Advances in Meteorology

Climate Risk Assessment, Coping, and Adaptation

Lead Guest Editor: Jayant K. Routray
Guest Editors: Sangam Shrestha, Sushil K. Dash, Bimal K. Paul, and Dev Niyogi

Climate Risk Assessment, Coping, and Adaptation

Advances in Meteorology

Climate Risk Assessment, Coping, and Adaptation

Lead Guest Editor: Jayant K. Routray
Guest Editors: Sangam Shrestha, Sushil K. Dash, Bimal K. Paul, and Dev Niyogi

Contents

Understanding the Effects of Changing Weather: A Case of Flash Flood in Morogoro on January 11, 2018

Offoro Neema Kimambo, Hector Chikoore, and Jabulani Ray Gumbo

Research Article (11 pages), Article ID 8505903, Volume 2019 (2019)

Hindawi
Advances in Meteorology
Volume 2019, Article ID 4053718, 10 pages
https://doi.org/10.1155/2019/4053718

Research Article

Temporal and Spatial Change Monitoring of Drought Grade Based on ERA5 Analysis Data and BFAST Method in the Belt and Road Area during 1989–2017

Changdi Xue,[1] **Hua Wu**,[1,2,3] **and Xiaoguang Jiang**[1,4]

[1]*University of Chinese Academy of Sciences, Beijing 100049, China*
[2]*State Key Laboratory of Resources and Environment Information System, Institute of Geographic Sciences and Natural Resources Research, Chinese Academy of Sciences, Beijing 100101, China*
[3]*Jiangsu Center for Collaborative Innovation in Geographical Information Resource Development and Application, Nanjing 210023, China*
[4]*Key Laboratory of Quantitative Remote Sensing Information Technology, Academy of Opto-Electronics, Chinese Academy of Sciences, Beijing 100094, China*

Correspondence should be addressed to Hua Wu; wuhua@igsnrr.ac.cn

Received 28 February 2019; Accepted 3 October 2019; Published 16 November 2019

Guest Editor: Jayant K. Routray

Drought is a worldwide natural disaster with a wide range of influences and a long duration, which has a huge impact on the agricultural production activities and social economy of local residents. The Belt and Road Initiative has always received much attention due to its special geographical location and great potential for economic development. At the same time, the Belt and Road region is also deeply affected by drought, especially in some countries and regions, where the agricultural infrastructure is weak and the ecological environment is fragile. How to effectively monitor and evaluate drought has become an urgent problem to be solved. In this study, the ERA5 atmospheric reanalysis data were used, and the self-calibrating Palmer Drought Severity Index was combined with Breaks for Additive Seasonal and Trend (BFAST) to study the temporal and spatial distribution of the 1989–2017 monthly scale of drought in different climate regions of the Belt and Road region. The results show that the overall change trend of arid area shows a change of "up-down-up-down." The winter drought area is larger than the summer drought area, and the drought center gradually moves from the Southeast Asia region in winter to the West–Central Asia region in summer. In the past five years, the drought area decreased gradually at the rate of approximately 0.38 million km^2 per year.

1. Introduction

Drought is an unusually dry incident over a period, causing water shortages for long enough to cause severe hydrological imbalances in the affected areas [1]. The imbalance of water budget is caused by the combined effects of climatic conditions, underlying surface, and human activities. Compared with floods, hurricanes, and other disasters, the process of drought is much slower [2, 3]. It usually takes several months or even several seasons [4]. It is easy to be ignored. Once it becomes a disaster, it has a large scope and lasts for a long time [5]. In the United States, drought causes an average of \$6–8 billion in annual losses, but in 1988, it reached \$40 billion [6]. Drought-related disasters in the 1980s caused more than half a million deaths in Africa [7].

Since the beginning of the last century, more and more researchers have realized the importance of drought monitoring, but due to technical limitations, most of them use weather station data to monitor and forecast drought [8–11]. With the development of remote sensing technology, the use of satellites to acquire long-term and large-scale meteorological data for monitoring environmental disasters has gradually become a mainstream method [12–14], such as the TRMM satellite. Its spatial resolution is 0.25°, and the time resolution is 1 hour, covering the area between 50°N and 50°S, spanning the period 1998 to 2018. It is a very powerful

source of meteorological data [15–18]. In recent years, reanalysis data have widely been used in climate simulation prediction [19, 20]. Several researchers use ERA-Interim reanalysis dataset from the European Centre for Medium-Range Weather Forecasts (ECMWF) and a refined version of a previously developed Lagrangian methodology to compile a global climatology of stratosphere-troposphere exchange (STE) from 1979 to 2011 [21]. Several researchers examined low-frequency variability and trends in temperature from 1979 to 2012, and near-surface behaviour of the ERA-Interim reanalysis is reviewed [22]. Several researchers model the climatic mass balance of the ice cap for the period September 2000 to August 2009 on ERA-Interim reanalysis [23].

Since the beginning of the 20th century, as the complexity of drought formation and the breadth of its effects have deepened, the researchers constructed a series of drought assessment indicators using easily available observational elements such as precipitation, temperature, evaporation, runoff, soil moisture, and remote sensing [24–26]. These assessment indicators study and depict drought from the perspective of meteorology, hydrology, agriculture, and other disciplines and begin to try to consider drought from a multifactor perspective. Representative drought indicators are as follows: Standardized Precipitation Index (SPI) [27], the Rainfall Deciles (RD) [28] reflect the water deficit of atmospheric process, and Computed Soil Moisture (CSM) [29] and Soil Moisture Deficit Index (SMDI) [30] reflect the water deficit of Soil process, and Total Water Deficit (S) [31] reflects the water deficit of the surface process. At the same time, there are a series of standardized comprehensive indexes, such as Normalized Difference Vegetation Index (NDVI) [32], Standardized Precipitation Evapotranspiration Index (SPEI) [33], Palmer Drought Severity Index (PDSI) [34], and Palmer Hydrological Drought Index (PHDI) [34]. On the one hand, these indicators reflect the water deficit in the atmosphere, soil, or surface, and on the other hand, their regional adaptability and transplantability are significantly enhanced, which can be applied to most parts of the world [35]. In view of these drought indexes, combining with modern climate statistical diagnosis technology, separating precipitation change trend from climate series can effectively monitor precipitation change and then monitor drought [36]. In addition to the traditional methods such as moving average [37], cumulative anomaly percentage [38], and linear tendency estimation [39], some researchers have also introduced new methods such as spline function to better reflect its real trend [40]. In addition, the significance test of the change trend is also emphasized. More commonly used are the Mann–Kendall detection [41], Yamamoto method [42], and so on.

Due to the large population and economic proportion of the Belt and Road, there are many cities with unbalanced cultural and economic development. Meteorological disasters, especially droughts, often have serious consequences for agricultural production in different countries. The region has a weak national agricultural infrastructure and relatively little investment in disaster prevention, mitigation, and relief, as the limitations of economic development lead to very heavy losses in the event of an accident [43]. Therefore, it is necessary to understand the distribution and variation of drought in the Belt and Road region. Due to the small coverage area of meteorological stations, some stations lack data, and the time series is not continuous, while the coverage area of satellite data is wide, but the time series is short for drought research. This paper calculates the self-calibrating Palmer Drought Severity Index (scPDSI) using ERA5 atmospheric reanalysis data and analyzes the distribution and change of drought in the Belt and Road region from 1989 to 2017 through Breaks for Additive Seasonal and Trend (BFAST) analysis [25, 44, 45]. We hope to contribute effectively to drought reduction by providing analysis of the drought situation in the Belt and Road region.

2. Materials and Methods

2.1. Area. The Belt and Road stretches across Asia, Europe, and Africa, from 0°North to 60°North and from 10°West to 110°East, and includes 70 countries and cities in the maritime regions, including the Western Pacific, Indian Ocean, Mediterranean Sea, Red Sea, and land. In the past research, most researchers use the state or national boundaries to study the distribution and change of drought in different regions. It is well known that the same geographical region usually contains different climatic types, and it may be inaccurate to compare drought under different climatic types in one region. In order to study the variation of drought under different climate regions better, according to the Wladimir Köppen climate zone classification [46], we divided the whole region into equatorial, arid, warm, snow, and polar. The climate classification system was proposed by a German climatologist Wladimir Köppen. Climate is classified according to temperature and precipitation, and according to the distribution of natural vegetation. First, the world's climate is divided into five climatic zones and expressed in majuscule terms: the tropical zone (equatorial), the arid zone (arid), the temperate zone (warm), the cold temperate zone (snow), and the polar climatic zone (polar). In the five climatic zones, except dry climate, all of them are bounded by isotherms. Precipitation and temperature were then used as secondary and tertiary classification indicators to divide the world into 31 climatic regions. For convenience and accuracy, this study used only Wladimir Köppen's classification of the world's five basic climate zones. The Belt and Road region is divided into five regions: namely, the tropical zone (equatorial), the arid zone (arid), the temperate zone (warm), the cold temperate zone (snow), and the polar zone (polar), see Figure 1 for classification of search area.

2.2. Data. The atmospheric reanalysis data, which have the advantages of long time series and high resolution, can be used not only for the diagnostic analysis of weather and climate but also for the assimilation of a large number of satellite data and routine data such as ground and upper air data. It can also be used in meteorological boundary fields for weather and climate models. ERA5 is a new climate reanalysis dataset (5th generation) from ECMWF (the

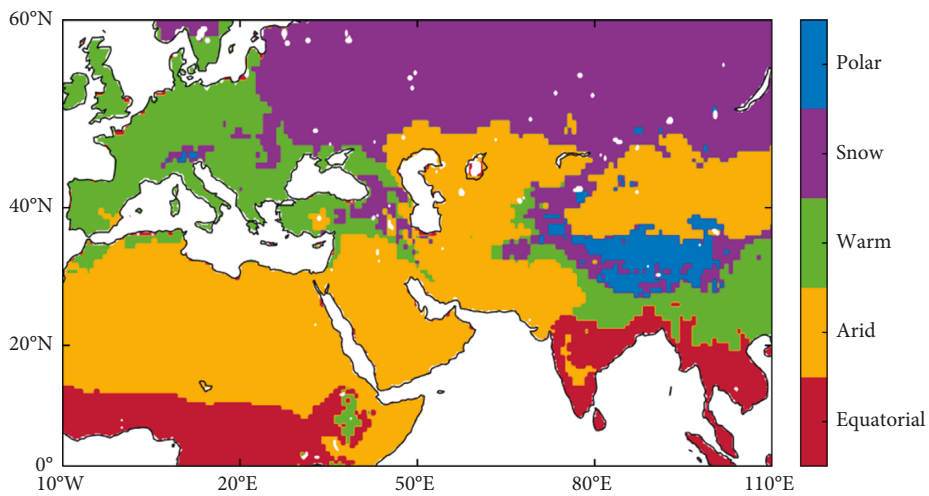

Figure 1: Research area and climate subregion.

European Centre for Medium-Range Weather Forecasts) [21]. The resolution was increased from 79 km to 31 km, the time resolution from 3 hours to 1 hour, the number of vertical layers from 60 to 137, and the time span from 1950 to the present (data for some years are still being processed). Based on the availability of the data, we selected atmospheric reanalysis data from 1989 to 2017, with the main variables being total precipitation and near-surface temperature. At the same time, in order to calculate the scPDSI, we used available water-holding capacity (AWC) from SoilGrids dataset [47–49], which was developed by random forest and gradient-enhanced tree algorithms combined with global soil profile data compilation (approximately 1,30,000 sites) and borehole data (approximately 1.6 million sites).

Daily atmospheric reanalysis data in the Belt and Road area from 1989 to 2017, which were collected from ECMWF, are used in this study. According to the world map of the Köppen–Geiger climate classification, we divide the study area into different climate types (available online at https://people.eng.unimelb.edu.au/mpeel/koppen.html). The soil data were downloaded from the World Soil Information (available online at https://www.isric.org/explore/soilgrids).

The ERA5 reanalysis data and soil data used to support the findings of this study can be downloaded from the corresponding website on the Internet (https://climate.copernicus.eu/). The scPDSI data used to support the finding of this study are available from the corresponding author upon request.

3. Method

3.1. scPDSI. This study uses the scPDSI [26], which is a drought index based on the relationship between water supply and demand proposed by Wayne Palmer in 1965. PDSI can take into account not only the current water supply and demand situation but also the effect of dry and wet situation and its duration on the current drought situation [34]. In order to improve the transplantability and spatial comparability of PDSI, wells and other researchers proposed scPDSI that can automatically modify the local climate [26].

Firstly, scPDSI has similar variation range under different climatic conditions. This makes it a more suitable indicator for comparing the relative availability of water in different regions. Secondly, potential evapotranspiration is calculated using the physical-based Penman–Monteith parameterization, using actual vegetation cover rather than reference crops. Thirdly, the seasonal dynamics of snow cover is considered in the water balance model [44, 50]. The scPDSI was calculated using a program developed by researchers at the University of Nebraska, Lincoln (http://greenleaf.unl.edu/).

3.2. Breaks for Additive Seasonal and Trend. BFAST was originally used to identify vegetation disturbance using remote sensing data. Compared with other change detection methods, such as PCA, Fourier analysis, wavelet analysis, and transform vector analysis, the advantages are as follows: firstly, BFAST can analyze all time series data and consider seasonal variation effectively avoiding the error caused by seasonal segmentation. Secondly, BFAST iteratively estimates the date and number of changes in the seasonal and trend components and characterizes the changes by extracting the magnitude and direction of the changes. Thirdly, BFAST is suitable for all types of remote sensing data and can be applied to other time series data without the need to select reference cycles, set thresholds, or define change trajectories [45, 51, 52].

The general pattern is as follows:

$$Y_t = T_t + S_t + e_t. \tag{1}$$

It is widely used and can be used in meteorology, hydrology, economics, and other fields. By decomposing the data over a period of time into long-term trend components, periodic components, and the remaining components, in which the trend components are fitted using a linear model, the model is (2), and the periodic components are fitted

using a periodic model. The model takes the form of formula (3):

$$T_t = \alpha_i + \beta_i t, \tag{2}$$

$$S_t = \sum_{k=1}^{j} \alpha_{j,k} \sin\left(\frac{2\pi kt}{f} + \delta_{j,k}\right). \tag{3}$$

Another key point is the identification of mutation points in time series. The BFAST algorithm uses the ordinary least squares (OLS) residual-based MOving SUM (MOSUM) test to determine whether there are mutation points and uses Bayesian information theory to determine the optimal number of mutation points. The position of the mutation point in the time series is estimated by the least squares.

As shown in Figure 2, the data preprocessing and scPDSI were firstly calculated based on the climate zone classification. The BFAST algorithm was then used to detect the presence of abrupt climate change points in the time series. The causes of abrupt climate change were finally analyzed. In this study, the BFAST algorithm is implemented in the R language BFAST algorithm package (http://bfast.r-forge.r-project.org/).

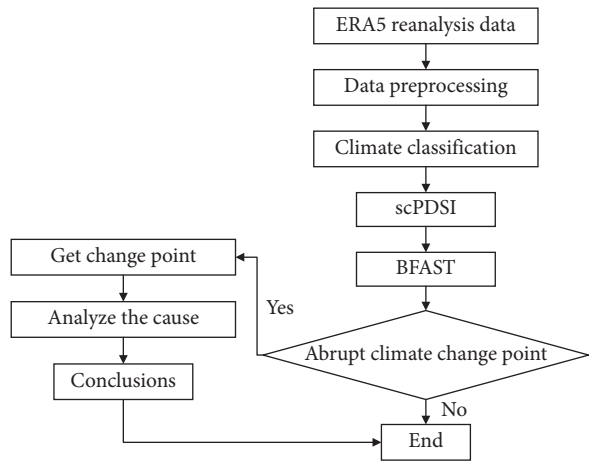

Figure 2: Graphical framework of methodology.

Table 1: Drought category based on the scPDSI value.

Rank	Category	scPDSI
1	No drought	>−1.0
2	Slight drought	−2.0 : −1.0
3	Medium drought	−3.0 : −2.0
4	Severe drought	−4.0 : −3.0
5	Extreme drought	<−4.0

4. Results

The scPDSI from 1989 to 2017 was calculated according to the calculation method of scPDSI mentioned in 3.1, and then the drought grades of 29 years were classified by using the drought index classification method in Table 1. Figure 3 shows the distribution of the average scPDSI drought index in 1998, with extreme droughts in central Africa, southern and Central Asia, and southern Europe, in contrast to increased precipitation in northern Europe and Central Asia. The rest are slightly and moderately dry. Figure 4 shows the distribution of drought grades from January to December 1998. For Europe, there were more severe droughts in February, April, and November, mainly in southern countries and regions, including Italy, Greece, Albania, Serbia, Austria, Hungary, and the West Coast of Spain; for Asia, West Asia is the main arid region, and the drought has also affected Central Asia in some months, with Saudi Arabia, Yemen, Iraq, Pakistan, and Iran being the main affected countries. Central Asia, on the other hand, is dominated by central Russia and Kazakhstan; for Africa, it's a perennial drought, with frequent droughts in Ethiopia, Djibouti, and northern Africa, mainly in winter and spring. It has a great impact on the daily life of the local people. As a region with abundant rainfall, Southeast Asia is prone to drought, which occurs mainly in autumn and winter, especially from September to December. The intensity of the drought gradually increased. Figure 5 illustrates the intensity change trend of PDSI from 1989 to 2017 in different climate regions, and Figure 5 illustrates the change trend of drought area (scPDSI < −1) from 1989 to 2017 in different climate regions, in order to better reflect the drought change.

Figure 5(e) shows the percentage change of drought area from 1989 to 2017. It is obvious that the drought area shows a trend of "up-down-up-down," which becomes clearer after BFAST algorithm decomposition. Among them, from 1989 to 1998, the drought area percentage gradually increased from 20% to 70%, which is the largest change in the past 30 years. From 1999 to the present, the trend of drought change basically accords with the change every five years. It can be seen from the periodic component that the drought area in the whole region of Belt and Road reaches the maximum in winter and spring and is lower in summer and autumn. The trend component T_t indicates that there are four arid climate change points from 1989 to 2017 and five periods of different periods of drought. The linear fitting of the monthly area change line of the five-stage drought period was obtained, and the slopes of the five-stage trend were 0.000191, 0.0053, −0.00513, 0.0034, and −0.00439. Based on the ERA5 resolution, the total area of the Belt and Road is estimated to be approximately 86.80 million km^2. So, the drought area decreased gradually at the rate of approximately 0.38 million km^2 per year from 2012 to 2017.

5. Discussion

5.1. Regional Variation Patterns of Drought Levels. The tropics have plenty of rainfall, with an annual average temperature of 800 mm or more, mainly in central Africa, much of India, and Southeast Asia; the arid regions include northern Africa, West Central Asia, and Northwest China. The annual precipitation is low, and the underlying surface is mainly desert and mountainous; the temperate zone mainly includes most of Europe and southwest China, which is strongly influenced by the monsoon, and the precipitation is seasonal. The cold temperate zone mainly includes northern Asia, eastern Europe, and the edge of the Qinghai–Tibet

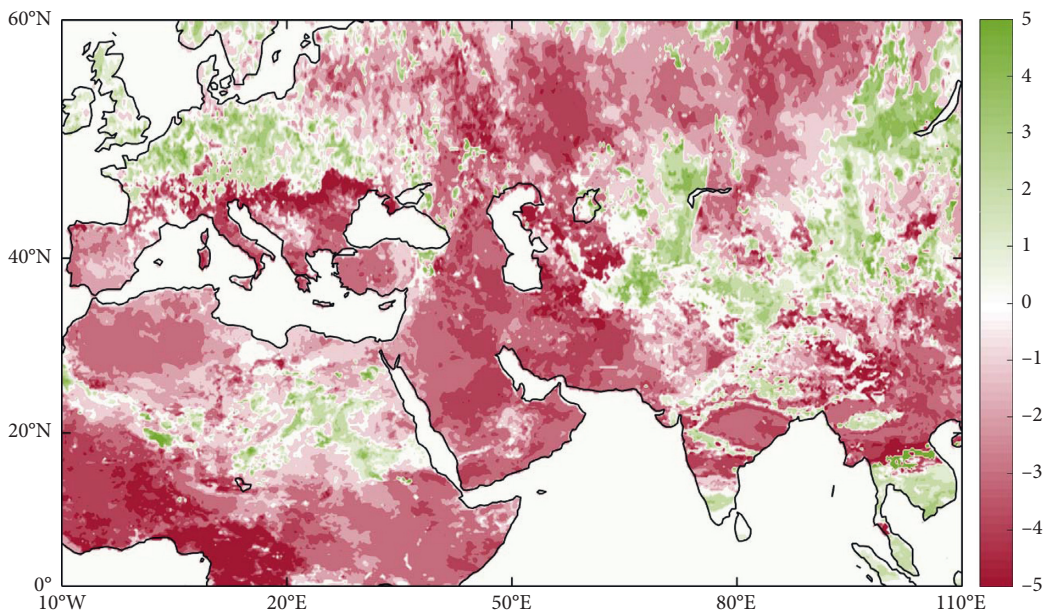

Figure 3: Monthly average scPDSI in 1998.

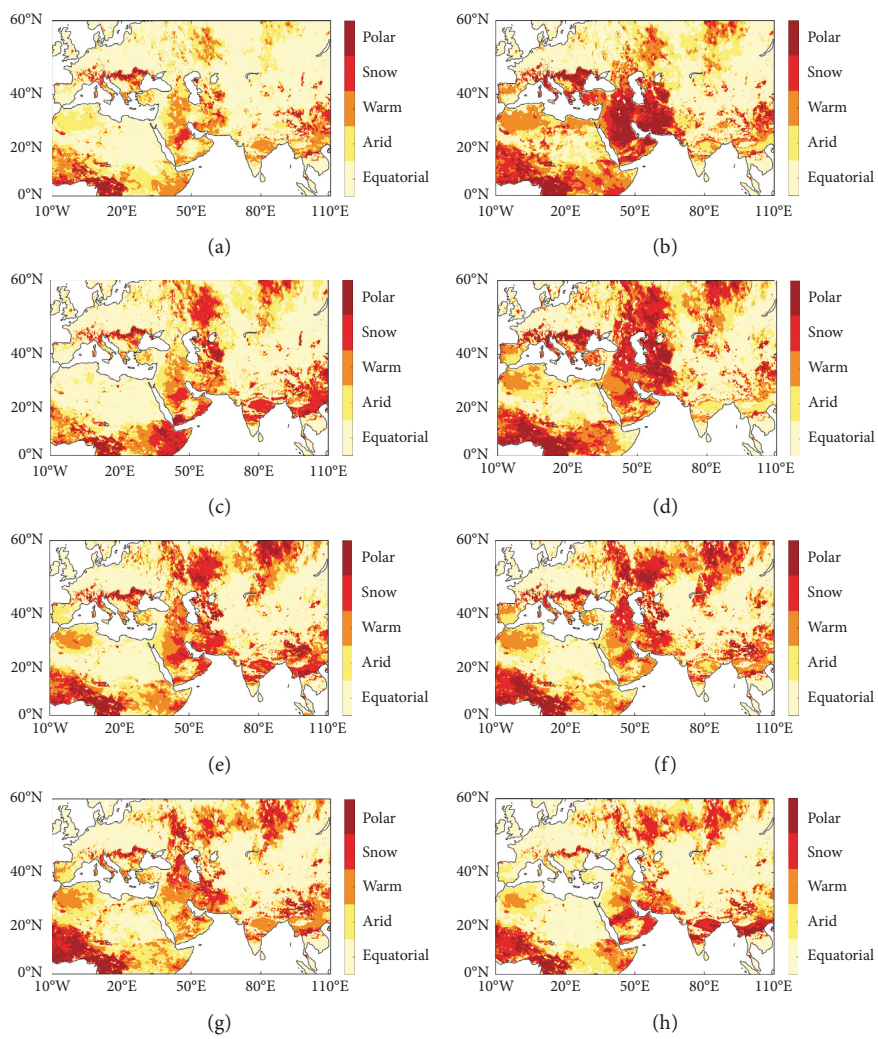

Figure 4: Continued.

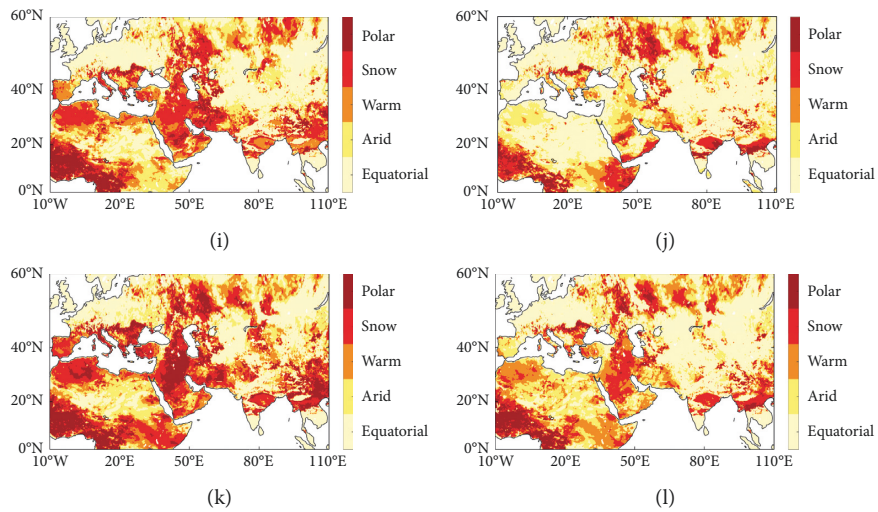

Figure 4: Spatiotemporal distribution of drought in Belt and Road area. (a) Jan. 1998. (b) Feb. 1998. (c) Mar. 1998. (d) Apr. 1998. (e) May. 1998. (f) Jun. 1998. (g) Jul. 1998. (h) Aug. 1998. (i) Sept. 1998. (j) Oct. 1998. (k) Nov. 1998. (l) Dec. 1998.

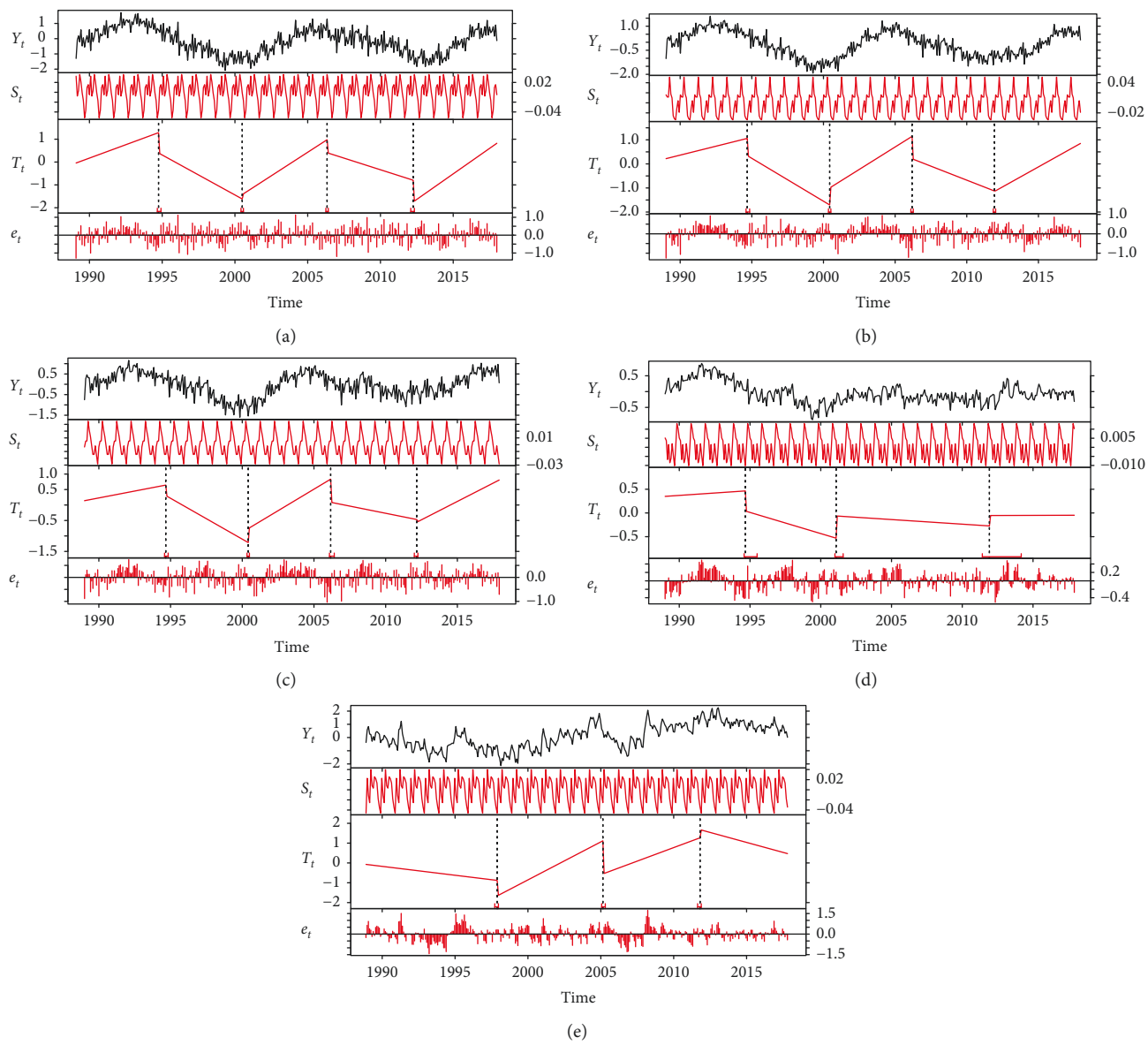

Figure 5: Trends of monthly scPDSI for the subregions. (a) Equatorial. (b) Arid. (c) Warm. (d) Snow. (e) Polar.

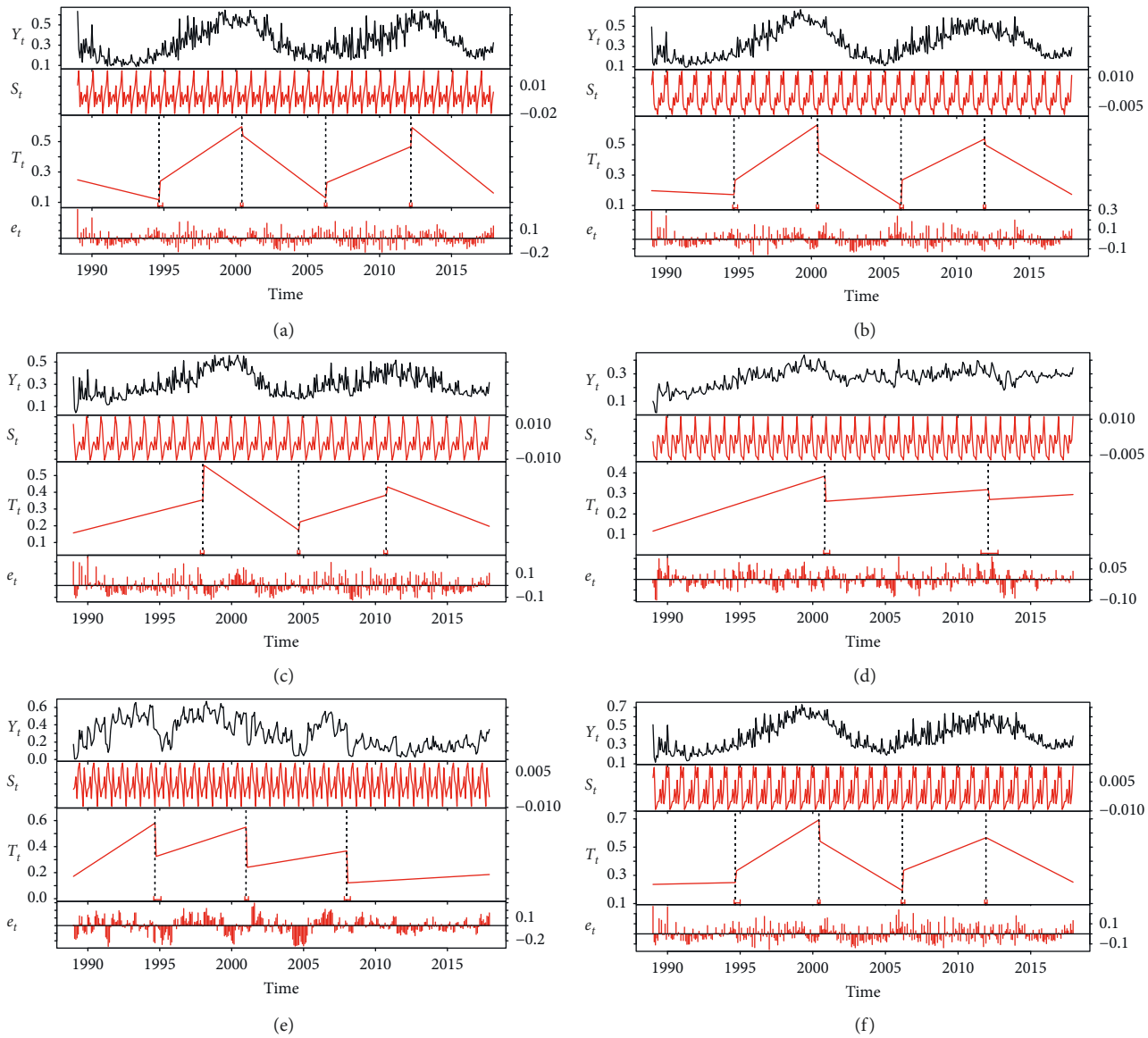

Figure 6: Trends of monthly average area percentage of the subregions in the Belt and Road area. (a) Equatorial. (b) Arid. (c) Warm. (d) Snow. (e) Polar. (f) Entire study area.

Plateau. The annual average temperature is relatively low, and ice and snow are the basic forms of precipitation in winter. For the tropical region (Figure 5(a)), it can be seen from the periodic component that the drought mainly occurs in autumn, and judging from the scPDSI of the monthly scale, it is a mild drought because of the mean value. So the drought is less severe than it actually is. According to the trend component, the slope of drought grade change in five periods was 0.0195, −0.0292, 0.0343, −0.017, and 0.0372, which showed obvious cycle change. For arid climate areas (Figure 5(b)), summer and autumn are frequent periods of drought, and most areas are moderate or extreme drought; from the perspective of the trend component, the slope of drought grade change in five periods was 0.0124, −0.0297, 0.0311, −0.0194, and 0.0277, and the drought degree increased between 1995 and 2000. For the temperate zone (Figure 5(c)), the drought is serious in winter, and most of the areas are mild and moderately drought. From the trend component, the slope of the five-stage period was 0.00742, −0.022, 0.0232, −0.00774, and 0.0198. The degree of drought increased between 1995 and 2000. For the cold temperate zone (Figure 5(d)), the summer drought was severe, and most of the areas were slightly arid. From the trend component, the slope of the four-stage period was 0.00168, −0.00743, −0.00162, and 0.00008, and the degree of drought tends to be stable between 2000 and 2015. For the polar climate region (Figure 5(e)), the drought is serious in spring and spring, and most areas are slightly dry. From the trend component, the slopes of the four periods were −0.00747, 0.0319, 0.0228, and −0.0168. The drought degree was gradually serious between 1990 and 1998 and then gradually improved from 1999 to 2005 and from 2006 to 2011, but it

can be seen that the annual average scPDSI shows a downward trend after 2012.

5.2. Regional Variation Patterns of Drought Areas. Comparing the changes of the arid area of the five climate type areas with the whole study area, it is found that the entire area shows a trend of "up-down-up-down." Of these, the percentage change in the arid area of the polar climate region was the largest, increasing from 11.33% in October 1995 to 67% in April 1998. For the polar climate region (Figure 5(e)), the trend of the percentage change of arid area is divided into four stages, which are the increasing trend of drought in different degrees, but when the arid area reaches a certain degree, there will be a sharp decline. This indicates that the duration of drought in polar climate region is short, and the slope of the four segments was 0.00601, 0.003, 0.00151, and 0.000541, respectively. This indicates that the rate of change in the extent of drought has gradually decreased over time, especially since 2008, the change in the area of drought has been moderate, and the tropical, arid, and temperate climatic regions basically conform to the overall trend of the change in the area of drought (Figures 6(a)–6(c)). But the variation range of adjacent months in tropical climate region is larger than that in arid climate region and temperate climate region. The proportion of arid areas in the cold temperate zone is relatively small (Figure 6(d)), ranging from 10 to 30 percent. On the one hand, because the cold temperate mainly in Russia, deep into the hinterland of the Asian continent, less precipitation. On the other hand, the cold temperate zone area is vast, but the change rate of drought area will be stable. For the cold temperate regions (Figure 6(e)), from 1989 to 2017, there were two major abrupt climate change points, the first in 2001 and the second in 2012. The slopes of the three aridity area curves were 0.00189, 0.000423, and 0.000353. The rate of increase in arid areas is levelling off.

6. Conclusions

Most previous studies were confined to smaller research areas, in which case, climate differences between different regions need not to be taken into account. Although the BFAST time series analysis method may get the trend and distribution characteristics of the drought index in different periods, the selected research area in this study is large, where it is not a good way to use the BFAST method alone. In addition, considering the long study period, the scPDSI may be more suitable for the reason that it can be self-calibrated according to the local climate and comprehensively and accurately describe the drought situation. Consequently, the authors tried to introduce the Köppen–Geiger climate zone into the change monitoring of the temporal and spatial distribution of the 1989–2017 monthly scale of drought with the scPDSI and the BFAST method. The classification by climate type avoids the selective error caused by subjective judgment. The change trend of drought and the abrupt change point of climate in the whole climate region can be well captured. In addition, by comparing the drought situation in different climatic regions, the degree of drought risk under different climatic influences can also be obtained. The development trend of drought in different climatic zones would be clarified. Based on the ERA5 data, the spatial distribution and temporal and spatial variation of drought in the Belt and Road region from 1989 to 2017 were studied by using the adaptive Palmer drought model. Overall, the results of our research and analysis of the distribution of drought in the Belt and Road are as follows.

In terms of spatial distribution, the area of winter drought is larger than that of summer drought, and winter drought mainly occurs in central Africa and West Asia, as well as parts of Southeast Asia summer droughts occur mainly in Central and Western Asia, much of Southeast Asia, and northern Africa. Taking into account the year-to-year distribution, the arid regional center moves eastward from West–Central Asia as the seasons change from winter to summer. In April 1999, 72.9 percent of the Belt and Road area was dry, the highest percentage in nearly three decades. According to the classification results of different climatic regions, the change trend of the percentage of arid area in arid, tropical, and temperate climate regions is "up-down-up-down." For the cold temperate zone and the polar climate zone, the trend of change increases slowly, and it is not clear whether the area of drought is likely to reduce the trend. In the past five years, the drought area decreased gradually at the rate of approximately 0.38 million km^2 per year.

This study used ERA5 atmospheric reanalysis data and self-calibrating Palmer Drought Severity Index to describe the occurrence and development trends of droughts in the Belt and Road from 1989 to 2017. It has a certain reference value for revealing the spatial and temporal distribution characteristics of drought in the Belt and Road area. From the view of data, extending the time span to 50 years may be more conducive to the estimation and analysis of drought trends. From the point of view of drought assessment, further research can be carried out using multiple drought indices for comprehensive assessment. For agricultural production, the next study will take into account agricultural factors such as crop drought tolerance and agricultural production data, and further study will take into account the direct impact of drought on agricultural production.

Data Availability

The ERA5 reanalysis data and soil data used to support the findings of this study can be downloaded from the corresponding website on the Internet. The scPDSI data used to support the finding of this study are available from the corresponding author upon request.

Conflicts of Interest

The authors declare that they have no conflicts of interest.

Authors' Contributions

The authors contributed equally to this paper.

Acknowledgments

This work was supported partly by the Strategic Priority Research Program of Chinese Academy of Sciences under grant nos. XDA20030302 and XDA19040403 and partly by the National Natural Science Foundation of China under grant no. 41871267.

References

[1] A. Dai, "Drought under global warming: a review," *Wiley Interdisciplinary Reviews: Climate Change*, vol. 2, no. 1, pp. 45–65, 2011.

[2] A. K. Mishra and V. P. Singh, "A review of drought concepts," *Journal of Hydrology*, vol. 391, no. 1-2, pp. 202–216, 2010.

[3] Z. Maosheng and S. W. Running, "Drought-induced reduction in global terrestrial net primary production from 2000 through 2009," *Science*, vol. 329, no. 5994, pp. 940–943, 2010.

[4] J. G. Charney, "Dynamics of deserts and drought in the Sahel," *Quarterly Journal of the Royal Meteorological Society*, vol. 101, no. 428, pp. 193–202, 2010.

[5] A. Dai, "Increasing drought under global warming in observations and models," *Nature Climate Change*, vol. 3, no. 1, pp. 52–58, 2013.

[6] J. Newton, "Federal legislation for disaster mitigation: a comparative assessment between Canada and the United States," *Earthquake and Atmospheric Hazards*, vol. 16, no. 2-3, pp. 219–241, 1997.

[7] G. Kallis, "Droughts," *Annual Review of Environment and Resources*, vol. 33, no. 1, pp. 85–118, 2008.

[8] M. J. Salerno, "Assessing the predictability of weekly drought improvement using nebraska's automated weather data network," ProQuest dissertations publishing, Creighton University, Omaha, NE, USA, 2015.

[9] K. L. Webster, J. W. Mclaughlin, Y. Kim, M. S. Packalen, and C. S. Li, "Modelling carbon dynamics and response to environmental change along a boreal fen nutrient gradient," *Ecological Modelling*, vol. 248, no. 1751, pp. 148–164, 2013.

[10] J. Fan, M. Zhang, G. Cao, X. Zhang, and J. Wu, "Integration of drought monitoring with remote sensing into the global drought information system," *Proceedings of SPIE—The International Society for Optical Engineering*, vol. 8531, no. 8, pp. 468–472, 2012.

[11] H. Ezzine, A. Bouziane, and D. Ouazar, "Seasonal comparisons of meteorological and agricultural drought indices in Morocco using open short time-series data," *International Journal of Applied Earth Observations & Geoinformation*, vol. 26, no. 1, pp. 36–48, 2014.

[12] Z. Tian, B. Nijssen, G. J. Huffman, and D. P. Lettenmaier, "Evaluation of real-time satellite precipitation data for global drought monitoring," *Journal of Hydrometeorology*, vol. 15, no. 4, pp. 1651–1660, 2014.

[13] H. Cui, J. Zhang, and F. Yao, "Combination of multi-sensor remote sensing data for drought monitoring over Southwest China," *International Journal of Applied Earth Observations & Geoinformation*, vol. 35, pp. 270–283, 2015.

[14] S.-B. Duan, Z.-L. Li, B.-H. Tang, H. Wu, and R. Tang, "Generation of a time-consistent land surface temperature product from MODIS data," *Remote Sensing of Environment*, vol. 140, pp. 339–349, 2014.

[15] A. Yaduvanshi, P. K. Srivastava, and A. C. Pandey, "Integrating TRMM and MODIS satellite with socio-economic vulnerability for monitoring drought risk over a tropical region of India," *Physics and Chemistry of the Earth, Parts A/B/C*, vol. 83-84, pp. 14–27, 2015.

[16] S. Park, J. Im, J. Eunna, and R. Jinyoung, "Peer review report 1 on "drought assessment and monitoring through blending of multi-sensor indices using machine learning approaches for different climate regions"," *Agricultural and Forest Meteorology*, vol. 217, p. 50, 2016.

[17] X. Cao, Y. Feng, and J. Wang, "An improvement of the Ts-NDVI space drought monitoring method and its applications in the Mongolian plateau with MODIS, 2000–2012," *Arabian Journal of Geosciences*, vol. 9, no. 6, p. 433, 2016.

[18] W. Yao, Z. Xu, Z. Bing, and L. Qi, "Monitoring the meteorological drought in the middle reaches of Heihe River basin based on TRMM precipitation data," in *Proceedings of the 2016 Geoscience & Remote Sensing Symposium*, Beijing, China, July 2016.

[19] S. Chen, T. Y. Gan, X. Tan, D. Shao, and J. Zhu, "Assessment of CFSR, ERA-Interim, JRA-55, MERRA-2, NCEP-2 reanalysis data for drought analysis over China," *Climate Dynamics*, vol. 53, no. 1-2, pp. 737–757, 2019.

[20] Z. Wang, K. Guan, J. Sheffield, and E. F. Wood, "Depiction of drought over sub-Saharan Africa using reanalyses precipitation datasets: depiction of drought using reanalyses," *Journal of Geophysical Research Atmospheres*, vol. 121, no. 18, pp. 10,555–10,574, 2016.

[21] B. Škerlak, M. Sprenger, and H. Wernli, "A global climatology of stratosphere–troposphere exchange using the ERA-Interim data set from 1979 to 2011," *Atmospheric and Physics*, vol. 14, no. 2, pp. 913–937, 2014.

[22] A. J. Simmons, P. Poli, D. P. Dee et al., "Estimating low-frequency variability and trends in atmospheric temperature using ERA-Interim," *Quarterly Journal of the Royal Meteorological Society*, vol. 140, no. 679, pp. 329–353, 2014.

[23] M. Möller, R. Finkelnburg, and M. Braun, "Climatic mass balance of the ice cap Vestfonna, Svalbard: a spatially distributed assessment using ERA-Interim and MODIS data," *Journal of Geophysical Research Earth Surface*, vol. 116, no. F3, 2011.

[24] J. K. Zhu, "Salt and drought stress signal transduction in plants," *Annual Review of Plant Biology*, vol. 53, no. 1, pp. 247–273, 2002.

[25] S. B. Duan, Z. L. Li, H. Li et al., "Validation of Collection 6 MODIS land surface temperature product using in situ measurements," *Remote Sensing of Environment*, vol. 225, pp. 16–29, 2019.

[26] S.-B. Duan, Z.-L. Li, and P. Leng, "A framework for the retrieval of all-weather land surface temperature at a high spatial resolution from polar-orbiting thermal infrared and passive microwave data," *Remote Sensing of Environment*, vol. 195, pp. 107–117, 2017.

[27] M. J. Hayes, M. D. Svoboda, D. A. Wilhite, and O. V. Vanyarkho, "Monitoring the 1996 drought using the standardized precipitation index," *Bulletin of the American Meteorological Society*, vol. 80, no. 3, pp. 429–438, 1999.

[28] Rainfall deciles, Climate Summary of South Africa, 2009.

[29] L. Telesca, S. M. Vicente-Serrano, and J. I. López-Moreno, "Power spectral characteristics of drought indices in the Ebro river basin at different temporal scales," *Stochastic Environmental Research and Risk Assessment*, vol. 27, no. 5, pp. 1155–1170, 2013.

[30] B. Narasimhan and R. Srinivasan, "Development and evaluation of soil moisture deficit index (SMDI) and evapotranspiration deficit index (ETDI) for agricultural drought

monitoring," *Agricultural and Forest Meteorology*, vol. 133, no. 1–4, pp. 69–88, 2005.

[31] K. Tankha and R. K. Gupta, "Effect of water deficit and sulphur dioxide on total soluble proteins, nitrate reductase activity and free proline content in sunflower leaves," *Biologia Plantarum*, vol. 34, no. 3-4, pp. 305–310, 1992.

[32] A. A. V. D. Griend and M. Owe, "On the relationship between thermal emissivity and the normalized difference vegetation index for natural surfaces," *International Journal of Remote Sensing*, vol. 14, no. 6, pp. 1119–1131, 1993.

[33] S. M. Vicente-Serrano, S. Beguería, and J. I. López-Moreno, "A multiscalar drought index sensitive to global warming: the standardized precipitation evapotranspiration index," *Journal of Climate*, vol. 23, no. 7, pp. 1696–1718, 2010.

[34] A. Dai, K. E. Trenberth, and T. Qian, "A global dataset of palmer drought severity index for 1870–2002: relationship with soil moisture and effects of surface warming," *Journal of Hydrometeorology*, vol. 5, no. 6, pp. 1117–1130, 2004.

[35] T. Qian, A. Dai, K. E. Trenberth, and K. W. Oleson, "Simulation of global land surface conditions from 1948 to 2004. Part I: forcing data and evaluations," *Journal of Hydrometeorology*, vol. 7, no. 5, pp. 953–975, 2006.

[36] V. K. Lohani and G. V. Loganathan, "An early warning system for drought management using the Palmer drought index," *Journal of the American Water Resources Association*, vol. 33, no. 6, pp. 1375–1386, 2010.

[37] R. Modarres, "Streamflow drought time series forecasting," *Stochastic Environmental Research and Risk Assessment*, vol. 21, no. 3, pp. 223–233, 2007.

[38] M. Yun, Z. Wu, H. Hai, G. Lu, H. Xu, and Q. Lin, "Spatio-temporal analysis of drought in a typical plain region based on the soil moisture anomaly percentage index," *Science of the Total Environment*, vol. 576, pp. 752–765, 2017.

[39] X. H. Xu, Z. Q. Lv, X. Y. Zhou, and N. Jiang, "Drought prediction and sustainable development of the ecological environment," *Environmental Science and Pollution Research*, vol. 24, no. 35, pp. 26974–26982, 2017.

[40] M. Sarfraz, M. Z. Hussain, and A. Nisar, "Positive data modeling using spline function," *Applied Mathematics and Computation*, vol. 216, no. 7, pp. 2036–2049, 2010.

[41] F. F. Zhao, Z. X. Xu, J. X. Huang, and J. Y. Li, "Monotonic trend and abrupt changes for major climate variables in the headwater catchment of the Yellow River basin," *Hydrological Processes*, vol. 22, no. 23, pp. 4587–4599, 2008.

[42] S. C. Babu and G. B. Mthindi, "Developing decentralized capacity for disaster prevention: lessons from food security and nutrition monitoring in Malawi," *Disasters*, vol. 19, no. 2, pp. 127–139, 1995.

[43] R. Ü. N. Geiger, "Köppen-geiger/Klima der Erde. (wandkarte 1:16 Mill.)," Klett-Perthes, Gotha, Germany, 1965.

[44] G. V. D. Schrier, J. Barichivich, K. R. Briffa, and P. D. Jones, "A scPDSI-based global data set of dry and wet spells for 1901–2009," *Journal of Geophysical Research: Atmospheres*, vol. 118, no. 10, pp. 4025–4048, 2013.

[45] J. Verbesselt, R. Hyndman, G. Newnham, and D. Culvenor, "Detecting trend and seasonal changes in satellite image time series," *Remote Sensing of Environment*, vol. 114, no. 1, pp. 106–115, 2010.

[46] M. C. Peel, B. L. Finlayson, and T. A. Mcmahon, "Updated world map of the Köppen-Geiger climate classification," *Hydrology and Earth System Sciences*, vol. 11, no. 5, pp. 1633–1644, 2007.

[47] T. Hengl, J. M. D. Jesus, G. B. M. Heuvelink et al., "SoilGrids250m: global gridded soil information based on machine learning," *PLoS One*, vol. 12, no. 2, Article ID e0169748, 2017.

[48] T. Hengl, J. M. D. Jesus, R. A. Macmillan, N. H. Batjes, and M. R. Gonzalez, "SoilGrids1km—global soil information based on automated mapping," *PLoS One*, vol. 9, no. 8, Article ID e105992, 2014.

[49] S. Wei, T. Hengl, J. M. D. Jesus, Y. Hua, and Y. Dai, "Mapping the global depth to bedrock for land surface modeling," *Journal of Advances in Modeling Earth Systems*, vol. 9, no. 1, pp. 65–88, 2017.

[50] N. Wells, S. Goddard, and M. J. Hayes, "A self-calibrating palmer drought severity index," *Journal of Climate*, vol. 17, no. 12, pp. 2335–2351, 2004.

[51] J. Verbesselt, R. Hyndman, A. Zeileis, and D. Culvenor, "Phenological change detection while accounting for abrupt and gradual trends in satellite image time series," *Remote Sensing of Environment*, vol. 114, no. 12, pp. 2970–2980, 2010.

[52] J. Verbesselt, A. Zeileis, and M. Herold, "Near real-time disturbance detection using satellite image time series," *Remote Sensing of Environment*, vol. 123, pp. 98–108, 2012.

Hindawi
Advances in Meteorology
Volume 2019, Article ID 1401402, 16 pages
https://doi.org/10.1155/2019/1401402

Research Article

Impact of Climate Change on the Growth of Typical Crops in Karst Areas: A Case Study of Guizhou Province

Jun Ma,[1,2] **Baisha Weng**,[1] **Wuxia Bi**,[1,3] **Dan Xu**,[4] **Ting Xu**,[1] **and Dengming Yan**[1,5]

[1]*State Key Laboratory of Simulation and Regulation of Water Cycle in River Basin, China Institute of Water Resources and Hydropower Research, Beijing 100038, China*
[2]*School of Water Conservancy and Hydroelectric Power, Hebei University of Engineering, Handan 056021, China*
[3]*College of Hydrology and Water Resources, Hohai University, Nanjing 210098, China*
[4]*Guizhou Climate Center, Guiyang 550002, China*
[5]*College of Environmental Science and Engineering, Donghua University, Shanghai 201620, China*

Correspondence should be addressed to Baisha Weng; baishaweng@163.com

Received 22 November 2018; Revised 10 May 2019; Accepted 20 August 2019; Published 3 November 2019

Guest Editor: Dev Niyogi

Climate change has emerged as a significant man-made global environmental challenge marked by rising temperature. The global rising temperature is supposed to alter climatic patterns like floods and droughts, thereby affecting human life supporting system and global food production. In order to clarify the impact of weather events on agricultural production in karst landforms, this study selected the indices of the growth period of crops (start time and duration), growing season precipitation, intense precipitation, number of consecutive rainless days, and number of drought-flood abrupt alternation events to evaluate the variation trend of future weather events and their impact on crop growth in Guizhou Province, China. The results show that (1) the climate is generally getting warmer. From 2019 to 2050, the sowing period of winter wheat and rice tends to be postponed. The duration of maize and rice's growth period will be shortened, and the life cycle of wheat also emerges as having a decreasing tendency except for those from the southern region. Comparing with the mean value during 1961 to 2018, the average crop cycle length of winter wheat, summer maize, and rice was shortened. The rate of shortening of crop cycle length is faster than the value during 1961 to 2018. (2) In the next 30 years, extreme precipitation concentrates in June and mainly falls in the central and southeast parts of Guizhou Province. In addition, summer is the outbreak period of drought events and drought-flood abrupt alternation events, which has a great impact on crop's growth. This study can provide references for the planting system, structure, layout, and management of crops in the karst region.

1. Introduction

Climate change has already affected global ecosystems, biodiversity, and social economy [1], and the impacts are likely to be more pronounced in the future [2]. IPCC Fifth Assessment Report has pointed out that global climate change is undoubtable [3]. Climate change has emerged as a significant man-made global environmental challenge marked by rising temperature. Global mean temperature has increased by 0.8°C over the past century and is anticipated to rise from 1.5°C to 4.8°C over the next hundred years [4]. Global warming trends may benefit crop production in cooler regions. Some areas such as northern Europe might benefit from climate change to some extent, in the short and medium terms, e.g., by increasing crop yield, better forest growth, and augmented tourism demand [5]. However, the negative impacts of climate change will be so severe in arid or semiarid areas such as Iran [6]. The agricultural water has been reducing with a steep downward trend in south of the Iran as a result of climate change [7]. Increased temperatures are likely to shorten the crop cycle, thus reducing crop production [8]. Recent increases in climate variability may have affected crop yields in countries across Europe since around the mid-1980s [9]. Global rising temperature is supposed to alter climatic patterns like floods, droughts, and incidents of the El Nino and La Nina, which could also

reduce the yield in other regions where optimal temperatures have already existed, thereby affecting human life supporting system and global food production, further leading to food insecurity in terms of food availability, accessibility, utilization, and food system stability [4, 10–13].

The existence of climate change in China is unequivocal. From 1961 to 2017, the average annual surface temperature in China increased by 0.24°C every 10 years, and the heating rate was higher than the global average. From 1961 to 2017, there was no significant increase or decrease in the average annual precipitation in China, but the extreme precipitation events showed an increasing trend [14]. The impact of climate change on Chinese agriculture is evident [15]. Statistics reveal that during a 28-year period from 1980 to 2008 in China, climatic changes led to a crop yield reduction of 1.27%, 1.73%, and 0.41% for wheat, corn, and soybean, respectively, while there was an increment of 0.56% in rice yield [16]. Lv et al. [17] reported a decrease in wheat yield in northern China and an increase in southern China in the future due to the presence of the rain-fed conditions.

Therefore, the study on the climate change impacts on crop growth was mainly in two aspects: one is the impact of normal climatic factors on agriculture, such as, temperature change, precipitation change, and others; the other is the impact of extreme climate events on the agriculture, such as rainstorm and drought. Southwest China is one of the main food producing areas. Guizhou Province has poor surface water storage capacity with karst topography. It has been found that a suitable climate plays a significant role in promoting food production [18]. Therefore, the growth period of crops (start time and duration), growing season precipitation, intense precipitation, number of consecutive rainless days, and number of drought-flood abrupt alternation events were selected as indices. Based on the observation data of 84 meteorological stations and climate model prediction simulation results, the evolution characteristics of extreme weather events and their effects on crop growth were evaluated. It is of great significance to the future agriculture development in Guizhou Province.

2. Study Site

Guizhou Province is located in the subtropical monsoon climate zone. The landform type is karst topography, with poor surface water storage capacity. Guizhou is the only province in China without plains. Thus, terrace fields are the main type of farmland. In 2017, the cultivated land area of Guizhou Province accounted for 2.72% of China's total cultivated land area, while the corn production and rice yield accounted for 2.03% and 1.45% of the national total output, respectively [19]. Guizhou has abundant agricultural biological resources, of 207 kinds [20], such as rice, corn, soybean, potato, sorghum, wheat, and so on. However, rice and corn account for about 70% of the total grain output, and winter wheat is responsible for about 50% of the summer harvest [21, 22]. Therefore, rice, corn, winter wheat, and other typical crops were selected to analyze the impact of climate change on crop growth and yield. Figure 1 shows the location of Guizhou Province.

3. Data and Methods

3.1. Research Idea. This paper conducts research according to the idea of "data sorting-model screening-extreme indices selection-future trend analysis-impact analysis" (details are shown in Figure 2).

3.2. Climatic Data

3.2.1. Measured Meteorological Data. Daily temperature and precipitation of 84 meteorological stations used in this study (from January 1961 to December 2016) were provided by the Meteorological Bureau of Guizhou Province. And daily temperature and precipitation of meteorological data (from January 2017 to December 2018) were obtained from http://data.cma.cn/site/index.html and https://www.wcrp-climate.org/data-etccdi, respectively. In this paper, the data in the province level were calculated through the Thiessen polygon based on the data of weather stations. The annual average temperature of 58 years in Guizhou was 15.6°C. The annual precipitation was 1183 mm.

3.2.2. Data Simulated by Model. The Inter-Sectoral Impact Model Intercomparison Project (ISIMIP) brought together 28 global impact models from five different sectors (water, agriculture, biomes, coastal infrastructure, and malaria). However, models involved in the agricultural component of ISIMIP were GFDL-ESM2M, IPSL-CM5A-LR, HadGEM2-ES, NorESM1-M, and MIROC-ESM-CHEM, with resolution of $0.5^\circ \times 0.5^\circ$, and were bias-corrected towards an observation-based dataset by using a trend-preserving method which is a common method in climate change studies [23–25]. Therefore, this study predicts the impact of climate change on agriculture based on these five models. Table 1 shows the details of five global climate models [26, 27].

3.3. Indicators for Evaluating Climate Events. In order to analyze the impact of climate change on crop growth, five indicators of growth period were selected based on accumulated temperature, growing season precipitation, intense precipitation, number of consecutive rainless days, and number of drought-flood abrupt alternation events.

3.3.1. Growth Period of Crops (Start Time and Duration). In order to analyze the impact of climate change on crops, the growth period is calculated based on the accumulated temperature threshold. The average daily temperature between 15°C and 18°C is most suitable for winter wheat sowing. When the daily average temperature is within the abovementioned temperature range (15°C to 18°C) during five consecutive days since late September, the first day of the period is defined as the sowing day of winter wheat [28]. Based on the research performed by Lu and Wang [29], the accumulated temperature ≥10°C (AT10) was chosen as an indicator to identify the stage of winter wheat growth. The AT10 threshold of each stage is given in Table 2 [30]. For

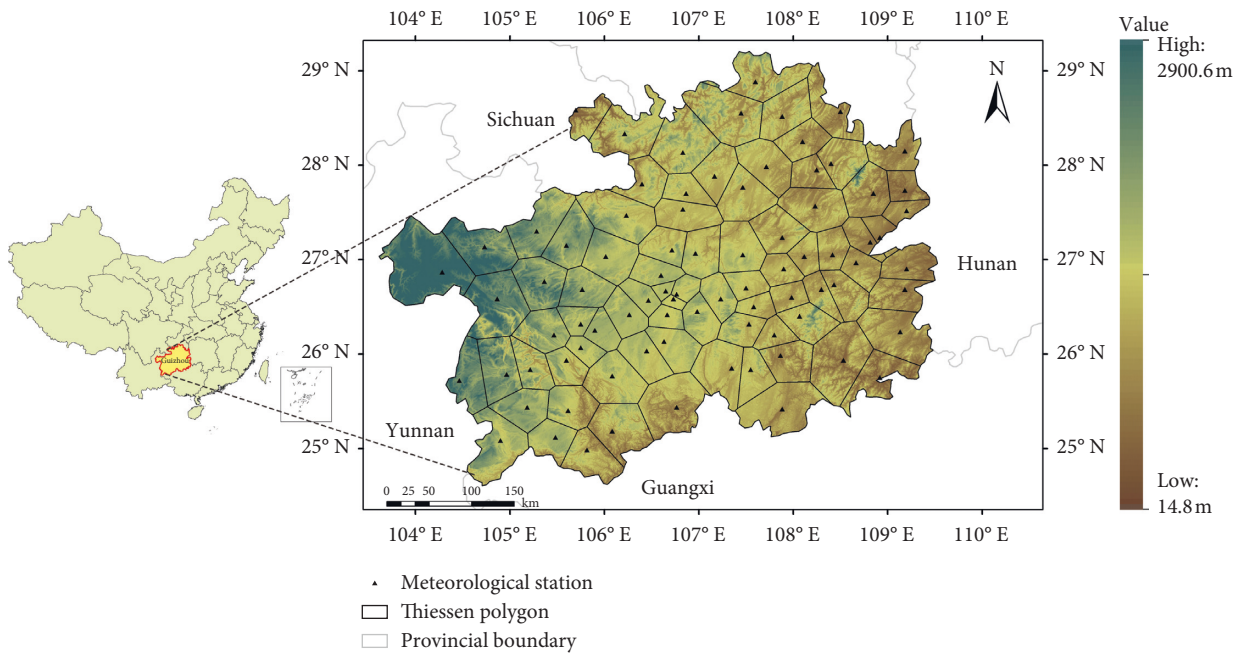

Figure 1: Location and meteorological monitoring points in Guizhou Province. Note: the figure includes the digital elevation model (DEM) data and the Thiessen polygons based on the location of the 84 weather stations.

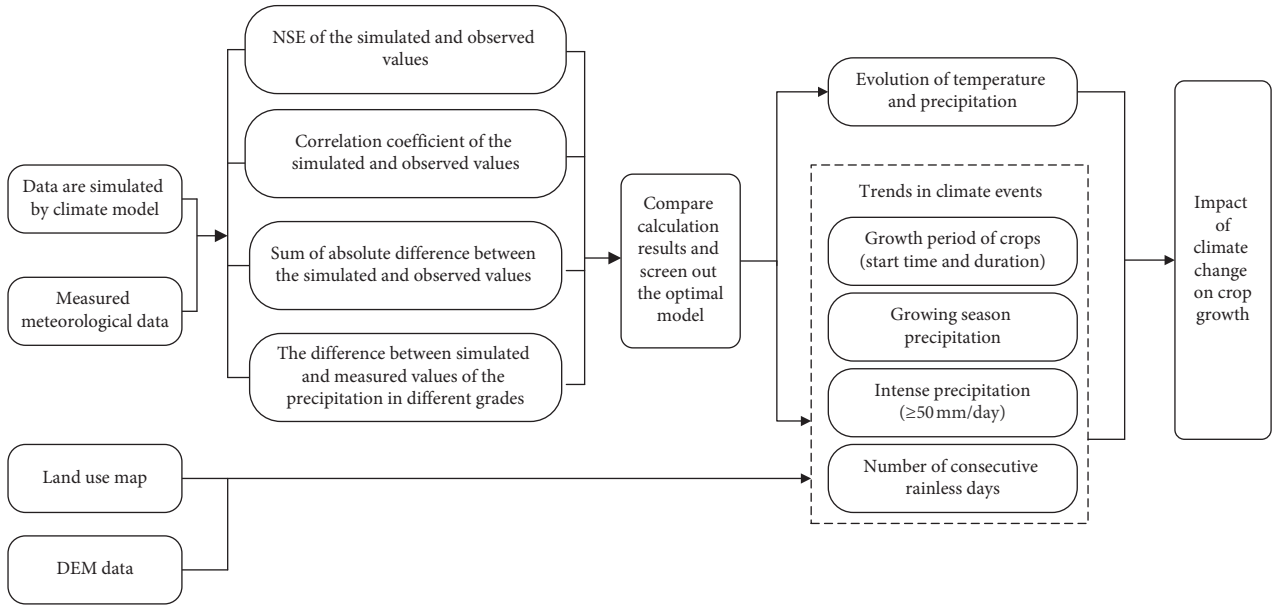

Figure 2: Technical steps for the study. Note: NSE represents the Nash–Sutcliffe efficiency coefficient.

summer maize, suitable sowing temperature ranges from 20°C to 25°C [31, 32]. When the average temperature for 5 consecutive days is within the abovementioned temperature range (20°C to 25°C) for the first time after 5 days before the ripening of winter wheat, the first day of the period is defined as the sowing day of summer maize. Table 3 shows the AT10 threshold of each stage [33]. The minimum temperature for safe seeding of japonica rice is 10°C and that of indica rice is 12°C [34, 35]. In this study, the next day when the average temperature for 5 consecutive days is finally lower than 12°C is selected as the date of rice planting [36]. AT10 thresholds of rice in different growth stages are given in Table 4 [29, 37].

3.3.2. Growing Season Precipitation. To study the effects of climate change on agriculture development in Guizhou, the precipitation changes during the crop growing season need to be clarified.

3.3.3. Intense Precipitation. Based on the daily precipitation, this study used the criteria in Table 5 to calculate the

Table 1: Details of five global climate models provided by ISIMIP.

R&D unit (country)	Name	Biogeochemical characteristics of the Earth system	External forcing factors considered in the simulation
Geophysical Fluid Dynamics Laboratory (GFDL) (USA)	GFDL-ESM2M	A (simple), LC, OBGC	GHG, SD, Oz, LU, SI, VI, SS, BC, MD, OC
Hadley Centre for Climate Prediction and Research, Met Office (UK)	HADGEM2-ES	A (complex), AC, LC, OBGC	GHG, SA, Oz, LU, SI, VI, BC, OC
L'Institut Pierre-Simon Laplace (IPSL) (France)	IPSL-CM5A-LR	A (simple), LC, OBGC	Nat, Ant, GHG, SA, Oz, LU, SS, Ds, BC, MD, OC, AA
Technology, Atmosphere and Ocean Research Institute, and National Institute for Environmental Studies (Japan)	MIROC-ESM-CHEM	A (complex), LC, OBGC	GHG, SA, Oz, LU, Sl, Vl, MD, BC, OC
Norwegian Climate Centre (Norway)	NORESM1-M	A (complex), AC	GHG, SA, Oz, S1, V1, BC, OC

Note. A: aerosol; AC: atmospheric chemistry; LC: terrestrial carbon cycle; OBGC: marine biogeochemistry; Nat: natural forcing; Ant: artificial forcing; GHG: completely mixed with greenhouse gases; SD: artificial sulphide aerosol (only direct effect); SI: a sulphide aerosol (only indirect effect); SA: a direct and indirect effect of sulphide aerosol; Oz: tropospheric and stratospheric ozone; LU: land use change; Sl: solar radiation; Vl: volcanic aerosol; SS: sea salt; Ds: dust; BC: black carbon; MD: mineral dust; OC: organic carbon; AA: artificial aerosol.

Table 2: AT10 thresholds of winter wheat at different growth stages.

Growth stage	Sowing-emergence	Emergence-tillering	Tillering-jointing	Jointing-heading	Heading-dough
AT10 (°C)	134	148	179	311	686

Table 3: AT10 thresholds of summer maize at different growth stages.

Growth stage	Sowing-emergence	Emergence-silking	Silking-dough
AT10 (°C)	158	1086	906

Table 4: AT10 thresholds of rice at different growth stages.

Growth stage	Sowing-transplanting	Transplanting-tillering	Tillering-jointing	Jointing-heading	Heading-dough
Medium japonica rice AT10 (°C)	800	384	588	557	636
Medium indica rice AT10 (°C)	810	584	494	484	590

Table 5: Precipitation grade standards.

Climatic factors	Light rain	Moderate rain	Heavy rain	Rainstorm	Heavy rainstorm	Extraordinary rainstorm
24 h precipitation (mm/day)	$S < 10$	$10 \leq S < 25$	$25 \leq S < 50$	$50 \leq S < 100$	$100 \leq S < 200$	$200 \leq S$

Note. S represents 24 h precipitation.

precipitation times in different grades and their change rate [38].

3.3.4. Number of Consecutive Rainless Days. In order to evaluate the degree of drought, this paper utilized the indicators of consecutive rainless days for analysis and calculation. The number of consecutive rainless days refers to the number of consecutive days without effective precipitation during the crop growth period. According to the Standard of Classification for Drought Severity (SL424-2008) [39], it is considered to be a rainless day when the daily precipitation is less than 3 mm in spring (from March to May), autumn (from September to November), and winter (from December to February) and when the daily precipitation is less than 5 mm in summer (from June to August) (Table 6).

3.3.5. Number of Drought-Flood Abrupt Alternation Events. According the analysis of drought-flood abrupt alternation, a drought-flood abrupt alternation event concludes longest consecutive rainless days and following intense precipitaion. The longest consecutive rainless days reach the level of moderate drought. That is, the longest consecutive rainless days are no less than 31 days in spring and autumn and no less than 21 days in summer. The first precipitation after the drought is intense precipitation (with 24 h accumulated precipitation of more than 25 mm). Figure 3 presents an intense precipitation after the summer drought [33].

3.4. Adaptive Analysis of Climate Models to Simulate Extreme Events. In order to reduce the impact of model uncertainty on the simulation of Guizhou, four indices were chosen to select the optimal plan: first is the Nash–Sutcliffe efficiency

Table 6: Consecutive rainless days: drought grade standards.

Season	Region	Number of consecutive rainless days in different drought grades (days)			
		Light drought	Moderate drought	Severe drought	Extraordinary drought
Spring (Mar–May)	North China	15~30	31~50	51~75	>75
	South China	10~20	21~45	46~60	>60
Summer (Jun–Aug)	North China	15~30	31~50	51~75	>75
	South China	10~20	21~45	46~60	>60
Autumn (Sep–Nov)	North China	10~20	21~30	31~50	>50
	South China	5~10	11~15	16~30	>30
Winter (Dec–Feb)	North China	20~30	31~60	61~80	>80
	South China	15~25	26~45	46~70	>70

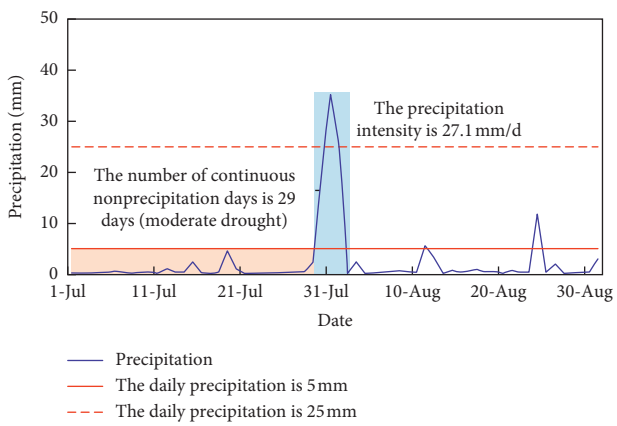

Figure 3: Drought-flood abrupt alternation event.

coefficient (NSE) of daily simulated value and measured value; second is the correlation coefficient of month simulated value and measured value; the third one is the sum of the absolute difference between the simulated value and the measured value of the annual average temperature or precipitation of each mode; and the fourth one is the proportion of precipitation amount of different grades in total precipitation amount.

$$E = 1 - \frac{\sum_{t=1}^{T}\left(Q_0^t - Q_m^t\right)^2}{\sum_{t=1}^{T}\left(Q_0^t - \bar{Q}_0\right)^2}, \quad (1)$$

where E is the value of NSE, Q_0 is the measured value, and Q_m is the value of simulation.

$$\rho_{xy} = \frac{\mathrm{Cov}(x, y)}{\sqrt{D(x)}\sqrt{D(y)}}, \quad (2)$$

where ρ_{xy} is the value of correlation coefficient, $\mathrm{Cov}(x, y)$ is the covariance of x and y, and $D(x)$ and $D(y)$ are the variances of x and y, respectively.

4. Result

4.1. Selection of Optimal Climate Model. Calculation results of four indices are presented in Tables 7–9 and Figures 4 and 5. A comparison and analysis of the four indicators has revealed that the mean of five models is the most accurate in temperature and precipitation simulation. For extreme precipitation, the simulation effect of the HadGEM2-ES model is better. Therefore, we chose the mean value of the five models to predict the future temperature and precipitation data and used the HadGEM2-ES model to predict extreme precipitation events.

4.2. Evolution of Temperature and Precipitation

4.2.1. The Variation Trend from 1961 to 2018. Figure 6 shows the evolution trend of the annual average temperature from 1961 to 2018. Figure 7 shows the evolution trend of annual precipitation from 1961 to 2018. Notably, we used linear trends and not some Mann-Kendall-like trend analysis because the linear trends could reflect the evolution trend and rate more directly. It can be seen that the temperature shows an increasing trend, with a rate of 0.14°C per 10 years. However, the precipitation shows a decreasing trend, with a rate of 15.02 mm per 10 years.

4.2.2. The Variation Trend from 2019 to 2050. Three RCPs (Representative Concentration Pathways) adopted in the IPCC's Fifth Assessment Report AR5 (RCPs 2.6, 4.5, and 8.5) were applied. For RCP4.5 scenario, the average temperature from 2019 to 2050 will go up, with a rate of 0.29°C per 10 years (Figure 8). The precipitation also shows an increasing tendency, with the rate being 27.9 mm/10 years (Figure 9). Compared with historical data, the increase rate of temperature is about 2 times that in history. The average annual precipitation in the next 30 years is lower than that in the past 60 years. The temperature increases the most in winter (Figure 10). The precipitation decreases in spring, autumn, and winter (Figure 11). In the next 30 years, annual average temperature increases from 1.36°C to 1.5°C compared with baseline period (from 1961 to 2018) (Figure 12).

4.2.3. Growth Period of Crops (Start Time and Duration). Climate change has changed the cycle length of crops [37, 40]. Studying the changes in crop growth period can provide a basis for adjusting crop types. A land use map, developed in 2014, was obtained from the Data Center for Resources and Environmental Sciences, Chinese Academy of Sciences. The spatial distribution of main crops in Guizhou was from the land use map in Geographic Information System (GIS) using the ArcMap platform (Figure 13(a)). This study chose the same precision as the climate model data and divided Guizhou Province into 65

Table 7: Comparison of simulated and measured values of temperature in Guizhou from 1961 to 2000.

Indices	GFDL-ESM2M	HadGEM2-ES	IPSL-CM5A-LR	MIROC-ESM-CHEM	NorESM1-M	Mean of 5 models
NSE	0.63	0.70	0.67	0.67	0.69	0.81
Correlation coefficient	0.82	0.85	0.84	0.84	0.84	0.90
T (°C)	23.04	20.19	23.62	26.12	22.33	17.42

Note. T represents the sum of the absolute difference between the measured value and the simulated value of the annual average temperature of each mode.

Table 8: Comparison of simulated and measured values of precipitation in Guizhou from 1961 to 2000.

Indices	GFDL-ESM2M	HadGEM2-ES	IPSL-CM5A-LR	MIROC-ESM-CHEM	NorESM1-M	Mean of 5 models
NSE	−0.67	−0.35	−0.83	−0.89	−0.44	−0.01
correlation coefficient	0.14	0.20	0.14	0.13	0.20	0.27
P (mm)	6398.98	5858.67	6854.68	7082.90	6432.12	4768.24

Note. P represents the sum of the absolute difference between the measured value and the simulated value of the annual average precipitation of each mode.

Table 9: The difference between simulated value of the precipitation of in different grades simulated by each mode and the measured precipitation from 1961 to 2000.

Prediction schemes	Light rain	Moderate rain	Heavy rain	Rainstorm	Heavy rainstorm	Extraordinary rainstorm
GFDL-ESM2M	−3.86	10.03	−0.54	−5.90	−0.20	0.30
HadGEM2-ES	3.86	2.91	−1.93	−4.71	−0.11	−0.18
IPSL-CM5A-LR	−7.44	9.14	0.43	−3.35	1.24	−0.18
MIROC-ESM-CHEM	−8.67	3.21	6.82	−1.26	−0.91	0.65
NorESM1-M	0.73	9.39	0.09	−7.70	−2.61	−0.18
Mean of 5 models	13.6	21.58	−17.60	−14.24	−3.32	−0.18

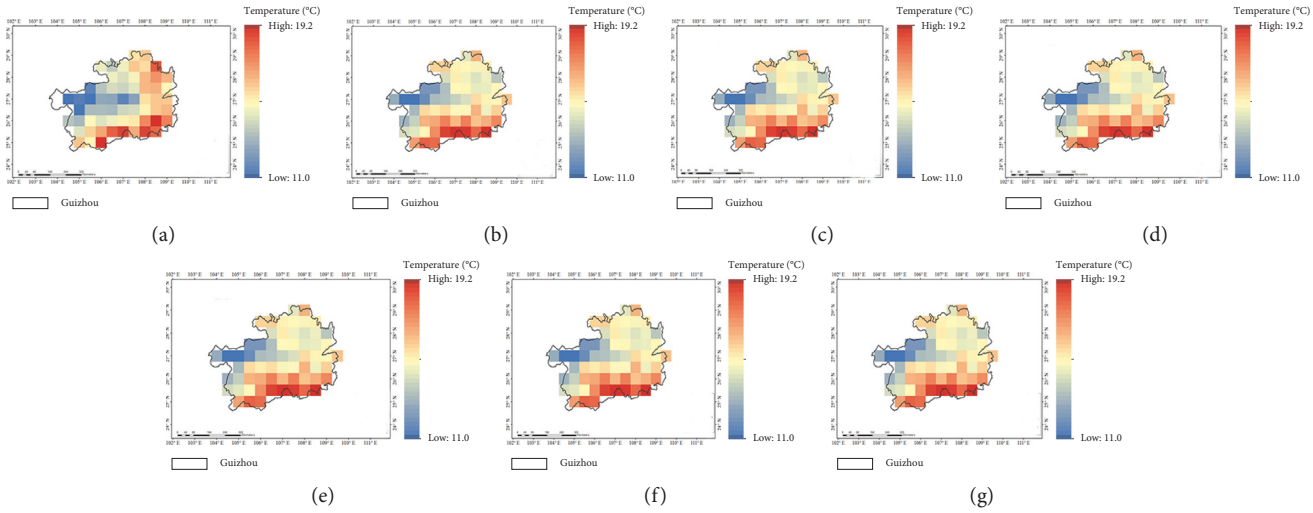

Figure 4: Spatial distribution of temperature. (a)–(g) represent measure, GFDL-ESM2M, IPSL-CM5A-LR, HadGEM2-ES, NorESM1-M, MIROC-ESM-CHEM, and the mean of the five models, respectively.

grid cells each with the size of 0.5° × 0.5° (Figure 13(b)). The main crops in Guizhou are winter wheat, summer maize, and rice. The varieties of rice mainly include single-cropping medium japonica rice and single-cropping medium indica rice [41, 42]. The spatial distribution of rice species is shown in Figure 13(c). According to the accumulated temperature, the growth period of 1961 to 2018 and 2019 to 2050 crops was analyzed. In the study, there is only one cultivar for each crop, from the past to the future.

From 1961 to 2018, the average winter wheat cycle length was 200 days. The growth period of winter wheat showed a decreasing trend with a rate of −2 days/10 years. The average summer maize cycle length was 98 days. The growth period of summer maize showed a decreasing trend with a rate of −0.9 days/10 years. The average summer maize cycle length was 141 days. The growth period of summer maize showed a decreasing trend with a rate of −1 days/10 years.

From 2019 to 2050, taking the RCP4.5 scenario as an example, the wheat sowing period will be postponed. The average crop cycle length of winter wheat, summer maize, and rice is 177 days, 94 days, and 132 days, respectively. From the spatial analysis (Figure 14(a)), the crop cycle length

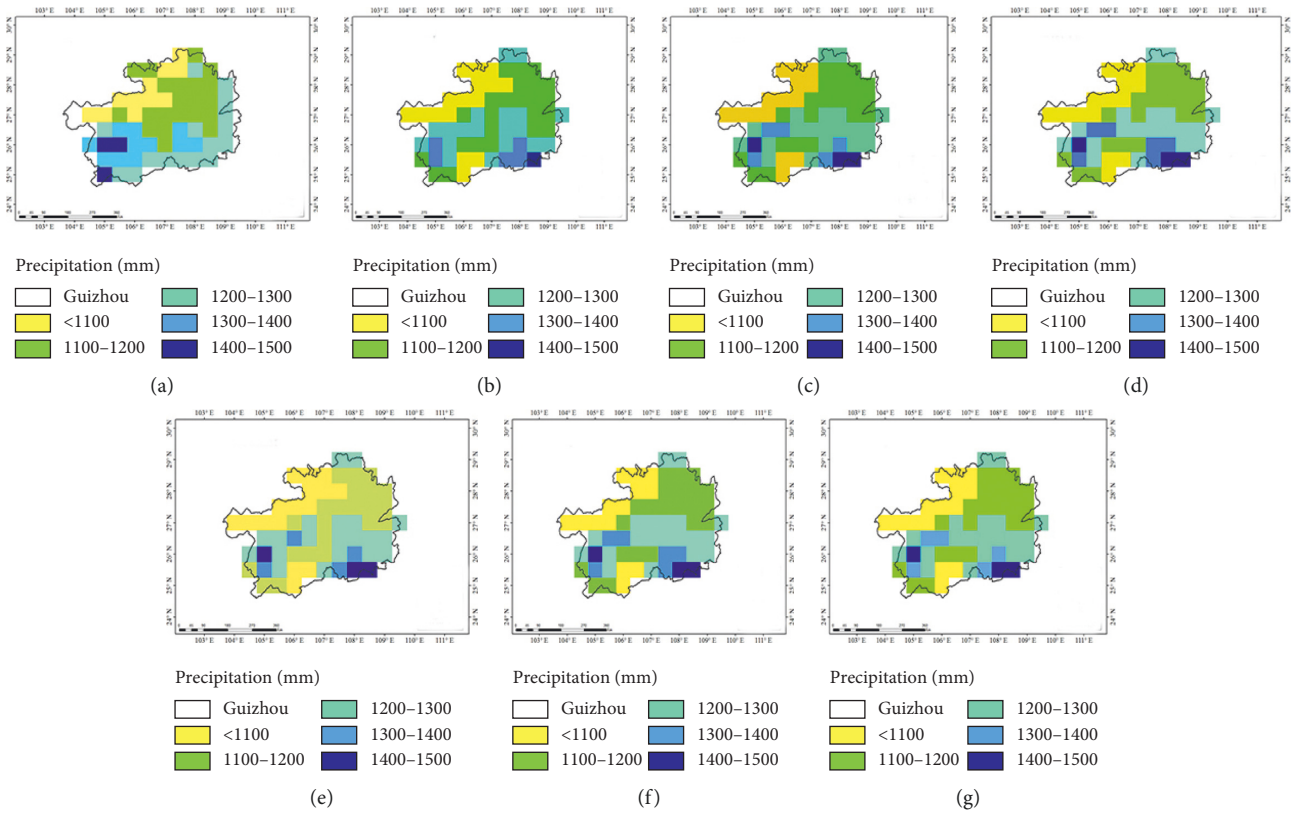

Figure 5: Spatial distribution of precipitation. (a)–(g) represent measure, GFDL-ESM2M, IPSL-CM5A-LR, HadGEM2-ES, NorESM1-M, MIROC-ESM-CHEM, and the mean of the five models, respectively.

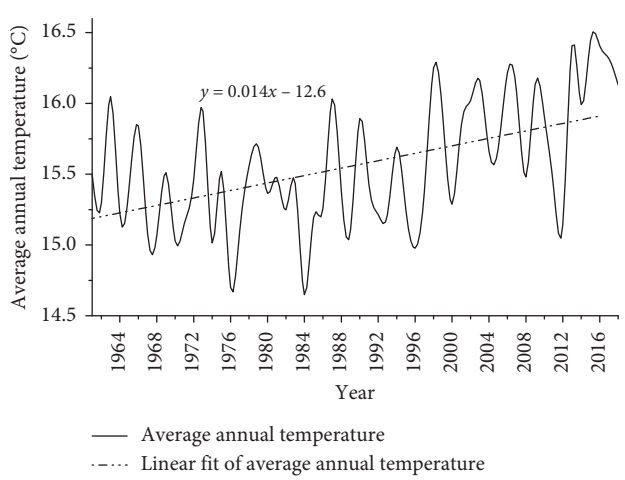

Figure 6: Evolution trends of the average annual temperature from 1961 to 2018.

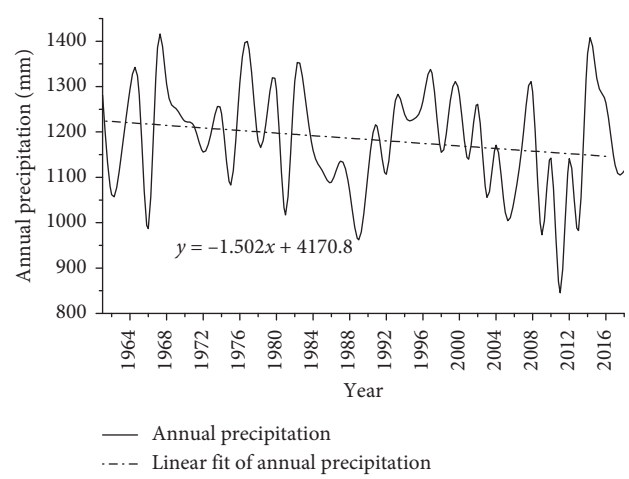

Figure 7: Evolution trends of annual precipitation from 1961 to 2018.

of winter wheat is shortened except for the southern region, with the rate of −2.1 days per 10 years. The linear tendency rate of corn planting date is small. From the spatial analysis (Figure 14(b)), the crop cycle length of summer maize is shortened in most areas of Guizhou, with the rate of −1.2 days per 10 years. The rice sowing period will be postponed in the next 30 years. From the spatial analysis (Figure 14(c)), the total number of days in rice growth period is shortened, with the rate of −1.6 days per 10 years.

4.2.4. Growing Season Precipitation. According to the calculation of the growth period of crops, the whole growth period of maize and rice is from April to September, and the growth period of wheat is from October to next April. The yield of wheat is positively correlated with the precipitation from December to March [43, 44].

For RCP4.5 scenario, the linear tendency rate of the precipitation tendency is small in the wheat growing season but large in the interannual variation (Figure 15). The

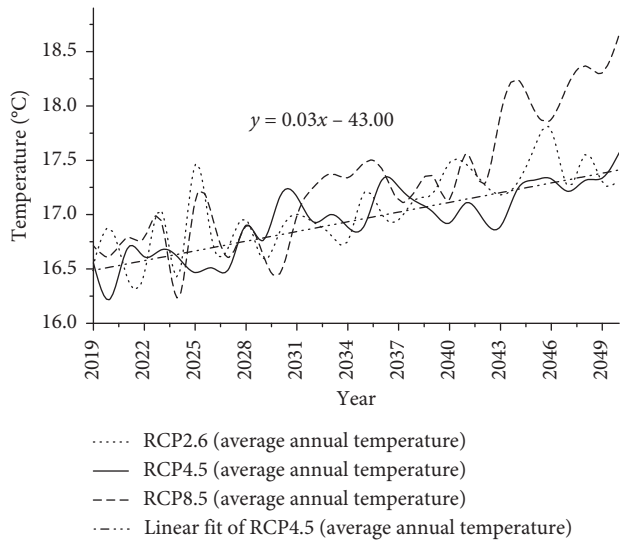

Figure 8: Evolution trends of the average annual temperature from 2019 to 2050.

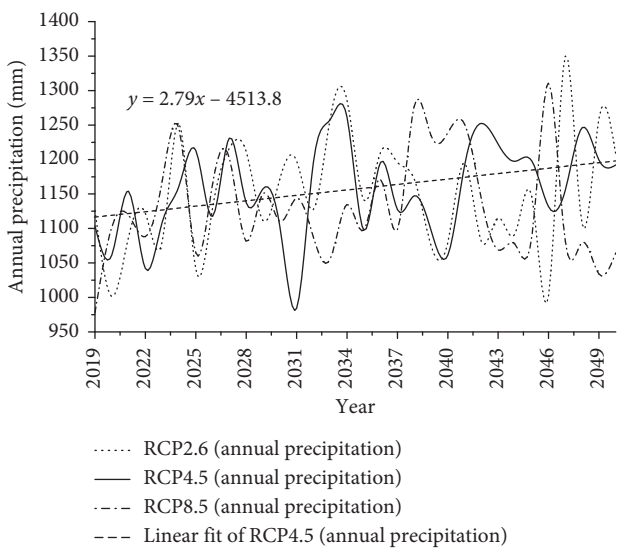

Figure 9: Evolution trends of annual precipitation from 2019 to 2050.

precipitation in the growing season of rice and corn showed an increasing trend, with a rate of 20.2 mm/10 years (Figure 16).

4.3. Trends in Extreme Events from 2019 to 2050

4.3.1. Intense Precipitation. In the next 30 years, intense precipitation (≥50 mm/day) events occur in April to October under three scenarios, with a difference in spatial distribution. For example, in the RCP4.5 scenario, extreme precipitation is mainly concentrated in the central and southeastern parts of Guizhou (Figure 17). And extreme precipitation accounts for 2.9% of total precipitation, with 1.1%, 0.56%, and 0.43% in June, July, and September, respectively.

4.3.2. Consecutive Rainless Days. Figure 18 plots the probabilities of different levels of drought in Guizhou from 2019 to 2050, and Figure 19 shows the probabilities of drought (except light drought) in different seasons from 2019 to 2050.

Drought is considered to be the most serious meteorological disaster affecting agriculture, and the drought in Guizhou Province has obvious seasonality and regionality [45]. Therefore, this paper analyzed the different levels of drought and seasonal drought in Guizhou in the next 30 years. Spring drought and summer drought are the main disaster-causing factors for rice and corn. Autumn and spring droughts are the main hazard factors for wheat and rapeseed [46]. This study mainly analyzed the probability of drought in spring, summer, and autumn.

Under the RCP4.5 scenario, in the next 30 years, the occurrence probability of drought in western Guizhou is higher than that in eastern Guizhou. In eastern Guizhou, drought is frequent in summer, while much less in spring and autumn. A number of droughts (except light drought) might occur most in the summer followed by spring. Therefore, the greatest impact on agriculture in the next 30 years is summer drought, followed by spring drought. Frequent drought events will increase the irrigation water demand and augment the pressure on freshwater resources.

4.3.3. Drought-Flood Abrupt Alternation Events. Soil fertility, rice growth period, physiological characteristics, and others will be affected by drought-flood abrupt alternation events, and the latter results in large reduction of production [47]. Figure 20 shows spatial distribution of drought-flood abrupt alternation events in Guizhou.

Low incidence of drought-flood abrupt alternation events is present in the RCP4.5 scenario, but each event has the longest drought duration with severe disasters. In the RCP4.5 scenario, drought-flood alternation change events might occur in spring, summer, and autumn.

5. Discussion

5.1. Effect of Normal Climatic Factors on Crop Growth. In Guizhou, the whole climate is getting warmer. Compared with historical data, the increase rate of temperature based on model projections is about 2 times that in history.

The temperature increase can lead to the northward shifting of suitable cropping areas of rice, maize, and wheat [48]. In the past 30 years, the north boundary of the double cropping rice growing area in southern China has been pushed northward for nearly 300 km [49]. Growth period is advanced and shortened [50]. The decomposition of soil organic matter is accelerated, and the soil fertility is reduced [51, 52]. It may also expand the activity scope of some pests subjected to temperature restrictions, further shorten the growth period of most pests, and increase the number of reproductive generations [53]. In the next 30 years, annual average temperature may increase from 1.36°C to 1.5°C compared with baseline period (from 1961 to 2018). It may change the suitable cropping areas in Guizhou and increase

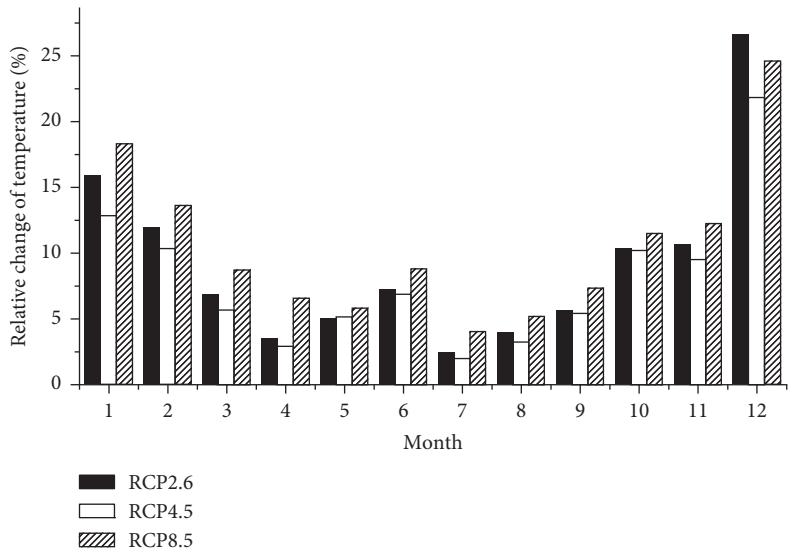

Figure 10: Relative changes of monthly average temperature between 2019–2050 and 1961–2018.

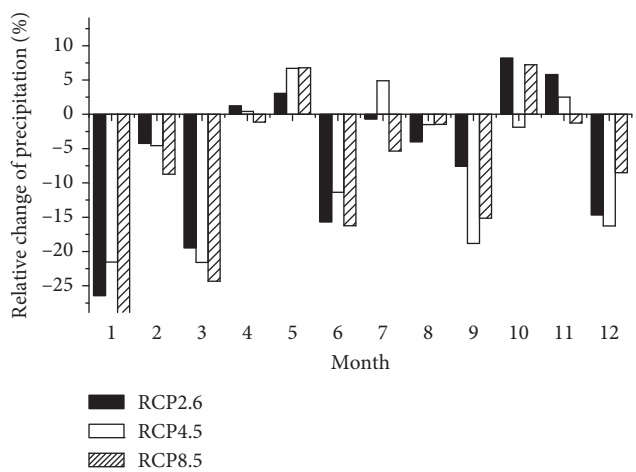

Figure 11: Relative change of monthly average precipitation between 2019–2050 and 1961–2018.

pests and diseases. Ao [54] also obtained this conclusion when she studied the Liupanshui area in Guizhou. It may also reduce crop yield while increasing utilization of fertilizers and pesticides, which will pollute the environment and water resources.

From 2019 to 2050, under RCP4.5 scenario, the sowing period of winter wheat and rice tends to be postponed. The duration of maize and rice's growth period will be shortened, and the life cycle of wheat also emerges as having a decreasing tendency except for those from the southern region. The average crop cycle length of winter wheat, summer maize, and rice was shortened by 23 days, 4 days, and 9 days, respectively, compared with the mean value of 1961 to 2018. Meanwhile, the rate of shortening of crop cycle length is faster than the value of 1961 to 2018. Changes in food quality are to be expected, e.g., decreased protein and mineral nutrient concentrations, as well as altered lipid composition [55]. The linear tendency rate of the precipitation tendency is small in the wheat growing season but large in the interannual variation, which increases the uncertainty of the irrigation amount of water resources. While most parts of Guizhou are rain-fed agricultural areas, the yield of wheat is positively correlated with the precipitation. Thus, the adverse effects will affect the wheat growth.

5.2. Effect of Extreme Events on Crop Growth. Extreme precipitation can affect soil fertility, and storm floods can cause sudden increase in diseases [56, 57]. The main stage of rice tillering in Guizhou is in June, which is the key period for rice growing [43]. Extreme precipitation in the next 30 years is mainly concentrated in June and July, which will increase the incidence of diseases. This phenomenon is more evident in central and southeastern Guizhou. In the future, the rice planting layout can be adjusted according to the distribution of extreme precipitation.

Rapeseed is also one of the crops in Guizhou. It blooms in March and matures in the end of April and early May. From the spatial distribution of extreme precipitation, it can

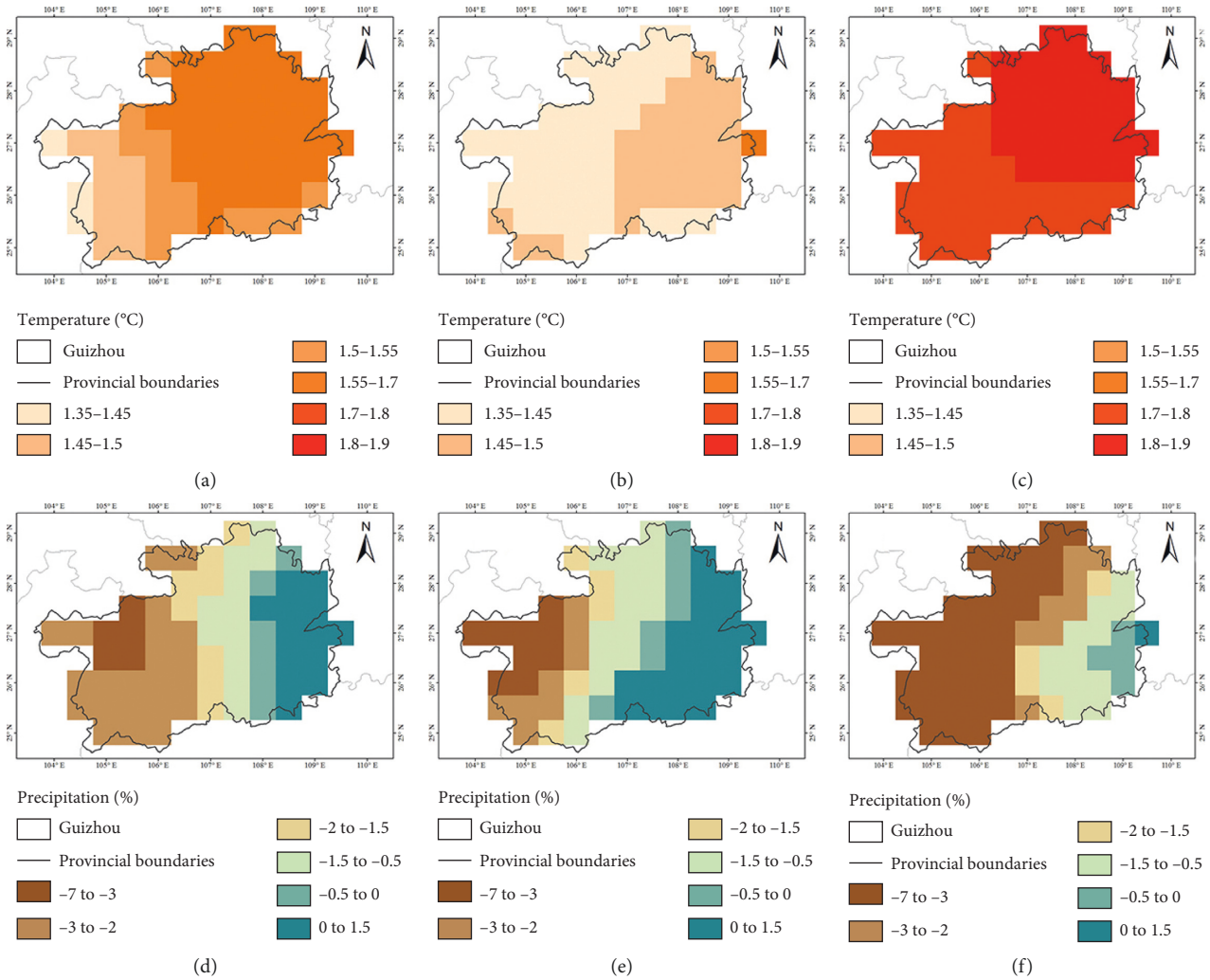

Figure 12: Change of annual average temperature and annual precipitation from 2019 to 2050 compared with the baseline period in Guizhou. (a) RCP2.6. (b) RCP4.5. (c) RCP8.5.

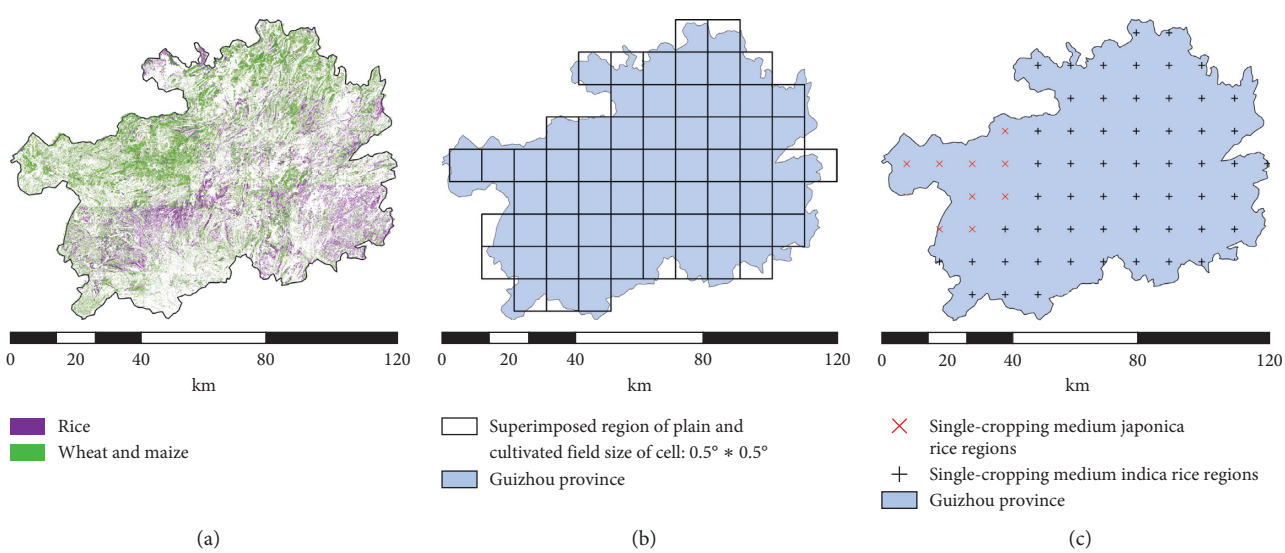

Figure 13: Cultivated field and grid map of superimposed area in Guizhou.

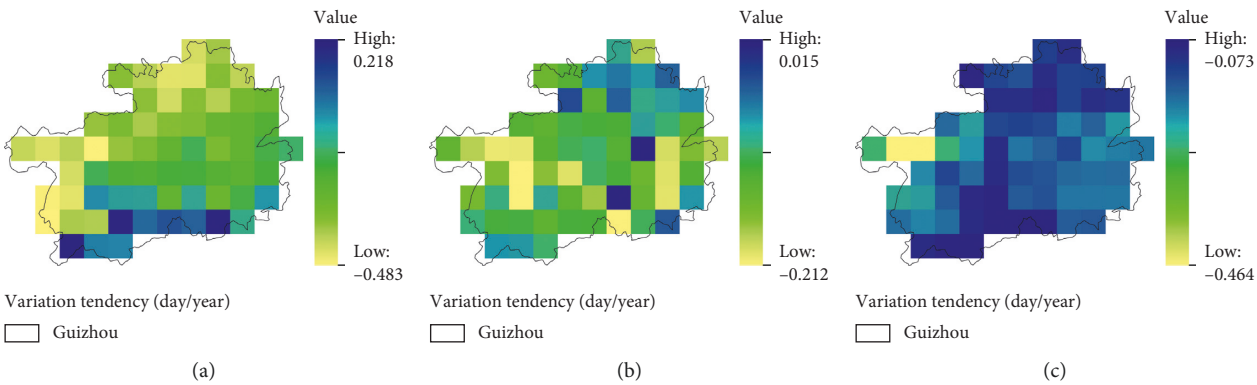

Figure 14: Distribution of the change rate of total days in crop growth period: (a) winter wheat, (b) summer maize, and (c) rice.

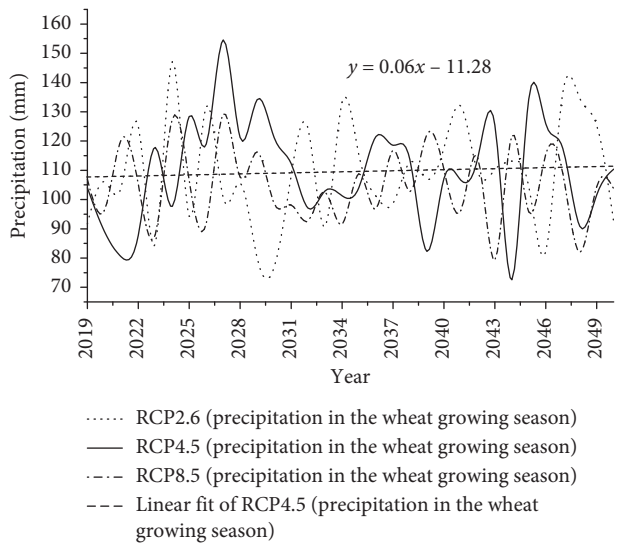

Figure 15: Precipitation trends during the wheat growing season (December to March) from 2019 to 2050.

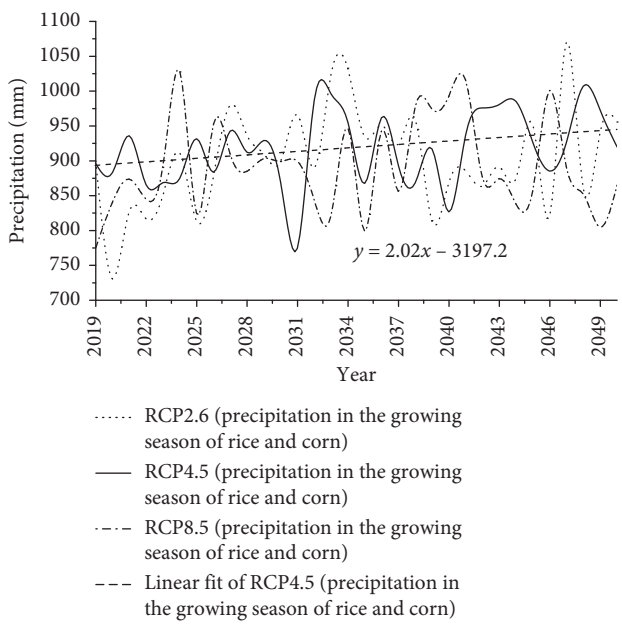

Figure 16: Precipitation trends during the growing season of rice and corn (April to September) from 2019 to 2050.

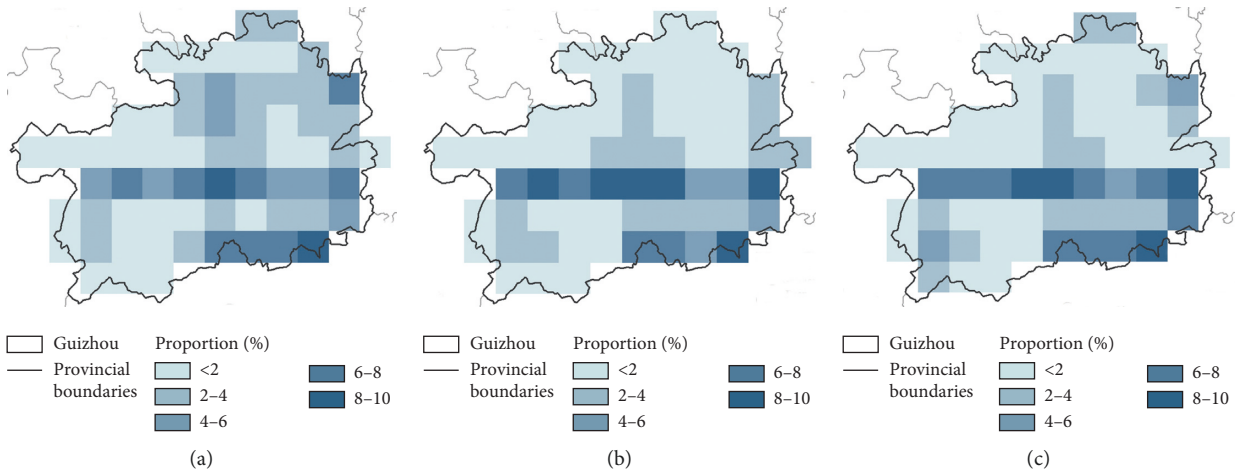

Figure 17: Spatial distribution of the proportion of extreme precipitation to total precipitation. (a) RCP2.6. (b) RCP4.5. (c) RCP8.5.

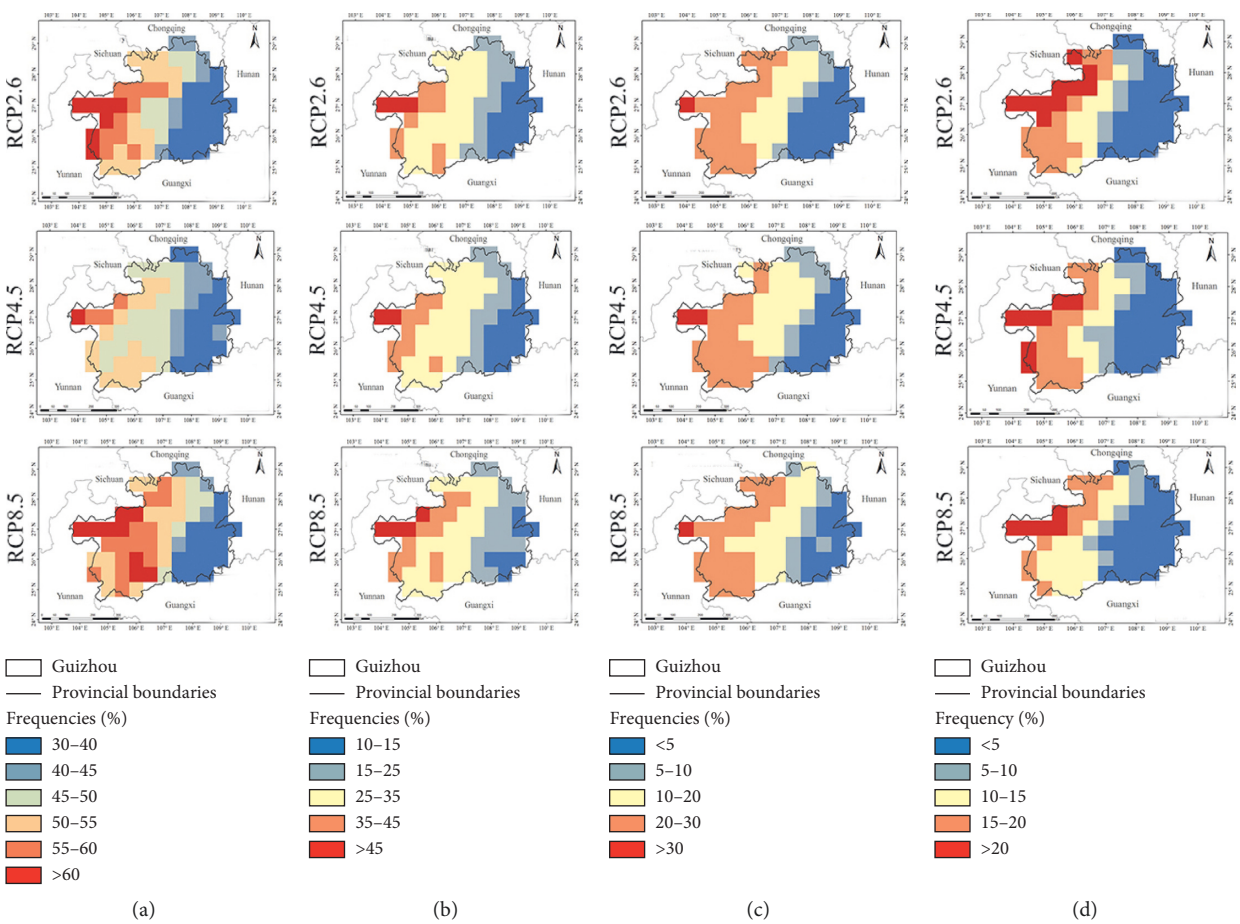

Figure 18: The probabilities of different levels of drought in Guizhou from 2019 to 2050. (a) Light drought. (b) Moderate drought. (c) Severe drought. (d) Extraordinary drought.

be explored that the occurrence probability of extreme precipitation is relatively high in the two major rapeseed producing areas, Buyei and Miao Autonomous Prefecture of QianNan and Guiyang. In April, extreme precipitation accounted for 0.16% of the annual precipitation.

Drought is considered to be the most serious meteorological disaster affecting agriculture. Under the RCP4.5 scenario, in the next 30 years, a number of droughts (except light drought) might occur most in the summer followed by spring. Therefore, the greatest impact on agriculture in the

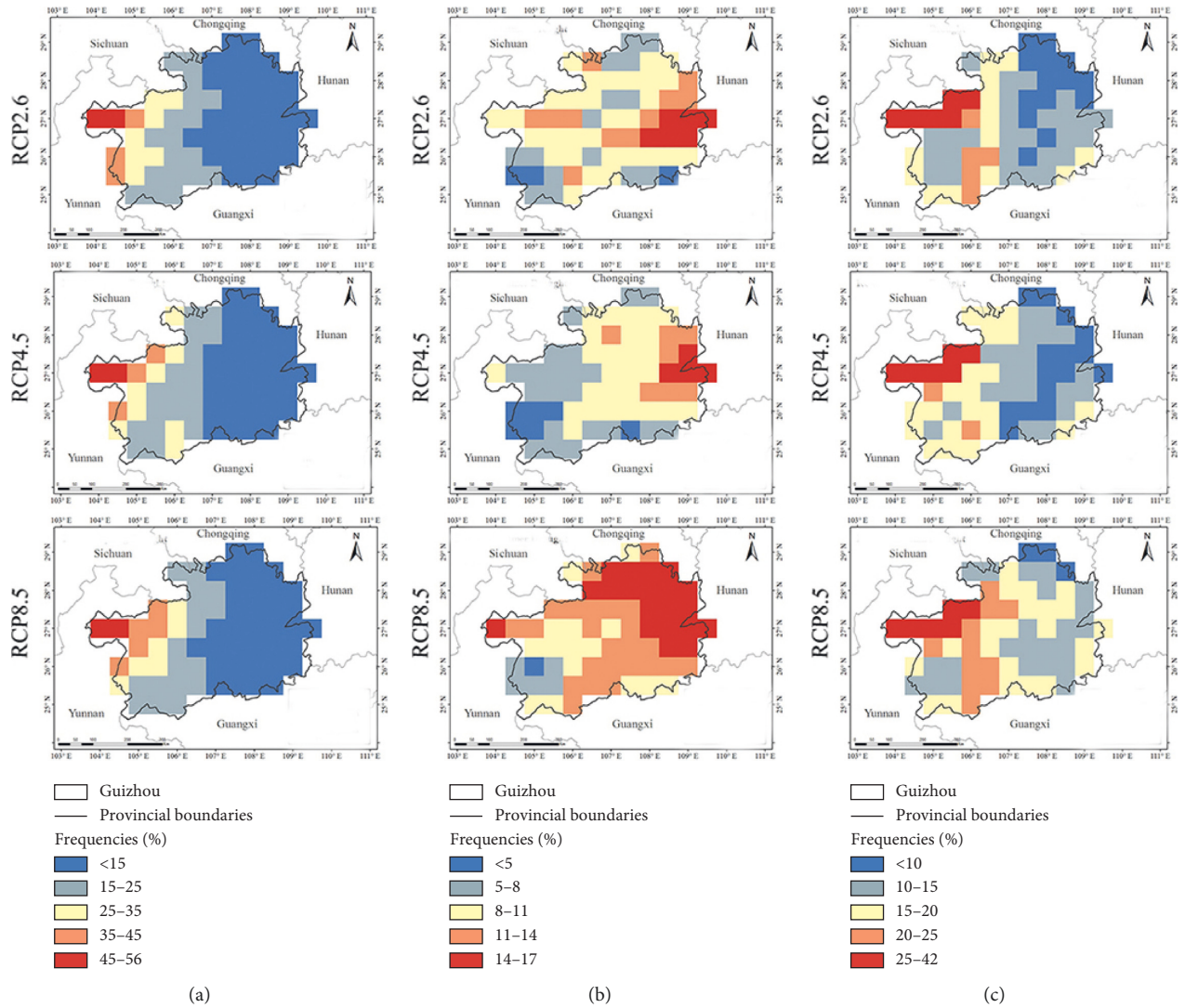

Figure 19: The probabilities of drought (except mild drought) in different seasons from 2019 to 2050. (a) Spring. (b) Summer. (c) Autumn.

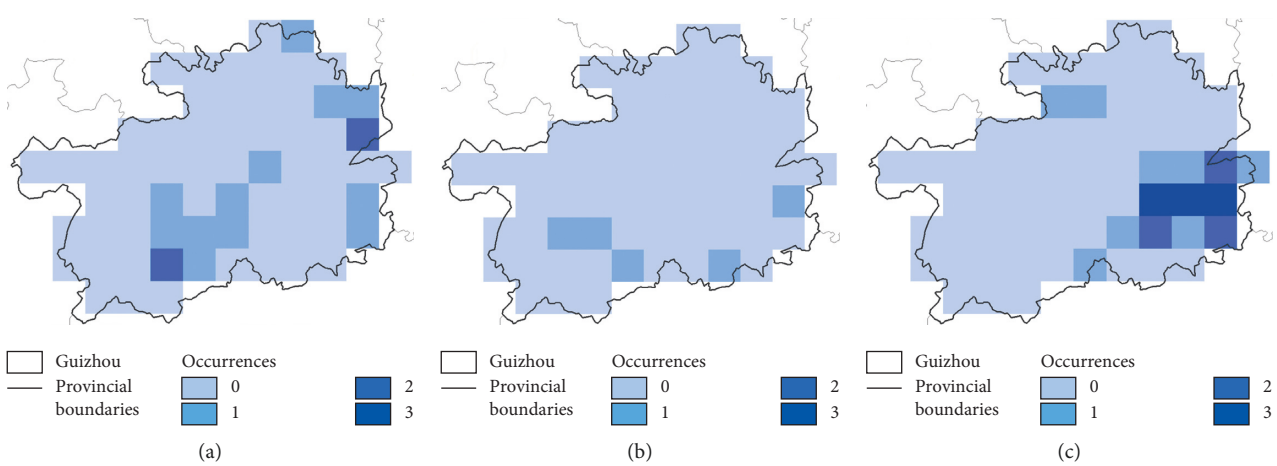

Figure 20: Spatial distribution of the frequency of drought-flood abrupt alternation events in Guizhou from 2019 to 2050. (a) RCP2.6. (b) RCP4.5. (c) RCP8.5.

next 30 years is summer drought, followed by spring drought. Frequent drought events will increase the irrigation water demand and augment the pressure on freshwater resources. In the RCP4.5 scenario, drought-flood abrupt alternation events might occur in spring, summer, and autumn, which will seriously affect soil quality and increase fertilizers.

6. Conclusions

(1) From 1961 to 2018, the temperature showed an increasing trend, with a rate of 0.14°C per 10 years. The precipitation showed a decreasing trend, with a rate of −15.02 mm per 10 years. Compared with historical data, under RCP4.5 scenario, the increase rate of temperature is about 2 times that in history.

(2) The growth period of crops has been influenced by climate change. The average crop cycle length of winter wheat, summer maize, and rice was shortened by 23 days, 4 days, and 9 days, respectively, compared with the mean value of 1961–2018. The sowing period of wheat and rice will be postponed in the next 30 years. The winter wheat cycle length is shortened except for the southern region, with the rate from −4.83 to 2.18 (days/10 years). The life cycle of corn also emerges as having a decreasing tendency in most areas of Guizhou, with the rate from −2.12 to 0.15 (days/10 years). The rice sowing period will be postponed in the next 30 years. The rice cycle length is shortened, with the rate from −4.65 to −0.07 (days/10 years). In the next 30 years. The precipitation tendency is low in the wheat growing season but large in the interannual variation, which increases the uncertainty of the irrigation amount of water resources. The precipitation in the growing season of rice and corn shows an increasing trend, with a rate of 16.6 mm/10 years.

(3) In the next 30 years, intense precipitation (≥50 mm/day) events might occur during April to October under three scenarios. Under the RCP4.5 scenario, extreme precipitation is mainly concentrated in the central and southeastern parts of Guizhou. And extreme precipitation accounts for 2.9% of total precipitation, 1.1% in June. The occurrence probability of extreme precipitation is relatively high in the two major rapeseed producing areas, Buyei and Miao Autonomous Prefecture of QianNan and Guiyang.

(4) Under the RCP4.5 scenario, in the next 30 years, the occurrence probability of drought in western Guizhou is higher than that in eastern Guizhou. In eastern Guizhou, drought is frequent in summer, while much less in spring and autumn. A number of droughts (except mild drought) might occur most in the summer followed by spring. Therefore, the greatest impact on agriculture in the next 30 years is summer drought, followed by spring drought. In the RCP4.5 scenario, drought-flood abrupt alternation events might occur in spring, summer, and autumn, which will seriously affect soil quality and increase fertilizers.

Data Availability

The data used to support the findings of this study are available from the corresponding author upon request.

Conflicts of Interest

The authors declare that there are no conflicts of interests regarding the publication of this article.

Acknowledgments

This research was supported by the National Key Research and Development Project (no. 2016YFA0601503), the Chinese National Natural Science Foundation (no. 51725905), the Research Fund of the State Key Laboratory of Simulation and Regulation of Water Cycle in River Basin (no. SKL2018TS02), and the Science and Technology Project in Guizhou Province (SY (2014) no. 3066). The authors would like to thank the Guizhou Climate Center for providing the basic data and full support during this study.

References

[1] J. H. Kotir, "Climate change and variability in Sub-Saharan Africa: a review of current and future trends and impacts on agriculture and food security," *Environment, Development and Sustainability*, vol. 13, no. 3, pp. 587–605, 2011.

[2] J.-M. Montaud, N. Pecastaing, and M. Tankari, "Potential socio-economic implications of future climate change and variability for Nigerien agriculture: a countrywide dynamic CGE-Microsimulation analysis," *Economic Modelling*, vol. 63, pp. 128–142, 2017.

[3] IPCC, *Working Group I Contribution to the IPCC Fifth Assessment Report Climate Change 2013: The Physical Science Basis: Headline Statements from the Summary for Policymakers*, Cambridge University Press, Cambridge, UK, 2014.

[4] S. Shankar and Shikha, "Chapter 7—impacts of climate change on agriculture and food security," in *Biotechnology for Sustainable Agriculture: Emerging Approaches and Strategies*, R. L. Singh and S. Mondal, Eds., pp. 207–234, Woodhead Publishing, Sawston, UK, 2018.

[5] S. Isoard, *Perspectives on Adaptation to Climate Change in Europe*, Springer, Dordrecht, The Netherlands, 2011.

[6] V. Karimi, E. Karami, and M. Keshavarz, "Climate change and agriculture: impacts and adaptive responses in Iran," *Journal of Integrative Agriculture*, vol. 17, no. 1, pp. 1–15, 2018.

[7] S. Jamshidi, S. Zand-parsa1, M. Pakparvar, and D. Niyogi, "Evaluation of evapotranspiration over a semi-arid region using multi-resolution data sources," *Journal of Hydrometeorology*, vol. 20, no. 5, pp. 1–50, 2015.

[8] M. A. Martins, J. Tomasella, and C. G. Dias, "Maize yield under a changing climate in the Brazilian Northeast: impacts and adaptation," *Agricultural Water Management*, vol. 216, pp. 339–350, 2019.

[9] J. R. Porter and M. A. Semenov, "Crop responses to climatic variation," *Philosophical Transactions of the Royal Society B: Biological Sciences*, vol. 360, no. 1463, pp. 2021–2035, 2005.

[10] W. N. Smith, B. B. Grant, R. L. Desjardins et al., "Assessing the effects of climate change on crop production and GHG emissions in Canada," *Agriculture, Ecosystems & Environment*, vol. 179, no. 5, pp. 139–150, 2013.

[11] R. Ortiz, K. D. Sayre, B. Govaerts et al., "Climate change: can wheat beat the heat?," *Agriculture, Ecosystems & Environment*, vol. 126, no. 1-2, pp. 46–58, 2008.

[12] A. Bhattacharya, *Changing Climate and Resource Use Efficiency in Plants*, Academic Press, Cambridge, MA, USA, 2019.

[13] D. Bocchiola, L. Brunetti, A. Soncini, F. Polinelli, and M. Gianinetto, "Impact of climate change on agricultural productivity and food security in the Himalayas: a case study in Nepal," *Agricultural Systems*, vol. 171, pp. 113–125, 2019.

[14] CMA, *China Blue Book on Climate Change*, Science Press, Beijing, China, 2018.

[15] R.-l. Li and S. Geng, "Impacts of climate change on agriculture and adaptive strategies in China," *Journal of Integrative Agriculture*, vol. 12, no. 8, pp. 1402–1408, 2013.

[16] F. Tao, Z. Zhang, S. Zhang, Z. Zhu, and W. Shi, "Response of crop yields to climate trends since 1980 in China," *Climate Research*, vol. 54, no. 3, pp. 233–247, 2012.

[17] Z. Lv, X. Liu, W. Cao, and Y. Zhu, "Climate change impacts on regional winter wheat production in main wheat production regions of China," *Agricultural and Forest Meteorology*, vol. 171-172, pp. 234–248, 2013.

[18] T. Dai, J. Wang, D. He, and N. Wang, "Impact simulation of climate change on potential and rainfed yields of winter wheat in Southwest China from 1961 to 2010," *Chinese Journal of Eco-Agriculture*, vol. 24, no. 3, pp. 293–305, 2016.

[19] NBS Statistical Communique of the National Economic and Social Development of Guizhou Province, 2017, http://www.gzgov.gov.cn/zfsj/tjgb/201805/P020180528542634287622.pdf.

[20] D. Zheng, W. Fang, R. Ruan et al., "Diversity of agro-biological resources in Guizhou province," *Journal of Plant Genetic Resources*, vol. 18, no. 2, pp. 367–371, 2017.

[21] L. Liu, J. Wu, and Y. Xu, "Study on the relationship between wheat growth and solar energy resources in Guizhou," *Journal of Guizhou Meteorology*, vol. 5, pp. 8–12, 2003.

[22] X. Chen, H. Lei, J. Xu et al., "Spatial and temporal distribution characteristics of drought during crop growth period in Guizhou province from climate change perspectives," *Journal of Natural Resources*, vol. 30, no. 10, pp. 1735–1749, 2015.

[23] L. Warszawski, K. Frieler, V. Huber, F. Piontek, O. Serdeczny, and J. Schewe, "The inter-sectoral impact model intercomparison Project (ISI-MIP): project framework," *Proceedings of the National Academy of Sciences*, vol. 111, no. 9, pp. 3228–3232, 2013.

[24] C. Piani, G. P. Weedon, M. Best et al., "Statistical bias correction of global simulated daily precipitation and temperature for the application of hydrological models," *Journal of Hydrology*, vol. 395, no. 3-4, pp. 199–215, 2010.

[25] S. Hagemann, C. Chen, J. O. Haerter et al., "Impact of a statistical bias correction on the projected hydrological changes obtained from three GCMs and two hydrology models," *Journal of Hydrometeorology*, vol. 12, no. 4, pp. 556–578, 2011.

[26] Z. Zhao, Y. Luo, and J. Huang, "The detection of the CMIP5 climate model to see the development of CMIP6 earth system models," *Climate Change Research*, vol. 14, no. 6, pp. 643–648, 2018.

[27] B. D. Santer, J. C. Fyfe, G. Pallotta et al., "Causes of differences in model and satellite tropospheric warming rates," *Nature Geoscience*, vol. 10, no. 7, pp. 478–485, 2017.

[28] Y. Wu and R. Wang, *Practical Techniques for Wheat Cultivation*, China Agricultural Science and Technology Press, Beijing, China, 2014.

[29] Q. Lu and L. Wang, "Accumulated temperature of the main varieties of rice, cotton and cotton in China," *Acta Agronomica Sinica*, vol. 4, no. 2, pp. 157–170, 1965.

[30] Z. Yuan, D. Yan, Z. Yang, J. Yin, P. Breach, and D. Wang, "Impacts of climate change on winter wheat water requirement in Haihe River Basin," *Mitigation and Adaptation Strategies for Global Change*, vol. 21, no. 5, pp. 677–697, 2016.

[31] X. Xi, Z. Guo, X. Hai et al., *High-yield Cultivation Techniques for Maize*, China Agricultural Science and Technology Press, Beijing, China, 2017.

[32] X. Wang, *Corn Cultivation Technology*, Northeastern University Press, Shenyang, China, 2014.

[33] Z. Yuan, "Drought risk assessment and its coping strategies under changing environments: a case study in Luanhe River Basin," Ph. D. thesis, China Institute of Water Resource and Hydropower Research, Beijing, China, 2016.

[34] Y. Zhang, "Planting upper limit and temperature conditions of different climate ecotype rice varieties in China," *Resources Science*, vol. 5, no. 2, pp. 65–72, 1983.

[35] Q. Yu, P. Lu, J. Liu et al., "Crop photo 2 temperature productivity model and numerical analysis of suitable growth season of rice in southern China," *Journal of Natural Resources*, vol. 14, no. 2, pp. 163–168, 1999.

[36] Y. Yang, *High-yield Cultivation Techniques for Rice*, China Agricultural Science and Technology Press, Beijing, China, 2017.

[37] Q. Ao, X. Gu, Y. Yao et al., "Yixiangyou1108': growth and yield under temperatures of different sowing dates," *ChineseAgricultural Science Bulletin*, vol. 32, no. 36, pp. 11–15, 2016.

[38] J. Xiao, B. Mu, and F. Hu, *Agrometeorology*, Vol. 2, Higher Education Press, Beijing, China, 2009.

[39] Ministry of Water Resources, *Standard of Classification for Drought Severity (SL424–2008)*, Ministry of Water Resources, Beijing, China, 2008.

[40] Y. Liu, Q. Chen, Q. Ge et al., "Modelling the impacts of climate change and crop management on phenological trends of spring and winter wheat in China," *Agricultural & Forest Meteorology*, vol. 248, pp. 518–526, 2018.

[41] J. Wu, "Guizhou major rice cultivation climate type area and variety distribution," *Rural Economy and Technology*, vol. 4, p. 41, 2002.

[42] J. Duan and G. Zhou, "Climatic suitability of double rice planting regions in China," *Scientia Agricultura Sinica*, vol. 45, no. 2, pp. 218–227, 2012.

[43] X. Gao, J. Xu, S. Yang et al., "Water requirement pattern and crop coefficient of main crops in Guizhou province," *China Rural Water and Hydropower*, vol. 1, pp. 11–19, 2015.

[44] S. Zhong, "Analysis of the relationship between meteorological factors and wheat yield in bijie," *Tillage and Cultivation*, vol. 1, no. 1, pp. 8–10, 1996.

[45] Y. Feng, N. B. Cui, Y. Xu, Z. P. Zhang, and J. P. Wang, "Temporal and spatial distribution characteristics of meteorological drought in Guizhou Province," *Journal of Arid Land Resources and Environment*, vol. 29, no. 8, pp. 82–86, 2015.

[46] J. Liao, Y. Su, Z. Feng et al., "Analysis on the effects of agricultural natural disasters on the agricultural economy in Guizhou in the past 54 years," *Journal of Anhui Agricultural Sciences*, vol. 25, pp. 11114–11117, 2008.

[47] X. Cheng, "Research on rice response regularity and water production function under drought-floods abrupt alternation

condition," Ph. D. thesis, Wuhan University, Wuhan, China, 2017.

[48] L. Xu and J.-j. Liu, "Climate change and issues of Chinese agricultural development," *Acta Agriculturae Zhejiangensis*, vol. 25, no. 1, pp. 192–199, 2013.

[49] Y. Song, B. Liu, and H. Zhong, "Impact of global warming on the rice cultivable area in southern China in 1961–2009," *Progressus Inquisitiones DE Mutatione Climatis*, vol. 7, no. 4, p. 259, 2011.

[50] Y. Liu and F. Tao, "Probabilistic change of wheat productivity and water use in China for global mean temperature changes of 1°, 2°, and 3°C," *Journal of Applied Meteorology and Climatology*, vol. 52, no. 1, pp. 114–129, 2013.

[51] D. Li, J. Fan, X. Zhang et al., "Hydrolase kinetics to detect temperature-related changes in the rates of soil organic matter decomposition," *European Journal of Soil Biology*, vol. 81, pp. 108–115, 2017.

[52] G. Ondrasek, H. Bakić Begić, M. Zovko et al., "Biogeochemistry of soil organic matter in agroecosystems & environmental implications," *Science of The Total Environment*, vol. 658, pp. 1559–1573, 2019.

[53] P. P. Reddy, *Climate Resilient Agriculture for Ensuring Food Security*, Springer, Delhi, India, 2015.

[54] X.-H. Ao, "Impact and adaptive strategies of climate change on agriculture in karst areas: a case study of Liupanshui city in western Guizhou," *Journal of Guiyang University*, vol. 11, no. 1, pp. 58–62, 2016.

[55] F. M. DaMatta, A. Grandis, B. C. Arenque, and M. S. Buckeridge, "Impacts of climate changes on crop physiology and food quality," *Food Research International*, vol. 43, no. 7, pp. 1814–1823, 2010.

[56] C. Gao, J. Zhu, J. Zhu et al., "Effect of extreme rainfall on the export of nutrients from agricultural land," *Acta Geographica Sinica*, vol. 6, pp. 113–119, 2005.

[57] Z.-g. Huo, M.-s. Li, L. Wang, J.-j. Xiao, D-p. Huang, and C.-y. Wang, "Impacts of precipitation variations on crop diseases and pests in China," *Scientia Agricultura Sinica*, vol. 45, no. 10, pp. 1935–1945, 2012.

Hindawi
Advances in Meteorology
Volume 2019, Article ID 4702139, 14 pages
https://doi.org/10.1155/2019/4702139

Research Article

Development of Downscaled Climate Projections: A Case Study of the Red River Basin, South-Central U.S.

Darrian Bertrand [1] **and Renee A. McPherson** [1,2]

[1] *Department of Geography and Environmental Sustainability, University of Oklahoma, Norman 73019, USA*
[2] *South Central Climate Adaptation Science Center, Norman 73019, USA*

Correspondence should be addressed to Darrian Bertrand; dmbertra@ncsu.edu

Received 1 March 2019; Revised 27 May 2019; Accepted 5 September 2019; Published 22 October 2019

Guest Editor: Jayant K. Routray

Climate models provide information that resource managers, policy makers, and researchers can use when planning for the future. While this information is valuable in the broad sense, the low spatial-resolution often lacks local details that resource managers and decision makers need to plan for their communities. Therefore, statistically downscaled climate projections provide a high-resolution output and offer local information that is more beneficial than coarse-resolution global climate model output. In the Red River Basin, located in the south-central U.S., this detailed information is used to develop long-term water plans. This area is prone to drought conditions and heavy precipitation events, and studies have consistently estimated that this will continue in the future. This paper introduces a dataset of statistically downscaled climate projections of daily minimum and maximum temperature and daily precipitation that is a useful tool for studies regarding climatological and hydrological aspects in the region. The dataset was created using two quantile mapping techniques to downscale the CCSM4, MPI-ESM-LR, and MIROC5 model outputs to a 0.1-degree spatial resolution. Furthermore, we describe the added value of coproduction of knowledge between climate scientists and end users, or in this case impacts modelers and decision makers, for creating climate projections that can be used for climate risk assessments. A case study of the data's development and application is provided, detecting the mean daily changes in temperature and precipitation through the end of the century in the Red River Basin for two representative concentration pathways. After applying the users' inputs to develop the datasets, results for this example estimate an increase in mean daily precipitation in the eastern portion of the basin and as much as a 15% decline in the west by the end of the century. Furthermore, mean daily temperature is expected to rise across the entire basin in all scenarios by up to 6–7°C.

1. Introduction

As the global climate changes, numerical projections from climate models provide information that aids resource managers, policy makers, and researchers in planning for the future [1, 2]. Although water resource managers and other decision makers can view global climate models (GCMs) for basic information, the associated low spatial-resolution output lacks the local information that they need to plan for their community [2] and implement into hydrologic models [3]. Therefore, high-resolution climate projections that are either model-generated in high resolution (less common) or are downscaled to high resolution (more common) are more useful to these local managers. For example, in the Red River Basin, located in the south-central United States (U.S.), this detailed climate information helps those who make long-term (e.g., 50 years) water plans. In many cases, stakeholders who desire to use downscaled climate projections may choose one dataset, looking for the "best" or "most likely" option, rather than recognizing that climate *risk assessment* requires them to acknowledge uncertainties and instead use a suite, or ensemble, of datasets.

This paper discusses the creation of downscaled datasets that include historical and future projections of daily minimum and maximum temperature and daily precipitation. The intent was to develop an ensemble of projections that stakeholders in the Red River Basin could use for climate risk assessment. During the process of

developing the datasets, we found that some methods provided results that we deemed unacceptable for our users and some choices within the method implementation were less appropriate than other choices for certain variables. We used what we learned to begin developing a new ensemble of climate projections for the entire south-central U.S.; yet, once users have access to one set of projections, they are reluctant to update to another set as science evolves. We will discuss some of these nuances for the case study of building an ensemble of projections for the Red River Basin in the south-central U.S. While we detail the methods for developing the dataset, we highlight some of the issues that arise as the climate science community works with those in other disciplines, including modelers and decision makers.

Before we delve into statistical downscaling and its uses, it is important to discuss GCMs, which are numerical models that represent atmospheric and oceanic processes [4] and can offer a large-scale view of future climate conditions, such as projected temperature and precipitation, under different representative concentration pathways (RCPs). The RCPs serve as scenarios of various radiative forcing trajectories from anthropogenic greenhouse gas emissions and changes in land cover [5]. Moss et al. [5] discussed the four RCPs—RCP 2.6, RCP 4.5, RCP 6.0, and RCP 8.5––where RCP 2.6 represents a scenario where radiative forcing peaks at 3.1 W/m^2 and the concentration of greenhouse gases reaches 490 parts per million in 2100 and then decreases, and RCP 8.5 represents a scenario with more than 8.5 W/m^2 of radiative forcing and a concentration of greenhouse gases that exceeds 1,370 parts per million by 2100.

Although GCMs provide an overall depiction of possible future conditions, they do not take local processes into account, having a coarse-resolution range of 50 to 600 kilometers, depending on the model [4, 6–9]. These local processes can include mountain meteorology and land-sea interactions [6]. Other GCM limitations include biases in rainfall intensity, responses to climate forcing, natural variability range, and simulated precipitation with a shortfall in convection and across mountainous areas [10, 11]. Downscaling can correct some of these GCM biases [11, 12] and allow us to project local changes in the future in greater detail where there are no observations to interpolate. Furthermore, downscaling provides a higher spatial resolution that allows local decision makers and resource managers to make more informed decisions about their area and to understand local phenomena to a higher degree [13].

Thrasher et al. [2] provided an example of the significance of downscaled climate projections to resource managers and decision makers. The spatial resolution of the projections offered enough detail to determine the changes in the freezing line in mountainous regions, relating to the amount of melting snowpack that affects the water supply. Resource managers also can learn about how their area may be affected by drought, causing them to change their community's water plans and usage of the water supply [14]. In addition, knowing how their region's climate is expected to change may alter food production areas, causing alteration in land use [15], especially where crops are rainfed.

Downscaled climate projections provide more localized information than GCMs through high-resolution data for applications by decision makers and can help them to create better drought and water resource management strategies [16]. For example, Bertrand and McPherson [17] use the dataset described in this study to determine that severe drought is expected to increase in the western Red River Basin and heavy precipitation events are projected to increase in the eastern basin, especially by the end of the 21st century under RCP 8.5. The high-resolution data allowed them to identify an east-west gradient in these changes that follows the natural precipitation gradient of the region.

2. Study Domain

This study focuses on a case study in the Red River Basin of the South (hereafter Red River Basin), with headwaters in far eastern New Mexico (Figure 1), flowing west to east through Texas, Oklahoma, and Arkansas, and exiting into the Mississippi River in Louisiana. The basin covers 239,361 km^2 and crosses a west-to-east gradient of precipitation with average yearly rainfall totals of approximately 500 to 1300 millimeters (20 to 50 inches). Because of this moisture gradient, the Red River Basin is home to many different ecoregions, from the High Plains in the west to the South Central Plains in the east [18].

This basin is vital for the area's drinking water supply and recreational and cultural activities [19]. However, because the basin benefits multiple states and metropolitan cities, such as Fort Worth, TX, and Oklahoma City, OK, there have been disagreements regarding water rights in this basin. Oklahoma, Texas, Arkansas, and Louisiana signed a water compact in 1978 to share the water resource fairly [20]; however, because Texas had been routinely exceeding its allotment of water, the Oklahoma Legislature restricted the state's apportioned water to remain within state boundaries in 2002, excluding Texas from any option to buy water from Oklahoma [21]. This new statute, Title 82-1B, upset decision makers in Texas because Tarrant County, including Fort Worth, previously bought water from Oklahoma. The issue eventually rose to a legal case that was brought before the U.S. Supreme Court—*Tarrant Regional Water District vs. Hermann* [22]—that wished to declare Oklahoma's new law as unconstitutional under interstate commerce laws. The case was dismissed, however, allowing Oklahoma to determine how to use its apportioned water.

Similarly, in 2016, a water rights issue between the City of Oklahoma City and both the Choctaw Nation of Oklahoma and Chickasaw Nation was resolved. This dispute arose in 2011, during a period of extreme drought in Oklahoma and Texas, when officials in Oklahoma City purchased rights to water in Sardis Lake, a reservoir in southeast Oklahoma that is within tribal boundaries of the Choctaw Nation of Oklahoma. Both tribes had views of water rights that conflicted with those of Oklahoma City, but all governments came to an agreement that allowed the State of Oklahoma to manage the water supply while ensuring that the tribes continued to have a voice in water resource and conservation issues for the region. These disagreements are important

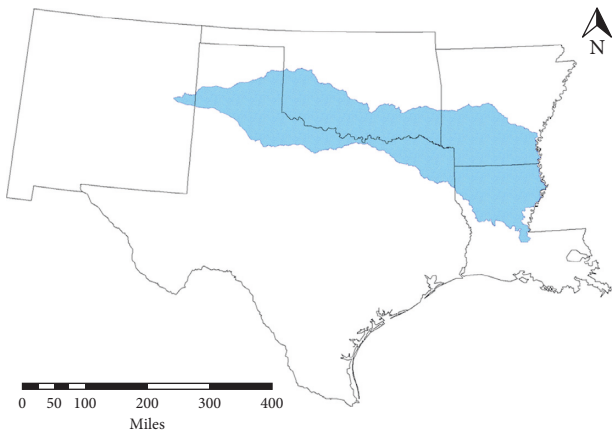

Figure 1: Red River Basin.

examples of the extremes that communities under pressure from water stress will undertake to gain or maintain their rights to water. With drought ravaging the U.S. Southern Plains in the decade of the 2010s, states have been forced to look for new water resources or reduce water use. Therefore, precipitation, temperature, and streamflow projections have become of important interest to water planners in the basin.

3. Data

3.1. Introduction to the Dataset. This study employs an ensemble of statistically downscaled, high-resolution climate projections that were generated by the Geophysical Fluid Dynamics Laboratory of the National Oceanic and Atmospheric Administration (NOAA) and disseminated by the South Central Climate Adaptation Science Center of the U.S. Geological Survey. A postdoctoral associate (supervised by the second author of this paper) of the South Central Climate Adaptation Science Center worked with scientists and engineers at the NOAA lab to produce the datasets. One purpose of the ensemble was to examine the representativeness of the dataset to aid water resource managers in the Red River Basin with their long-term water plans. The ensemble of historical and future climate data was generated by statistically downscaling output from three representative GCMs using empirical relationships between a predictor, or large-scale climate variable, and a predictand, or local-scale surface variable, by diverse techniques [23]. Appropriate transfer functions, described below, were used to link the predictor and the predictand. Statistical downscaling was a better option for this study, compared to dynamical downscaling, because it allowed us to create projections for multiple models and scenarios without being as computationally demanding and expensive.

Downscaled daily surface maximum and minimum temperatures and daily precipitation were computed for historical and future periods using over 3600 grid points throughout the region. The historical outputs were trained from an observational dataset from Livneh et al. [24] that originally included daily minimum and maximum temperature and daily precipitation data from 1915–2011 with a 1/16-degree resolution. From these data, a time frame of January 1st, 1961, to December 31st, 2005, was selected and the data were downscaled to 0.1°, which is sufficient spatial resolution to capture regional climatic differences but is larger than the microscale so that we are not capturing noise. The downscaled projections included a time frame of 1961–2005 for the historical period, which is a common definition of the historical period when using CMIP5 models, and 2006–2099 for the future period, seeking results for the end of the 21st century. This dataset allowed us to view projections in the future directly or to analyze change maps and examine future changes in the region.

To force the projections on the large scale, three GCMs were chosen from the Coupled Model Intercomparison Project Phase 5 (CMIP5) [25]: the low-resolution version of the Max Planck Institute's Earth System Model (MPI-ESM-LR) [26], the Community Climate System Model (CCSM4) [27], and the fifth version of the Model for Interdisciplinary Research on Climate (MIROC5) [28]. The CCSM4 model has a resolution of 0.9° by 1.3° and couples the atmosphere, ocean, land surface, and sea ice, and the sixth realization was used for this study, which spans from 1850 to 2005. For the MPI-ESM-LR model with a 1.9-degree resolution, the r1 realization was used, which has a time frame from 1880 through 2005; future simulations included natural forcings but excluded volcanic aerosols after 2005. The r1 realization was used for the MIROC5 model with a resolution of 1.4°. In addition, the first version of the perturbed physics model was used for all models.

Only three GCMs were selected due to computational demand of downscaling and running the data through the VIC model. Although the end users wanted only one model, our team compromised on three so as to include some range of uncertainty. For climate risk assessment, it is important to include multiple scenarios, multiple GCMs, and multiple downscaling techniques (e.g., Wootten [29]) to represent uncertainties that can affect decision making. These models were selected based on their historical performance from the evaluation of Sheffield et al. [30], which included consideration of model biases in seasonal temperature and precipitation over North America and central North America. We subjectively selected the final three GCMs because 1) they have relatively smaller biases compared to the full suite of CMIP5 models and 2) they span a range of one standard deviation above and below the ensemble mean in both temperature and precipitation (Figures 2(a) and 2(b)), thus incorporating much of the uncertainty. Additionally, the climate sensitivity of the models was included in the overall selection process [31] (Figure 2(c)). For example, MIROC5, CCSM4, and MPI-ESM-LR represent the lower 50% mean, and upper 50% of the distribution of model sensitivities, showing that these models are representative of the general spread of the GCMs and are not on the extreme end of the spectrum.

3.2. Quantile Mapping Approaches. After model selection, we selected three of the four available RCP scenarios (RCP 2.6, RCP 4.5, and RCP 8.5) because they represent the full range of existing scenarios. Using these for each of the three

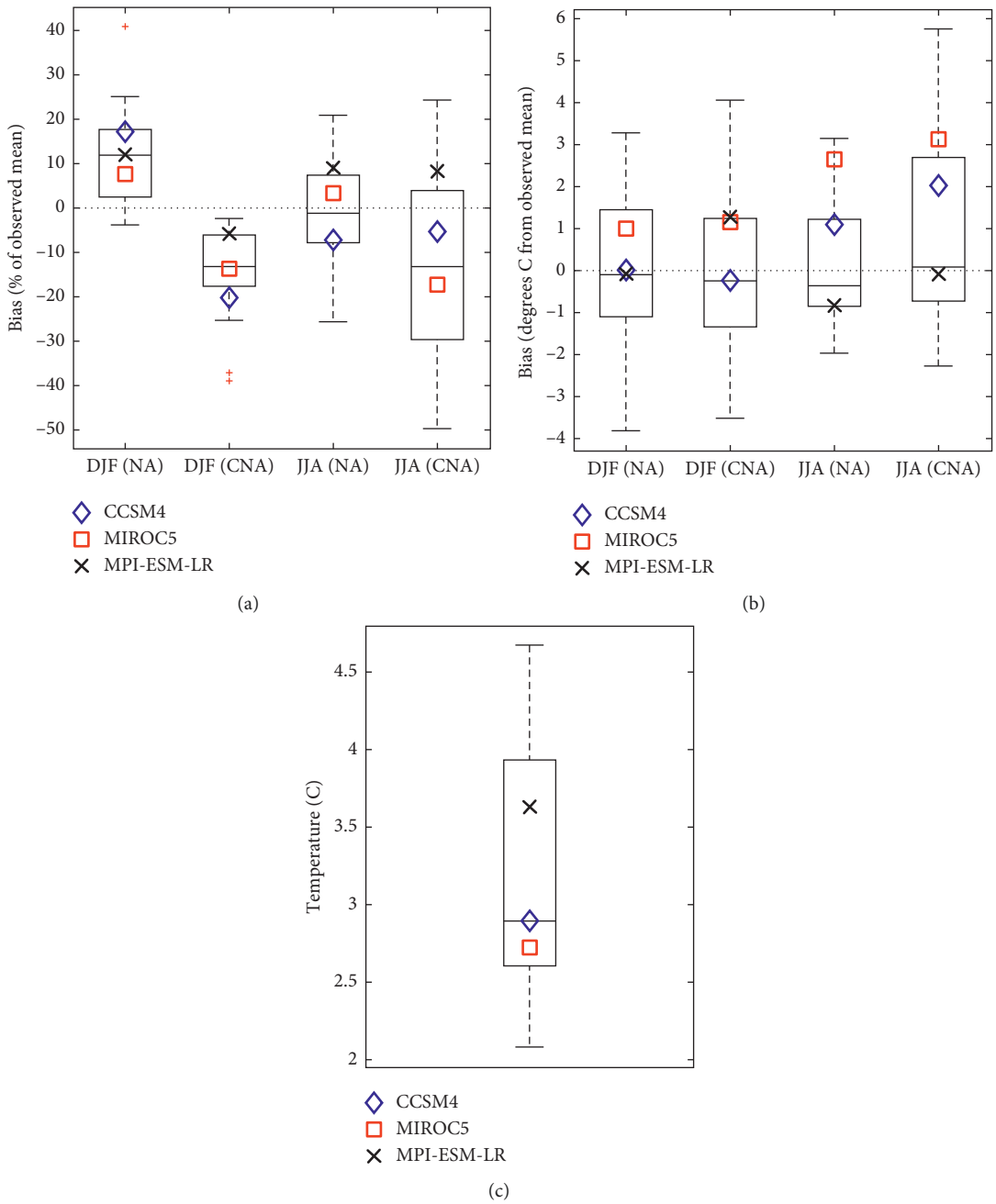

Figure 2: Performance assessment of the selected 3 GCMs (CCSM4, MIROC5, and MPI-ESM-LR) from the CMIP5 suite based on North American (NA) and central North American (CNA) winter (DJF) and summer (JJA) bias in (a) precipitation and (b) temperature, and (c) climate sensitivity (based on Sheffield et al. [30] and personal communication with Dr. Derek Rosendahl).

GCMs, we implemented quantile mapping techniques to downscale the output, also reducing biases in the large-scale climate models during postprocessing [32]. For example, all three chosen models have been shown to underestimate precipitation in the winter, and two of the models overestimate temperature in the summer for the central North America region [30]. In this case, quantile mapping helped to correct these biases in the probability distributions of the GCMs and were tested to find the sensitivity of the projections. Quantile mapping incudes a stationarity assumption, meaning that biases and patterns that occur in the historical period are assumed to also occur in the future period [33–36]. In addition, for precipitation downscaling, we used a threshold of 0.127 mm to classify rainfall days, while dry days were defined as those days with precipitation amounts falling below the threshold. This threshold is defined by the National Climatic Data Center [37].

3.3. Cumulative Density Function Transform (CDFt) Method. We selected the downscaling techniques of cumulative density function transform (CDFt) [38], equidistant quantile

mapping (EDQM) [33, 39], and bias correction quantile mapping (BCQM) [40]. The CDFt downscaling technique uses a transfer function, shown in equation (1) [39], to identify the quantitative relationship between the modeled historical and the observed cumulative distribution functions and uses the same relationship to generate the future cumulative distribution function (F) [41]:

$$\hat{x}_{\mathrm{m,p}}(t) = F_{\mathrm{o,h}}^{-1}\left(F_{\mathrm{m,h}}\left(x_{\mathrm{m,p}}\right)\right), \tag{1}$$

where subscripts represent observed (o), historical (h), modeled (m), and predicted (p) data; $x_{\mathrm{m,p}}$ is the modeled climate variable that is being predicted; and $\hat{x}_{\mathrm{m,p}}$ is the bias corrected climate variable. This equation improves the tail behavior of the projections by keeping the distribution within the bounds of the observed data, and the technique preserves the initial GCM means in the downscaled output by transforming the mean of the GCMs to match the historical observed means.

The two parameters used by CDFt are *dev*, the coefficient of development, which is the difference between the historical and future GCM mean and is used to extend the range for quantiles to be calculated, and *npas*, the number of quantiles that are being estimated. For this study, $dev = 1$ and $npas = 100$, the default. Pierce et al. [41] analyzed the CDFt method and their results revealed that this method generally produces lower precipitation estimates across the U.S. However, in the Red River Basin region, their findings indicated a wet bias across a large part of the region, especially during the summer. Daily maximum temperature was underestimated in their end-of-century projections for much of the basin in the summer as well.

3.4. Equidistant Quantile Mapping (EDQM) Method. The second method we used was EDQM and the downscaling was performed through the transfer functions in equations (2) and (3) [33, 39]. The modeled mean for the historical and predicted period is represented by $\overline{x}_{\mathrm{m,h}}$ and $\overline{x}_{\mathrm{m,p}}(t)$ [33]. A ratio approach (equation (2)) for EDQM versus an additive approach (equation (3)) for precipitation eliminates the possibility of negative precipitation values occurring after bias correction, which generally arises when a model has a wet bias and projects a decrease in precipitation [42]. Therefore, both methods were applied in the calculation of EDQM, with a ratio approach being implemented for precipitation and an additive approach for temperature.

$$\hat{x}_{\mathrm{m,p}}(t) = F_{\mathrm{o,h}}^{-1}\left\{F_{\mathrm{m,h}}\left[\frac{\overline{x}_{\mathrm{m,h}} x_{\mathrm{m,p}}(t)}{\overline{x}_{\mathrm{m,p}}(t)}\right]\right\}\frac{\overline{x}_{\mathrm{m,p}}(t)}{\overline{x}_{\mathrm{m,h}}}, \tag{2}$$

$$\hat{x}_{\mathrm{m,p}}(t) = x_{\mathrm{m,p}} + F_{\mathrm{o,h}}^{-1}\left(F_{\mathrm{m,p}}\left(x_{\mathrm{m,p}}\right)\right) - F_{\mathrm{m,h}}^{-1}\left(F_{\mathrm{m,p}}\left(x_{\mathrm{m,p}}\right)\right). \tag{3}$$

EDQM assumes that the historical model error will persist in the future, and the technique bias corrects future temperature values by adding the historical bias value to the modeled change in that estimate at a given quantile across the grid points [41]. This method also upholds the modeled median change in the future. Pierce et al. [41] projected very wet and dry regions to have a higher error in precipitation; however, in the Red River Basin region, their estimates showed an underestimation of precipitation in the winter and an overestimation in summer. Temperature was relatively consistent between winter and summer, with a smaller mean error of −0.5 to 0.5 degrees Celsius.

Quantile mapping methods do not require a temporal structure, or sequence, that represents the historical record; however, the resulting downscaled projections are used for hydrologic impacts studies, applying the variable infiltration capacity model [43] for rainfall runoff and input to the RiverWare [12, 19] water management tool. Thus, it was essential to link the daily variability of the GCM and downscaled output from both techniques to create temporal consistency by creating an algorithm to reorganize the downscaled output to improve the correlation of the projections with the coarse-resolution GCM time-sequenced values. Once this process was complete, the downscaled data were quality controlled.

3.5. Bias Correction Quantile Mapping (BCQM) Method. It is worth noting that we intended to use the BCQM method [40] as a third downscaling technique; however, there were substantive issues found with our computations of this method. BCQM uses the transfer equation in equation (1), but it only includes historical observations for data training and disregards information from future projections [33]. This technique can alter the trends of the GCMs after bias correction substantially, which affects precipitation analyses and skews the data distribution [44]. The tail distribution becomes skewed when the model projects values that fall outside of the historical range used for training. When the variance is overestimated in the historical period, the mean and quantiles also are overestimated after bias correction and vice versa for underestimation [33]. Because of time constraints, we were unable to correct and rerun computations for this method and include it in our study. Therefore, the BCQM technique could not be recommended to decision makers in the Red River Basin and, therefore, was not used in our analyses, in impacts modeling, or for management decisions.

4. Results

The resulting ensemble of statistically downscaled climate projections for the Red River Basin was made publicly available in NetCDF format. The data include daily minimum and maximum temperatures (in degrees Kelvin) and daily precipitation (in kg/m^{2}s) from the described three GCMs and two downscaling techniques for the historical time period (1961–2005) and future period (2006–2099). There are 72 statistically downscaled projections created at a resolution of 0.1°, or approximately 11 kilometers latitude by 9 kilometers longitude, including 18 projections for the historical period and 54 projections for the future period. The gridded observational dataset [24] used as the downscaling training dataset is also available for validation purposes.

Many analyses can be executed from these data. For example, in Section 4.1, we provide an analysis for the difference in mean daily values between the most recent 25 years in the historical period (1981–2005) and two 25-year segments of the future period (2046–2070 and 2075–2099) under RCP 2.6 and RCP 8.5 scenarios. We then computed the mean daily changes of precipitation for each season, which we discuss in Section 4.2. Detailed analyses of the dataset are available in Bertrand and McPherson [17].

4.1. Changes in Precipitation and Temperature. Our first example of an analysis that can be conducted from these data is a simple calculation of the projected changes in mean daily precipitation and daily minimum and maximum temperature between the historical and future time frames. We converted temperature to degrees Celsius and precipitation to millimeters per day. Overall, we determined that the models generally project an increasing precipitation trend in eastern portions of the Red River Basin and a decreasing trend in the west for both downscaling techniques, especially during the end-of-century period under RCP 8.5 (Figure 3). Under the CDFt technique, the CCSM4 and MPI-ESM-LR models estimate mean daily precipitation to decrease in the west up to 0.5 mm/day and increase in the east by up to 0.7 mm/day (Figure 3). In the historical period, 4–5 mm/day of mean daily precipitation occurred in the east, which indicates a 15% increase by the end of the 21st century (Figure 4). In the west, historical mean daily precipitation ranged from 1–3 mm/day, which is a 15% decrease in the future.

The EDQM technique yielded a smaller range in precipitation differences, spanning from a 0.5-mm/day decrease to a 0.4-mm/day increase but exhibited the same spatial patterns as CDFt. On the other hand, the MIROC5 simulations demonstrated a basin-wide increase in precipitation for all RCPs and time frames with the exception of the end-of-century scenario with RCP 8.5, where a basin-wide decrease was projected from both downscaling techniques. Sillmann et al. [45] found that the MIROC5 model projects the highest precipitation totals among the CMIP5 models, which may explain the model's generally higher estimates. The differing results between models represent uncertainties in the models, downscaling methods, emission scenarios, and natural variability [46].

Projections for mean daily minimum temperature differed greatly between RCP 2.6 and RCP 8.5 scenarios. In a lower emission scenario, mean minimum daily temperatures increased up to 2°C for both time frames, while estimates in the higher emission scenario increased by as much as 6.6°C by the end of the century (Figures 5(a)–5(f)) compared to the historical value of approximately 10°C (Figure 6). Mean daily maximum temperature is similar, and each projection revealed a basin-wide increase with no decreases in either minimum or maximum temperature (Figures 7(a)–7(f)).

The largest warming was projected to occur in the end-of-century time period of 2075–2099 under the RCP 8.5 scenario for all models and downscaling methods. However, MIROC5 exhibited warmer mean temperatures in the future time periods, with values being 1°C higher than the other two models. This difference can be explained by the warm bias in MIROC5 temperatures, as described in Sheffield et al. [30]. Sheffield also estimated a warm bias in MPI-ESM-LR for the central North America region. The CDFt and EDQM results were nearly equivalent in regard to temperature variables. Based on our results, precipitation and temperature seem to be more influenced by the GCM versus the downscaling technique, indicating more variability in the GCMs due to their own inherit biases and little variability in the downscaling technique. Nover et al. [47] describes this well, stating that locations driven by large-scale features are more affected by the GCM selection.

4.2. Seasonal Changes in Precipitation. To better understand the changes seen in Section 4.1, we computed the mean daily precipitation differences between the historical and future periods for each climatological season, categorized as December through February (DJF), March through May (MAM), June through August (JJA), and September through November (SON). Because modeled precipitation is more variable than temperature, we chose to only analyze the seasonal precipitation changes. Model projections indicated that the two downscaling techniques yielded similar results and spatial patterns.

In the mid-century period, the models generally projected a change of 0.5 mm/day from the historical value; however, there were distinct patterns in some models. For example, the CCSM4 model exhibited the largest changes in mean daily precipitation. This model estimated the mean daily precipitation to increase by 2 mm/day in the MAM time frame, compared to less than 0.5 mm/day in the other models (Figure 8). This substantial amount revealed a 40% increase compared to historical values. Furthermore, the model projected a basin-wide decrease in the JJA time frame with some locations having a reduction of 0.85 mm/day, while the other two models included a large-scale increase in mean daily precipitation. This result shows that the CCSM4 model projects more extreme values during the spring and balances its annual average by a widespread reduction during the summer in the mid-century period. Qiao et al. [48] analyzed seasonal precipitation in the Red River Basin and used the same dataset as our study for the mid-century time frame. Their results showed that the highest increases in precipitation occur in the spring and largest decreases were in the fall for the mid-century period. In addition, they discovered that precipitation amounts in the upper quantiles are driving the precipitation totals in spring, which may validate that CCSM4 projects more extreme events in spring. Their results are consistent with ours.

On the other hand, larger changes were seen in the end-of-century period under RCP 8.5. We noticed the same previous patterns for the CCSM4 model, but the largest changes emerged in the MPI-ESM-LR model (Figure 9). For example, mean daily precipitation in the DJF period increased by 1.68 mm in the eastern basin, which is more than 30% greater than the historical value. Precipitation increased

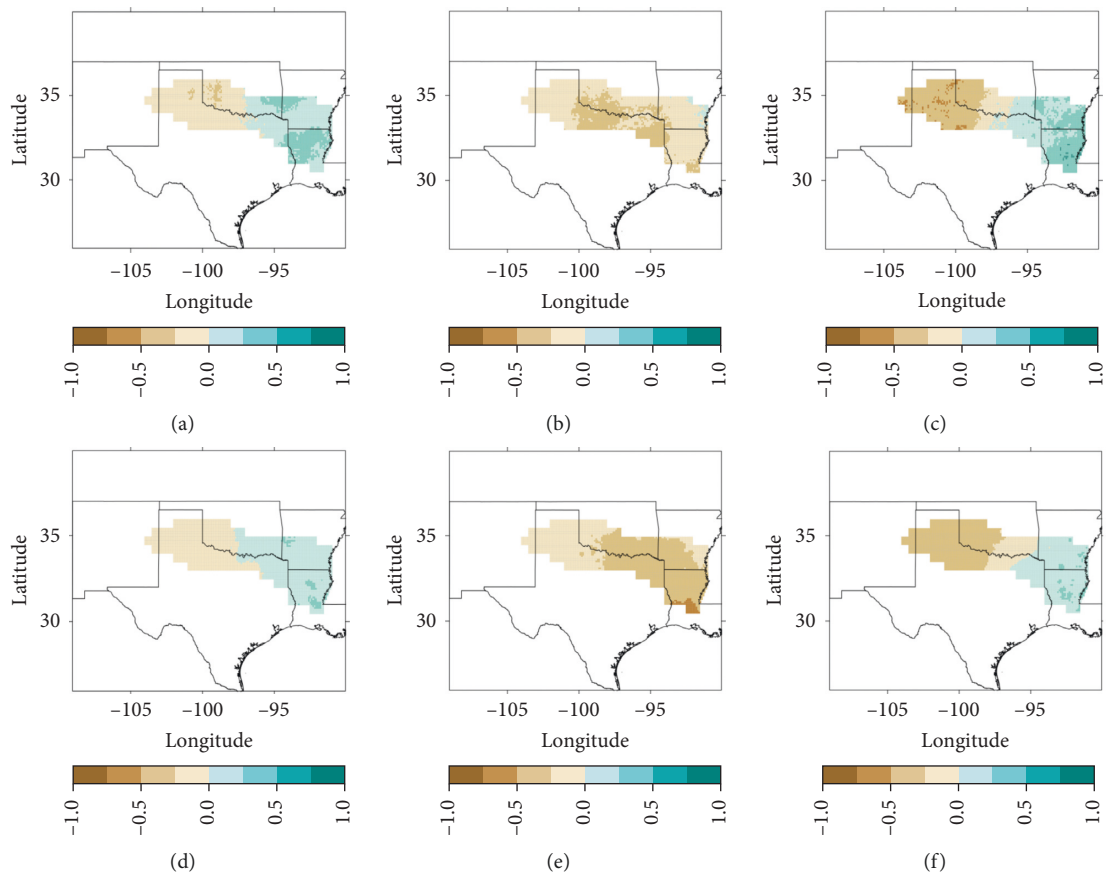

Figure 3: Difference fields for mean daily precipitation (in mm/day) between historical (1981–2005) and end-of-century (2075–2099) time frames for RCP 8.5. Columns represent the GCMs (CCSM4, MIROC5, and MPI-ESM-LR, from left to right respectively); rows represent downscaling methods, with CDFt on top and EDQM on bottom. Brown and tan colors represent future decreases in precipitation compared to the historical period; blue-green colors represent future increases in precipitation. (a) Model: CCSM4, SD: CDFt. (b) Model: MIROC5, SD: CDFt. (c) Model: MPI-ESM-LR, SD: CDFt. (d) Model: CCSM4, SD: EDQM. (e) Model: MIROC5, SD: EDQM. (f) Model: MPI-ESM-LR, SD: EDQM.

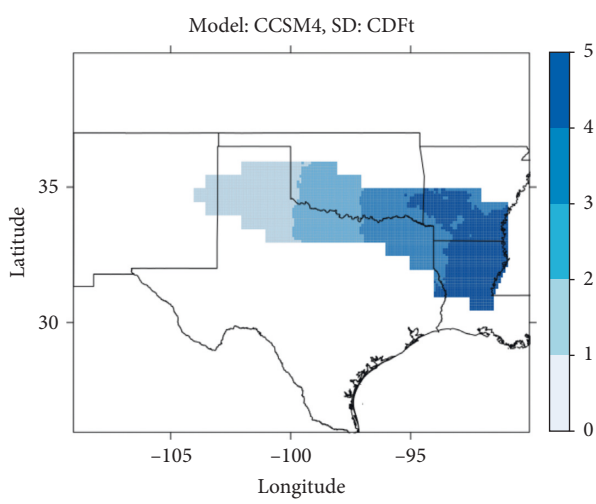

Figure 4: Difference fields for the CCSM4 mean daily precipitation (in mm/day) for the historical (1981–2005) time frame. Darker shades of blue represent higher rainfall values.

in the JJA period as well, along with a decrease of 1.3 mm/day in the Texas Panhandle. Furthermore, this model projected the largest MAM decreases. Meanwhile, the MIROC5 model included small changes throughout most of the year. Precipitation uncertainties are evident by the end of the 21st century and two of the three models show that extreme values are likely driving the seasonal trends.

5. Discussion about Climate Risk Assessment

Although it is important to document the methods that created the ensemble of climate projections for this case study in the Red River Basin, much of what was learned from the process of generating the dataset involved coproduction of knowledge with impacts modelers (in this case, for streamflow and channel routing) and decision makers (in this case, water resource managers). First, impacts modelers and decision makers both must rely on climate scientists to value their management outcomes in order to produce useable climate projections. In Section 3.5, we noted that all variables for all scenarios, GCMs, and time periods were generated using the BCQM downscaling technique; however, instabilities in the resulting output led the climate scientists to remove that dataset from further processing and analyses for their coproduction partners. Without the expertise of the climate scientists, it is probable (perhaps even

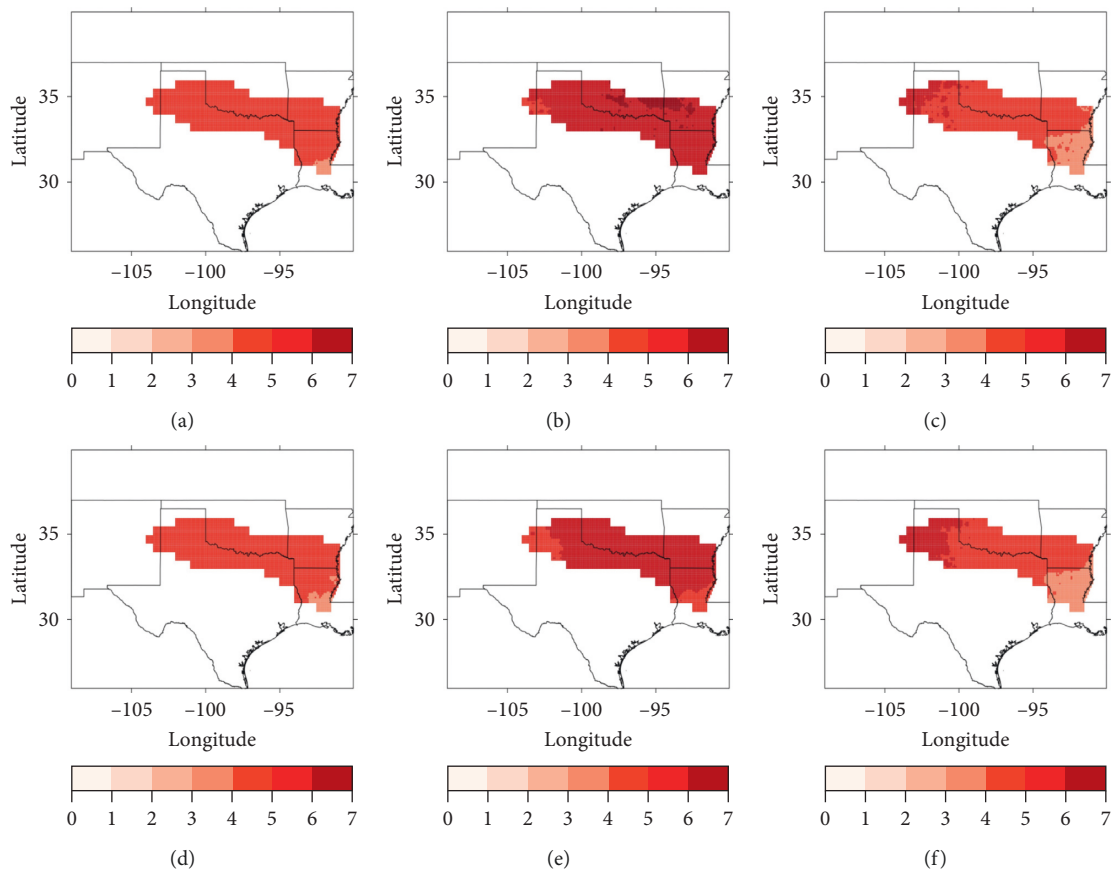

Figure 5: Difference fields for mean daily minimum temperature (°C) between historical (1981–2005) and end-of-century (2075–2099) time frames for RCP 8.5. Columns represent the GCMs (CCSM4, MIROC5, and MPI-ESM-LR, from left to right respectively); rows represent downscaling methods, with CDFt on top and EDQM on bottom. Darker shades of red represent higher minimum temperature values. (a) Model: CCSM4, SD: CDFt. (b) Model: MIROC5, SD: CDFt. (c) Model: MPI-ESM-LR, SD: CDFt. (d) Model: CCSM4, SD: EDQM. (e) Model: MIROC5, SD: EDQM. (f) Model: MPI-ESM-LR, SD: EDQM.

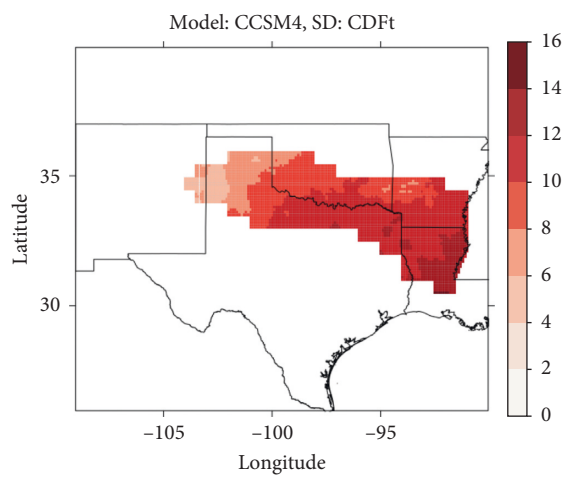

Figure 6: Difference fields for mean daily minimum temperature (°C) for the historical (1981–2005) time frame for CCSM4. Dark shades of red represent higher minimum temperature values.

likely) that impacts modelers or water resource managers would have included these anomalous results in their work.

Similarly, in Section 3.4, we discussed how we implemented a ratio approach for precipitation and an additive approach for temperature in the calculation of the EDQM datasets. This choice is one of many that can be applied during the creation of a downscaled dataset, and each of these choices can affect the resulting output (e.g., Wootten

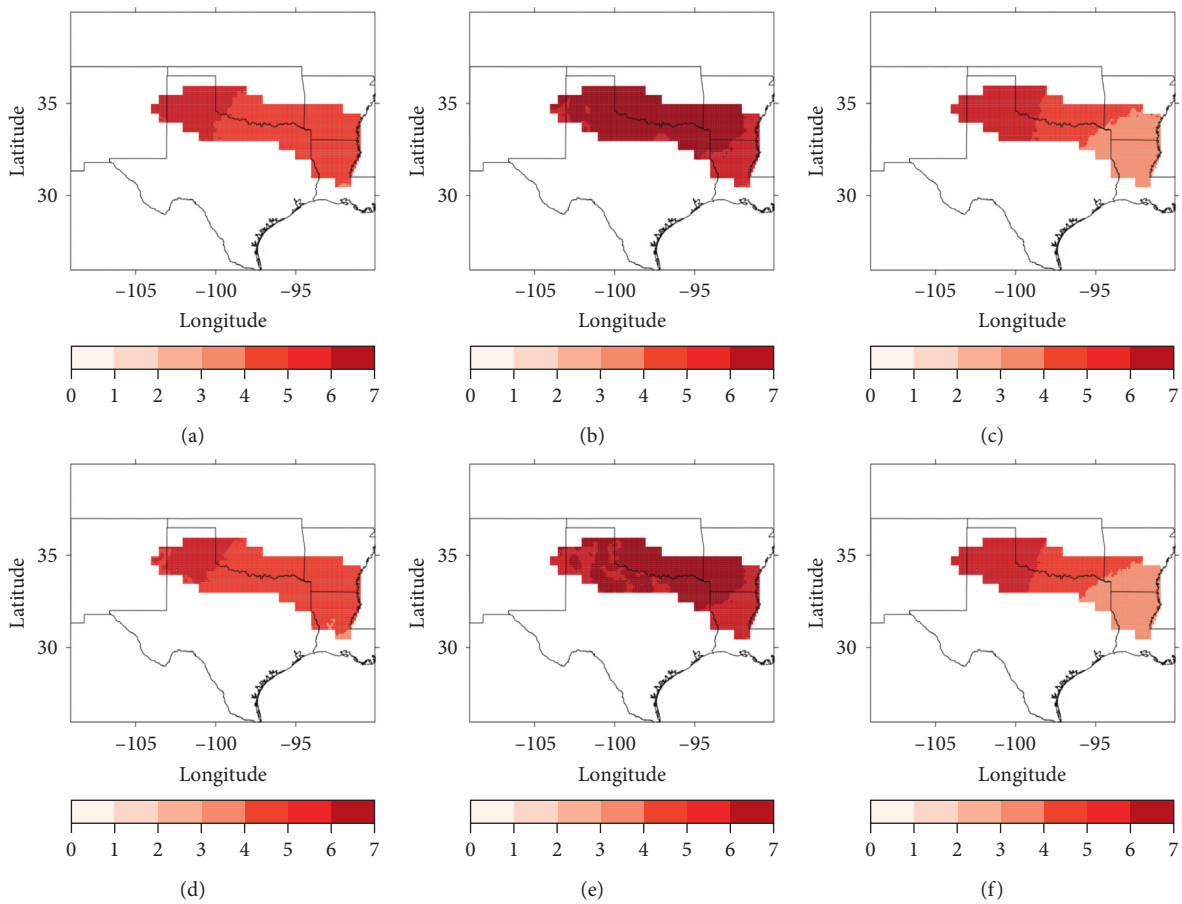

Figure 7: Difference fields for mean daily maximum temperature (°C) between historical (1981–2005) and end-of-century (2075–2099) time frames for RCP 8.5. Columns represent the GCMs (CCSM4, MIROC5, and MPI-ESM-LR, from left to right respectively); rows represent downscaling methods, with CDFt on top and EDQM on bottom. Darker shades of red represent higher maximum temperature values. (a) Model: CCSM4, SD: CDFt. (b) Model: MIROC5, SD: CDFt. (c) Model: MPI-ESM-LR, SD: CDFt. (d) Model: CCSM4, SD: EDQM. (e) Model: MIROC5, SD: EDQM. (f) Model: MPI-ESM-LR, SD: EDQM.

[29]), especially for extreme values and longer projections. Other choices include data transformations (e.g., to transform non-Gaussian distributions like precipitation for application to statistical techniques that assume Gaussian distributions), regridding or interpolating GCM output to the same spatial and temporal resolution of the gridded observational dataset used in training the statistical technique and implementing a tail adjustment (for extreme values) within the downscaling process. Again, because these choices affect the resulting downscaled projections, users of the projections need to work closely with climate scientists to understand how these choices may affect their own decisions.

On the other hand, value is added to the development of downscaled datasets through coproduction with impacts modelers and decision makers in the field. In this case study, we teamed with hydrologists at the University of Oklahoma and Aqua Strategies Inc., a private water resources consulting firm, to use the output of our downscaling processes as input to the variable infiltration capacity (VIC) model [43, 49], which is a physically based, semidistributed water and energy balance model that outputs surface hydrological variables, including streamflow. Xue et al. [19] detail results from the VIC model using downscaled input for this Red River case study. Many other river basin studies have used the VIC model for climate change impact assessments as well [50, 51]. Hydrologic projections from the VIC model then were used as input to RiverWare™ [52], developed by the Center for Advanced Decision Support for Water and Environmental Systems (CADSWES), to model the river/reservoir system of the Red River Basin. RiverWare is used extensively for water planning because it allows users to simulate management operations across a complex basin, including various types of reservoirs, canals, diversions, and users. Water managers from the Chickasaw Nation and Choctaw Nation of Oklahoma ultimately were users of the resulting information as they worked on a 50-year water plan. Conversations between the climate scientists, hydrologic modelers, and water managers resulted in many of the choices discussed above in the downscaling development. When climate scientists understood the *kinds* of decisions that were being made, it became apparent when a given set of output would be unhelpful or even harmful to the risk assessment process. Given the project timeline, it was

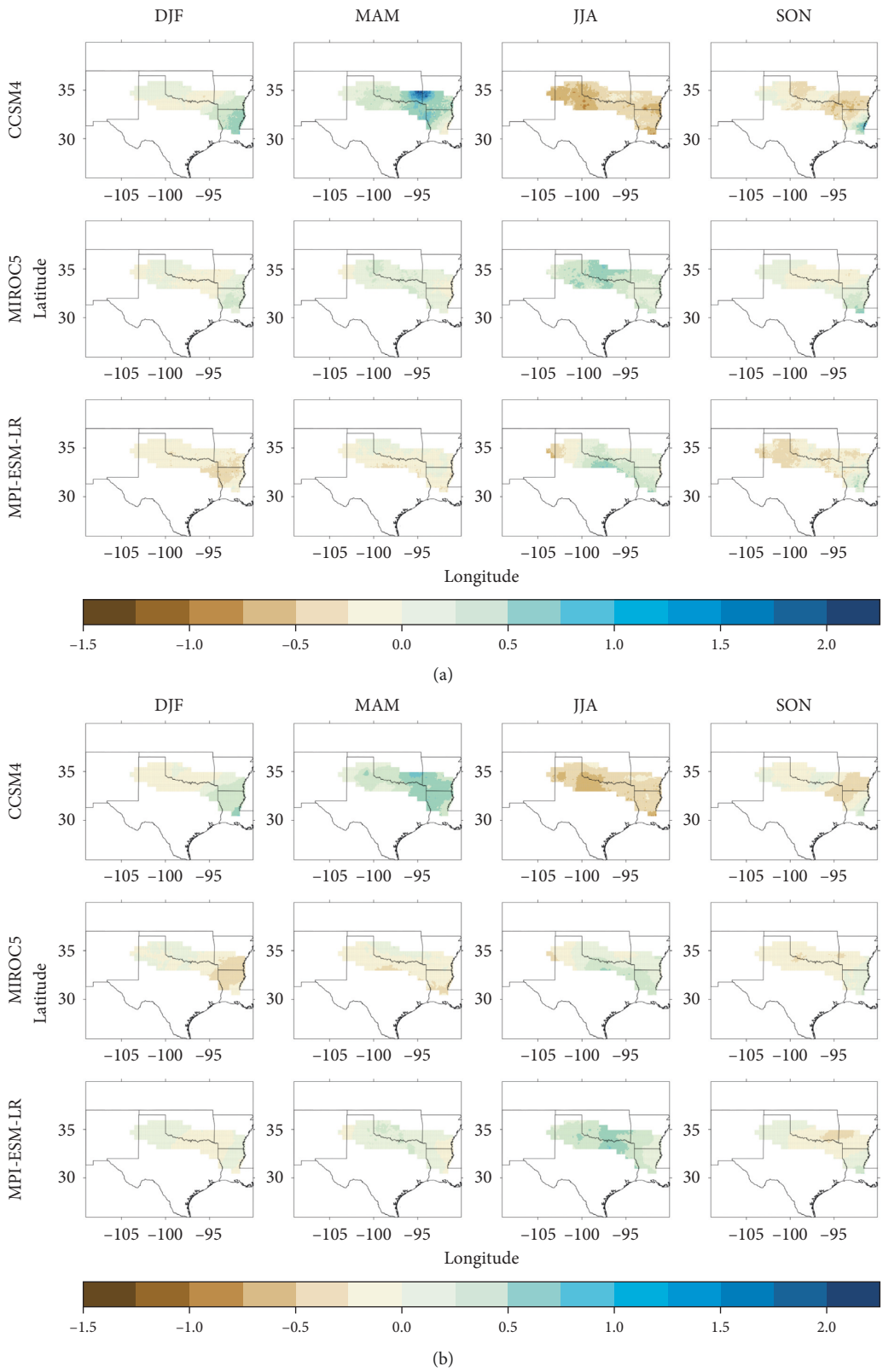

Figure 8: Difference field in seasonal changes in mean daily precipitation (mm/day) between the historical (1981–2005) and mid-century (2046–2070) time frames for RCP 2.6 using the (a) CDFt downscaling technique and (b) EDQM technique. Columns represent seasons (DJF, MAM, JJA, and SON). Brown colors represent a decrease in daily precipitation and blues represent an increase.

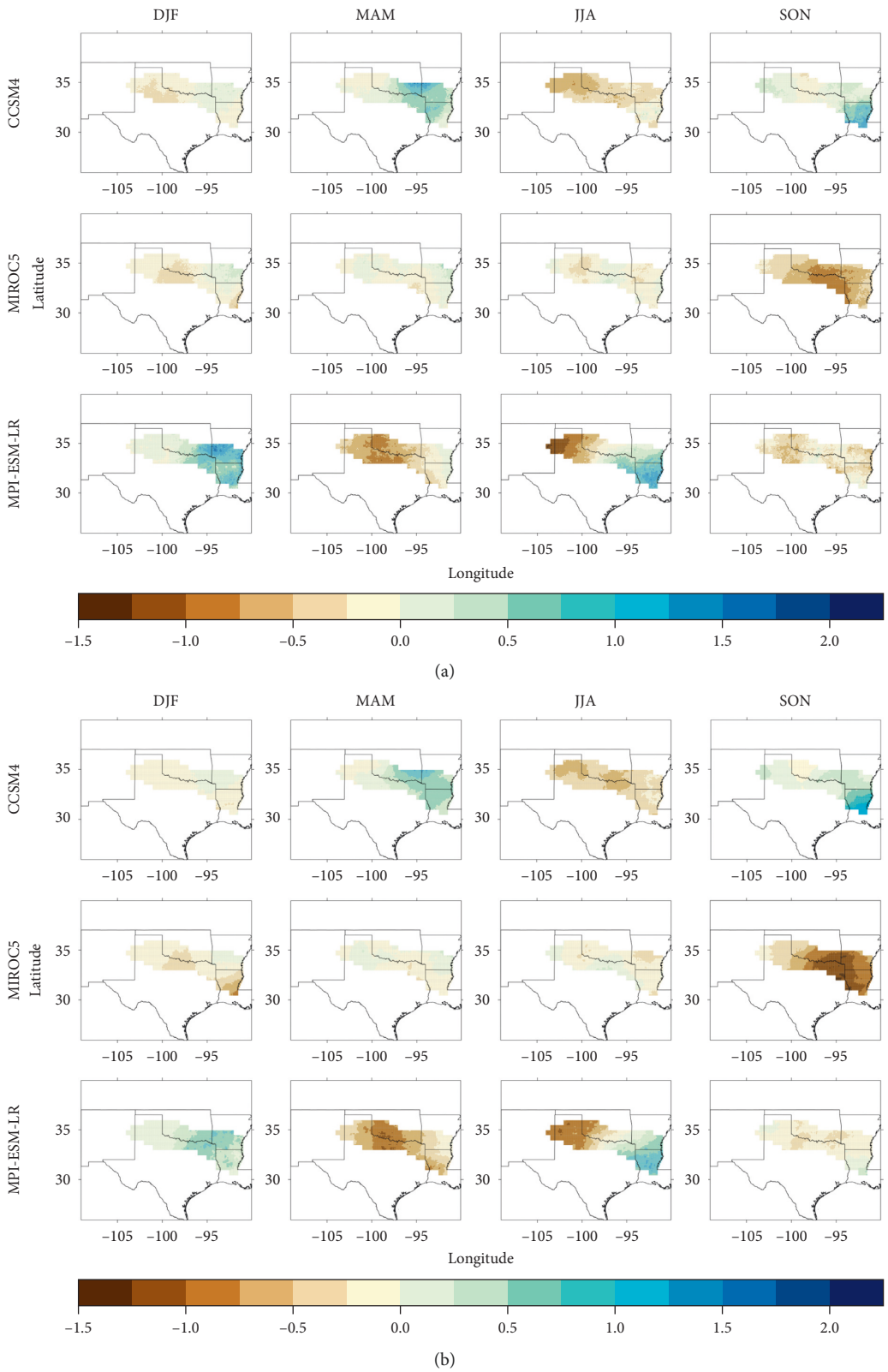

Figure 9: Difference fields in seasonal changes in mean daily precipitation (mm/day) between the historical (1981–2005) and end-of-century (2075–2099) time frames for RCP 8.5 using the (a) CDFt downscaling technique and (b) EDQM technique. Columns represent seasons (DJF, MAM, JJA, and SON). Brown colors represent a decrease in daily precipitation and blues represent an increase.

impossible to apply a different downscaling technique, for example, when BCQM resulted in spurious output for some cases, but at least the communications among the three groups could result in the nations not using problematic climate projections for their planning process.

6. Conclusions

Statistically downscaled climate projections provide high-resolution output that is more useful to water managers, decision makers, and researchers than coarse-resolution global climate models. This study introduced datasets that include downscaling from three GCMs (CCSM4, MPI-ESM-LR, and MIROC5) using two statistical downscaling techniques (CDFt and EDQM) at a resolution of 0.1° for the Red River Basin. The datasets contain a historical time period (1961–2005) and a future period (2006–2099) and project daily minimum and maximum temperature and daily precipitation through the end of the 21st century. Value was ultimately added to these datasets through coproduction of knowledge with impacts modelers and decision makers, which created usable climate projections for the end users' climate risk assessments. By working with these groups, we were able to identify their needs and make the appropriate decisions for the downscaling development.

While there are uncertainties in the models, downscaling techniques, and future emissions, results of the mean daily differences between historical and future climate variables indicate a decrease in mean daily precipitation in western portions of the basin and an increase in the east by the end of the century. Our seasonal analysis indicates that extreme values in some seasons may be driving the trends in mean daily precipitation, especially in the end-of-century period under RCP 8.5. In addition, daily minimum and maximum temperatures were projected to increase across the basin by up to 7°C, especially toward the end of the century and under a higher emission scenario. Results suggest that water resource managers and decision makers should not focus on one model or one downscaling technique, but the general trends show that they may need to plan for drier and hotter conditions in the western Red River Basin and wetter and hotter conditions in the east. Our analysis explores one possibility of the use of these datasets; however, it can be beneficial for many other studies regarding climatological and hydrological aspects in the region. Coproduction of knowledge between climate scientists and end users leads to data that are usable for those making decisions and climate risk assessments.

Data Availability

The NetCDF data used to support the findings of this study have been deposited in the Downscaling—Red River Basin repository (statistically downscaled time series for the Red River Basin (South Central U.S.A.), DOI: 10.15763/DBS.SCCSC.RR; (a) 1/10th of a degree observation based dataset, DOI: 10.15763/DBS.SCCSC.RR.0001; (b) downscaled climate variables from the CCSM4 GCM, DOI: 10.15763/DBS.SCCSC.RR.0002; (c) downscaled climate variables from the MIROC5 GCM, DOI: 10.15763/DBS.SCCSC.RR.0003; (d) downscaled climate variables from the MPI-ESM-LR GCM, DOI: 10.15763/DBS.SCCSC.RR.0004).

Conflicts of Interest

The authors declare that there are no conflicts of interest regarding the publication of this paper.

Acknowledgments

This material is based on the work supported by The National Science Foundation (Grant number OIA-1301789). In addition, support was provided by the Oklahoma Established Program to Stimulate Competitive Research (EPSCoR), the South Central Climate Adaptation Science Center, and the Southern Climate Impacts Planning Program. The authors give thanks to Keith, John L., Carlos, and others at GFDL for developing the datasets and thanks to impacts modelers at the University of Oklahoma and Aqua Strategies and water managers at Chickasaw Nation and Choctaw Nation of Oklahoma for working with us on the project.

References

[1] E. P. Maurer, L. Brekke, T. Pruitt et al., "An enhanced archive facilitating climate impacts and adaptation analysis," *Bulletin of the American Meteorological Society*, vol. 95, no. 7, pp. 1011–1019, 2014.

[2] B. Thrasher, J. Xiong, W. Wang, F. Melton, A. Michaelis, and R. Nemani, "Downscaled climate projections suitable for resource management," *Eos, Transactions American Geophysical Union*, vol. 94, no. 37, pp. 321–323, 2013.

[3] A. W. Wood, L. R. Leung, V. Sridhar, and D. P. Lettenmaier, "Hydrologic implications of dynamical and statistical approaches to downscaling climate model outputs," *Climatic Change*, vol. 62, no. 1–3, pp. 189–216, 2004.

[4] IPCC, "What is a GCM?," 2013, http://www.ipcc-data.org/guidelines/pages/gcm_guide.html.

[5] R. H. Moss, J. A. Edmonds, K. A. Hibbard et al., "The next generation of scenarios for climate change research and assessment," *Nature*, vol. 463, no. 7282, pp. 747–756, 2010.

[6] F. Feser, B. Rockel, H. von Storch, J. Winterfeldt, and M. Zahn, "Regional climate models add value to global model data: a review and selected examples," *Bulletin of the American Meteorological Society*, vol. 92, no. 9, pp. 1181–1192, 2011.

[7] C. Prudhomme, N. Reynard, and S. Crooks, "Downscaling of global climate models for flood frequency analysis: where are we now?," *Hydrological Processes*, vol. 16, no. 6, pp. 1137–1150, 2002.

[8] M. A. Semenov and E. M. Barrow, "Use of a stochastic weather generator in the development of climate change scenarios," *Climatic Change*, vol. 35, no. 4, pp. 397–414, 1997.

[9] UCAR, "Climate modeling," 2011, http://scied.ucar.edu/longcontent/climate-modeling.

[10] J. M. Eden, M. Widmann, D. Grawe, and S. Rast, "Skill, correction, and downscaling of GCM-simulated precipitation," *Journal of Climate*, vol. 25, no. 11, pp. 3970–3984, 2012.

[11] J. Schmidli, C. Frei, and P. L. Vidale, "Downscaling from GCM precipitation: a benchmark for dynamical and statistical downscaling methods," *International Journal of Climatology*, vol. 26, no. 5, pp. 679–689, 2006.

[12] E. A. Zagona, T. J. Fulp, R. Shane, T. Magee, and H. M. Goranflo, "Riverware: a generalized tool for complex reservoir system modeling1," *JAWRA Journal of the American Water Resources Association*, vol. 37, no. 4, pp. 913–929, 2001.

[13] R. L. Wilby, S. P. Charles, E. Zorita, B. Timbal, P. Whetton, and L. O. Mearns, "Guidelines for use of climate scenarios developed from statistical downscaling methods. Intergovernmental panel on climate change (IPCC) task group on data and scenario support for impacts and climate analysis (TGICA)," 2004, http://ipcc-ddc.cru.uea.ac.uk/guidelines/StatDown_Guide.pdf.

[14] K. Venkataraman, S. Tummuri, A. Medina, and J. Perry, "21st century drought outlook for major climate divisions of Texas based on CMIP5 multimodel ensemble: implications for water resource management," *Journal of Hydrology*, vol. 534, pp. 300–316, 2016.

[15] Q. Zhang and J. Zhang, "Drought hazard assessment in typical corn cultivated areas of China at present and potential climate change," *Natural Hazards*, vol. 81, no. 2, pp. 1323–1331, 2016.

[16] W.-H. Nam, M. J. Hayes, M. D. Svoboda, T. Tadesse, and D. A. Wilhite, "Drought hazard assessment in the context of climate change for South Korea," *Agricultural Water Management*, vol. 160, pp. 106–117, 2015.

[17] D. Bertrand and R. A. McPherson, "Future hydrologic extremes of the Red River basin," *Journal of Applied Meteorology and Climatology*, vol. 57, no. 6, pp. 1321–1336, 2018.

[18] U.S. Environmental Protection Agency, "Level III ecoregions of the continental United States," 2013, ftp://newftp.epa.gov/EPADataCommons/ORD/Ecoregions/us/Eco_Level_III_US.pdf.

[19] X. Xue, K. Zhang, Y. Hong et al., "New multisite cascading calibration approach for hydrological models: case study in the Red River basin using the VIC model," *Journal of Hydrologic Engineering*, vol. 21, no. 2, Article ID 05015019, 2015.

[20] Oklahoma Water Resources Board, "Red River Compact Commission," 2016, https://www.owrb.ok.gov/rrccommission/rrccommission.html.

[21] J. Malewitz, "Red river showdown: Texas-Oklahoma water war could reverberate across US," McClatchy—Tribune Business News, Tribune Content Agency LLC, 2013.

[22] Tarrant Regional Water District versus Herrmann, 569 U. S. (2013).

[23] F. Giorgi, B. Hewitson, J. Christensen, M. Hulme, and H. von Storch, "Regional climate information—evaluation and projections," in *Climate Change 2001: The Scientific Bases*, Cambridge University Press, Cambridge, UK, 2001.

[24] B. Livneh, E. A. Rosenberg, C. Lin et al., "A long-term hydrologically based dataset of land surface fluxes and states for the conterminous United States: update and extensions," *Journal of Climate*, vol. 26, no. 23, pp. 9384–9392, 2013.

[25] K. E. Taylor, R. J. Stouffer, and G. A. Meehl, "An overview of CMIP5 and the experiment design," *Bulletin of the American Meteorological Society*, vol. 93, no. 4, pp. 485–498, 2012.

[26] M. A. Giorgetta, J. Jungclaus, C. H. Reick et al., "Climate and carbon cycle changes from 1850 to 2100 in MPI-ESM simulations for the Coupled Model Intercomparison Project phase 5," *Journal of Advances in Modeling Earth Systems*, vol. 5, no. 3, pp. 572–597, 2013.

[27] P. R. Gent, G. Danabasoglu, L. J. Donner et al., "The community climate system model version 4," *Journal of Climate*, vol. 24, no. 19, pp. 4973–4991, 2011.

[28] M. Watanabe, T. Suzuki, R. O'ishi et al., "Improved climate simulation by MIROC5: mean states, variability, and climate sensitivity," *Journal of Climate*, vol. 23, no. 23, pp. 6312–6335, 2010.

[29] A. Wootten, "The subtle processes in statistical downscaling and the potential uncertainty," *US Clivar Variations*, vol. 16, no. 3, pp. 8–13, 2018, https://usclivar.org/newsletter/newsletters.

[30] J. Sheffield, A. P. Barrett, B. Colle et al., "North American climate in CMIP5 experiments. Part I: evaluation of historical simulations of continental and regional climatology," *Journal of Climate*, vol. 26, no. 23, pp. 9209–9245, 2013.

[31] P. M. Forster, T. Andrews, P. Good, J. M. Gregory, L. S. Jackson, and M. Zelinka, "Evaluating adjusted forcing and model spread for historical and future scenarios in the CMIP5 generation of climate models," *Journal of Geophysical Research: Atmospheres*, vol. 118, no. 3, pp. 1139–1150, 2013.

[32] M. J. Themeßl, A. Gobiet, and A. Leuprecht, "Empirical-statistical downscaling and error correction of daily precipitation from regional climate models," *International Journal of Climatology*, vol. 31, no. 10, pp. 1530–1544, 2011.

[33] A. J. Cannon, S. R. Sobie, and T. Q. Murdock, "Bias correction of GCM precipitation by quantile mapping: how well do methods preserve changes in quantiles and extremes?," *Journal of Climate*, vol. 28, no. 17, pp. 6938–6959, 2015.

[34] K. W. Dixon, J. R. Lanzante, M. J. Nath et al., "Evaluating the stationarity assumption in statistically downscaled climate projections: is past performance an indicator of future results?," *Climatic Change*, vol. 135, no. 3-4, pp. 395–408, 2016.

[35] D. Maraun, "Nonstationarities of regional climate model biases in European seasonal mean temperature and precipitation sums," *Geophysical Research Letters*, vol. 39, no. 6, Article ID L06706, 2012.

[36] P. C. D. Milly, J. Betancourt, M. Falkenmark et al., "Stationarity is dead: whither water management?," *Science*, vol. 319, no. 5863, pp. 573-574, 2008.

[37] National Climatic Data Center, *Surface Land Daily Cooperative Summary of the Day. NCDC Data Documentation for Data Set 3200*, National Climatic Data Center, Asheville, NC, USA, 2009.

[38] P. A. Michelangeli, M. Vrac, and H. Loukos, "Probabilistic downscaling approaches: application to wind cumulative distribution functions," *Geophysical Research Letters*, vol. 36, no. 11, Article ID L11708, 2009.

[39] H. Li, J. Sheffield, and E. F. Wood, "Bias correction of monthly precipitation and temperature fields from intergovernmental panel on climate change AR4 models using equidistant quantile matching," *Journal of Geophysical Research: Atmospheres*, vol. 115, no. D10, Article ID D10101, 2010.

[40] C. K. Ho, D. B. Stephenson, M. Collins, C. A. T. Ferro, and S. J. Brown, "Calibration strategies: a source of additional uncertainty in climate change projections," *Bulletin of the American Meteorological Society*, vol. 93, no. 1, pp. 21–26, 2012.

[41] D. W. Pierce, D. R. Cayan, E. P. Maurer, J. T. Abatzoglou, and K. C. Hegewisch, "Improved bias correction techniques for hydrological simulations of climate change," *Journal of Hydrometeorology*, vol. 16, no. 6, pp. 2421–2442, 2015.

[42] L. Wang and W. Chen, "Equiratio cumulative distribution function matching as an improvement to the equidistant approach in bias correction of precipitation," *Atmospheric Science Letters*, vol. 15, no. 1, pp. 1–6, 2014.

[43] X. Liang, E. F. Wood, and D. P. Lettenmaier, "Surface soil moisture parameterization of the VIC-2L model: evaluation and modification," *Global and Planetary Change*, vol. 13, no. 1–4, pp. 195–206, 1996.

[44] E. P. Maurer and D. W. Pierce, "Bias correction can modify climate model simulated precipitation changes without adverse effect on the ensemble mean," *Hydrology and Earth System Sciences*, vol. 18, no. 3, pp. 915–925, 2014.

[45] J. Sillmann, V. V. Kharin, X. Zhang, F. W. Zwiers, and D. Bronaugh, "Climate extremes indices in the CMIP5 multimodel ensemble: Part 1. Model evaluation in the present climate," *Journal of Geophysical Research: Atmospheres*, vol. 118, no. 4, pp. 1716–1733, 2013.

[46] R. Knutti and J. Sedláček, "Robustness and uncertainties in the new CMIP5 climate model projections," *Nature Climate Change*, vol. 3, no. 4, pp. 369–373, 2013.

[47] D. M. Nover, J. W. Witt, J. B. Butcher, T. E. Johnson, and C. P. Weaver, "The effects of downscaling method on the variability of simulated watershed response to climate change in five U.S. basins," *Earth Interactions*, vol. 20, no. 11, pp. 1–27, 2016.

[48] L. Qiao, C. B. Zou, C. F. Gaitán, Y. Hong, and R. A. McPherson, "Analysis of precipitation projections over the climate gradient of the Arkansas Red River basin," *Journal of Applied Meteorology and Climatology*, vol. 56, no. 5, pp. 1325–1336, 2017.

[49] X. Liang, D. P. Lettenmaier, E. F. Wood, and S. J. Burges, "A simple hydrologically based model of land surface water and energy fluxes for general circulation models," *Journal of Geophysical Research*, vol. 99, no. D7, pp. 14415–14428, 1994.

[50] N. Nyaupane, B. Thakur, A. Kalra, and S. Ahmad, "Evaluating future flood scenarios using CMIP5 climate projections," *Water*, vol. 10, no. 12, p. 1866, 2018.

[51] V. Sridhar, P. Modi, M. M. Billah, P. Valayamkunnath, and J. L. Goodall, "Precipitation extremes and flood frequency in a changing climate in southeastern Virginia," *JAWRA Journal of the American Water Resources Association*, vol. 55, no. 4, pp. 780–799, 2019.

[52] RiverWare, "RiverWare overview," 2015, http://www.riverware.org/riverware/overview.html.

Hindawi
Advances in Meteorology
Volume 2019, Article ID 9461513, 14 pages
https://doi.org/10.1155/2019/9461513

Research Article

Drought Early Warning and the Timing of Range Managers' Drought Response

Tonya R. Haigh,[1] **Jason A. Otkin**,[2] **Anthony Mucia**,[3] **Michael Hayes**,[4] **and Mark E. Burbach**[5]

[1]*National Drought Mitigation Center, University of Nebraska-Lincoln, Lincoln 68583, USA*
[2]*Cooperative Institute for Meteorological Satellite Studies, Space Science and Engineering Center, University of Wisconsin-Madison, Madison 53706, USA*
[3]*CNRM UMR 3589, Météo-France/CNRS, Toulouse 31057, France*
[4]*School of Natural Resources, University of Nebraska-Lincoln, Lincoln 68583, USA*
[5]*Conservation and Survey Division, School of Natural Resources, University of Nebraska-Lincoln, Lincoln 68583, USA*

Correspondence should be addressed to Tonya R. Haigh; thaigh2@unl.edu

Received 1 March 2019; Revised 15 July 2019; Accepted 25 July 2019; Published 9 October 2019

Guest Editor: Jayant K. Routray

The connection between drought early warning information and the timing of rangeland managers' response actions is not well understood. This study investigates U.S. Northern Plains range and livestock managers' decision-making in response to the 2016 flash drought, by means of a postdrought survey of agricultural landowners and using the Protective Action Decision Model theoretical framework. The study found that managers acted in response to environmental cues, but that their responses were significantly delayed compared to when drought conditions emerged. External warnings did not influence the timing of their decisions, though on-farm monitoring and assessment of conditions did. Though this case focused only on a one-year flash drought characterized by rapid drought intensification, waiting to destock pastures was associated with greater losses to range productivity and health and diversity. This study finds evidence of unrealized potential for drought early warning information to support proactive response and improved outcomes for rangeland management.

1. Introduction

The goal of monitoring and early warning of natural hazards is the provision of reliable and timely information to inform decision-making in ways that reduce harm of loss [1]. Scientists recommend that agricultural producers, like other resource managers, use climate data as well as on-site observations to monitor and predict drought in order to manage it effectively and minimize damages [2, 3]. In the U.S., for example, monitoring tools such as the U.S. Drought Monitor [4] and NOAA Climate Prediction Center Seasonal Drought Outlook (http://droughtmonitor.unl.edu) may be used to enhance producers' decision-making. However, inserting additional information into the decision-making process does not guarantee effective use of that information. Rather, research has found a significant gap between information provision and information use [5, 6]. The realization of successful drought early warning, therefore, lies as much with the potential users as with the providers of monitoring information. It requires (1) that the information will be accessed and understood by decision-makers; (2) that decision-makers will use the information to make timely and effective coping and adaptation decisions as a result of incorporating the information; and (3) that the decisions made will result in fewer, or less severe, impacts (harm or loss) due to drought [7, 8].

The integration of drought early warning into rangeland managers' coping and adaptive decision-making requires an understanding of the complexity of livestock-rangeland systems and drought response options [9]. Decision-making in agricultural systems is complex even before drought begins to emerge. Rangeland managers act within multifaceted,

interconnected socioecological systems that encompass rangeland ecosystems, livestock production, markets, and business and family systems [10]. Their decision-making to-do lists includes tasks that need to be carried out in the next few days, over the coming weeks or months, as well as into future seasons or years [11]. When a drought event occurs, range and livestock managers' responses are varied in type, scope, and timing [12–15]. While some managers make incremental modifications to their management in response to drought, others act in ways that may transform their operations for the long term; and while some focus on on-farm responses, others may hope for off-farm (governmental) assistance. Managers' decisions to take actions—proactively before drought emerges, concurrently as it emerges, and/or responsively after drought has clearly taken hold—are likely to have unique outcomes in terms of impacts to the socioecological system [16]. Yet, there is little documentation of the outcomes of proactive, concurrent, and responsive decision-making in rangeland-based livestock systems or the timing of decision-making that might classify an action as proactive versus responsive.

The timing of decision-making is a critical, yet understudied, aspect of drought early warning [17]. In some regions of the world, the timing of response is of concern because of the risk of emergent food insecurity or even famine [18]. In these instances, the timing of agricultural producers' response to drought may provide cues to relief agencies as to how quickly relief may be needed [19]. In the U.S. Great Plains, drought has not been associated with famine. However, the timing of producers' responses, as much as what their responses are, affects the long-term ecological health of grasslands and croplands, water supplies, agricultural markets, farm economics, and the health of decision-makers, families, and communities [20, 21]. Despite the importance of the timing of response, little is known about how agricultural producers make their decisions to begin a drought response action, or the degree to which drought monitoring information is used to trigger the beginning the response.

2. Conceptual Framework

The use of early warning information in coping and adaptation is a focus of a body of research in short-term emergency responses to fires, hurricanes, and other disasters. One prominent guiding theoretical model, the Protective Action Decision Model (PADM) [22], locates the role of early warning information in a social-psychological process of decision-making in response to hazards. Specifically, warnings are seen as cues to action that inform an individual's processes of perceiving and comprehending the nature of the threat [22, 23]. Warnings include all sources of information that convey a threat, commonly communicated through the media, alarms, presentations, or decision tools [24]. Cues to action may also come from the natural or social environment [22]. For the range-based livestock manager, for example, deviations from normal in precipitation or forage growth may be natural environmental cues that a drought threat is at hand. Social cues may come in the form of heightened awareness due to observations of increased sales at the livestock barn or increases in local forage prices.

The existence of a cue does not itself spontaneously lead to an individual taking protective action. Rather, the individual must observe, pay attention to, and comprehend the cue, then establish that the cue represents enough of a personal risk to necessitate taking action, and finally identify and choose among options for response [22]. Individuals who process and move through these stages quickly may take protective action earlier than those who spend more time addressing uncertainty and processing information [25, 26]. Thus, examining drought coping response within this framework may lead to better understanding of the drivers of proactive and responsive or reactive coping actions [16].

Drought is a notoriously difficult natural hazard to perceive, adding to the uncertainty and complexity of decision-making [27]. In complex decision-making environments, managers may encounter multiple and conflicting types of cues to action. Environmental and social cues may be asynchronous or contradict one another. Sources of warning may not provide consistent messages of the nature or severity of the threat. And warnings may differ in timing, precision, visibility, message specificity to the audience, and other characteristics that have been summarized by Cash et al. [28] as information salience, credibility, and legitimacy and by Lemos et al. [5] as the perceived fit, interplay, and interaction of the information by decision-makers. A better understanding of the choices and timing of rangeland managers' drought coping responses in the context of environmental, social, and early warning cues will enable information providers, risk communicators, and educators/advisors to more effectively provide information that meets decision-maker needs.

3. Materials and Methods

3.1. Selection of the Study Area. This study investigates the triggers of drought response and examines the role of early warning information in timely drought response decision-making. To do so, U.S. Northern Great Plains livestock producers were surveyed about their coping decisions (related to feed, forage, and grazing pressure) in response to a 2016 flash drought. As reported in Otkin et al. [29], the 2016 drought event developed by the end of March, in response to a prolonged period of warmer than normal temperatures and near- to below-normal precipitation during the preceding fall and winter. April brought wetter conditions to much of the region, but by the end of May, very dry conditions returned to most of the region, and temperatures were also much cooler than normal. Several hard freezes occurred across the region, heavily damaging the vegetation in some locations. In June, rapid drought intensification occurred, with much warmer than normal temperatures and continued below-normal precipitation and drought intensity peaked across the region by the middle of July. Precipitation began normalizing toward the end of August.

The drought event affected parts of a four-state region including portions of South Dakota, Wyoming, Nebraska, and Montana. Livestock production in the study region is dominated by cow-calf enterprises that depend upon local

rangelands as well as regional supplies of hay and feed. The predominant land cover of the region ranges from tall-grass to short-grass prairie and contains mixed shrub/grassland, forage, wheat, corn, and sugar beet-producing cropland, and forestland. The area is largely dependent upon precipitation for agricultural production, with limited areas of irrigated cropland (https://earlywarning.usgs.gov/images/usewem/2012_MIrAD_CONUS.png). In 2016, the primarily rural region experienced drought impacts such as forest and grassland fires, reductions in grain yields, reduced forage production, water quality and quantity problems, and economic losses [30]. Economic losses may have been compounded by low prices for feeder cattle, while also somewhat alleviated by plentiful hay stocks nationally and locally [31]. These characteristics make the area and drought event appropriate for studying rangeland managers' drought response and use of drought monitoring/early warning information.

3.2. Sampling Design and Survey Instrument. Livestock producers were identified through a Farm Services Agency list of agricultural landowning households with a history of production forage, wheat, corn, or sugar beets, whose addresses place them within the study region. The sample was stratified based on the location of their addresses in relation to the 2016 drought's extent and severity. Four strata were defined by the U.S. Drought Monitor (USDM) severity level (D0, D1, D2, and D3) of the landowner's county in mid-July 2016 (representing the greatest severity and geographic extent of the drought event) (Figure 1). The USDM is a composite measure of drought stress [4] used to depict abnormally dry conditions (D0) and four drought categories including moderate (D1), severe (D2), extreme (D3), and exceptional (D4) drought. In order to ensure representation of landowners experiencing all four levels of drought severity, landowners living in USDM D0 and D1 strata (which happened to include more highly populated counties) were undersampled, while landowners living in USDM D2 and D3 strata (which happened to include less populated counties) were oversampled.

The survey was administered by the National Drought Mitigation Center via the U.S. Postal Service following the Dillman [32] protocol, with a presurvey letter mailed in early November 2016, an initial survey mailing in late November 2016, and a follow-up survey mailing in early January 2017. Of the 2,389 surveys that were mailed out, 516 (22%) were returned/not refused. Of these, 252 were received from eligible agricultural producers who reported raising livestock and used in this analysis.

The survey instrument was developed with the input of content and theory experts and pretested with agricultural extension personnel volunteers. The questionnaire focused on the 2016 drought and included questions about timing of drought-related conditions as observed by the respondents, the types and timing of drought management actions that they took, the types and influence of drought monitoring information they used, and the impacts they experienced. Specific question wording is listed in Appendix A. Measures of outcome variables included

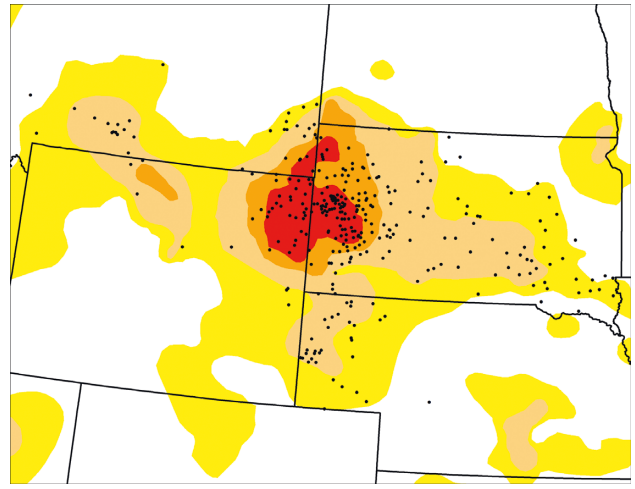

Figure 1: Points represent the approximate locations of survey respondents and are randomly distributed within respondents' zip codes, to protect individual identities. The colors on the map represent the U.S. Drought Monitor designation as of July 26, 2016, with yellow indicating abnormal dryness, tan indicating moderate drought, orange indicating severe drought, and red indicting extreme drought.

(i) Whether or not respondents took any of the following actions in response to drought: purchasing more hay or feed than usual to supplement existing feed stocks; grazing fall or winter pastures earlier than planned; destocking pastures more than usual through culling, early weaning, ending grazing contracts, sending to feedlot, etc. of any livestock; and culling and selling more breeding animals, specifically, than usual. If a respondent took none of the listed actions in 2016, they were considered to have not responded to the drought for the sake of this analysis.

(ii) If the respondent took action in any of the ways listed above, in what month they began doing so (January–December 2016). Respondents who did not take an action were listed as missing for this variable.

(iii) The respondent-reported impacts of the 2016 drought, by percentage of yield or productivity lost (0–100%), on each of the following: pasture hay yield; range productivity; range health or diversity; animal gain/productivity; net income of the operation; and cash reserves or savings.

(iv) Respondents' perceptions as to whether better information would have led them to respond differently and whether responding differently would have led to different impacts.

Measures of predictor variables included

(i) Respondents' observations of various conditions related to drought and the timing of the observations, including decreased topsoil moisture; delayed/lack of plant emergence; delayed/lack of plant growth; deteriorating range conditions; and

decreased forage productivity. For respondents who reported not observing a condition at all, their date of observing the condition was reported as 366, rather than as missing.

(ii) Respondents' use and perceived influence of their own methods of monitoring drought, including on-farm rain gauges or soil moisture sensors and/or their own assessment of crop, range, and livestock conditions. Respondents not using a source were coded as "0" while respondents using were coded as the level of influence from "1" (not influential) to "3" (very influential).

(iii) Respondents' use and perceived influence of external sources of drought monitoring or early warning information, including local extension, the U.S. Department of Agriculture, National Weather Service, and the U.S. Drought Monitor. These sources were chosen as known sources of weekly, monthly, and seasonal drought monitoring and/or outlook products and information. The U.S. Drought Monitor (https://www.droughtmonitor.unl.edu) is released weekly throughout the year and is featured by news media outlets, included in extension and USDA publications, shared via social media, and accessed online. The Climate Prediction Center provides temperature and precipitation outlooks and monthly and seasonal drought outlooks (http://www.weather.gov). The USDA provides a Weekly Weather and Crop Bulletin (https://www.usda.gov/oce/weather/pubs/Weekly/Wwcb/), and local extension offices provide drought information to producers through reports and presentations (https://drought.unl.edu/archive/Documents/NDMC/Workshops/795/Pres/Edwards-SD2016USDM.pdf). Respondents not using a source were coded as "0" while respondents using were coded as the level of influence from "1" (not influential) to "3" (very influential).

Specific research hypotheses evaluated during this study included

(1) The decision whether or not to take drought response actions is predicted by
   (a) Drought severity experienced
   (b) Respondents' observation of drought conditions, and/or
   (c) Respondents' use and influence of their own monitoring or external early warning information

(2) The timing of respondents' drought response actions is predicted by
   (a) Drought severity experienced
   (b) The timing of respondents' observation of drought conditions, and/or
   (c) Respondents' use and influence of their own monitoring/assessments or external early warning information

(3) Respondents who are delayed in their actions experience drought impacts differently from those who acted earlier

3.3. Measures of Drought Emergence and Severity. Multiple measures of drought emergence and severity were examined throughout the analysis, as measures of environmental cues to action and as a control variable for determining statistical relationships. The median 3-month Standardized Precipitation Evapotranspiration Index (SPEI) for the months of October 2015 through June 2016 was used to represent measures of the overall dryness experienced by each survey respondent during the months that drive forage productivity in the region [33]. The 3-month SPEI depicts the balance between precipitation and potential evapotranspiration over the previous 3 months, calculated at weekly intervals [3]. County-level weighted averages were computed using station-based historical data that were interpolated using inverse distance weighting.

Other indicators of drought were examined because of their direct relationship with our measures of respondent-perceived drought conditions. The North American Land Data Assimilation System topsoil and total column moisture (NLDAS TS and TC) provide model-based objective measures of topsoil and subsoil moisture that correlate with respondent-perceived emergence of depleted topsoil and subsoil moisture. These measures are based on models that simulate changes in soil moisture and temperature throughout layers of the soil profile [29]. For this analysis, gridded soil moisture analyses were obtained from NLDAS at 0.1258 degree resolution [34], with soil moisture anomalies computed over 4-week time periods using data from 1979–2017. Ensemble mean analyses were used for topsoil (TS; 0–10 cm) and total column (TC; 0–2 m) soil moisture measures. Each dataset was aggregated to the zip code level for the study region. As reported in Otkin et al. [29], respondents' recollection of the timing of top soil moisture depletion generally aligned with drought development as indicted by NLDAS TS.

The Evaporative Stress Index (ESI) was examined to depict moisture-related stress in vegetation, both related to vegetation health and to soil moisture availability [35]. The ESI depicts standardized anomalies in the ratio of actual to reference evapotranspiration, and deteriorating conditions as measured by ESI have been shown to correspond with the timing of respondent reports of plant stress [29]. For this analysis, the ESI was computed at 4 km horizontal grid spacing, with 4 week ESI anomalies at weekly intervals using data from 2001 to 2017 [29, 35]. Each dataset was aggregated to the zip code level for the study region.

3.4. Time Series Comparisons. The relationships between the emergence and development of drought conditions and the timing of drought response actions were examined through a novel method introduced by Otkin et al. [29]. The relationships between drought response action timing and the associated 4 week ESI, NLDAS TS, and NLDAS TC trends were quantified by averaging each dataset over all zip codes during a 12 week period centered on the date that each response action was first taken (week zero). For a given zip code, a shape file was used to identify all of the grid points on

the 4-km resolution grid located within that zip code. Values for these grid points were then used to compute the mean for each dataset. An average time series for each survey question and dataset was then generated using the recentered time series from all respondents who responded with a month that they began taking drought response actions. These recentered time series were used to evaluate relationships between the timing of the reported management actions and the timing of drought development in the drought monitoring datasets. Recentering the time series for each response prior to computing the average time series promotes a more robust comparison of the datasets because the differential timing of drought development across the region is included in the measure.

3.5. Statistical Analysis. Testing the hypotheses and identifying factors that predict actions taken, the timing of actions, and drought impacts required controlling for average drought severity. Regression models were used to estimate the coefficient of predictive variables with the control variable in the model. Predictors of whether or not drought response actions were taken, as binary categorical outcomes, were examined using logistic regression models. Predictors of the month respondents began taking action, as ordinal categorical outcomes, were examined using ordered logistic regressions (proportional odds models [36]). Predictors of integer variables, including the date of observed drought conditions, as well the percent loss impact of drought, were examined using linear regression models. Logical skip-patterns in data led to substantial missing data for some variables. Cases with missing data were eliminated from analysis using pairwise deletion. Data were unweighted, but stratification was accounted for in the analysis using the STATA "svy" method (STATA v. 11) [37]. Statistical significance was determined with a 95% confidence level at an alpha = 0.05.

4. Results and Discussion

4.1. Description of Respondents and Drought Response. Respondents almost all raised beef cattle, owned and ranted/leased a mean land base of 1,983 ha (range 16 ha–15,176 ha), and had gross sales ranging from less than $25,000 to more than $500,000 annually. Consistent with the sampling frame, all respondents lived in areas that experienced some level of dryness in 2016, ranging from abnormal dryness to extreme drought. Some respondents began observing drought conditions as early as the winter of 2015-2016, but most reported seeing early indications of dryness (decreased topsoil moisture and/or delayed or lack of plant emergence) in May. The most frequently reported month for beginning to observe decreased subsoil moisture, delayed/lack of plant growth, and/or decreased forage productivity was June. The most frequently reported month for beginning to observe deteriorating range conditions was July. Descriptive statistics for all predictor and outcome variables can be found in Table 1.

In response to the drought, respondents took a number of coping actions and varied in the timing of their actions. Figure 2 shows the timeline of actions taken. Two-thirds of respondents grazed fall or winter pastures early, primarily in August and September 2016. Over half of respondents destocked their pastures more than usual due to drought, through any culling, early weaning, ending grazing contracts, or sending livestock to feedlots. While some respondents began destocking as early as May or June, most waited to begin destocking until September 2016. Of the 57% of respondents who purchased supplemental hay or feed in 2016, some began in early summer but most waited to begin purchasing until October 2016. Similarly, of the 46% of respondents who culled their breeding herd, the peak month for beginning that particular action was October 2016. Most respondents used multiple response strategies. Respondents who used both early grazing fall/winter pastures and destocking as drought response strategies tended to begin destocking later in the season compared to those who destocked but did not early graze fall/winter pastures. Other actions did not affect the timing of one another.

In terms of drought monitoring and early warning information, respondents were more likely to use and be influenced by their own on-farm monitoring or assessments of drought conditions than any external source of early warning information. Of the external sources of monitoring/drought early warning information listed, respondents perceived the National Weather Service to be the most influential to their farm management during drought and local Extension information to be the least influential. Other sources, including the U.S. Drought Monitor and resources provided by the U.S. Department of Agriculture, fell towards the middle.

4.2. Factors Affecting Respondents' Drought Response. Approximately 87% of respondents reported taking some type of management action in response to drought conditions. Table 2 lists the log-odds coefficients of variables used to predict the likelihood of respondents' taking action, controlling for the median 3-month SPEI. Respondents who observed delayed or lack of plant emergence or growth, decreased forage production, and/or deteriorated range conditions, even controlling for drought severity (SPEI), were more likely than others to purchase supplemental hay or feed, graze fall/winter pastures earlier than usual, destock any livestock more than usual, and/or reduce the size of breeding herds. The degree to which managers used and were influenced by USDA resources was also associated with the likelihood of culling the breeding herd, regardless of drought severity. The 13% of the respondents in this study who did not take any of the listed actions experienced significantly less dryness over the October 2015–June 2016 timeframe than did the rest of the sample and were less likely than others to observe any drought-related conditions. These findings support hypothesis 1, providing some evidence that respondents' use and influence of early warning information contributed to their perceptions of personal risk and

Table 1: Descriptive statistics.

Operation characteristics	Proportions or means (n)
Types of livestock produced	Beef cattle—97% ($n = 237$)
Total hectares	Mean 1,893 (SE 2,369) ($n = 234$)
Operation gross sales ($)	<25,000—10 25,000–99,999—30% 100,000–249,000—33% 250,000–499,999—17% 500,000+—9% ($n = 229$)
Use and influence of drought monitoring information	On-farm rain gauge ($n = 237$), mean = 1.58 (SD 1.19) Own assessment ($n = 234$), mean = 2.13 (SD 1.17) Local extension resources ($n = 236$), mean = 0.60 (SD 0.95) National weather service ($n = 235$), mean = 1.60 (SD1.08) U.S. drought monitor ($n = 236$), mean = 1.23 (SD 1.15) USDA resources ($n = 232$), mean = 0.88 (SD 1.08) Television/radio reports ($n = 234$), mean = 1.69 (SD 0.98)
Average 3-month SPEI between October 2015 and June 2016 experienced by respondents	Mean = −0.10 (SD 0.26), with a range of −0.60 to 0.57 ($n = 246$)
Conditions observed by respondents	Decreased topsoil moisture ($n = 250$)—96%, May (mode) Delayed or lack of plant emergence ($n = 225$)—74%, May Decreased subsoil moisture ($n = 239$)—96%, June Delayed or lack of plant growth ($n = 243$)—91%, June Decreased forage productivity ($n = 235$)—94%, June Deteriorating range conditions (=n235)—94%, July
Actions taken and mode month	Graze fall or winter pastures earlier than planned ($n = 228$), 68%, Sept Destock pastures more than usual ($n = 224$), 56%, Sept Purchase more supplemental hay/feed than usual ($n = 224$), 57%, Oct Cull and sell more breeding animals than usual ($n = 221$), 47%, Oct Took none of these actions ($n = 235$), 14% N/A
Mean percent loss from 2016 drought	Pasture hay yield ($n = 197$), 65.76% (31.86) Range productivity ($n = 180$), 49.17% (24.72) Range health or diversity ($n = 134$), 38.31% (30.37) Animal gain or productivity ($n = 158$), 12.18% (16.68) Net income of operation ($n = 196$), 32.52% (22.50) Cash reserves or savings ($n = 151$), 25.15% (26.27)
Would have acted earlier or differently, given earlier warning	28% yes ($n = 243$)
Would have seen less harm, given different/earlier action	25% yes ($n = 241$)

Data sources: 2016 survey, SPEI (droughtatlas.unl.edu).

influenced their decisions to take at least one of the actions, as predicted by the PADM [22].

4.3. Factors Affecting the Timing of Respondents' Drought Response. On average, managers did not begin responding to the drought until the fall of 2016, even if drought was severe months earlier. Average dryness, as measured by the 3-month SPEI, between October 2015 and June 2016 was useful for predicting the start of early grazing, with more severe drought associated with earlier start dates. SPEI did not predict the timing of other actions. Table 2 lists the log-odds coefficients of other variables used to predict the timing of respondents' actions, controlling for the median 3-month SPEI. The timing of respondents' observations of emerging drought conditions was statistically unrelated to the timing of actions, with one exception: the timing of observation of

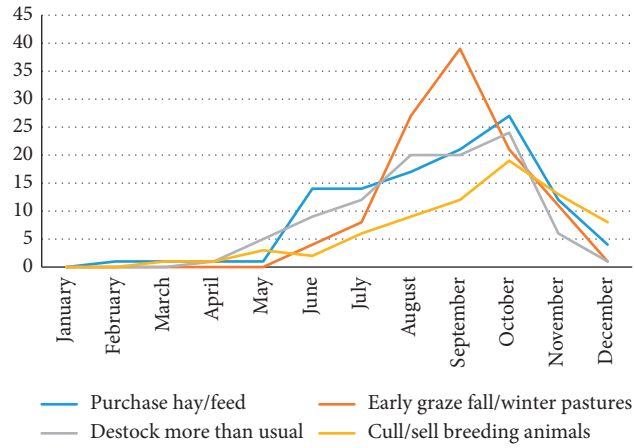

Figure 2: Number of respondents who took each action in response to drought conditions in 2016 by month.

delayed plant emergence was negatively correlated with the timing of destocking pastures. In other words, respondents who observed delayed plant emergence earlier in the year reported later destocking dates than those who observed the condition later or not at all, which is the opposite of the expected relationship predicted by the PADM model.

In general, respondents observed conditions that indicated the development of drought well in advance of taking drought response actions. While respondents' observations of on-the-ground drought conditions were largely synchronous with the development of the drought as measured by NLDAS TS, NLDAS TC, and ESI (as reported in Otkin et al. [29]), the timing of their drought response actions was not. Figures 3 and 4 demonstrate the relationships between objective drought measures and respondents' observations and the lack of relationships with respondents' actions. Figure 3 shows the average trends in the three measures in relation to the date of respondents' first observations (week 0) of decreased topsoil moisture, delayed/lack of plant emergence, delayed/lack of plant growth, plant stress, deteriorating range conditions, and decreased forage productivity. In all cases, on average, NLDAS TS, NLDAS TC, and ESI indicated the emergence and increased severity of drought in time with respondents' observations. Each time series shows a downward trend from normal conditions to drought (falling below −0.5 on each mean standardized anomaly).

Analysis of the trends in the emergence and development of the drought, as measured by NLDAS TS, NLDAS TC, and ESI, demonstrates the lack of relationship between the timing of the emergence of drought and the timing of drought response (Figure 4). Whereas drought-related conditions were observed in time with increasing deviation from normal in soil moisture or evaporative stress, the drought response actions began (on average) during either an upward trend or no trend in drought indices. Time series lines that show neither an upward nor a downward trend indicate either stable conditions or no trend in drought conditions on average. Time series lines showing an upward trend indicate that drought conditions (as measured by these indices) were generally improving by the time the action was taken, on average.

A return to normal conditions does not imply that drought impacts have disappeared or that drought management actions are not necessary. ESI, for example, may show improvements with late-season green-up that do not necessarily indicate adequate forage availability [17]. It has been demonstrated that, for the study region, precipitation over the winter months and spring is a critical determinant of forage productivity during the summer [33]. In western South Dakota, over 60% of annual forage production occurs by July 1 and 90% by August 15, while in eastern Montana, 90% of annual forage production occurs by July 1 [38]. Grazing preferred forages during late-season green-up after drought is generally not recommended, as it can damage the following years' production (https://hayandforage.com/article-1253-recovering-pastures-after-a-drought.html; https://newsroom.unl.edu/announce/beef/6982/39981; https://www.ag.ndsu.edu/archive/dickinso/grassland/news/news5.htm; https://www.drovers.com/article/grazing-considerations-dr). Thus, respondents were likely respondent to observed drought impacts when they chose to take action, rather than responding to leading indicators of drought emergence and development. These results provide only weak support for hypotheses 2(a) and 2(b).

There is some evidence that respondents who conducted their own on-farm monitoring or other assessments of local conditions timed their drought response actions differently from others, providing some support for hypothesis 2(c). First, respondents who said that their own assessments of conditions were influential in their decision-making reported earlier observations of decreased topsoil moisture (Table 3) and also tended to destock earlier than those who did not (significant at 0.10). This relationship with the timing of destocking, while only marginally significant, is in the direction that would be expected theoretically. It is possible that managers who assessed conditions throughout the drought were somewhat faster in determining that drought posed a risk to them and deciding that action needed to be taken sooner rather than later, as would be predicted by the PADM [22]. However, another relationship between monitoring and the timing of action is in the opposite direction. Respondents who said that their on-farm monitoring (rain gauge or soil moisture sensors) was influential

Table 2: Factors affecting respondents' drought response coping actions and timing.

	Purchase supplemental feed (*y*/*n*)	Early graze fall/winter pastures (*y*/*n*)	Destock (*y*/*n*)	Cull breeding herd (*y*/*n*)	Timing—purchasing feed	Timing—early grazing	Timing—destocking	Timing—culling breeding herd
SPEI	−2.87** (224)	−1.54** (228)	−1.55** (224)	−2.17** (221)	1.52 (112)	1.78** (111)	−0.31 (97)	−1.12 (74)
Observed decreased topsoil moisture (*y*/*n*)	0.65 (221)	2.12* (225)	1.59 (222)	Omit (210)	n/a	n/a	n/a	n/a
Observed delayed/lack of plant emergence (*y*/*n*)	0.81** (212)	1.01** (215)	0.42 (213)	0.87** (210)	n/a	n/a	n/a	n/a
Observed delayed/lack of plant growth (*y*/*n*)	−0.06 (219)	2.19** (223)	1.45** (219)	−0.05 (217)	n/a	n/a	n/a	n/a
Observed deteriorating range conditions (*y*/*n*)	0.85 (218)	3.28** (222)	1.96** (217)	2.27** (214)	n/a	n/a	n/a	n/a
Observed decreased forage productivity (*y*/*n*)	0.62 (217)	1.71** (221)	1.13* (219)	0.86 (216)	n/a	n/a	n/a	n/a
Timing of decreased topsoil moisture	n/a	n/a	n/a	n/a	0.00 (111)	0.00 (110)	0.00 (97)	−0.00 (72)
Timing of delayed/lack of plant emergence	n/a	n/a	n/a	n/a	0.00 (109)	−0.00 (105)	−0.00** (94)	−0.00 (71)
Timing of delayed/lack of plant growth	n/a	n/a	n/a	n/a	0.00 (106)	0.00 (109)	−0.00 (96)	−0.00 (73)
Timing of deteriorating range conditions	n/a	n/a	n/a	n/a	0.00 (109)	−0.00 (110)	−0.00 (96)	−0.01* (73)
Timing of decreased forage productivity	n/a	n/a	n/a	n/a	0.00 (110)	−0.00 (108)	−0.00 (95)	−0.00 (72)
Use/influence on-farm monitoring	−0.06 (213)	−0.09 (216)	0.07 (212)	0.14 (210)	−0.05 (108)	0.33** (107)	−0.09 (92)	0.01 (68)
Use/influence own assessment of conditions	−0.21 (212)	0.04 (215)	0.07 (211)	−0.11 (208)	−0.04 (107)	−0.13 (108)	−0.39* (93)	−0.23 (68)
Use/influence local extension	0.37** (213)	0.04 (216)	−0.09 (212)	0.15 (209)	0.11 (107)	0.13 (108)	0.06 (92)	−0.13 (67)
Use/influence NWS	0.25* (214)	0.15 (217)	0.08 (213)	0.09 (210)	0.09 (108)	0.14 (108)	−0.06 (93)	−0.11 (68)
Use/influence U.S. drought monitor	0.30** (212)	0.04 (215)	0.24* (211)	0.13 (208)	0.12 (106)	−0.09 (107)	0.03 (92)	−0.10 (68)
Use/influence USDA resources	0.43** (213)	0.15 (216)	0.16 (212)	0.31** (209)	−0.09 (107)	−0.18 (107)	0.09 (93)	0.04 (68)
Use/influence TV/radio	−0.01 (211)	0.09 (214)	0.16 (210)	0.00 (207)	−0.04 (106)	0.08 (108)	0.10 (93)	−0.41* (68)
Purchase supplemental feed (*y*/*n*)	n/a	n/a	n/a	n/a	n/a	−0.26 (104)	0.21 (90)	0.58 (70)
Early graze fall/winter pastures (*y*/*n*)	n/a	n/a	n/a	n/a	−0.32 (108)	n/a	1.17** (92)	−0.41 (70)
Destock (*y*/*n*)	n/a	n/a	n/a	n/a	−0.19 (104)	−0.12 (103)	n/a	−0.33 (70)
Cull breeding herd (*y*/*n*)	n/a	n/a	n/a	n/a	−0.039 (106)	−0.35 (104)	−0.17 (89)	n/a

Reporting coefficients listed in log-odds units, significance of test that coefficient is different from 0, and (*n*). For SPEI, the coefficient is determined without other covariates. For other predictors, coefficients are determined when controlling for SPEI. Data sources: 2016 survey, SPEI (droughtatlas.unl.edu). $^{*}p < 0.10$; $^{**}p < 0.05$.

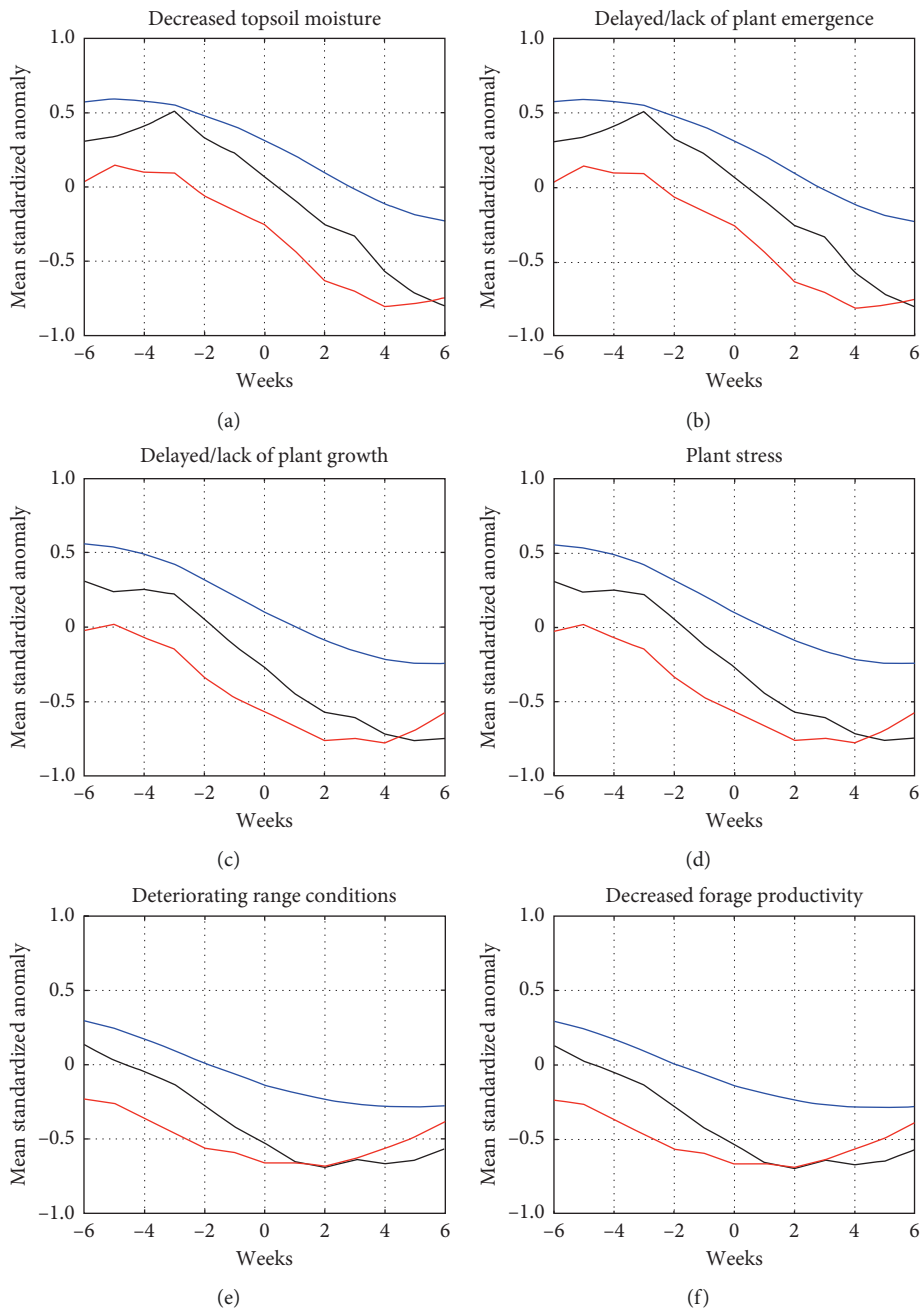

Figure 3: Time series showing the average condition depicted by anomalies in the ESI (black line) NLDAS TS (red line) and NLDAS TS (blue line) data sets at weekly intervals from six weeks prior to six weeks after the onset: (a) decreased topsoil moisture, (b) delayed/lack of plant emergence, (c) delayed/lack of plant growth, (d) plant stress, (e) deteriorating range conditions, and (f) decreased forage productivity as reported by the respondents.

tended to begin grazing fall/winter pastures later than others did, even though more severe SPEI predicted earlier fall/winter grazing. Using the PADM framework, this may indicate that managers using on-farm rain gauges or soil moisture sensors were later than others to determine the need for protective action in the form of early grazing fall/winter pastures or decided that later action was desirable. One possibility is that managers who used on farm monitoring were more likely than others to be able to reserve fall/winter pastures for their intended purpose, rather than as an emergency feed source. Other covariates not included in this analysis may be necessary to explain the relationship.

The degree to which respondents used and were influenced by external sources of early warning information did not predict the timing of respondents' drought actions, providing lack of support for hypothesis 2(c). That is not to say that drought early warning had no effect on respondents at all. Increased use/influence of multiple sources of drought early warning information was associated with earlier observations of delayed/lack of plant growth and decrease

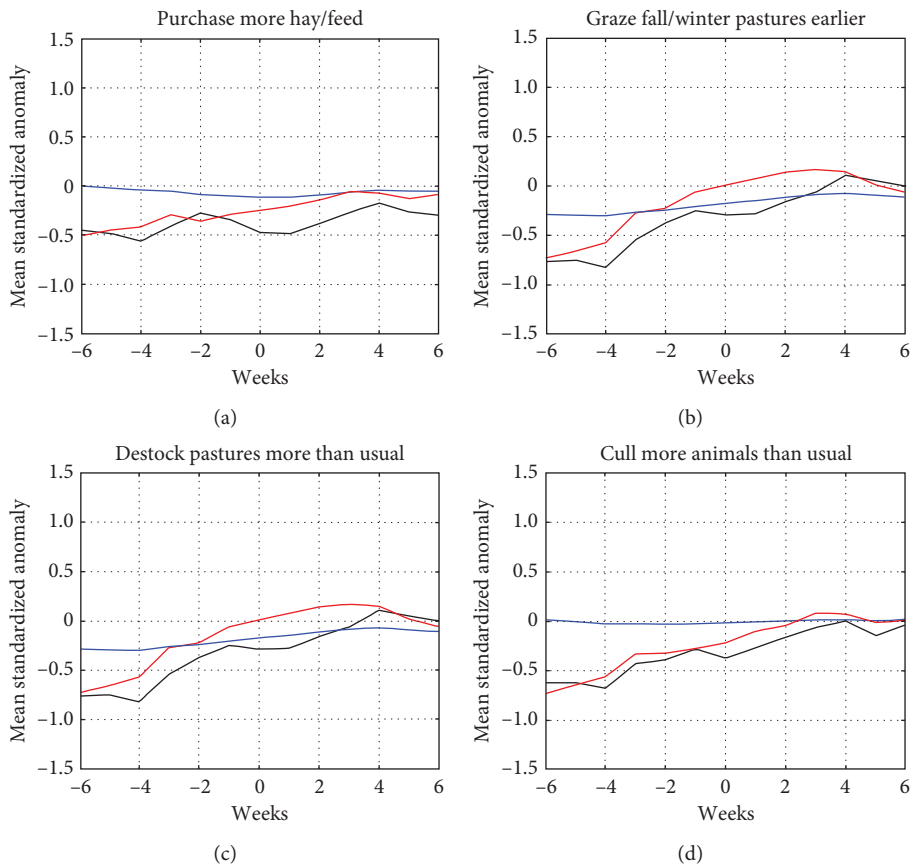

Figure 4: Time series showing the average condition depicted by anomalies in the ESI (black line) NLDAS TS (red line) and NLDAS TS (blue line) data sets at weekly intervals from six weeks prior to six weeks after the average beginning of drought response actions, including (a) purchasing more hay or feed than usual, (b) grazing fall/winter pastures earlier than usual, (c) destocking pastures more than usual, and (d) culling more breeding animals than usual.

forage productivity (Table 3). However, just as the timing of observing these drought conditions was unrelated with the timing of action, so was the use and influence of drought early warning information. These findings indicate that while drought early warning is perceived and understood by managers as an alert about deteriorating conditions, it is not currently being perceived by managers as a primary cue to take action.

External sources of uncertainty may slow managers' decision-making processes about drought response. Managers may not immediately be able to determine what the financial or other implications of their actions could be, as markets for their supplies and products change and as policy responses are announced expectedly or unexpectedly [39]. For example, farm commodity (including corn, soy, and wheat) and livestock prices had been on a downward trend throughout 2016 (https://www.bloomberg.com/graphics/2016-farm-economy/), which may have affected decisions that weighed purchasing feed against destocking livestock. Further, administration of the USDA Livestock Forage Disaster Program (LFP) may have played a role in the timing of drought response. As legislated in the 2014 Farm Bill (https://www.fsa.usda.gov/Assets/USDA-FSA-Public/usdafiles/FactSheets/archived-fact-sheets/2016_livestock_forage_disaster_program.pdf), producers who live in counties that meet conditions triggered by the U.S. Drought Monitor automatically become eligible to apply for LFP, but the amount a producer will be eligible to receive depends upon both drought intensity and length of time in drought. The promise of an LFP payout may lessen a manager's feeling at risk of running out of feed due to drought because they will have financial assistance for purchasing feed for livestock if the drought continues. This possibility may lead some to wait until later in the year to decide whether they will actually need to destock.

4.4. Factors Affecting Drought Impacts. Individuals varied in the losses that they experienced as a result of the 2016 drought event. On average, the largest percentage losses were to pasture hay yield and range productivity and the smallest percentage losses were to livestock gain/productivity (Table 1). Table 4 lists the coefficients of variables used to predict the percent loss, controlling for the 3-month SPEI. When controlling for drought severity, the timing of action was useful in predicting some impacts, providing support for hypothesis 3. The timing of destocking was related to the percentage loss of range productivity and to range health and diversity, with those destocking later reporting higher losses. Holding 3-month SPEI constant, for every month later that

Table 3: Factors affecting the timing of observed conditions.

	Timing decreased topsoil moisture	Timing delayed/lack of plant emergence	Timing delayed/lack of plant growth	Timing deteriorating range conditions	Timing decreased forage productivity
SPEI	102.27** (250)	122.14** (239)	139.72** (248)	113.26** (242)	90.03** (243)
Use/influence on-farm monitoring	−3.80 (237)	8.40 (227)	−3.58 (236)	−2.67 (230)	0.51 (231)
Use/influence own assessment of conditions	−8.38** (236)	−3.00 (225)	−6.66 (234)	−7.99* (229)	−5.56 (229)
Use/influence local extension	3.93 (237)	2.76 (226)	−8.48** (235)	5.39 (230)	3.29 (230)
Use/influence NWS	1.33 (238)	−7.48 (227)	−6.51* (236)	−5.54 (231)	−11.84** (231)
Use/influence U.S. drought monitor	−0.73 (236)	−5.98 (225)	−4.74 (234)	−3.21 (229)	−4.90 (229)
Use/influence USDA resources	−1.13 (237)	−10.72 (226)	−12.03** (235)	−2.12 (230)	−1.80 (230)
Use/influence TV/radio	2.39 (235)	−4.64 (224)	−8.18** (233)	1.73 (228)	−1.35 (228)

Reporting coefficients, significance of test that coefficient is different from 0, and (n). For SPEI, the coefficient is determined without other covariates. For other predictors, coefficients are determined when controlling for SPEI. Data sources: 2016 survey, SPEI (droughtatlas.unl.edu). $^{*}p < 0.10$; $^{**}p < 0.05$.

respondents began destocking, they reported an additional 3.49% loss to range productivity and an additional 4.78% loss to range health/diversity. Timing of destocking was related to loss of range productivity even when holding the early-grazing-of-fall/winter-pastures (y/n) variable constant. This study provides evidence that livestock producers are continuing to see negative impacts to herbage production and range health and diversity, in part due to failure to decrease grazing pressure early enough in the season. While some researchers report increased drought preparedness among rangeland managers [13], this study would indicate that there continues to be room for improvement in timely decision-making.

Later actions were not always associated with greater losses, however. The timing of buying supplemental feed was correlated with loss of cash reserves or savings and loss of animal gain or productivity—those who started purchasing supplemental feed later in the year also experienced less loss to their savings and animal gain. For every month later in 2016 that respondents began buying supplemental feed, they experienced 5.10% less loss to their cash reserves or savings and 2.11% less loss to their animal gain/productivity (Table 4). Unlike the effect of delayed destocking on rangeland health, there may not be harm in waiting to purchase supplemental hay or feed, as long as local supplies remain available and affordable. In 2016, national hay supplies were plentiful, though local hay prices did increase starting in July in response to local demand (https://www.ams.usda.gov/market-news/hay-reports). While those who waited until later in the year were likely to pay slightly more for hay than those who purchased earlier in the year, if they were purchasing for a fewer number of months than those who began purchasing earlier, they may still have benefitted economically. However, other drought events may be geographically more widespread or coincide temporally with high hay and feed prices, which would make waiting to purchase supplemental hay/feed a gamble.

After the 2016 drought event, approximately 28% of all respondents said that they would have acted earlier or differently if they had had information earlier that drought was emerging, and 25% of respondents said they thought they would have seen less harm had they acted earlier or differently. The timing of drought response actions was useful in predicting whether they had regrets after the drought (Table 5). Respondents who began destocking later in the year were more likely than others to say that they would have seen less harm to their operations if they had acted earlier or differently, controlling for SPEI. This relationship aligns with the correlation between later destocking and increased harm to rangeland resources. Respondents who used on-farm monitoring and/or NWS early warning were more likely than others to say that they would have taken action earlier or differently with earlier warning of drought. These results support prior research finding that producers who are already users of monitoring information see the greatest value in the information [40], in part because those not currently using the information may be "unconsciously incompetent" with regard to the potential use of the information [41].

5. Conclusion

This study informs the literature on proactive drought response and the current and potential role of drought early warning in supporting it. Smit and Skinner [16] classify adaptation in terms of intent, purposefulness, timing, duration, scale, responsibility, and form. The intent of decisions can be considered in light of the managers' goals and the particular impacts that managers hope to avoid or minimize [15]. And, the proactive versus reactive nature of decisions may depend upon the ultimate intent of the decisions. Thus, it is important to consider drought response within the context of decision-making goals and calendars in order to understand the implications for earlier versus later response, lending support to the need for better understanding and documentation of crop-specific decision calendars (e.g., [9, 17]).

Findings provide support for encouraging Great Plains range-based livestock producers to make stocking decisions based on spring drought conditions, regardless of later

Table 4: Factors affecting drought impacts.

	Loss of pasture hay yield	Loss of range productivity	Loss of range health or diversity	Loss of livestock gain or productivity	Loss of net income	Loss of cash reserves or savings
SPEI	−55.46** (188)	−32.96** (171)	−43.96** (111)	−13.24** (112)	−9.32 (175)	3.49 (119)
Timing of purchasing supplemental feed	1.31 (104)	1.74 (91)	1.03 (60)	−2.11** (60)	−0.70 (87)	−5.10** (59)
Timing of early grazing fall/winter pastures	3.21 (103)	0.87 (97)	1.87 (63)	−0.33 (63)	0.18 (91)	−2.80 (58)
Timing of destocking	1.56 (88)	3.49** (85)	4.78** (60)	−0.78 (58)	−0.03 (77)	−0.49 (51)
Timing of culling breeding herd	0.26 (71)	0.98 (60)	−0.58 (44)	−2.22 (45)	−1.28 (59)	0.73 (43)

Reporting coefficients, significance of test that coefficient is different from 0, and (n). For SPEI, the coefficient is determined without other covariates. For other predictors, coefficients are determined when controlling for SPEI. Data sources: 2016 survey, SPEI (droughtatlas.unl.edu). $^{*}p < 0.10$; $^{**}p < 0.05$.

Table 5: Factors affecting perceived capacity to improve drought response.

	Would have acted differently with information	Would have seen less impact if acted differently
SPEI	0.14 (241)	0.29 (239)
Timing of purchasing supplemental feed	−0.05 (109)	0.08 (109)
Timing of early grazing fall/winter pastures	−0.04 (109)	0.35* (108)
Timing of destocking	0.11 (92)	0.32** (93)
Timing of culling breeding herd	0.03 (68)	0.10 (68)
Use/influence on-farm monitoring	0.41** (236)	0.21 (235)
Use/influence own assessment of conditions	0.23* (235)	0.12 (235)
Use/influence local extension	0.23 (236)	0.05 (235)
Use/influence NWS	0.43** (237)	0.17 (236)
Use/influence U.S. Drought monitor	0.20 (235)	0.12 (234)
Use/influence USDA resources	0.04 (236)	−0.05 (235)
Use/influence TV/radio	0.04 (234)	0.10 (233)

Reporting coefficients listed in log-odds units, significance of test that coefficient is different from 0, and (n). For SPEI, the coefficient is determined without other covariates. For other predictors, coefficients are determined when controlling for SPEI. Data sources: 2016 survey, SPEI (droughtatlas.unl.edu). $^{*}p < 0.10$; $^{**}p < 0.05$. n varies, dependent upon variable n (listed in Table 1).

season precipitation [33]. This study shows that actions taken with the intent of avoiding rangeland harm only do so when taken proactively and as soon as it can be determined that drought is likely to reduce forage growth. The same actions, taken reactively after damages have already occurred, have the effect of coping with damages instead of lessening them. Though this study focused only on a one-year flash drought, waiting to destock pastures was associated with greater losses to range productivity, health, and diversity. And, respondents who waited to destock saw the potential for less harm to their operations had they acted differently or sooner. These findings are important because, while range and pastures may be likely to recover after a one-year drought [42], degraded range health increases the vulnerability of the operation to harm from future multi-year droughts and recurring drought events. Future research should examine the connections between drought, management, and impacts to provide additional analysis of feedback relationships such as these that are difficult to quantify.

A key finding of this study is that the timing of drought response actions did not align with the timing of drought development. Spring drought conditions did not, for most respondents, lead them to begin taking drought response action in the spring or summer months. More research is needed to investigate other factors influencing the timing of these decisions. Respondents' use of drought early warning information did not influence the timing of their actions, though federal disaster assistance did. Respondents' efforts to monitor and pay attention to environmental cues, through on-farm moisture monitoring and/or other means of assessing conditions, may have led them to strategically alter their timing of response. This supports efforts to increase on-farm monitoring as a strategy for increasing proactive drought response in the future.

This study suggests opportunities for improved management, given the development of improved drought early warning information that clearly links emerging drought conditions with expected impacts and actions that can be taken to minimize those impacts. New decision support tools, such as the USDA GrassCast Tool, should be explored and developed further as strategies to provide more management-specific early warning of drought to rangeland managers (http://grasscast.agsci.colostate.edu/). This study provides evidence of opportunities to use such tools in concert with drought early warning information to improve the timing of rangeland managers' drought responses and the outcomes of drought management.

Data Availability

The drought monitoring datasets used to support the findings of this study are available from the corresponding

author upon request. Station-based datasets for the SPI and SPEI can be accessed at https://droughtindex.unl.edu. Survey descriptive statistics are available from the corresponding author upon request.

Conflicts of Interest

The authors declare that there are no conflicts of interest regarding the publication of this paper.

Acknowledgments

The authors are grateful to the agricultural producers and advisors who pretested the survey and to the producers who participated in the survey. The authors are also grateful to Yared Ashenafi Bayissa for calculating county-level SPEI values and to Deborah Wood for proofreading. Errors remain the authors' own. This work was supported by the National Oceanic and Atmospheric Administration (NOAA) Sectoral Application Research Program (SARP) via grants NA160AR4310131 and NA16OAR4310130 and by the National Integrated Drought Information System.

Supplementary Materials

Appendix A provides the full wording and formatting of questionnaire-based measured used in this analysis. (*Supplementary Materials*)

References

[1] International Strategy for Disaster Reduction UNISDR, *Terminology on Disaster Risk Reduction*, UNISDR, Geneva Switzerland, 2009.

[2] C. Knutson and T. Haigh, "A drought-planning methodology for ranchers in the Great Plains," *Rangelands*, vol. 35, no. 1, pp. 25–33, 2013.

[3] J. D. Derner and D. J. Augustine, "Adaptive management for drought on rangelands," *Rangelands*, vol. 38, no. 4, pp. 211–215, 2016.

[4] M. Svoboda, D. LeComte, M. Hayes et al., "The drought monitor," *Bulletin of the American Meteorological Society*, vol. 83, no. 8, pp. 1181–1190, 2002.

[5] M. C. Lemos, C. J. Kirchhoff, and V. Ramprasad, "Narrowing the climate information usability gap," *Nature Climate Change*, vol. 2, no. 11, pp. 789–794, 2012.

[6] C. J. Kirchhoff, M. Carmen Lemos, and S. Dessai, "Actionable knowledge for environmental decision making: broadening the usability of climate science," *Annual Review of Environment and Resources*, vol. 38, no. 1, pp. 393–414, 2013.

[7] M. Buchanan-Smith, "Role of early warning systems in decision making processes," in *Early Warning Systems for Drought Preparedness and Drought Management*, World Meteorological Organization, Geneva, Switzerland, 2000.

[8] R. S. Pulwarty and M. V. K. Sivakumar, "Information systems in a changing climate: early warnings and drought risk management," *Weather and Climate Extremes*, vol. 3, pp. 14–21, 2014.

[9] T. Haigh, E. Takle, J. Andresen, M. Widhalm, J. S. Carlton, and J. Angel, "Mapping the decision points and climate information use of agricultural producers across the U.S. Corn Belt," *Climate Risk Management*, vol. 7, pp. 20–30, 2015.

[10] B. Walker, S. R. Carpenter, J. M. Anderies et al., "Resilience management in social-ecological systems: a working hypothesis for a participatory approach," *Conservation Ecology*, vol. 6, no. 1, p. 14, 2002.

[11] S. E. Hollinger, "Meteorological forecasting for agricultural production," in *Systems Analysis and Modeling in Food and Agriculture*, K. C. King, D. H. Fleisher, and L. F. Rodriguiz, Eds., p. 488, EOLSS Publications, Oxford, UK, 2009.

[12] C. T. Bastian, C. Ponnamaneni, P. Mooney et al., "Range livestock strategies given extended drought and different price cycles," *ASFMRA*, pp. 153–163, 2009.

[13] D. L. Coppock, "Ranching and multiyear droughts in Utah: production impacts, risk perceptions, and changes in preparedness," *Rangeland Ecology & Management*, vol. 64, no. 6, pp. 607–618, 2011.

[14] E. Kachergis, J. D. Derner, B. B. Cutts et al., "Increasing flexibility in rangeland management during drought," *Ecosphere*, vol. 5, no. 6, pp. 1–14, 2014.

[15] T. R. Haigh, W. Schacht, C. L. Knutson et al., "Socioecological determinants of drought impacts and coping strategies for ranching operations in the Great Plains," *Rangeland Ecology & Management*, vol. 72, no. 3, pp. 561–571, 2019.

[16] B. Smit and M. W. Skinner, "Adaptation options in agriculture to climate change: a typology," *Mitigation and Adaptation Strategies for Global Change*, vol. 7, no. 1, pp. 85–114, 2002.

[17] E. S. Takle, C. J. Anderson, J. Andresen et al., "Climate forecasts for corn producer decision making," *Earth Interactions*, vol. 18, no. 5, pp. 1–8, 2014.

[18] D. Hillier and B. Dempsey, *A Dangerous Delay*, Oxfam Intenational, Nairobi, Kenya, 2012.

[19] S. Davies, "Are coping strategies a cop out?," *IDS Bulletin*, vol. 24, no. 4, pp. 60–72, 1993.

[20] H. Wilmer, E. York, W. K. Kelley, and M. W. Brunson, ""In every rancher's mind": effects of drought on ranch planning and practice," *Rangelands*, vol. 38, no. 4, pp. 216–221, 2016.

[21] T. R. Shrum, W. R. Travis, T. M. Williams, and E. Lih, "Managing climate risks on the ranch with limited drought information," *Climate Risk Management*, vol. 20, pp. 11–26, 2018.

[22] M. K. Lindell and R. W. Perry, "The protective action decision model: theoretical modifications and additional evidence," *Risk Analysis*, vol. 32, no. 4, pp. 616–632, 2012.

[23] E. Kuligowski, "Predicting human behavior during fires," *Fire Technology*, vol. 49, no. 1, pp. 101–120, 2013.

[24] S. P. Church, T. Haigh, M. Widhalm et al., "Agricultural trade publications and the 2012 Midwestern U.S. drought: a missed opportunity for climate risk communication," *Climate Risk Management*, vol. 15, pp. 45–60, 2017.

[25] T. Terpstra and M. K. Lindell, "Citizens' perceptions of flood hazard adjustments: an application of the protective action decision," *Environment and Behavior*, vol. 45, no. 8, pp. 993–1018, 2013.

[26] M. K. Lindell and D. J. Whitney, "Correlates of household seismic hazard adjustment adoption," *Risk Analysis*, vol. 20, no. 1, pp. 13–26, 2000.

[27] D. A. Wilhite, "Drought as a natural hazard," in *Drought: A Global Assessment*, D. A. Wilhite, Ed., vol. 1, pp. 3–18, Routledge, Abingdon, UK, 2000.

[28] D. Cash, W. Clark, F. Alcock, N. Eckley, and J. Jäger, *Salience, Credibility, Legitimacy and Boundaries: Linking Research Assessment and Decision Making RWP02-046*, Harvard University, John F. Kennedy School of Government, Cambridge, MA, USA, 2002.

[29] J. Otkin, T. Haigh, A. Mucia, M. C. Anderson, and C. Hain, "Comparison of agricultural stakeholder survey results and drought monitoring datasets during the 2016 U.S. Northern Plains flash drought," *Weather, Climate, and Society*, vol. 10, no. 8, pp. 867–883, 2018.

[30] USDA National Agricultural Statistics Service, *Agricultural Prices*, USDA National Agricultural Statistics Service, Washington, DC, USA, 2017.

[31] NCEI, *Drought—Annual 2016 State of the Climate*, National Centers for Environmental Information (NCEI), Asheville, NC, USA, 2019, https://www.ncdc.noaa.gov/sotc/drought/201613.

[32] D. A. Dillman, "The design and administration of mail surveys," *Annual Review of Sociology*, vol. 17, no. 1, pp. 225–249, 1991.

[33] A. J. Smart, B. H. Dunn, P. S. Johnson, L. Xu, and R. N. Gates, "Using weather data to explain herbage yield on three great plains plant communities," *Rangeland Ecology & Management*, vol. 60, no. 2, pp. 146–153, 2007.

[34] Y. Xia, J. Sheffield, M. B. Ek et al., "Evaluation of multi-model simulated soil moisture in NLDAS-2," *Journal of Hydrology*, vol. 512, pp. 107–125, 2014.

[35] M. C. Anderson, J. M. Norman, J. R. Mecikalski, J. A. Otkin, and W. P. Kustas, "A climatological study of evapotranspiration and moisture stress across the continental United States based on thermal remote sensing: 1. Model formulation," *Journal of Geophysical Research: Atmospheres*, vol. 112, no. 10, 2007.

[36] D. W. Hosmer, S. Lemeshow, and R. X. Sturdivant, *Applied Logistic Regression*, Wiley, vol. 23, no. 1, Hoboken, NJ, USA, 1994.

[37] StataCorp LP, *Stata Statistical Software: Release 12*, StataCorp LP, College Station, TX, USA, 2011.

[38] A. J. K. Smart, J. D. Harmoney, M. B. Scasta et al., "Forum: critical decision dates for drought management in central and norther Great Plains rangelands," *Rangeland Ecology and Management*, vol. 72, 2019.

[39] B. Dunn, A. Smart, and R. Gates, "Barriers to successful drought management: why do some ranchers fail to take action?," *Rangelands*, vol. 27, no. 2, pp. 13–16, 2005.

[40] J. R. Ziolkowska and J. Zubillaga, "Importance of weather monitoring for agricultural decision-making—an exploratory behavioral study for Oklahoma Mesonet," *Journal of the Science of Food and Agriculture*, vol. 98, no. 13, pp. 4945–4954, 2018.

[41] L. Turner, L. Irvine, and S. Kilpatrick, "Incorporating data into grazing management decisions: supporting farmer learning," *Animal Production Science*, 2019.

[42] R. K. Heitschmidt, K. D. Klement, and M. R. Haferkamp, "Interactive effects of drought and grazing on northern great plains rangelands," *Rangeland Ecology & Management*, vol. 58, no. 1, pp. 11–19, 2005.

Hindawi
Advances in Meteorology
Volume 2019, Article ID 3849210, 13 pages
https://doi.org/10.1155/2019/3849210

Research Article

Farmers' Perceptions of Climate Change Trends and Adaptation Strategies in Semiarid Highlands of Eastern Tigray, Northern Ethiopia

Hailay Tsigab Kahsay,[1] Dawit Diriba Guta,[1] Belay Simane Birhanu,[1] and Tagel Gebrehiwot Gidey[2]

[1]*Center for Environment and Development Studies, Addis Ababa University, P.O. Box 1176, Addis Ababa, Ethiopia*
[2]*Environment and Climate Research Center, Ethiopian Development Research Institute, P.O. Box 2479, Addis Ababa, Ethiopia*

Correspondence should be addressed to Hailay Tsigab Kahsay; hailay20@gmail.com

Received 27 January 2019; Accepted 17 July 2019; Published 15 August 2019

Guest Editor: Jayant K. Routray

This study examined smallholder farmers' perception about climate change and variability compared with the observed metrological data and their adaptation strategies in response to the perceived impacts of climate change. The multistage sampling method was employed to select 358 rural farmers in Hawzen and Irob districts located in semiarid highlands of Eastern Tigray, northern Ethiopia. Moreover, areal gridded surface monthly rainfall and temperature data between 1983 and 2015 were collected from National Meteorology Agency of Ethiopia. The results revealed that about 98.56 and 92 percent of farmers perceived a decrease in annual rainfall. In addition, 87 and 90 percent of farmers noticed that temperature was increased in Hawzen and Irob districts, respectively. Harmoniously, the modified Mann–Kendall trend test confirmed that annual rainfall was decreased by 32.38 mm and 121.33 mm during the period of analysis. Furthermore, mean annual temperature increased statistically significant ($p < 0.001$) by about 0.40°C and 0.39°C per decade during the period of analysis cognate with the farmers' perception. To reduce the perceived impacts of climate change, farmers adopted various farm-level adaptation strategies that vary significantly between the two groups. Soil and water conservation, planting trees, crop varieties, changing crop calendar, biological conservation, and irrigation were among the dominant adaptation strategies, respectively, in the study area. The results of this study provide baseline information for local governments, subsequent researchers, and policy-makers in terms of farmers' perception of climate change and adaptation strategies.

1. Introduction

An increase in intensity and frequency of extreme weather events and climate variability have raised broad concerns over global climatic changes since they affected human livelihood activities and strategies [1, 2]. Rainfall and temperature are the most indispensable hydrology climatic variables often used for characterization of climate change and variability [3]. Rainfall variability and other climatic risks account for a significant share of agricultural production decline in developing countries [4, 5]. The global mean surface temperature (GMST) increased by 0.89°C during 1901–2012 because of human action greenhouse gas concentrations [6]. As a result, globally, the average temperature will warm between 1.48°C and 5.88°C by 2100 that leads to frequent extreme weather events and risks [7].

In sub-Saharan Africa, warming temperature is expected to be higher than the global average temperature, and in some parts of the region, rainfall will decline [8]. The overall summer rainfall had an increasing trend during 1901–1955 but a decreasing trend since the 1950s [9]. Farm households in rural Ethiopia primarily depend on low-productivity rainfed agriculture that determines the socioeconomic challenges including food insecurity [10]. Ethiopia's GDP

growth is strongly correlated with rainfall and negatively affected by rainfall variability [11, 12].

Several studies have been conducted to investigate the spatiotemporal variability of rainfall and temperature in Ethiopia [13–17], among others. However, their results were inconclusive because of the difference in time and unit of analysis in addition to being carried out at regional, basin, and national levels. Ahmad et al. [18] suggested that, for efficient and effective decision-making, climate variable trend analysis on low-scale time-series data is more preferential. The spatio-temporal variation in temperature and rainfall existing around the globe confounds generalities over large areas because nonuniformity is expected to occur [19]. Moreover, none of the above empirical studies in Ethiopia incorporated local people's perception because actual climatic trends are often not equally perceived among small-scale farmers [20]. Ayal and Leal Filho [21] confirmed farmers' perceptions of changes in temperature were similar with meteorological station data but different with meteorological rainfall trends in Ethiopia. Similarly, Limantol et al. [22] reported that farmers' perceptions of increased temperature coincided with climatic data, but their perception of decreased rainfall did not corroborate with rainfall climatic data in Ghana. Contrary to these studies, Moroda et al. [23] revealed that the majority of respondents' perceived changes in temperature and rainfall tally with meteorological data in East Shewa, Ethiopia. Hence, climate change system modeling and impacts may coincide with the perception of farmers in some cases but not in others. But the link between the two is helpful for climate change adaptation by influencing farmers' risk perception behaviors [24]. Tripathi and Mishra [25] identified although farmers are aware of temperature and rainfall change, they fail to recognize these changes as climate change. Farm households distinctly perceive the same stimulus depending on their past personal experiences and cultural differences [26, 27]. Local people's perception of rainfall behavior is an idiosyncratic manifestation of their experience and various environmental aspects [28].

Little is known about farmers' climate perceptions and their effects on adaptation decision as a result of climate information facility although farmers' perception of climate change impacts is a prerequisite for the adaptation strategy [25, 29]. Recently, the integration of local farmers' climate change awareness with nearby weather monitoring stations or meteorology data has received broad attention to improve farmers' adaptation strategies [30]. Therefore, the objective of this study is to examine rural farmers' perceptions of climate change and variability as compared with the observed metrological data of rainfall and temperature. Besides, it assesses the adaptation strategies in response to the perceived impacts of climate change in Hawzen and Irob districts located in semiarid eastern highlands of Tigray, northern Ethiopia.

2. Materials and Methods

2.1. Selection of the Study Area. The study area located in Eastern Tigray National Regional State, northern Ethiopia, is a semiarid climate zone characterized by a heavy rainy season (June to August), a small rainy season (March to May), and a major dry season (October to March) [31, 32]. The eastern highlands receive an average annual rainfall of 520–680°mm, and the average annual temperature ranges between 16°C and 20°C with diurnal variations being larger than seasonal changes [33]. This study involves Hawzen and Irob districts (*woredas* in Amharic), a local administrative unit above village (*kebele* in Amharic), the smallest administrative unit. Geographically, the districts are found between latitude 13°78′ and 14°18′N and longitude 39°18′ and 39°58′E and latitude 14°35′ and 14°58′N and longitude 39°50′ and 40°26′E, respectively. According to population estimation [34], the total population of Hawzen and Irob districts in 2018 was 127,265 (52.4 percent females) and 33,912 (50.77 percent females), respectively. Out of them, 93 and 95 percent live in rural areas mainly dependent on a subsistence mixed agriculture livelihood system. The main crops grown in the rainy season are barley (*Hordeum vulgare*), sorghum (*Sorghum bicolor*), wheat (*Triticum aestivum*), maize (*Zea mays*), and teff (*Eragrostis tef*). The total area estimated was about 1,892.69 km^2 and 850 km^2 for Hawzen and Irob, respectively, characterized by rugged mountains, hills, high plateaus, and deep valley bottoms. The average elevation of the study districts ranges from 2000 m in Irob to 2243 m.a.s.l. in Hawzen, respectively.

Of the Hawzen district climatically, 60 percent belongs to midlands (*woinadega*, 1500–2500 m.a.s.l.), 35 percent lowlands (*kolla*, 500–1500 m.a.s.l.), and 5 percent highlands (*dega*, 2500–3500 m a.s.l.) according to the country's traditional agroecological zones, respectively. Likewise, Irob accounts for 75 percent midland, 15 percent highland, and 10 percent lowland agroecological zones. Rainfall is marked by a weakly bimodal pattern, with small showers of rain during the months of March to May with a long rainy season in summer during the months of June to August. Irob and Hawzen received the mean annual rainfall ranging from 470 to 613 mm during 1983–2015, respectively, with erratic, highly spatial, and temporal variations. The mean annual temperature varies from 19°C in Hawzen to 20°C for Irob with diurnal variations being larger than seasonal changes. According to information from the Finance and Planning Office, both districts are identified among the most vulnerable areas exposed to chronic food insecurity, adverse extreme climate events, severe land degradation, and declining soil fertility. Specifically, during the *El Niño*-induced drought conditions in 2016, about 40 percent of the total population of the Hawzen district were exposed to chronic food insecurity. Likewise, about 74 percent of the total population of Irob were beneficiaries of the Productive Safety Net Program in the same year.

2.2. Sampling and Data Collection. In this study, a multistage sampling method was employed to select rural farm households. In the first stage, Hawzen and Irob districts were selected using the purposive sampling method since both districts represent the semiarid eastern highlands of Tigray that involve diverse ecological zones, socioeconomic

conditions, and occurrences of frequent extreme weather events. In the second stage, using the stratified sampling method, two *kebeles* were selected from each district considering the available similarities. In this study, the sampled Selam Kebele and Alitena Kebele fall under midlands, while Degamba Kebele and Hareze-Sebata Kebele were categorized under highland agroecological zones. In Hawzen, 1856 and 1395 household heads in Selam and Degamba, were found, respectively, while in Irob, 1607 and 355 household heads in Alitena and Hareze-Sebata were found, respectively, in 2016. Finally, using the simple random sampling method, 208 and 150 households were selected from Hawzen and Irob districts proportional to the total number of farm household heads. Hence, a total of 358 rural household heads were enumerated from the study area.

In addition, a structured questionnaire was designed, pretested, and administered at the household level to obtain the primary data. The survey was conducted between January and February 2018, administered by trained enumerators who speak the local language, and supervised by local agricultural extension agents in the study districts. Moreover, to compare farmers' perceptions of climate change with the actual meteorological data monthly maximum, minimum temperatures and monthly total rainfall data were collected. The data are based on areal gridded data (4 km by 4 km) spatial resolution over the period between 1983 and 2014. The gridded dataset merging two datasets includes station gauge data (rainfall and temperature) from National Meteorology Agency of Ethiopia and satellite rainfall and temperature estimates from European Organisation for the Exploitation of Meteorological Satellites (EUMETSAT) and the US National Aeronautics and Space Administration (NASA). Finally, the satellite temperature and rainfall estimates were combined with station gauge data by National Meteorological Services Agency together with its international partners.

The total sample size from each kebele was computed using the following standard formula:

$$n = \frac{N}{1} + N(e)^2, \tag{1}$$

where N = total population of the sample kebele, n = sample size to be computed, and e^2 = acceptable error (level of precision), which is assigned a value of 5 percent (0.05).

Then, the sample size distributed to each kebele proportional to the total household size is calculated using the following formula:

$$n_i = n * \frac{N_i}{\sum N_i}, \tag{2}$$

where n_i = sample size of the ith kebele to be computed, n = sample size of the ith kebele, and N_i = total household heads of the ith kebele.

2.3. Trend Analysis Methods. Tests for the detection of significant trends in climatologic time series are grouped as parametric and nonparametric methods [35]. Coefficient of variation (CV) and standardized rainfall anomaly (SRA) from parametric methods and Mann–Kendall's test and Sen's slope estimator from nonparametric methods were applied to examine the temporal trends of temperature and rainfall. CV is a widely used technique to analyze interannual variability of rainfall computed as the ratio of standard deviation to mean value over the given period [21, 36]. A rainfall amount with a CV less than 0.20 is less variable, that with a CV between 0.20 and 0.30 is moderately variable, and that with a CV greater than 0.30 is highly variable [37]. SRA is calculated as the difference between long-term mean annual rainfall and observed annual rainfall to the ratio of standard deviation assuming that the observations are normally distributed [38]. It helps to examine the pattern of rainfall that exhibits dry and wet years over time [36]. A negative anomaly of rainfall at 25% and 50% refers to dry and very dry conditions, respectively [37].

2.3.1. Mann–Kendall's Trend Test. The basic assumption of the Mann–Kendall trend (MKT) test, proposed in [39, 40], is a test of random series ordered against nonrandom series in time [41]. The null hypothesis H_0 of the MK test assumes that the data are independent and randomly ordered; that is, there is no significant trend against the alternative hypothesis which assumes there is a trend [42]. The test has been suggested by the World Meteorological Organization to assess trends in environmental time-series data because it does not require normally distributed data [43]. The Mann–Kendall test is useful to identify the direction and magnitude of significant trends because of its low sensitivity to abrupt breaks and permitted missing values [44]. The Mann–Kendall test is not significantly affected by single data errors or outliers [41]. Moreover, the data should be free from serial independence that causes unreliable results. In case any serial autocorrelation exists, the modified Mann–Kendall (MMK) test was employed to remove the impact of autocorrelation [45]. Hence, before starting a monotonic trend test, lag 1 autocorrelation for temperature and rainfall time series was checked using the autocorrelation function. The test has been applied by many researchers using the same applications [41, 45, 46].

The MKT test method primarily involves the standardized test statistic Z and Sen's slope β parameters. The Mann–Kendall test statistic computes the difference between the later measured values and all early measured values for a time series of interest over time. If a data value from a later time period is higher than a data value from an earlier time period, the statistic S is incremented by 1. On the contrary, if the data value from a later time period is lower than a data value sampled earlier, S is decremented by 1. The net result of all such increments and decrements yields the final value of S using the following formula:

$$S = \sum_{k=1}^{n-1} \sum_{j=i+1}^{n} \operatorname{sgn}\left(x_j - x_i\right), \tag{3}$$

where n denotes the length of a dataset and x_j and x_i are the sequential data values at times j and i ($j > i$):

$$\operatorname{sgn}\left(X_j - X_i\right) = \begin{cases} +1, & \text{if } \left(x_j - x_i\right) > 0, \\ 0, & \text{if } \left(x_j - x_i\right) = 0, \\ -1, & \text{if } \left(x_j - x_i\right) < 0, \end{cases} \quad (4)$$

where sgn denotes the sign function that takes the values 1, 0, or −1 if $x_j > x_i$, $x_j = x_i$, or $x_j < x_i$, respectively. Positive S values indicate an increasing (upward) trend, and negative values of S reveal a decreasing (downward) trend in the time-series data.

For samples, $n \geq 10$, the S statistic is approximately normally distributed with mean and variance as follows [47]:

$$E(S) = 0, \qquad \sigma^2 = \frac{1}{18}\left[n(n-1)(2n+5)\right]. \quad (5)$$

If there is a tie in the data, then the variance (σ^2) statistic is given as

$$\sigma^2 = \frac{1}{18}\left[n(n-1)(2n+5) - \sum_{i=1}^{m} t_i\left(t_i - 1\right)\left(2t_i + 5\right)\right], \quad (6)$$

where m is the number of tied groups and t_i is the number of observations in the ith group. The standardized MK test statistic Z_{MK} which follows the standard normal distribution with mean zero and variance one is as follows:

$$Z_{\text{MK}} = \begin{cases} \dfrac{s-1}{\sqrt{\delta^2}}, & \text{if } s > 0, \\ 0, & \text{if } s = 0, \\ \dfrac{s+1}{\sqrt{\delta^2}}, & \text{if } s < 0. \end{cases} \quad (7)$$

A positive (negative) value of S indicates an increasing (decreasing) trend for the period. The trend is insignificant if Z_{MK} is less than the standard normal variate $Z\alpha/2$, where α is the significance level. Testing trends is done at the specific α significance level. When $|Z_s| > Z_{1-\alpha/2}$, the null hypothesis is rejected and a significant trend exists in the time series.

The parameter β (the trend magnitude), indicating the variation rate within the time series, given by Sen's slope estimation test computes both the slope and intercept [48, 49]. A positive value of β indicates an "upward trend" (increasing values with time), while a negative value of β indicates a "downward trend." In general, the slope between any two values of a time series x can be estimated from the following formula:

$$\beta = \text{median}\left[\frac{X_j - X_k}{j - k}\right], \quad (8)$$

where X_j and k are data values at times j and k ($j > k$), respectively.

Tau [50] measures the strength of the monotonic relationship between x and y. Therefore, Kendall's tau correlation coefficient is given by

$$\tau = \frac{S}{n(n-1)/2}. \quad (9)$$

A positive value of τ indicates an increasing trend, and vice versa. The summation of the Mann–Kendall test statistic (S) indicates how strong the trend of temperature and precipitation is and whether it is increasing or decreasing. The final analyses of the socioeconomic data and MKT tests were carried out using STATA v.14 and XLSTAT 2018 statistical software packages.

3. Results and Discussion

3.1. Sample Household Characteristics. Table 1 presents the summary of sociodemographic and local institution environments of the sampled household heads. Therefore, of the surveyed households, 77 percent were male-headed households, with an aggregate mean age of 52.4 years implying that respondents were relatively elderly with more farming experience. Studies [51, 52] used age as a proxy measure of farming experience; hence, farmers with more farming experience are more likely to have perceived climate change. Household heads on average had 2.26 years of education that may impair their climate change perception behavior and understanding skills [53].

The self-reported subjective measurement of climate information indicated that 71 percent of household heads received access to weather information from various media outlets and rural local institutions. Climate information services involve provision of climate forecasts together with agronomic advice to overcome the uncertainties that constrain farm decision-making against climate risks [54]. Furthermore, Table 1 presents ANOVA, chi-square, and bivariate correlation tests. ANOVA Scheffe's and χ^2 tests were used to examine whether there was a difference in means of continuous and categorical variables between the two districts, respectively. Hence, a statistically significant mean difference was found ($p < 0.001$) between Hawzen and Irob sample household groups.

Pearson's correlation test was also used to measure the strength and direction of the linear relationship between access to climate information and household characteristics [55]. Climate information or access to weather forecast was positively correlated with training received at the farmer training center (FTC) ($r = 0.22$, $p < 0.001$) and a number of social networks ($r = 0.22$, $p < 0.001$) but negatively correlated with distance to the market ($r = -0.48$, $p < 0.001$). Households who have limited contacts with local farmer institutions can get agricultural technology information from their family social networks [56]. But increased distance from local market centers is a proxy measure of poor access to local weather condition information [57].

Furthermore, household age was negatively correlated with access to weather information ($r = -0.15$, $p < 0.001$). Older farmers have limited social networks and poor interactions with local institutions, which ultimately negatively influences access to climate information [58]. Moreover, Kirui et al. [59] underlined that older farmers preferred indigenous knowledge over modern climate information

Table 1: Means, standard deviations, and pairwise correlations among variables ($n = 358$).

Variables	Mean	SD	p value	1	2	3	4	5	6	7	8	9
Sex of HH (% males)	0.77	0.42	0.001									
Age of HH	52.4	12.27	0.001	0.28[a]								
Education of HH	2.26	2.98	0.359	0.29[a]	−0.34[a]							
Access to AESs (% yes)	0.62	0.48	0.001	−0.08	−0.13[b]	0.07						
Climate information (% yes)	0.71	0.45	0.001	−0.14	−0.15[a]	0.04	0.66[a]					
HH's own radio/TV (% yes)	0.40	0.49	0.196	0.11[b]	−0.05	0.17[a]	0.14[b]	0.04				
Access to FTC	0.28	0.45	0.001	0.01	−0.08	0.13[b]	0.27[a]	0.22[a]	0.11[b]			
Number of off-farm activities	0.86	0.66	0.001	0.10[b]	−0.16[a]	0.12[b]	−0.21[a]	−0.08	0.06	−0.03		
Distance to the market (minutes)	52.48	69.87	0.001	0.13[b]	0.13[a]	−0.08	−0.47[a]	−0.48[a]	−0.01	−0.15[a]	0.16[a]	
Number of social networks	1.41	1.53	0.001	0.02	−0.14[a]	0.22[a]	0.25[a]	0.22[a]	0.22[a]	0.26[a]	−0.05	0.22[a]

[a]Significant at the 0.01 level; [b]significant at the 0.05 level; HH = household head. p value stands for ANOVA and chi-square tests of continuous and categorical variables, respectively.

services. However, access to agricultural extension services (AESs) positively correlated with access to climate information ($r = 0.66$, $p < 0.001$). Agricultural extension services influence farmers' decision to change their farming practices in response to climate change [60]. Generally, households' access to climate information was enriched through provision of training at the FTC, access to agricultural extension services, and the number of social network households participated. Access to rainfall forecast information is helpful to farmers for better selection and timely growth of crops [51].

3.2. Farmers' Perceptions of Climate Change and Variability

3.2.1. Farmers' Perception of Rainfall Variability. Table 2 shows the households' perception of climate change and variability in terms of rainfall distribution, amounts, and increasing temperatures over the last fifteen years. Households had no wide perception in climate change, and an undeniable majority of households perceived a notable change in rainfall and temperature. Out of the total households, 98.56% and 92% perceived a decrease in rainfall amount in Hawzen and Irob, respectively. The χ^2 test was employed to determine whether there were differences between the household groups in their perception behaviors. A significant difference was found (χ^2 test, $p < 0.01$), indicating that households who had been in Hawzen were more likely to perceive a decrease in rainfall compared to those in Irob. Besides to perceiving the decreased rainfall in the study area, almost 40 percent and 20 percent of households believed that variability in onset and cessation time of rainfall is more in the last 15 years, respectively.

Furthermore, around 29 percent and 39 percent of households in the Hawzen and Irob districts noted that the number of rainy days decreased; that is, there was no rain for a full month within the rainy season. Nonetheless, few households suggested that even when it rains, the intensity of rainfall is increased. Only 5 percent of households from Hawzen observed abnormality in rainfall timing, and distribution was increased. Furthermore, almost 37 percent of households in Irob understood that the occurrence of drought frequency was increased, while only 2.4 percent viewed contrarily to this opinion in Hawzen. Regarding rainfall patterns of the last summer, around 82 and 92 percent of households from Hawzen and 99 and 98 percent of households from Irob report that rainfall came too late and stoped too early, respectively. In addition, around 25 percent of households in Hawzen witnessed rain during the harvest time last year. This inadequacy of rainfall and unreliability of raining time impede the agricultural planning that attracts appropriate adaptation strategies and reliable scientific climate information to mitigate the climatic shocks.

3.2.2. Farmers' Perception of Temperature Variability. Moreover, 87 and 90 percent of households felt that temperature increased, while about 3 and 8 percent believed that temperature decreased in the last 15 years in Hawzen and Irob, respectively. The significance (χ^2 test, $p < 0.001$) showed that households who had been in Irob were more likely to perceive an increase in temperature compared to those in Hawzen. Furthermore, about 77 and 78 percent of households perceived an increase in hot days, while 7 and 5 percent noted the decrease of coldness in cold seasons, respectively. Generally, the majority of households are aware about the presence of climate change and variability. They revealed their local experience of climate change and variability using variability in onset and cessation time of the rainy season, the decreased number of rainy days, a raise of drought severity, and the increased number of hot days.

3.3. Actual Variability and Trends of Rainfall and Temperature

3.3.1. Variability of Rainfall. Monthly values of rainfall were aggregated to obtain seasonal rainfall for each district. Seasons were defined using the standard meteorological definition: winter (December, January, and February), spring (March, April, and May), summer (June, July, and August), and autumn (September, October, and November) which is also aligned with study [61].

Table 3 illustrates that the long-term mean annual rainfall varies from about 614 mm in Hawzen to 471 mm in Irob, respectively, during the period of analysis analogous to the semiarid climate zone [31]. Kiros et al. [17] found 555 mm and 633 mm mean annual rainfall for the Hawzen

Table 2: Farmers' perception of climate change and climate shocks ($n = 358$).

Perceptions of climate parameters	Hawzen Percent*	Irob Percent	χ^2 test	p value
Rainfall decrease in the last 15 years			13.32	0.004
Yes	98.56	92.00		
No	—	4.67		
Stayed the same	0.96	3.33		
Do not know	0.48	—		
Local perceptions of rainfall variability			120.78	0.001
Variability in onset and cessation time of the rainy season	39.42	19.33		
Decreased number of rainy days	28.85	38.67		
Increased intensity of rainfall	4.33	2.00		
Increased occurrence of untimely rainfall	5.23	—		
Increased frequent drought occurrence	2.40	36.67		
Temperature increase in the last 15 years			13.32	0.004
Yes	87.02	90		
No	2.88	8.00		
Stayed the same	7.69	2.00		
Do not know	2.40	—		
Local perceptions of temperature variability			36.38	0.001
Increased number of hot days	76.92	78.33		
Increased number of warm nights	2.00	3.33		
Decreased coldness in cold seasons	7.21	5.33		
Rainfall occurrence last summer			28.06	0.001
On time	16.82	0.00		
Too early	1.44	1.33		
Too late	81.73	98.66		
Rainfall termination last summer			11.84	0.003
On time	7.21	0.00		
Stopped too late	0.96	2.00		
Stopped too early	91.82	98.00		
Rain during the harvest time last year			42.88	0.001
Yes	24.52	0.00		
No	75.48	100		

*Does not add up to 100 because of multiple responses.

Table 3: Mean (μ), standard deviation (σ), and CV (%) of rainfall (mm) during 1983–2015.

Annual and seasonal	Hawzen			Irob		
	μ	σ	CV	μ	σ	CV
Annual	613.71	294.02	47.90	470.97	280.06	59.46
Spring	118.18	110.82	93.77	153.43	119.39	77.83
Summer	425.46	184.87	43.45	236.01	155.67	65.96
Autumn	60.04	44.82	74.65	71.35	44.68	62.62
Winter	10.02	11.99	119.66	10.16	13.15	129.43

district and northern Tigray region over the period 1971–2013, respectively. Summer, the main rainy season, and spring, the short rainy season, rainfall contributes around 69% and 50%, and 19% and 33% to mean annual rainfall for Hawzen and Irob, respectively. Hence, about 88% and 83% of the total annual rainfall occurs in the two seasons over the period of analysis. Summer rainfall dominates the seasonal pattern, and spring also considerably contributes to the annual rainfall in northern Tigray [62]. The contribution of spring rainfall over the north and northeastern highlands is ranging from 5% to 30% [10].

The long-term mean annual and seasonal rainfall was unevenly distributed in both districts. High long-term mean annual rainfall variability (CV) ranged from 47.9% in Hawzen to 59.46% in Irob, respectively. A rainfall amount with CV above 30% is an indication that both districts were vulnerable to drought [37]. Hadgu et al. [63] consistently reported a high coefficient variation in the main rainy season in Tigray, northern Ethiopia. Summer CV is less than spring CV in both districts, indicating that summer rainfall was relatively less variable than spring rainfall. Higher rainfall variability is experienced during the small rainy season than the main rainy season and annual rainfall [64]. Rainfall variability and uncertainty in semiarid areas have substantial influence on agricultural production [31]. One-way ANOVA was employed to test the null hypothesis constructed that there is no significant difference in mean annual and mean summer season rainfall between Hawzen and Irob districts. The F-test result revealed that the observed significance value F for annual and summer rainfall is 3.95 ($p < 0.050$) and 19.66 ($p < 0.001$), implying that there is a significant difference in annual and summer rainfall between the two districts.

The mean annual SRA analysis showed that there were 8 and 6 very dry and 10 and 4 dry years in Hawzen and Irob, respectively, over the period of analysis. 3-month and 12-month accumulated precipitation SRA is calculated to determine seasonal and intermediate-term drought indexes [65]. Drought occurs when the SRA initially drops below zero and ends with the first positive value [66]. The proportion of negative mean annual rainfall anomalies in Irob ranges between 63% and 79%, while summer rainfall in Hawzen ranges between 61% and 63% of the total observations, respectively. Certain rainfall patterns show that a dry year is followed by another one or two very dry years and *vis-à-vis* for the wet years. Rainfall has been declining in northeast Ethiopia since 1996 [67].

3.3.2. Trends of Rainfall. The monotonic trend of temperature and rainfall time series was measured using the Mann–Kendall trend test assuming no serial correlation in the dataset. The most widely applied test for detecting serial correlation is the Durbin–Watson d statistic that is defined as the ratio of the sum of squared differences in successive residuals to the residual sum of squares [68]. Prior to the Mann–Kendall test, a serial correlation analysis for rainfall and temperature was assessing the Durbin–Watson d statistic. The estimated Durbin–Watson d statistic values were above one and less than 2, hence not rejecting the null hypothesis suggesting that there is statistically significant evidence of positive autocorrelation in the residuals.

Therefore, the modified Mann–Kendall (MMK) test was used in order to analyze the true trend value. The trend test for annual and seasonal rainfall did not show statistically significant results for both districts (Table 4). However, negative trends are evident in both annual and seasonal rainfall except a positive trend observed in summer rainfall for Hawzen during the period of analysis. In Hawzen and Irob, annual rainfall has been decreasing by about 32.38 and 121.33 mm per decade. Contrarily, in Hawzen, the main rainy season rainfall was increasing by 28.5 mm per decade although there was an absolute decrease in mean annual rainfall amount. This implies no circumstances of agricultural drought and enhanced crop production and livelihoods. For Hawzen and Irob, total annual rainfall decreased by 106.85 mm and 400.39 mm, respectively, in the period of analysis (Table 4 and Figure 1). This result agreed with the results in [17] where no statistically significant trends with a blend of positive and negative trends were found in annual rainfall except at one of the seven stations, Geba River Basin located in the Tigray region of northern Ethiopia, over the period of 1971 to 2013. Correspondingly, Hadgu et al. [63] confirmed a nonsignificant trend in both annual and seasonal rainfall measures in five stations in Tigray, northern Ethiopia, between 1980 and 2009. Overall, studies [10, 62] reported a nonsignificant trend of annual and seasonal rainfall in northern Ethiopia.

3.3.3. Variability of Temperature. The mean annual temperature data were computed as an average of the maximum and minimum temperatures. Mean and standard deviation values of temperature during the study period of analysis are presented in Table 5. The mean maximum (T_{max}), minimum (T_{min}), and annual (T_{mean}) temperatures were 27.06°C, 11.30°C, and 19.18°C for Hawzen. Correspondingly, 27.96°C, 11.88°C, and 19.92°C were for Irob, respectively, over the period of analysis. Generally, Irob had been recording slightly higher mean temperatures compared to the Hawzen district. In Hawzen, the lowest and the highest mean annual temperature variability was 25.61°C and 28.38°C recorded in 1986 and 2013, respectively. Similarly, 26.86°C and 30.00°C were the lowest and highest temperatures recorded in 1989 and 2008 for Irob, respectively, implying that temperature was recently rising in both districts. In Hawzen, spring and summer were the hottest and coldest seasons that reported $20.73°C \pm 0.96\sigma$ and $9.73 \pm 0.67\sigma$, while in Irob, summer and winter were the hottest and coldest seasons with $22.45°C \pm 0.69\sigma$ and $17.96°C \pm 0.68\sigma$, respectively.

3.3.4. Trends of Temperature. Warming trends of maximum and mean annual temperatures were observed in Hawzen and Irob districts at statistically significant levels ($p < 0.001$ and $p < 0.05$, respectively). The warming trends of maximum and mean annual temperatures were 0.65°C and 0.4°C per decade in Hawzen. Likewise, for Irob, the warming trends of maximum and mean annual temperatures were 0.55°C and 0.39°C per decade over the period of analysis, respectively. Generally, the mean annual temperature trend was increased by about 1.32°C and 1.29°C for Hawzen and Irob, respectively, in the period of analysis (Table 6 and Figures 2 and 3). Moreover, the maximum temperature increased faster than the minimum temperature for both districts. However, Gebrehiwot and van der Veen [69] found the average annual minimum temperature (0.72°C) increased faster than the average annual maximum temperature (0.36°C) per decade in the Tigray region of northern Ethiopia during the period 1954–2008.

3.4. Farmers' Perceptions of Climate Change and Meteorological Data. Farmers' self-reported climate perception is not sufficient to generalize about the actual trends of climate change and variability. Their perception of climate change is highly personal, site specific, and influenced by a number of factors [20]. Therefore, it is helpful in comparing farmers' climate change perception and the actual meteorological data in the study area to know the adaptation strategies. The majority of farmers believed total rainfall decreased in the last fifteen years in their localities (Table 2). Meteorological rainfall data analysis was also congruous with farmers' perception of rainfall decline in both districts (Table 4). In Hawzen, the mean main rainy season rainfall showed an increased trend somewhat consistent with farmers' local perception that the intensity of rainfall increased by about 4% (Table 2). Except the main rainy season for Hawzen, the perceived reduction in annual and seasonal rainfall is consistent with meteorological results in agreement with the findings in [70]. Households' local perceptions of increased numbers of hot days and warm nights were in harmony with the meteorological records of mean temperature trends in their vicinities (Tables 2 and 6). This

Table 4: Annual and seasonal rainfall trend analysis for Hawzen and Irob in 1983–2015.

District	Annual rainfall (mm)				Main rainy season (mm)				Spring season (mm)			
	Kendall's tau	S	p value*	Sen's slope	Kendall's tau	S	p value	Sen's slope	Kendall's tau	S	p value	Sen's slope
Hawzen	−0.170	−90.00	0.916	−3.238	0.053	28.00	0.285	0.285	−0.371	−196.00	0.999	−3.328
Irob	−0.481	−254.00	0.500	−12.133	−0.352	−186.00	0.998	−3.904	−0.496	−262.00	1.000	−5.422

*Two-tailed test.

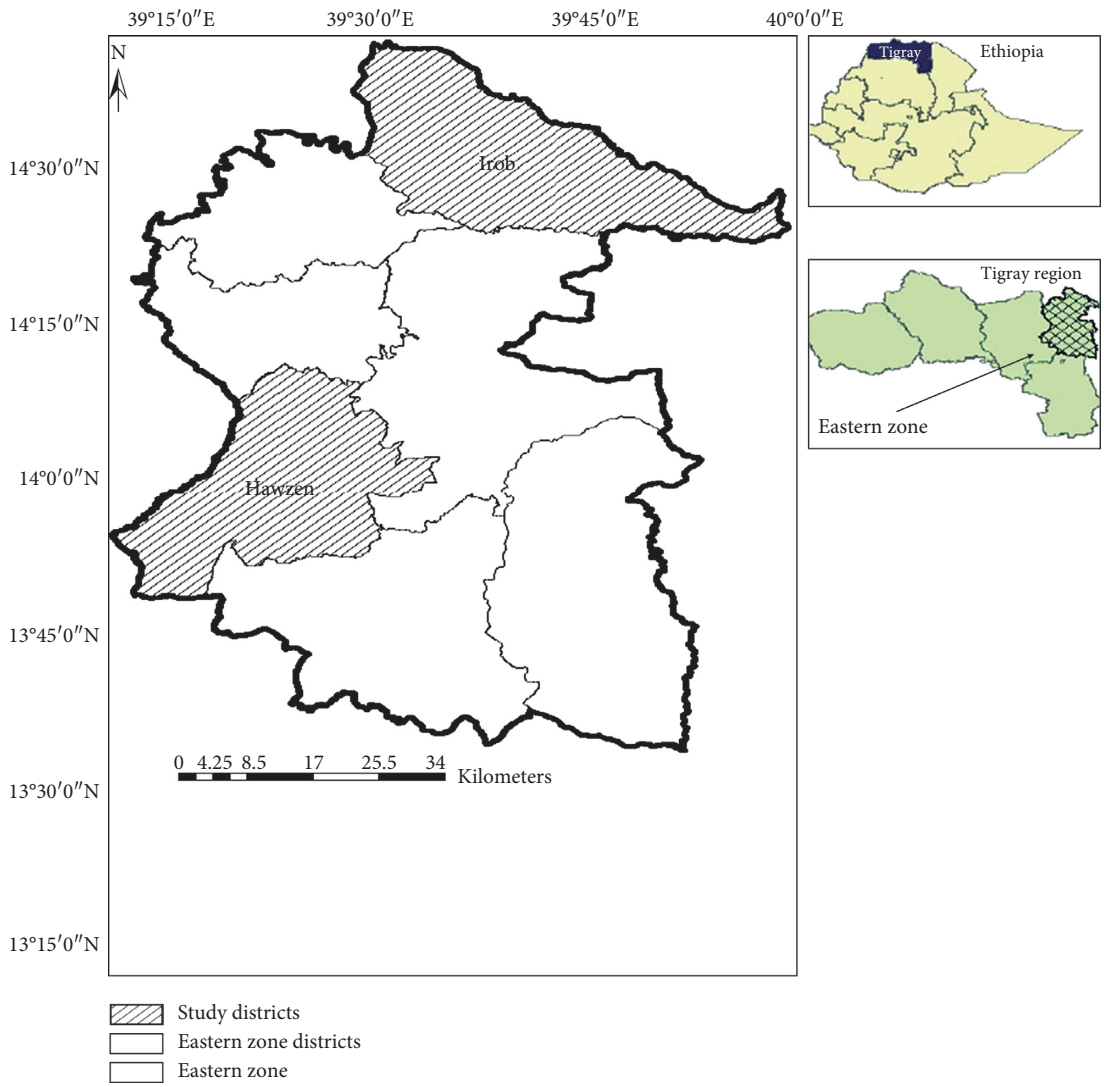

Figure 1: Map of the study areas.

Table 5: Mean maximum, minimum, and annual temperatures (°C) in Hawzen and Irob in 1983–2015.

Annual and seasonal	T_{max} (°C)				T_{min} (°C)				T_{mean} (°C)			
	Hawzen		Irob		Hawzen		Irob		Hawzen		Irob	
	μ	σ	μ	σ	μ	σ	μ	σ	μ	σ	μ	σ
Annual	27.06	0.70	27.96	0.65	11.30	0.60	11.88	0.62	19.18	0.65	19.92	0.64
Spring	28.85	1.06	28.70	0.97	12.60	0.85	12.85	0.75	20.73	0.96	20.78	0.86
Summer	25.86	0.72	29.61	0.72	13.60	0.63	15.28	0.65	9.73	0.67	22.45	0.69
Autumn	26.47	0.85	27.61	0.61	10.14	0.76	10.45	0.76	18.31	0.81	19.03	0.67
Winter	27.06	0.71	25.91	0.89	8.85	0.64	8.93	0.67	17.96	0.68	17.42	0.78

Table 6: Annual and seasonal temperature trend analysis by the MKT test for Hawzen and Irob in 1983–2014.

District	T_{max} (°C)				T_{min} (°C)				T_{mean} (°C)			
	Kendall's tau	S	p value	Sen's slope	Kendall's tau	S	p value	Sen's slope	Kendall's tau	S	p value	Sen's slope
Hawzen	0.685	340.00	0.001	0.065	0.181	90.00	0.140	0.025	0.500	248.00	0.001	0.040
Irob	0.657	326.00	0.001	0.056	0.181	90.00	0.153	0.027	0.492	244.00	0.001	0.039

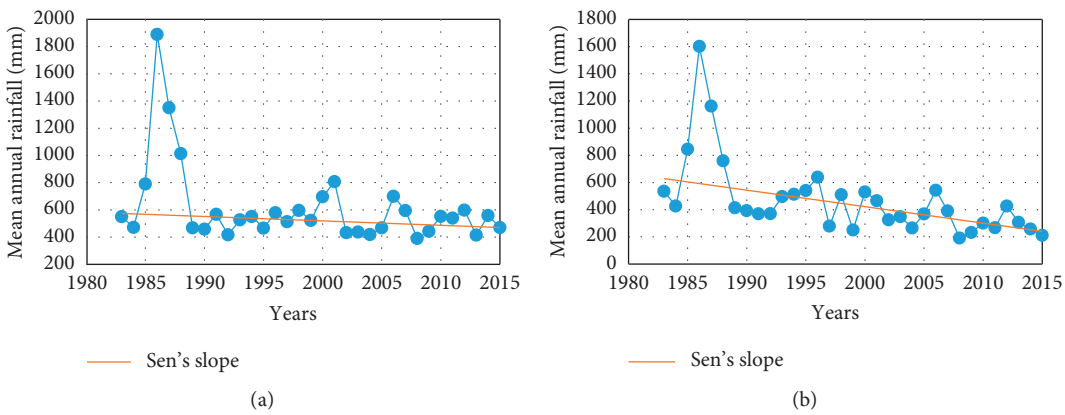

Figure 2: Mean annual rainfall trends for Hawzen (a) and Irob (b) districts during 1983–2015.

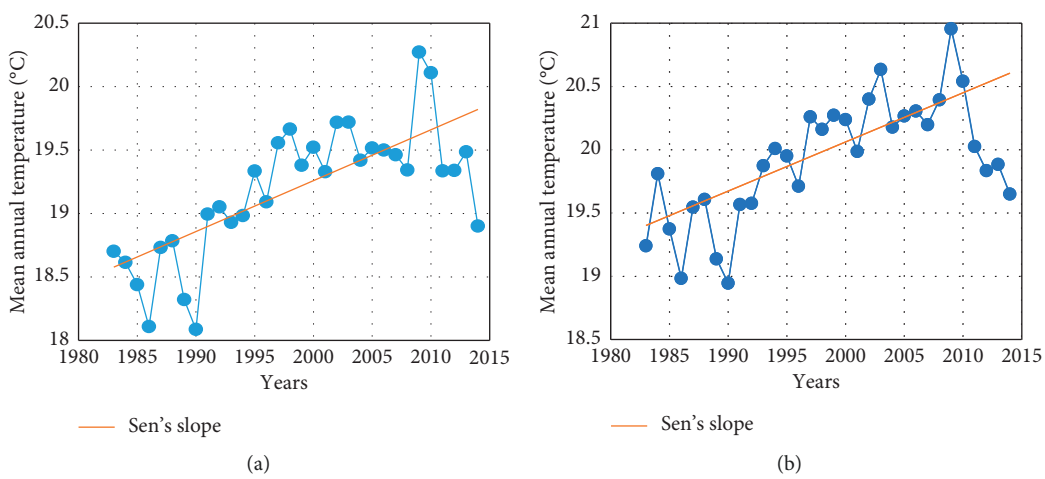

Figure 3: Mean annual temperature trends for (a) Hawzen and (b) Irob districts during 1983–2015.

harmony between farmers' perception of an increased temperature trend and meteorological results is also supported by previous works [23, 70, 71].

3.5. Adaptation Strategies to Perceived Climate Change. Rural farmers in developing countries are vulnerable to climatic and nonclimatic induced stressors that caused high income and consumption fluctuations [72, 73]. Nevertheless, they are not passive receivers of shocks; rather employing an adaptation strategy is a policy option to reduce the negative impact of climate change [74]. According to ([75]: 225), adaptation in the climate change context refers to "adjustments in ecological-social-economic systems in response to actual or expected climatic stimuli, their effects, or impacts." Adaptation based on purposefulness can be classified as autonomous and planned adaptation [75]. An autonomous adaptation also referred to as reactive adaptation is an action undertaken by vulnerable people without direct interventions of a public agency to reduce risks posed by climatic stimuli [7]. However, Stern [76] argued that an autonomous adaptation is inefficient and reduces courtesy to necessary planned interventions. Conversely, planned adaptation is the result of deliberate policy decisions by government agencies aimed at promoting appropriate and effective adaptation measures. Generally, households can adopt more than one adaptation strategies based on their long-term knowledge and perceptions of climate changes.

The main climate change adaptation strategies were soil and water conservation (SWC) (87.71%), planting

trees (84.64%), crop varieties (81%), changing crop planting times (64.25%), biological conservation (43.58), and irrigation (19%) in the study area. These adaptation strategies have been widely in use in Ethiopia for a long period of time in response to historic climate change [36, 51, 77]. But it is not required to link all of these strategies directly to reduce climate change impacts [29]. For instance, the aim of adoption of new crop varieties might be to increase production and household income.

SWC is the dominant planned adaptation strategy farmers employed to ease the adverse effects of climate change and variability. Specifically, in Irob, currently 2 percent land is under cultivation of the total area because of severe land degradation and steeped land slope. Consequently, the average land holding size per household head is estimated around 0.02 hectares. Hence, farmers adopted different SWC practices including built bench terrace, soil bunds, and check dam based on the land use types to improve soil fertility and extensive farming. Besides, SWC farmers planted trees as an adaptation and mitigation measure to prevent land erosion caused by heavy rainfall. The rainfall of the area is a weakly bimodal pattern; hence, during the short rain season, farmers grow potato and sorghum that are drought-resistant and short maturing varieties of crops followed by maize, wheat, and barley crop varieties with a long main rainy season. The rainfall variability in terms of length of the growing season has always been indeterminate because of high variability of onset and cessation of the rainy season (Table 2). This demands a correct planning of the lean period (sowing, growing, and harvesting) and selection of the crop type and variety. During the late-onset small rainy season, farmers reschedule the crop calendar by sowing crop varieties to be harvested (barely, teff, and wheat) on the onset of the main rainy season in October–December. Overall, yields damage meaningfully with either a late onset or an early cessation of the growing season in the study area.

However, there were differences in the intensity of the adaptation strategy between the districts except for planting trees (Table 7). This indicates that households living in the Hawzen district were in a better position to ameliorate climate change risk impacts compared to households in the Irob district employing these adaptation measures. Generally, local knowledge-based adaptation strategies are more effective over the national-level adaptation strategy [78].

Table 7: Adaptation strategies to perceived temperature and rainfall changes ($n = 358$).

Adaptation strategy	Hawzen Percent	Irob Percent	p value
Improved crop varieties	96.15	60.00	0.001
Soil and water conservation	83.65	93.33	0.006
Planting trees	83.60	86.00	0.544
Changing planting time	79.81	42.67	0.001
Biological conservation	57.69	24.00	0.001
Irrigation	13.46	26.67	0.002

4. Conclusion and Policy Implications

Integrating farmers' perceptions of climate change and variability with the observed meteorological data that influence adaptation strategies has not been extensively studied. This study analyzed farmers' perceptions about rainfall and temperature corresponding to the observed metrological data and their adaptation strategies to the perceived climate change. The multistage sampling method was employed to select 358 rural farmers in Hawzen and Irob districts located in semiarid highlands of Eastern Tigray, northern Ethiopia. Moreover, areal gridded data on rainfall and temperature were collected from National Meteorology Agency of Ethiopia.

There is a positive correlation among farmers' access to weather information, farmers' access to training in agronomic practices, access to agricultural extension services, and number of social networks in which farmers have membership. The majority of the farmers had perceived climate change and extreme weather events in their locality in the last fifteen years. Specifically, about 98.56 percent and 92 percent farmers perceived a decrease in rainfall amount in Hawzen and Irob districts, respectively. However, a statistically significant difference was found between the two districts, indicating that farmers who had been in Hawzen were more likely to perceive a decrease in rainfall compared to those in Irob. The mean annual rainfall variability in Hawzen and Irob varies between 47.9 percent and 59.5 percent. As a result, a significant difference in annual rainfall was observed in the two districts. Furthermore, in Hawzen and Irob, the proportion of negative anomalies ranges from 63 percent to 79 percent of the total observations. Farmers realized the manifestation of rainfall variability in terms of change in the onset and cessation of the rainy season, decreased number of rainy days, increased intensity, and unpredictable rainfall distribution. Moreover, 87 percent and 90 percent of farmers felt that temperature was increased in the last 15 years in Hawzen and Irob, respectively. The statistical result indicated that households who had been in Irob were more likely to perceive an increase in temperature compared to those in Hawzen. The noticed increased temperature evidences the increase in the number of hot days, warm nights, and decreased coldness in cold seasons.

The actual meteorological data coincide with farmers' perceptions of climate change and variability that demonstrate decreasing mean annual rainfall and increasing temperatures. Specifically, the modified MKT test showed that, in Hawzen and Irob, mean annual rainfall had decreased by 32.38 mm and 121.33 mm per decade, respectively, except an increased trend that was observed at the summer rainy season in the Hawzen district. Conversely, the mean annual temperature had been increasing by about 0.4°C and 0.39°C per decade, respectively, during the period of analysis.

The study results indicated that SWC, planting trees, crop varieties, changing crop calendar, biological conservation, and irrigation were the dominant adaptation strategies farmers adopted to ameliorate the perceived impact of climate change risks. Thus, the results of this

study provide valuable information to policy-makers and extension works. First, an increase in local weather station sites improves access to weather information, thereby advancing the adaptation strategies against adverse climate change impacts. Second, local government and NGOs are required to disseminate and present weather information in newspapers and Internet to promote the capacity of rural agricultural extension workers and farmers. Third, since farmers used family social networks to find weather information under poor climate information dissemination, local governments should strengthen social networks' capacity and develop a link with local public institutions.

Data Availability

The household survey primary data and climate data used to support the findings of this study are available from the corresponding author upon request.

Conflicts of Interest

The authors declare that there are no conflicts of interest regarding the publication of this paper.

Acknowledgments

This study was carried out with the financial support from Adigrat University and Addis Ababa University as part of the first author's Ph.D. program. The authors wish to thank the farmers for their collaboration in interview and National Meteorology Agency of Ethiopia for providing the gridded monthly rainfall and temperature data.

References

[1] A. Rahman and M. Begum, "Application of non-parametric test for trend detection of rainfall in the largest island of Bangladesh," *Journal of Earth Sciences*, vol. 2, no. 2, pp. 40–44, 2013.

[2] P. C. Chen, Y. H. Wang, G. J. Y. You, and C. C. Wei, "Comparison of methods for non-stationary hydrologic frequency analysis: case study using annual maximum daily precipitation in Taiwan," *Journal of Hydrology*, vol. 545, pp. 197–211, 2017.

[3] C. S. Sharma, S. N. Panda, R. P. Pradhan, A. Singh, and A. Kawamura, "Precipitation and temperature changes in eastern India by multiple trend detection methods," *Atmospheric Research*, vol. 180, pp. 211–225, 2016.

[4] Food and Agricultural organization (FAO), *Climate Change Adaptation and Mitigation in the Food and Agriculture Sector*, FAO, Rome, Italy, 2008.

[5] World Bank, *Social Protection Sector Strategy: From Safety Net to Springboard*, The World Bank Group, Washington, DC, USA, 2002.

[6] Intergovernmental Panel on Climate Change (IPCC), *Climate Change 2013: The Physical Science Basis. Contribution of Working Group I to the Fifth Assessment Report of the Intergovernmental Panel on Climate Change*, T. F. Stocker, D. Qin, G. K. Plattner et al., Eds., Cambridge University Press, Cambridge, UK, 2013.

[7] Intergovernmental Panel on Climate Change (IPCC), *Climate Change 2001: Synthesis Report. A Contribution of Working Groups I, II and III to the Third Assessment Report of the Intergovernmental Panel on Climate Change*, Cambridge University Press, Cambridge, UK, 2001.

[8] Intergovernmental Panel on Climate Change (IPCC), *Climate Change 2007: Impacts, Adaptation and Vulnerability. Contribution of Working Group II to the Fourth Assessment Report of the Intergovernmental Panel on Climate Change*, M. L. Parry, O. F. Canziani, J. P. Palutikof, P. J. van der Linden, and C. E. Hanson, Eds., Cambridge University Press, Cambridge, UK, 2007.

[9] L. Zhang and T. Zhou, "An assessment of monsoon precipitation changes during 1901–2001," *Climate Dynamics*, vol. 37, no. 1-2, pp. 279–296, 2011.

[10] W. H. Cheung, G. B. Senay, and A. Singh, "Trends and spatial distribution of annual and seasonal rainfall in Ethiopia," *International Journal of Climatology*, vol. 28, no. 13, pp. 1723–1734, 2008.

[11] World Bank, *Managing Water Resources to Maximize Sustainable Growth: A World Bank Water Resources Assistance Strategy for Ethiopia*, World Bank, Washington, DC, USA, 2006.

[12] S. N. Ali, "Climate change and economic growth in a rain-fed economy: how much does rainfall variability cost Ethiopia?," *SSRN Electronic Journal*, 2012.

[13] W. Bewket and D. Conway, "A note on the temporal and spatial variability of rainfall in the drought-prone Amhara region of Ethiopia," *International Journal of Climatology*, vol. 27, no. 11, pp. 1467–1477, 2007.

[14] S. Rosell, "Regional perspective on rainfall change and variability in the central highlands of Ethiopia, 1978–2007," *Applied Geography*, vol. 31, no. 1, pp. 329–338, 2011.

[15] M. R. Jury and C. Funk, "Climatic trends over Ethiopia: regional signals and drivers," *International Journal of Climatology*, vol. 33, no. 8, pp. 1924–1935, 2013.

[16] N. Wagesho, N. K. Goel, and M. K. Jain, "Temporal and spatial variability of annual and seasonal rainfall over Ethiopia," *Hydrological Sciences Journal*, vol. 58, no. 2, pp. 354–373, 2013.

[17] G. Kiros, A. Shetty, and L. Nandagiri, "Analysis of variability and trends in rainfall over northern Ethiopia," *Arabian Journal of Geosciences*, vol. 9, no. 6, 2016.

[18] I. Ahmad, F. Zhang, M. Tayyab et al., "Spatiotemporal analysis of precipitation variability in annual, seasonal and extreme values over upper Indus River basin," *Atmospheric Research*, vol. 213, pp. 346–360, 2018.

[19] O. O. Akinremi, S. M. McGinn, and H. W. Cutforth, "Seasonal and spatial patterns of rainfall trends on the Canadian prairies," *Journal of Climate*, vol. 14, no. 9, pp. 2177–2182, 2001.

[20] M. T. Niles and N. D. Mueller, "Farmer perceptions of climate change: associations with observed temperature and precipitation trends, irrigation, and climate beliefs," *Global Environmental Change*, vol. 39, pp. 133–142, 2016.

[21] D. Y. Ayal and W. Leal Filho, "Farmers' perceptions of climate variability and its adverse impacts on crop and livestock production in Ethiopia," *Journal of Arid Environments*, vol. 140, pp. 20–28, 2017.

[22] A. M. Limantol, B. E. Keith, B. A. Azabre, and B. Lennartz, "Farmers' perception and adaptation practice to climate variability and change: a case study of the Vea catchment in Ghana," *SpringerPlus*, vol. 5, no. 1, 2016.

[23] G. T. Moroda, D. Tolossa, and N. Semie, "Perception and adaptation strategies of rural people against the adverse effects of climate variability: a case study of Boset district, East Shewa,

Ethiopia," *Environmental Development*, vol. 27, pp. 2–13, 2018.

[24] S. Luís, C. M. Vauclair, and M. L. Lima, "Raising awareness of climate change causes? Cross-national evidence for the normalization of societal risk perception of climate change," *Environmental Science & Policy*, vol. 80, pp. 74–81, 2018.

[25] A. Tripathi and A. K. Mishra, "Knowledge and passive adaptation to climate change: an example from Indian farmers," *Climate Risk Management*, vol. 16, pp. 195–207, 2017.

[26] E. U. Weber, "What shapes perceptions of climate change?," *Wiley Interdisciplinary Reviews: Climate Change*, vol. 1, no. 3, pp. 332–342, 2010.

[27] S. B. Broomell, D. V. Budescu, and H. H. Por, "Personal experience with climate change predicts intentions to act," *Global Environmental Change*, vol. 32, pp. 67–73, 2015.

[28] E. Meze-Hausken, "Contrasting climate variability and meteorological drought with perceived drought and climate change in northern Ethiopia," *Climate Research*, vol. 27, no. 1, pp. 19–31, 2004.

[29] G. M. M. Alam, K. Alam, and S. Mushtaq, "Climate change perceptions and local adaptation strategies of hazard-prone rural households in Bangladesh," *Climate Risk Management*, vol. 17, pp. 52–63, 2017.

[30] Intergovernmental Panel on Climate Change (IPCC), *Climate Change 2014: Synthesis Report. Contribution of Working Groups I, II and III to the Fifth Assessment Report of the Intergovernmental Panel on Climate Change*, R. K. Pachauri and L. A. Meyer, Eds., IPCC, Geneva, Switzerland, 2014.

[31] J. Nyssen, H. Vandenreyken, J. Poesen et al., "Rainfall erosivity and variability in the northern Ethiopian highlands," *Journal of Hydrology*, vol. 311, no. 1–4, pp. 172–187, 2005.

[32] S. Tesfaye, E. Birhane, T. Leijnse, and S. E. A. T. M. van der Zee, "Climatic controls of ecohydrological responses in the highlands of northern Ethiopia," *Science of the Total Environment*, vol. 609, pp. 77–91, 2017.

[33] B. Grum, R. Hessel, A. Kessler et al., "A decision support approach for the selection and implementation of water harvesting techniques in arid and semi-arid regions," *Agricultural Water Management*, vol. 173, pp. 35–47, 2016.

[34] Central Statistical Agency (CSA), *Population Projection of Ethiopia for All Regions at Woreda Level from 2014–2017*, Central Statistical Agency (CSA), Addis Ababa, Ethiopia, 2013.

[35] M. Gocic and S. Trajkovic, "Analysis of changes in meteorological variables using Mann-Kendall and Sen's slope estimator statistical tests in Serbia," *Global and Planetary Change*, vol. 100, pp. 172–182, 2013.

[36] A. Alemayehu and W. Bewket, "Determinants of smallholder farmers' choice of coping and adaptation strategies to climate change and variability in the central highlands of Ethiopia," *Environmental Development*, vol. 24, pp. 77–85, 2017.

[37] National Meteorological Services Agency (NMSA), *Assessment of Drought in Ethiopia: Meteorological Research Report Series*, Vol. 1, NMSA, Addis Ababa, Ethiopia, 1996.

[38] E. Viste, D. Korecha, and A. Sorteberg, "Recent drought and precipitation tendencies in Ethiopia," *Theoretical and Applied Climatology*, vol. 112, no. 3-4, pp. 535–551, 2013.

[39] H. B. Mann, "Nonparametric tests against trend," *Econometrica*, vol. 13, no. 3, pp. 245–259, 1945.

[40] M. G. Kendall, *Rank Correlation Methods*, Griffin, London, UK, 1955.

[41] K. H. Hamed, "Enhancing the effectiveness of prewhitening in trend analysis of hydrologic data," *Journal of Hydrology*, vol. 368, no. 1–4, pp. 143–155, 2009.

[42] B. Önöz and M. Bayazit, "The power of statistical tests for trend detection," *Journal of Engineering and Environmental Sciences*, vol. 27, no. 4, pp. 247–251, 2003.

[43] World Meteorological Organization (WMO), "Scientific assessment of ozone depletion," Global Ozone Research and Monitoring Project—Report no. 55, World Meteorological Organization, Geneva, Switzerland, 2014.

[44] E. McBean and H. Motiee, "Assessment of impacts of climate change on water resources—a case study of the Great Lakes of North America," *Hydrology and Earth System Sciences Discussions*, vol. 3, no. 5, pp. 3183–3209, 2006.

[45] K. H. Hamed and A. R. Rao, "A modified Mann–Kendall trend test for autocorrelated data," *Journal of Hydrology*, vol. 204, no. 1–4, pp. 182–196, 1998.

[46] S. H. Bari, M. T. U. Rahman, M. A. Hoque, and M. M. Hussain, "Analysis of seasonal and annual rainfall trends in the northern region of Bangladesh," *Atmospheric Research*, vol. 176-177, pp. 148–158, 2016.

[47] D. R. Helsel and R. M. Hirsch, *Statistical Methods in Water Resources*, United States Geological Survey, Reston, VA, USA, 2002.

[48] H. Theil, "A rank-invariant method of linear and polynomial regression analysis," in *Advanced Studies in Theoretical and Applied Econometrics*, vol. 23, pp. 345–381, Springer, Berlin, Germany, 1992.

[49] P. K. Sen, "Estimates of the regression coefficient based on Kendall's tau," *Journal of the American Statistical Association*, vol. 63, no. 324, pp. 1379–1389, 1968.

[50] M. G. Kendall, *Rank Correlation Methods*, Griffin, London, UK, 4th edition, 1948.

[51] T. T. Deressa, R. M. Hassan, C. Ringler, T. Alemu, and M. Yesuf, "Determinants of farmers' choice of adaptation methods to climate change in the Nile Basin of Ethiopia," *Global Environmental Change*, vol. 19, no. 2, pp. 248–255, 2009.

[52] A. Asfaw and A. Admassie, "The role of education on the adoption of chemical fertiliser under different socioeconomic environments in Ethiopia," *Agricultural Economics*, vol. 30, no. 3, pp. 215–228, 2004.

[53] E. Hisali, P. Birungi, and F. Buyinza, "Adaptation to climate change in Uganda: evidence from micro level data," *Global Environmental Change*, vol. 21, no. 4, pp. 1245–1261, 2011.

[54] World Bank, *Climate Information Services Providers in Kenya, No. 103186-KE*, World Bank, Washington, DC, USA, 2016.

[55] Y. Dong, S. Hu, and J. Zhu, "From source credibility to risk perception: how and when climate information matters to action," *Resources, Conservation and Recycling*, vol. 136, pp. 410–417, 2018.

[56] P. Wainaina, S. Tongruksawattana, and M. Qaim, "Tradeoffs and complementarities in the adoption of improved seeds, fertilizer, and natural resource management technologies in Kenya," *Agricultural Economics*, vol. 47, no. 3, pp. 351–362, 2016.

[57] A. R. Kaliba, H. Verkuijl, and W. Mwangi, "Factors affecting adoption of improved maize seed and use of inorganic fertilizer for maize production in the intermediate and lowland zone of Tanzania," *Journal of Agricultural and Applied Economics*, vol. 48, no. 1, pp. 1–12, 2000.

[58] E. Muema, J. Mburu, J. Coulibaly, and J. Mutune, "Determinants of access and utilization of seasonal climate information services among smallholder farmers in Makueni county, Kenya," *Heliyon*, vol. 4, no. 11, pp. 1–19, 2018.

[59] V. C. Kirui, M. Waiganjo, and S. Cheplogoi, "Evaluating access and use of dissemination pathways for delivering

climate information and services to women farmers in semi-arid Kenya," *International Journal of Advanced Research*, vol. 2, no. 9, pp. 44–53, 2014.

[60] D. Maddison, *The Perception of and Adaptation to Climate Change in Africa: Policy Research Working Paper 4308*, The World Bank, Washington, DC, USA, 2007.

[61] M. Belihu, B. Abate, S. Tekleab, and W. Bewket, "Hydro-meteorological trends in the gidabo catchment of the rift valley lakes basin of Ethiopia," *Physics and Chemistry of the Earth, Parts A/B/C*, vol. 104, pp. 84–101, 2018.

[62] D. Conway, "Some aspects of climate variability in the northeast Ethiopian highlands-Wollo and Tigray," *SINET: Ethiopian Journal of Science*, vol. 23, no. 2, pp. 139–161, 2000.

[63] G. Hadgu, K. Tesfaye, G. Mamo, and B. Kassa, "Trend and variability of rainfall in Tigray, Northern Ethiopia: analysis of meteorological data and farmers' perception," *Academia Journal of Agricultural Research*, vol. 1, no. 6, pp. 88–100, 2013.

[64] B. Pohl and P. Camberlin, "Influence of the Madden–Julian oscillation on east african rainfall. I: intraseasonal variability and regional dependency," *Quarterly Journal of the Royal Meteorological Society*, vol. 132, no. 621, pp. 2521–2539, 2006.

[65] WMO, "Standardized precipitation index user guide," Technical Report 1090, WMO, Geneva, Switzerland, 2012.

[66] T. B. McKee, N. J. Doesken, and J. Kleist, "The relationship of drought frequency and duration to time scales," *American Meteorological Society*, vol. 17, no. 22, pp. 179–183, 1993.

[67] J. Verdin, C. Funk, G. Senay, and R. Choularton, "Climate science and famine early warning," *Philosophical Transactions of the Royal Society B: Biological Sciences*, vol. 360, no. 1463, pp. 2155–2168, 2005.

[68] D. N. Gujarati, *Basic Econometrics*, Tata McGraw-Hill Education, New York, NY, USA, 2009.

[69] T. Gebrehiwot and A. van der Veen, "Assessing the evidence of climate variability in the northern part of Ethiopia," *Journal of Development and Agricultural Economics*, vol. 5, no. 3, pp. 104–119, 2013.

[70] D. Y. Ayal, M. Radeny, S. Desta, and G. Gebru, "Climate variability, perceptions of pastoralists and their adaptation strategies: implications for livestock system and diseases in Borana zone," *International Journal of Climate Change Strategies and Management*, vol. 10, no. 4, pp. 596–615, 2018.

[71] B. Legesse, Y. Ayele, and W. Bewket, "Smallholder farmers' perceptions and adaptation to climate variability and climate change in Doba district, West Hararghe, Ethiopia," *Asian Journal of Empirical Research*, vol. 3, no. 3, pp. 251–265, 2012.

[72] J. Gao and B. F. Mills, "Weather shocks, coping strategies, and consumption dynamics in rural Ethiopia," *World Development*, vol. 101, pp. 268–283, 2018.

[73] J. McCarthy, O. F. Canziani, N. A. Leary, D. J. Dokken, and C. White, *Climate Change 2001: Impacts, Adaptation, and Vulnerability. Contribution of Working Group II to the Third Assessment Report of the Intergovernmental Panel on Climate Change*, Cambridge University Press, Cambridge, UK, 2001.

[74] S. Dercon, "Income risk, coping strategies, and safety nets," *The World Bank Research Observer*, vol. 17, no. 2, pp. 141–166, 2002.

[75] K. Smith, C. B. Barrett, and P. W. Box, "Participatory risk mapping for targeting research and assistance: with an example from east African pastoralists," *World Development*, vol. 28, no. 11, pp. 1945–1959, 2000.

[76] N. Stern, *The Economics of Climate Change: The Stern Review*, Cambridge University Press, Cambridge, UK, 2007.

[77] Y. A. Tessema, C. S. Aweke, and G. S. Endris, "Understanding the process of adaptation to climate change by small-holder farmers: the case of east Hararghe zone, Ethiopia," *Agricultural and Food Economics*, vol. 1, no. 1, pp. 1–17, 2013.

[78] S. Eriksen and J. Lind, "Adaptation as a political process: adjusting to drought and conflict in Kenya's drylands," *Environmental Management*, vol. 43, no. 5, pp. 817–835, 2009.

Hindawi
Advances in Meteorology
Volume 2019, Article ID 1935719, 15 pages
https://doi.org/10.1155/2019/1935719

Research Article

Climate Change Characteristics of Extreme Temperature in the Minjiang River Basin

Ting Chen,[1,2] **Tianqi Ao**,[1] **Xu Zhang**,[1,3,4] **Xiaodong Li**,[1] **and Kebi Yang**[1]

[1]*State Key Laboratory of Hydraulics and Mountain River Engineering, College of Water Resource and Hydropower, Sichuan University, Chengdu 610065, China*
[2]*Heavy Rain and Drought-Flood Disasters in Plateau and Basin Key Laboratory of Sichuan Province, Chengdu 610072, China*
[3]*State Key Laboratory of Hydrology-Water Resources and Hydraulic Engineering, Nanjing Hydraulic Research Institute, Nanjing 210029, China*
[4]*Research Center for Climate Change, Ministry of Water Resources, Nanjing 210029, China*

Correspondence should be addressed to Tianqi Ao; aotianqi@scu.edu.cn

Received 28 February 2019; Accepted 10 June 2019; Published 14 July 2019

Guest Editor: Sushil K. Dash

Based on the daily temperature data from 26 meteorological stations in the Minjiang River Basin, for 1961 to 2016, the temporal trend and spatial distribution of extreme temperature in this region were analyzed using 16 extreme temperature indices. The results show that in terms of time variation, determined using linear trend analysis and a Mann–Kendall trend test, the warm and day indices mainly show an upward trend while the cold and night indices mainly show a downward trend in the entire basin. Among them, FD0, TN10, and CSDI significantly decrease at −1.3, −2.9, and −1.1 d/10a, respectively. TN90, TX90, SU25, and TR20 significantly increase at 3.0, 2.6, 2.1, and 2.2 d/10a, respectively. The crop growth period in the basin showed a significant increasing trend at 1.4 days/decade, while the diurnal temperature range showed a nonsignificant increasing trend at 0.03 days/decade. On comparing the change range of each index, it was found that the change range of the warm index is greater than that of the cold index, while the change range of the day index is smaller than that of the night index; thus, the change trends of the maximum and minimum temperatures in the whole basin are not obvious. Analysis of the changing trend at each station showed that the relative index of the extreme temperature in the basin has good climatic consistency in terms of spatial distribution. The distributions of the absolute and extreme indices are not uniform, which is consistent with the change in elevation in the basin. Further, the diurnal temperature range in the upper reaches of the basin is greater than that in the middle and lower reaches. However, because of the more obvious upward trends of the day and warm indices in the middle and lower reaches, and the more obvious downward trends of the night and cold indices in the upper reaches, the daily temperature differences in the upper, middle, and lower reaches of the Minjiang River Basin tend to be consistent. Therefore, the precipitation in the Minjiang River Basin shows a significant decreasing trend; thus, the basin shows a trend of drying and warming.

1. Introduction

According to the Intergovernmental Panel on Climate Change Fifth Assessment Report, the mean global surface temperature has risen by 0.85°C from 1880 to 2012. It is an undisputed fact that the globe has warmed resulting in a serious impact on human society [1–6]. With the increase in temperature, the ability of the atmosphere to retain water is increased, and the extreme value of temperature has changed significantly, resulting in frequent droughts and forest fires. Meanwhile, with the change of temperature, the global average sea level rose by 19 centimeters between 1901 and 2010. In the past 10 years, the speed of glacier melting has been several times faster than that in the 1990s. The changes in temperature extremes have increased the frequency and intensity of extreme climatic events such as high temperatures, droughts, rainstorms, and flooding. Some extreme climatic phenomena cannot be described by a single meteorological element. For example, when the temperature increases, evaporation will intensify and soil moisture and

infiltration intensity will also change. A change in the water cycle is caused by an increase in temperature. An increase in temperature will also change the redistribution of river runoff and water resource characteristics of a basin. Extreme temperature events are an important part of extreme climatic events; thus, it is of great significance to study the changes in extreme temperature under global warming.

Thus far, many studies have been completed regarding extreme temperature [7, 8]. For example, Alexander et al. [9] found that 70% of the world's regions underwent a significant decrease in cold nights and a significant increase in warm nights during the past 50 years. Manton et al. [10] analyzed 91 temperature stations of 15 countries in Southeast Asia where climate change is extremely evident. The result showed that the number of warm days and nights significantly increased, while the number of cold days and nights significantly decreased during 1961–1988. Overall, the annual average temperature shows a relatively consistent and significant increasing trend worldwide, but the temperature indicators in different regions have different characteristics, particularly extreme temperature indicators.

In China, the annual average surface temperature increased by 1.1°C at a rate of 0.22°C/10a [11], which is higher than the global average during the last 50 years. However, regarding extreme temperature, Ren et al. [12] found that cold extreme events such as cold waves, nights, and days and frost days significantly decreased. In contrast, warm events such as warm nights and days significantly decreased, particularly warm nights in China. Zhang et al. [13] found that the annual and seasonal extreme low temperatures in China showed a steady increasing trend by calculating the daily maximum and minimum temperatures of 234 meteorological stations in China from 1955 to 2005. Wang et al. [14] considered that the cold index increased more than the warm index, and the night index increased more than the day index. From the aforementioned studies, it is clear that due to global warming, extreme temperature indices in different regions do respond differently, and the variation range of cold and warm indices in different regions varies from day to night. Overall, studies show that the frequency and intensity of cold wave events in most parts of China have significantly decreased, but the intensity of heat wave events in China shows regional asymmetry [15–17]. The frequency of heat wave events has strong interdecadal characteristics, and the long-term linear trend is not obvious. This shows that with an increase in temperature, the frequency of cold extreme events decreases while the frequency of warm extreme events has different characteristics in different regions. The Yangtze River is the largest river in China, and the third largest river in the world. The basin has a dense population and is among the areas with a highly developed economy. The Yangtze River is affected not only by the southeast and southwest monsoons but also by the Qinghai-Tibet Plateau. It is a vulnerable area of climate change and a frequent area of drought and flood disasters [18]. Zhou et al. [19] considered that extreme low temperature days began to decrease and extreme high temperature days began to increase after 1987 in the lower reaches of the Yangtze River. Both extreme high temperature and extreme low temperature showed a significant upward trend, particularly extreme low temperature. Zhong et al. [20] found that the annual and seasonal mean temperature of the Yangtze River Basin showed a significant upward trend from 1961 to 2013 and is more obvious during winter than summer. Wang et al. [21] showed that the annual average temperature in most areas of the upper reaches of the Yangtze River showed an upward trend, particularly during the 1990s; the most significant increase in temperature occurring during winter mainly distributed in the source area of the Yangtze River and the Jinsha River Basin. Wang et al. [14] noted that the average temperature in the upper reaches of the Yangtze River showed an upward trend and, at the same time, the increase in temperature reflected a trend of drought aggravation. At present, a large number of studies have focused on the Yangtze River Basin or the upper and middle reaches of the Yangtze River as a whole, to study its trend changes. Analysis of extreme temperature indicators in the Yangtze River Basin is relatively general, mainly focusing on changes in the highest and lowest temperatures and average temperatures. At the same time, the results show that there is regional asymmetry in the upper reaches and in the middle and lower reaches of the Yangtze River. The mean summer temperature in the middle and lower reaches of the Yangtze River has significantly decreased because of the obvious decrease in the maximum temperature, while the upper reaches of the Yangtze River showed an upward trend [12]. The change trend of high temperature days is also different. There is a significant decreasing trend in the middle and lower reaches of the Yangtze River, while there is an increasing trend in the upper reaches [15].

The Minjiang River Basin is in a transitional area from high altitudes to basins on the eastern side of the Qinghai-Tibet Plateau. There are great differences in altitude, topography, and climatic conditions. There are differences between the extreme temperature changes and the overall situation in the Yangtze River Basin. Therefore, it is of great significance to study the spatial differences within the Minjiang River Basin. Based on the daily temperature data of 26 meteorological stations in the Minjiang River Basin from 1961 to 2016, the temporal and spatial variations of extreme temperature in the Minjiang River Basin were analyzed by linear trend analysis and Mann–Kendall (MK) tests. The reasons for the spatial variations in extreme temperature are discussed.

1.1. Study Area. The Minjiang River is the first tributary on the west bank of the upper reaches of the Yangtze River. Figure 1 is the drainage map of the Minjiang River. The Minjiang River is also the largest tributary of runoff in the Yangtze River Basin. Its total length is 790 km. The total elevational drop of the Minjiang River is 3560 m. It originates from the southern foot of Minshan Mountain in Aba Prefecture, Sichuan Province. The area of the basin is 135,881 square km. Because it is rich in hydropower resources, it is an important area for hydropower development in Southwest China. The upper reaches of the Dujiangyan River are mainly hydroelectric power generation and the middle

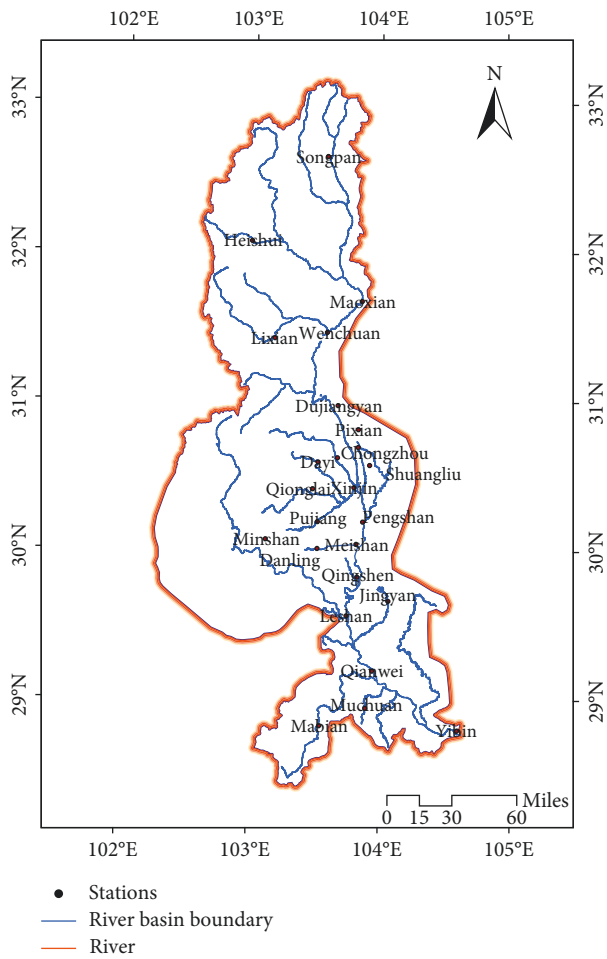

Figure 1: Minjiang River drainage map.

reaches of the Dujiangyan to Leshan flow through the Chengdu Plain area, together with the Tuojiang River system and many artificial river networks, forming the Dujiangyan irrigation area. The lower reaches, from Leshan to Yibin, are mainly used for shipping. It finally flows into the Yangtze River in Yibin.

2. Materials and Methods

2.1. Materials. In this study, the daily temperature data of 26 national basic stations and national general stations (Table 1) in the Minjiang River Basin provided by the China Meteorological Administration (CMA) were used, including daily average temperature, daily maximum temperature, and daily minimum temperature. The time period was 1961–2016. The data have passed strict quality control, including extreme value and time consistency tests.

2.2. Extreme Temperature Index. In this study, 16 important extreme temperature indices recommended and defined by the World Meteorological Organization (WMO) were used, as shown in Table 2. These indices reflect the changes in different aspects of extreme climate [9] and have the characteristics of weak extremes, low noise, and strong significance.

2.2.1. Linear Tendency Estimation Method. In this study, the linear trend estimation method was used to analyze the trend of climate change. The arithmetic of the climatic tendency rate is as follows: Let the time series of a meteorological element of a station be $y_1, y_2, \ldots, y_n$, which can be expressed by a polynomial as follows:

$$y(t) = a_0 + a_1 t_1 + a_2 t_2 + \cdots + a_m t_n. \quad (1)$$

In the formula, t is the time in unit a (year). $a_1{}^*10$ is termed the climatic tendency rate in d/10a or °C/10a. The coefficients in the equation can be determined by the least squares method or an empirical orthogonal polynomial.

2.2.2. MK Trend Test. A MK test is a nonparametric test recommended and widely used by the WMO. It was first proposed by Mann and Kendall and has been applied by many scholars [22–25]. A MK trend test was used to analyze the trend change of time series of precipitation, runoff, temperature, and water quality. A MK test does not require samples to follow a certain distribution, nor is it disturbed by a few abnormal values. It is suitable for non-normal distribution data such as hydrology and meteorology and is easy to calculate [6, 26–29].

In the MK test, the zero hypothesis H_0 and alternative hypothesis H_1 are equal to each other for the question of whether there is a time series trend in the observed data. Statistical value S and standard test statistic value Z_{MK} are calculated as follows:

$$S = \sum_{i=1}^{n-1} \sum_{j=i+1}^{n} \operatorname{sgn}(X_j - X_i),$$

$$\operatorname{sgn}(X_j - X_i) = \begin{cases} +1, & \text{if}(X_j - X_i) > 0, \\ 0, & \text{if}(X_j - X_i) = 0, \\ -1, & \text{if}(X_j - X_i) = 0, \end{cases} \quad (2)$$

$$Z_{MK} = \begin{cases} \dfrac{S+1}{\sqrt{\operatorname{Var}(S)}}, & \text{if } S > 0, \\ 0, & \text{if } S = 0, \\ \dfrac{S-1}{\sqrt{\operatorname{Var}(S)}}, & \text{if } S < 0. \end{cases}$$

In the formula, X_i and X_j are the corresponding values of X of the i-th and j-th years; n is the length of time series data; and Z_{MK} is the trend of the data. If $Z_{\mathrm{MK}} > 0$, the time series data show an increasing trend over time; conversely, the time series data show a decreasing trend over time. When $|Z_{MK}| > Z_{(1-(a/2))}$, the zero hypothesis is rejected and the time series data have a significant trend. The $Z_{(1-(a/2))}$ value can be found in the

Table 1: Basic information of the meteorological stations in the Minjiang River Basin.

Station number	Longitude (°E)	Latitude (°N)	Altitude (m)	Station name	Station class
The upper reaches					
56182	103.57	32.65	2850	Songpan	Bbase station
56185	102.98	32.08	2400	Heishui	Ggeneral stations
56180	103.85	31.68	1591	Maoxian	Ggeneral stations
56183	103.58	31.47	1326	Wenchuan	Ggeneral stations
56184	103.17	31.43	1885	Lixian	Ggeneral stations
The middle reaches					
56188	103.67	30.98	699	Dujiangyan	Bbase station
56189	103.93	30.98	582	Pengzhou	Ggeneral stations
56187	103.83	30.7	539	Wenjiang	Bbase station
56288	103.92	30.58	495	Shuangliu	Ggeneral stations
56181	103.67	30.63	534	Chongzhou	Ggeneral stations
56272	103.83	30.82	559	Pixian	Ggeneral stations
56276	103.8	30.43	468	Xinjin	Ggeneral stations
56285	103.52	30.6	524	Dayi	Ggeneral stations
56284	103.48	30.42	501	Qionglai	Ggeneral stations
56281	103.52	30.2	511	Pujiang	Ggeneral stations
56391	103.82	30.05	415	Meishan	Ggeneral stations
56289	103.87	30.2	437	Pengshan	Ggeneral stations
56381	103.52	30.02	496	Dangling	Ggeneral stations
56383	103.83	29.83	455	Qingshen	Ggeneral stations
56386	103.75	29.57	424	Leshan	Bbase station
56280	103.12	30.08	691	Minshan	Ggeneral stations
The lower reaches					
56390	104.07	29.67	404	Jingyan	Ggeneral stations
56389	103.95	29.2	388	Qianwei	Ggeneral stations
56480	103.55	28.83	541	Mabian	Ggeneral stations
56490	103.9	28.95	397	Muchuan	Ggeneral stations
56492	104.6	28.8	341	Yibin	Bbase station

Table 2: Mean extreme temperatures in the upper, middle, and lower reaches of the Minjiang River Basin from 1961 to 2016 (°C or days).

Index	The upper reaches	The middle reaches	The lower reaches
TX10p	35.77	34.63	36.10
TN10p	35.81	34.47	35.33
TX90p	35.92	37.13	35.78
TN90p	35.76	36.91	36.21
ID0	2.92	0.28	0.00
FD0	95.16	7.60	2.23
SU25	59.14	126.64	139.05
TR20	5.09	86.04	98.29
TXn	9.91	14.29	15.06
TNn	0.13	8.43	10.00
TXx	23.55	26.19	27.55
TNx	9.98	17.34	18.70
WSDI	7.07	7.08	6.94
CSDI	8.91	10.61	11.70
GSL	120.32	171.43	178.28
DTR	23.21	17.28	17.20

standard normal distribution table. When the significance level $a = 5\%$, the corresponding $Z_{(1-(a/2))}$ value is 1.96.

3. Results

3.1. Spatial Distribution. As can be seen from Table 2, the annual average of the relative index of the upper and middle reaches is basically the same as that of the lower and middle reaches of the Minjiang River Basin. In the extreme index, the high values of the extreme cold index and extreme warm index are in the downstream of the basin, while the low values are in the upstream of the basin. In the absolute index, the high value of the cold index (ID0, FD0) is in the upstream of the basin, the low value is in the downstream of the basin, the high value of the warm index (SU25, TR20) is in the downstream of the basin, and the low value is in the upstream of the basin. Among other indicators, DTR in the upper reaches of the basin is higher than that in the middle and lower reaches of the basin. The high values of WSDI is in the upper and middle reaches of the basin, and the difference between the upper, middle, and lower reaches is not obvious. The high values of CSDI and GSL are in the lower reaches of the basin, while the low values are in the upper reaches of the basin.

3.1.1. Relative Index (TX10p, TN10p, TX90p, and TN90p). Figure 2 shows the spatial distribution characteristics of the extreme temperature indicators in the Minjiang River Basin. It can be seen that the spatial distribution of cold nights (TN10p) and cold days (TX10p) in the Minjiang River Basin is relatively uniform, except for the lower days at Shuangliu and Meishan stations in the middle reaches of the Minjiang River Basin, most of which are 34–36 days and 34-35 days, respectively. At the same time, the number of warm nights (TN90p) and warm days (TX90p) at Shuangliu and Meishan

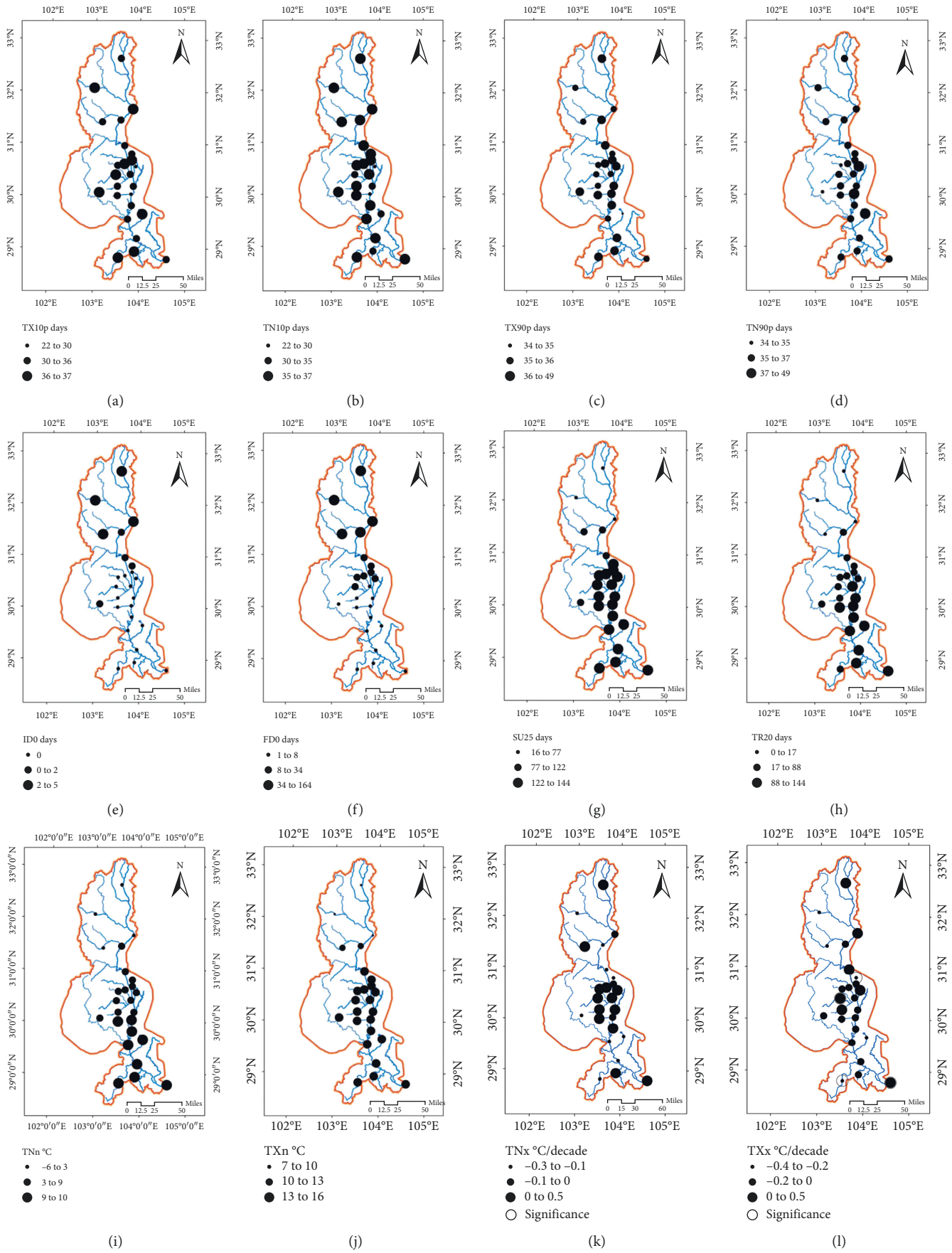

Figure 2: Continued.

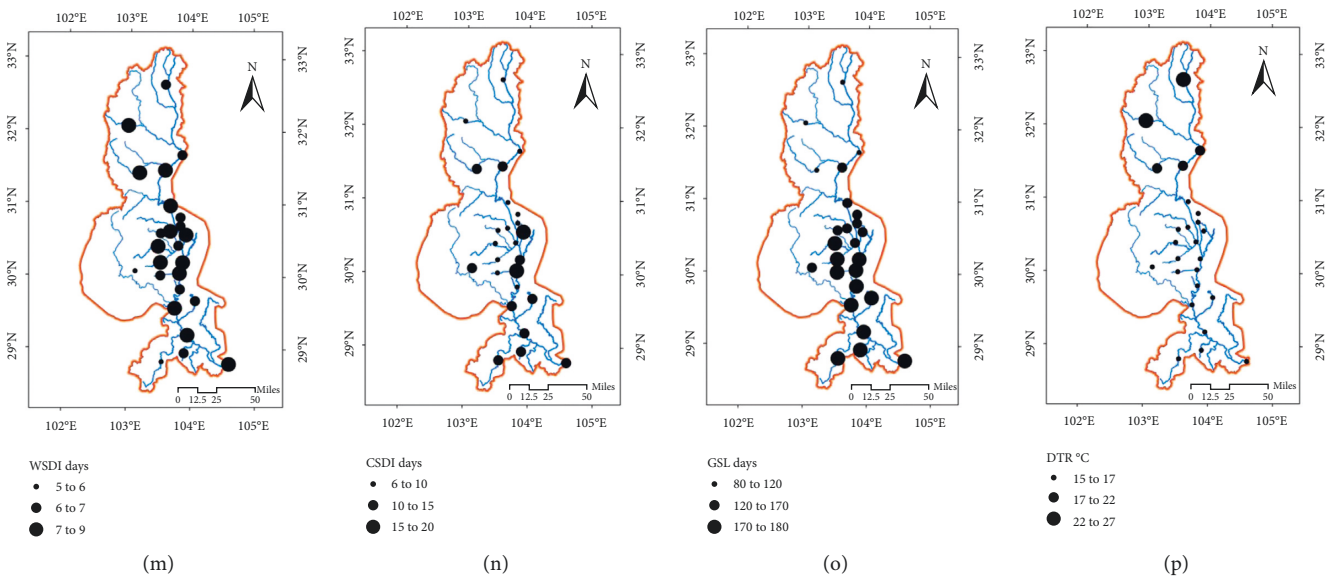

Figure 2: Spatial distribution of extreme temperature index in the Minjiang River Basin from 1961 to 2016.

stations in the middle reaches of the Minjiang River Basin was higher than average, while the remainder was 34–36 days and 36-37 days, respectively. This shows that the climatic consistency of the relative index in the Minjiang River Basin is good.

3.1.2. Absolute Index (ID0, FD0, SU25, and TR20). It can be seen that the high value of ID0 and FD0 in the Minjiang River Basin mainly occurs in the upper reaches of the basin. The maximum value of ID0 is at Maoxian station in the upper reaches of 4.4 days, and the maximum value of FD0 is at Songpan station in the upper reaches of 163 days. The low value of SU25 is in the upper reaches of the basin, while the high value area is in the middle and lower reaches of the basin. The minimum value is at Songpan station in the upper reaches of 16 days, and the maximum value is at Yibin station in the lower reaches of 144 days. The value of the TR20 is zero at Songpan and Heishui stations in the upper reaches of the basin. This shows that the distribution of the absolute index is not uniform in the basin. The number of ID0 and FD0 mainly occurs in the upper reaches of the basin at high altitude, while the high value of SU25 and TR20 mainly occurs in the middle and lower reaches of the basin in the Sichuan basin. The extreme values occur in the lower reaches of the basin.

3.1.3. Extreme Value Index (TXn, TNn, TXx, and TNx). TXn in the upper reaches of the basin is 7–12°C, and the lowest is 7.2°C at Songpan station in the upper reaches. TXn in the middle and lower reaches of the basin is 13–15°C, and the highest value is 15.4°C at Yibin station in the lower reaches. TNn in the upper reaches of the basin is −6 to −4°C, and the lowest is −6.5°C at Songpan station in the upper reaches. TNn in the middle and lower reaches of the basin is 7–10°C, and the highest value is 10.8°C at Yibin station in the lower reaches. TXx in the upper reaches of the basin is 21–25°C, and the lowest value is 21.4°C at Songpan station in the upper reaches. TXx in the middle and lower reaches of the basin is 25–27°C, and the highest value is 27.9°C at Yibin station in the lower reaches. In summary, the low value of the basin extreme value index is in the upper reaches of the basin, while the high value is in the middle and lower reaches of the basin.

3.1.4. Other Indices (GSL, DTR, WSDI, and CSDI). WSDI of the Minjiang River Basin is 5–8 days, and the difference between the upper, middle, and lower reaches is not obvious. CSDI in the upper reaches of the Minjiang River Basin is 6–11 days, and the minimum value of the basin is 6 days at Songpan station. CSDI in the middle and the lower reaches of the Minjiang River Basin is mostly 8–13 days, and the maximum value of the basin is 13 days at Meishan station in the middle reaches of the Minjiang River Basin. There is no obvious difference between the upper, middle, and lower reaches. GSL in the upper reaches of the Minjiang River Basin is lower than that in the middle and lower reaches of the basin. The minimum value of the basin is 86 days at Songpan station in the upper reaches. GSL in the middle and lower reaches of the Minjiang River Basin is greater than 160 days. The maximum value in the basin is 178 days at Qianwei, Mabian, Muchuan, and Yibin stations in the lower reaches. The maximum daily temperature difference in the upper reaches of the Minjiang River Basin is 27°C at Songpan station, while that in the remainder of the basin is greater than 20°C. DTR in the middle and lower reaches of the Minjiang River Basin is between 16 and 17°C. Because there are more FD0 values in the upper reaches of the basin, GSL in the middle and lower reaches of the basin is obviously longer than that in the upper reaches of the basin (approximately twice as long as that in the upper reaches). At the same time, DTR in the upper reaches of the basin is

larger than that in the middle and lower reaches of the basin. In summary, the extreme cold temperature indices such as FD0 and ID0 in the upper reaches are higher than those in the middle and lower reaches. At the same time, the extreme warm temperature indices such as TN90, TX90, SU25, TR20, and GSL are lower in the upper reaches than in the middle and lower reaches. DTR is higher in the upper reaches than in the middle and lower reaches.

3.2. Spatial Variation Trend of Extreme Temperature Indicators. From Table 3, it can be seen that the change trend of relative indices in the upper, middle, and lower reaches of the basin is relatively consistent. The extreme cold temperature indices are consistently decreasing. The decreasing trend of TX10 in the middle and lower reaches is greater than that in the upper reaches, while that of TN10 in the upper reaches is greater than that in the middle and lower reaches. The extreme warm temperature indices are consistently increasing. The increasing trend of TX90 in the middle and lower reaches is greater than that in the upper reaches, and the increasing trend of TN90 in the upper reaches is greater than that in the middle and lower reaches. It can be seen that the relative index in the middle and lower reaches has a greater trend during the day, while the relative index in the upper reaches has a greater trend during the night.

The change trend of the absolute index indices in the upper, middle, and lower reaches of the basin is relatively consistent. The decreasing trend of FD0 in the upper reaches is greater than that in the middle and lower reaches. SU25 showed an increasing trend in the Minjiang Basin, and the increasing trend of SU25 in the middle reaches is greater that in the upstream and downstream. It can be seen that the absolute warm index in the middle and lower reaches has a greater trend while the absolute cold index in the upper reaches has a greater trend in the upper reaches. The trend of the extreme index is weak.

Among other indicators, WSDI has an upward trend and the upward trend in the middle and lower reaches is greater than that in the upper reaches. CSDI has a downward trend, and the downward trend in the upper reaches is greater than that in the middle and lower reaches. It can be seen that the other indicators are similar to the absolute indicators. Warm indicators are larger in the middle and lower reaches than in the upstream, while cold indicators are larger in the upstream than in the middle and lower reaches. In the middle reaches for GSL, the trend is increasing, while the trend is decreasing in the upstream and downstream. DTR is decreasing in the upstream, middle, and downstream.

3.2.1. Relative Index (TX10p, TN10p, TX90p, and TN90p). Figure 3 shows the spatial distribution of the extreme temperature variation trend in Minjiang River Basin. It can be seen that TX10p is increasing at 60% of the stations in the upper reaches of the Minjiang River Basin and decreasing at 80% of the stations in the middle reaches and 100% of the stations in the lower reaches. In total, 7% of the stations in the Minjiang River Basin passed the 0.05 significance test. TN10p showed a downward trend in 92% of the stations in the Minjiang River Basin; 57% of the stations in the basin passed the 0.05 significance test. TN90p is increasing in 100% of the stations in the Minjiang River Basin, while TX90p is increasing in 96% of the stations in the Minjiang River Basin; 81% and 77% of the stations in the basin passed the 0.05 significance test, respectively. This shows that TN90p and TX90p in the basin show mainly an upward trend, while TN10p shows mainly a downward trend. TX10p shows mainly a downward trend in the middle and lower reaches of the basin and an upward trend in the upper reaches.

Table 3: Mean values of trends in the upper, middle, and lower reaches of the Minjiang River Basin from 1961 to 2016 (°C/10a or d/10a).

Index	Upper reaches	Middle reaches	Lower reaches
TX10p	−0.12	−0.50	−0.50
TN10p	−3.98	−2.28	−1.73
TX90p	1.52	3.81	2.49
TN90p	4.86	3.50	2.34
FD0	−2.93	−1.07	−0.14
SU25	2.00	4.82	1.63
TXn	−0.06	0.12	0.04
TNn	−0.66	0.11	0.05
TXx	0.00	0.03	−0.04
TNx	−0.05	0.08	−0.02
WSDI	0.62	1.12	1.00
CSDI	−1.67	−0.90	−1.17
GSL	−3.87	1.49	−2.34
DTR	−0.27	−0.12	−0.09

3.2.2. Absolute Index (ID0, FD0, SU25, and TR20). FD0 is decreasing at 96% of the stations in the Minjiang River Basin; 57% of the stations in the Minjiang River Basin passed the 0.05 significance test. SU25 is increasing at 92% of the stations in the Minjiang River Basin; 65% of the stations in the basin passed the 0.05 significance test, particularly Pengshan, Danling, and Qingshen stations in the middle reaches of the basin. The change rate is 17 d/10a, 11 d/10a, and 11 d/10a, respectively. Because the middle and lower reaches of the Minjiang River Basin are in a subtropical zone, ID0 is mostly 0. The upper reaches of the Minjiang River Basin are at a high altitude and the TR20 value is mostly 0, so trend analysis was not completed for ID0 and TR20. This shows that the FD0 in the basin mainly decreases, while SU25 in the basin mainly increases, particularly in the middle reaches of the basin.

3.2.3. Extreme Value Index (TXn, TNn, TXx, and TNx). TXn showed a downward trend at 60% of the stations in the upper reaches of the Minjiang River Basin, an upward trend at 68% of the stations in the middle reaches of the Minjiang River Basin, and a downward trend at 60% of the stations in the lower reaches of the basin; 15% of the stations in the basin passed the significance test. TNn showed a downward trend at 57% of the stations in the Minjiang River Basin. TXx

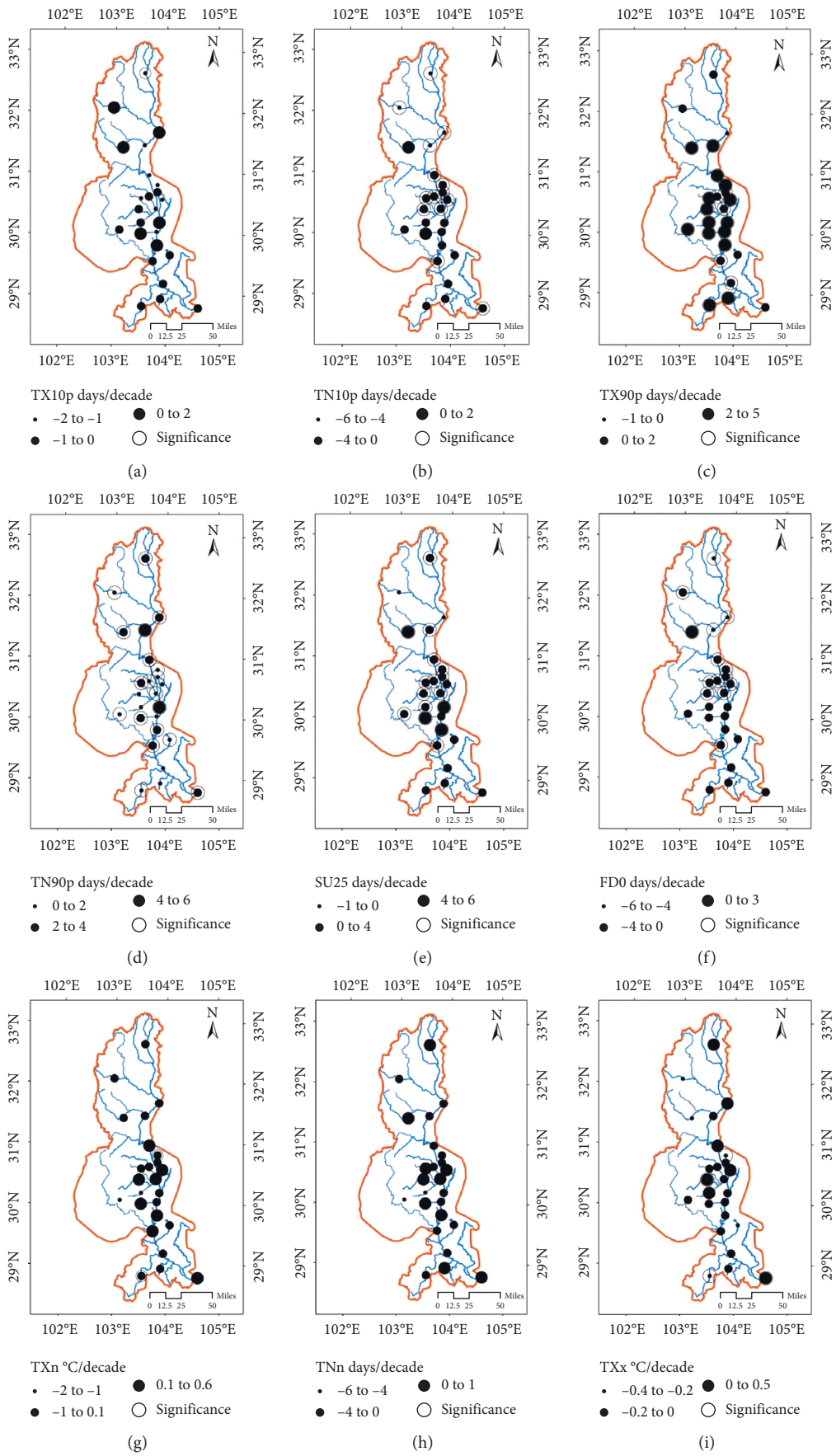

Figure 3: Continued.

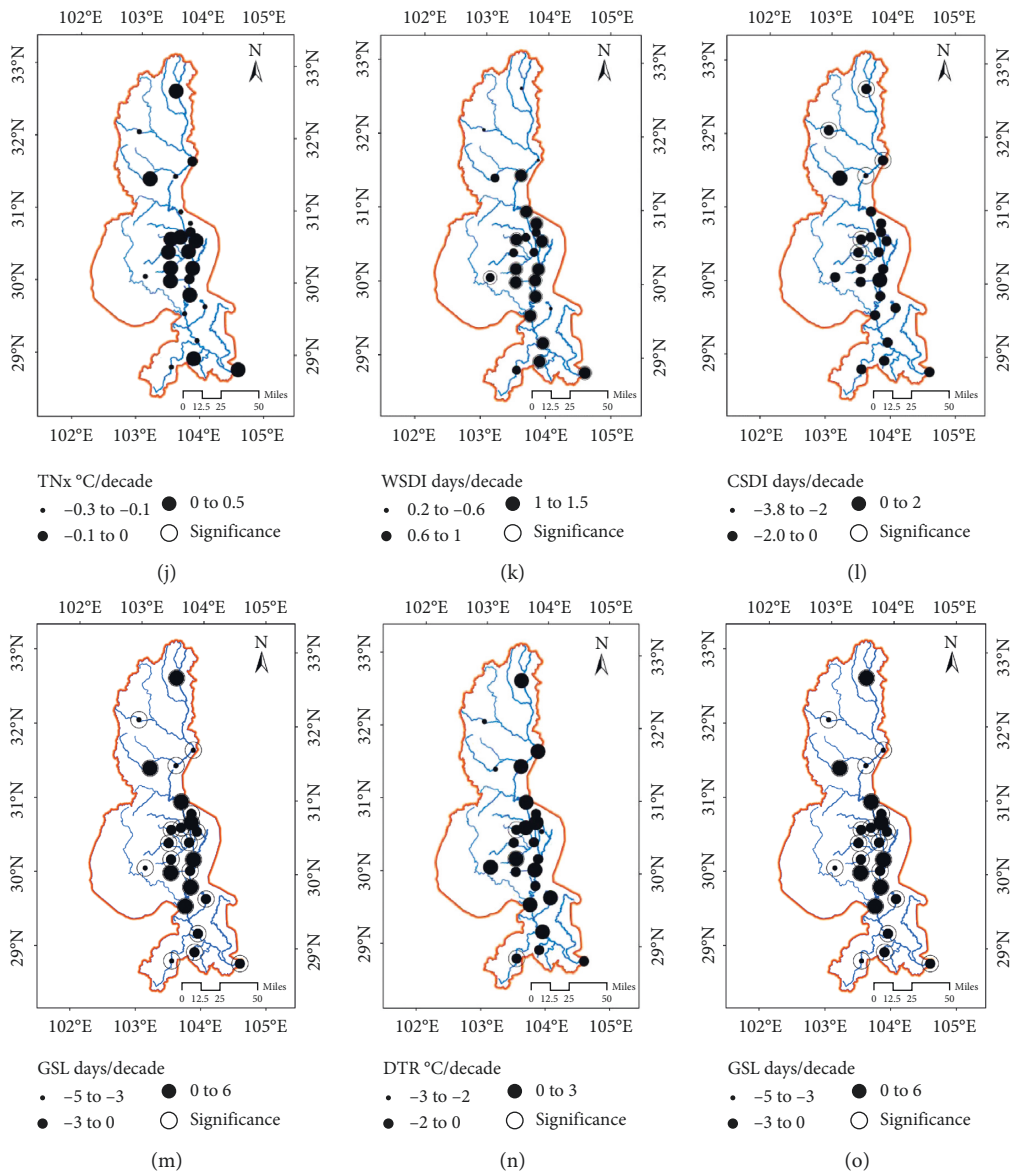

Figure 3: Spatial distribution of the extreme temperature variation trend in the Minjiang River Basin from 1961 to 2016.

showed an upward trend at 73% of the stations in the Minjiang River Basin; 15% of the stations in the basin passed the significance test. The TNx showed an upward trend at 50% of the stations. This shows that the minimum values of the maximum temperature and minimum temperature are increasing mainly in the basin, while the maximum values of the maximum temperature and minimum temperature are mainly decreasing in the basin.

3.2.4. Other Indices (WSDI, CSDI, GSL, and DTR). WSDI is increasing at 100% of the stations in the basin and 61% of which passed the significance test. CSDI is decreasing at 92% of the stations in the basin; 26% of the stations in the basin passed the significance test. GSL is decreasing at 69% of the stations in the basin; 15% of the stations in the basin passed the significance test. DTR is not obvious in the whole basin. This shows that the heat persistence index of the basin is mainly increasing, the cold persistence days of the basin are mainly decreasing, and DTR is mainly decreasing in most parts of the basin except for some parts of the middle reaches.

3.3. Time Trend of Extreme Temperature Indicators

3.3.1. Relative Index (TX10p, TN10p, TX90p, and TN90p). Figure 4 shows the interannual variation in the extreme temperature index in the Minjiang River Basin. It can be seen that TN10p and TX10p are decreasing in the Minjiang River Basin. Their annual tendency rates are −2.9 d/10a and −0.8 d/10a, respectively. TN90p and TX90p are increasing in the Minjiang River Basin. Their annual tendency rates are 3.0 d/10a and 2.6 d/10a, respectively. Combining the MK trend test results in Table 4, it can be seen that the linear trend analysis and MK trend test results are consistent. TX10p

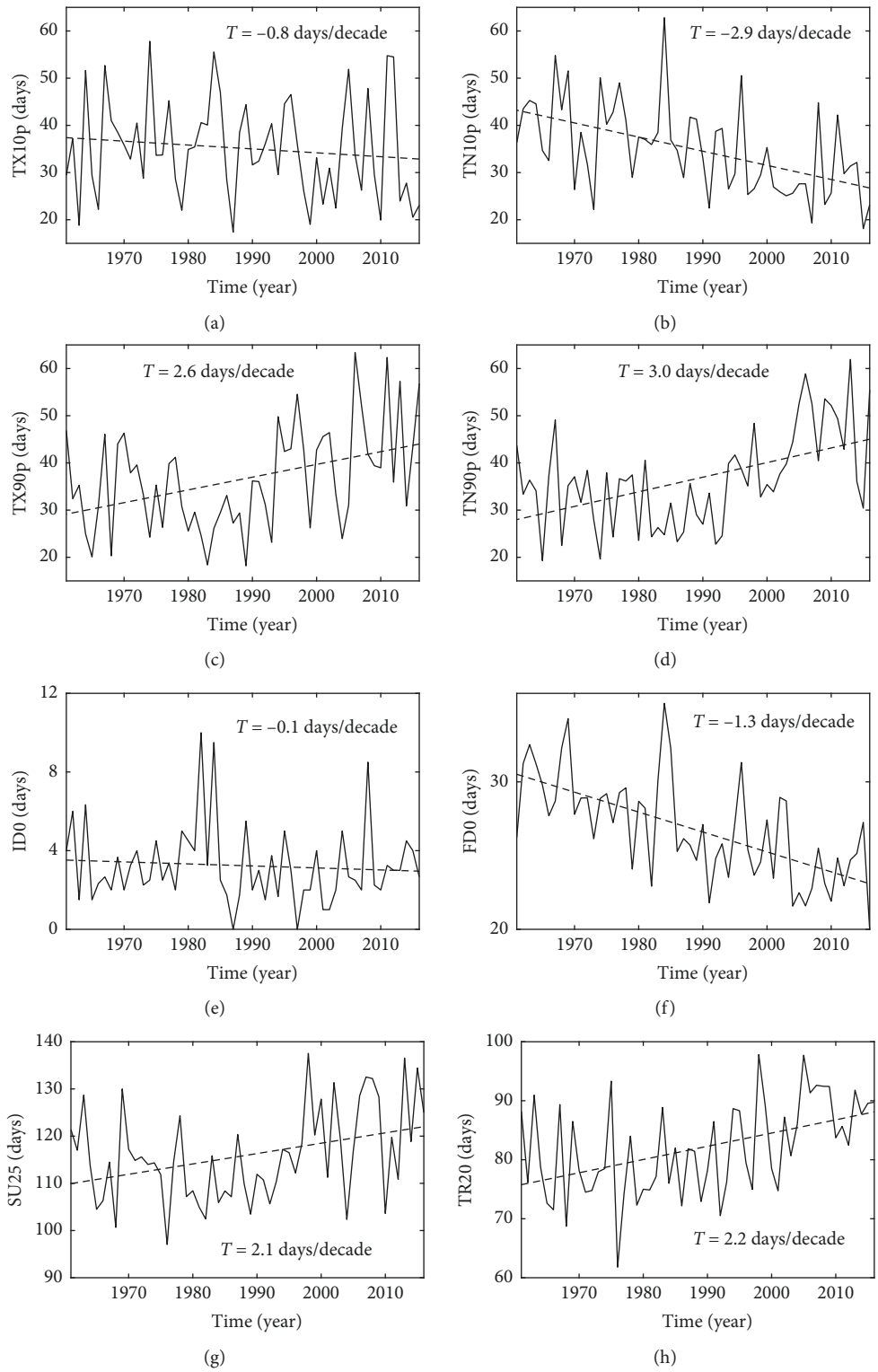

Figure 4: Continued.

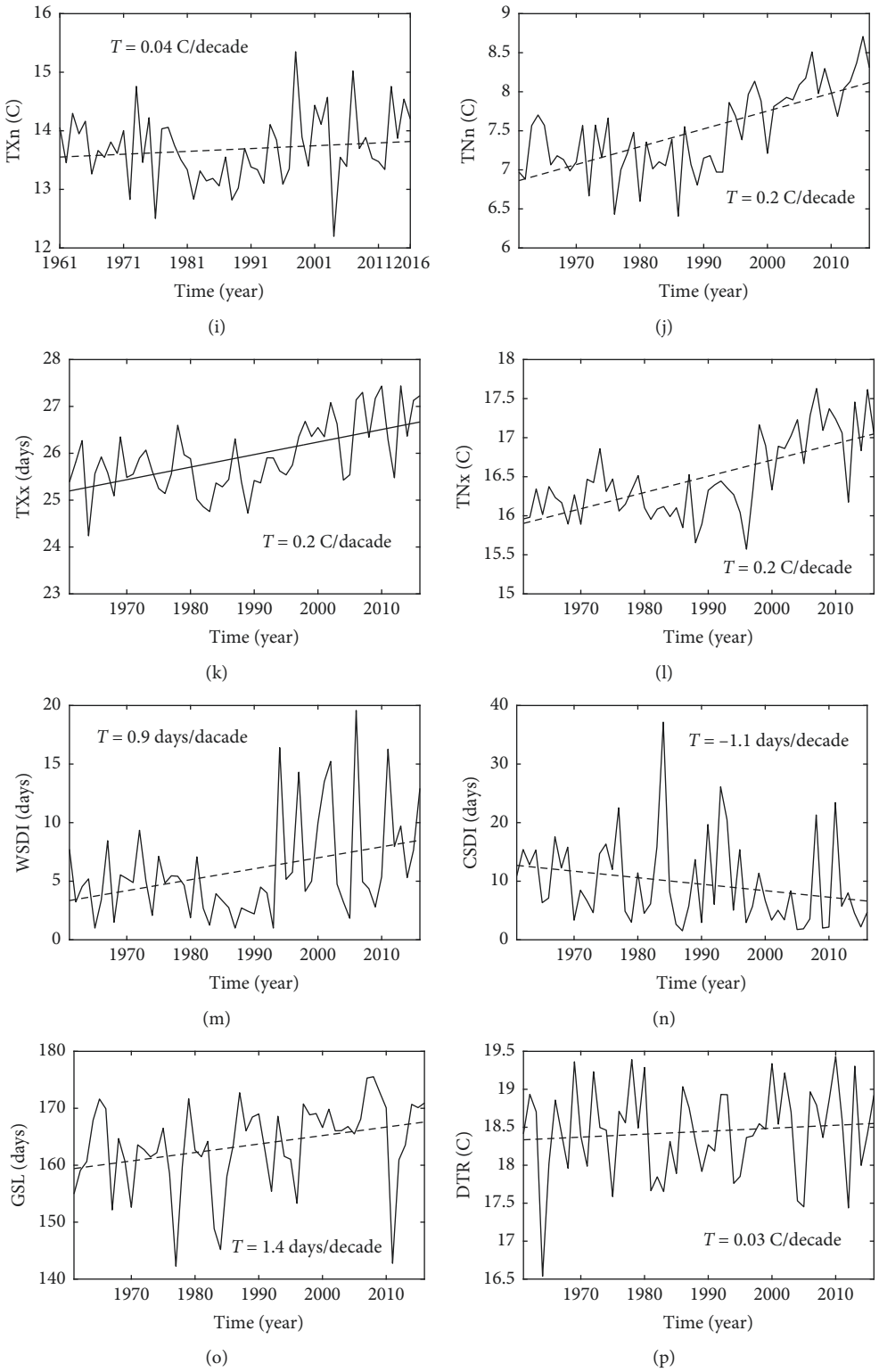

Figure 4: Interannual variation in the extreme temperature index in the Minjiang River Basin from 1961 to 2016.

shows a nonsignificant decrease, TN10p shows a significant decrease, and the TX90p and TN90p show a significant increase. The change trend of the night index (TN10p and TN90p) is more obvious than that of the day index (TX10p and TX10p).

3.3.2. Absolute Index (ID0, FD0, SU25, and TR20). During the past 56 years, the absolute index and relative index of the Minjiang River Basin have a similar change trend. The cold index shows a decreasing trend, while the warm index shows an increasing trend, but the degree of

Table 4: Temporal trends of the extreme temperature indicators in the Minjiang River Basin.

Index	MK	T
TX10p	−1.13	−0.8
TN10p	**−4.09**	−2.9
TX90p	**2.51**	2.6
TN90p	**3.49**	3
ID0	−0.36	−0.1
FD0	**−4.93**	−1.3
SU25	**2.45**	2.1
TR20	**3.39**	2.2
TXn	0.68	0.04
TNn	**4.79**	0.2
TXx	**4.1**	0.2
TNx	**4.63**	0.2
WSDI	1.8	0.9
CSDI	**−2.58**	−1.1
GSL	**3.13**	1.4
DTR	0.79	0.03

MK denotes MK statistics. T denotes trends (decade^{-1}). Values for the trends at the 0.05 significance level are shown in bold.

change in the cold and warm indices is different. FD0 and ID0 show a downward trend. The change rates are −1.3 d/10a and −0.1 d/10a, respectively, while SU25 and TR20 show an upward trend of 2.1 d/10a and 2.2 d/10a, respectively. The trend of the warm index is more obvious than that of the cold index. At the same time, the results of the MK trend test shown in Table 4 show that the linear trend analysis and MK trend test have the same results. This shows that FD0 has significantly decreased over the past 56 years, ID0 nonsignificantly decreased, while summer days and heat wave days significantly increased.

3.3.3. Extreme Value Index (TXn, TNn, TXx, and TNx). From the change trend of the extreme value index, we can see that TXn shows a nonsignificant increase; TNn, TXx, and TNx show a significant increase; and the change rate is 0.2°C/10a, 0.2°C/10a, 0.04°C/10a, and 0.2°C/10a, respectively. Combining with the linear trend analysis and MK trend test shown in Table 4, we can see that TXn shows a nonsignificant increase, TNn shows a significant increase, and TXx and TNx show a significant increase.

3.3.4. Other Indices (WSDI, CSDI, GSL, and DTR). WSDI is increasing in the Minjiang River Basin, with a change trend of 0.9 d/10a, while CSDI is decreasing, with a change trend of −1.1 d/10a. The GSL is increasing with a change trend of 1.4 d/10a and DTR is increasing with a change rate of 0.03°C/10a. From the time variation trend of the extreme temperature index in the Minjiang River Basin shown in Table 4, it can be seen that the linear trend analysis and MK trend test show the same trend. WSDI shows a nonsignificant upward trend, CSDI shows a significant downward trend, and GSL shows a significant upward trend. And, DTR is nonsignificantly trending upward.

As can be seen from Figure 4, the interannual variation of the Minjiang River Basin can be divided into two phases. Table 5 calculates the variation rates of extreme temperature indices before and after 1990. It can be seen that the change rates of warm and cold indices before 1990 are mainly decreased, while after 1990, the change rates of warm indices are mainly increased, cold indices are mainly decreased, and the change rate of the warm index is higher than that of the cold index.

4. Results

In this study, 16 extreme temperature indices were used to study the temporal and spatial characteristics of extreme temperature events in the Minjiang River Basin during the recent 56 years. The main conclusions are as follows:

(1) The spatial distribution of the relative index of extreme temperature in the basin is consistent. The distribution of the absolute index and extreme index is not consistent. The cold extreme temperature index (FD0 and ID0) mainly occurs in the upper reaches of the basin at high altitude, while the warm extreme event index (TXx, TNx, TN90p, TX90p, TN90p, SU25, and TR20) mainly occurs in the Sichuan basin. In the middle and lower reaches of the basin, the extreme values are distributed in the lower reaches of the basin. Because the high values of FD0 occur in the upper reaches of the basin, the GSL in the middle and lower reaches of the basin is obviously greater than that in the upper reaches and is approximately twice as large as that in the upper reaches. At the same time, the DTR in the upper reaches of the basin is greater than that in the middle and lower reaches.

(2) The spatial variation in each index is consistent, but the degree of variation shows a spatial difference. The warm index and daytime index mainly show an upward trend in the whole basin. The cold index and nighttime index mainly show a downward trend in the whole basin. The warm index and daytime index are more obvious in the middle and lower reaches, while the cold index and nighttime index are more obvious in the upper reaches.

(3) The variation range between the cold and warm extreme temperature indices and the variation range between the daytime and nighttime in the Minjiang River Basin show an obvious asymmetry. The variation range of the warm index (SU25, TR20) is greater than that of the cold index (ID0, FD0), and that of the night index (TN10p, TN90p) is greater than that of day index (TX10p, TX90p). The increasing trend of the warm index in the middle and lower reaches of the basin is greater than that in the upper reaches, and the decreasing trend of the night index in the upper reaches of the basin is greater than that in the middle and lower reaches of the basin.

(4) On a time scale, cold extreme temperature indices such as FD0, TN10p, and CSDI significantly decrease

Table 5: Temporal trends of the extreme temperature indicators in the Minjiang River Basin before and after 1990.

	T (before 1990)	T (after 1990)	T (1961–2016)
TX10p	0.7	−1.7	−0.8
TN10p	−1	−2.1	−2.9
TX90p	−3.2	4.4	2.6
TN90p	−2.9	7.5	3
ID0	0.1	0.5	−0.1
FD0	−1.2	−0.9	−1.3
SU25	−3	5	2.1
TR20	−1	3.8	2.2
TXn	−0.3	0.2	0.04
TNn	−0.1	0.4	0.2
TXx	−0.1	0.5	0.2
TNx	−0.04	0.4	0.2
WSDI	−1	1	0.9
CSDI	−1.2	−3.5	−1.0
GSL	0.6	2.1	1.4
DTR	−0.1	0.1	0.03

from 1961 to 2016 at −1.3, −2.9, and −1.1 d/10a, respectively, while TX10p and ID0 nonsignificantly decrease at −0.8 and −0.1 d/10a, respectively. The warm extreme temperature indices TXx and TNx increase from 1961 to 2016 at 0.2 and 0.2°C/10a, respectively. Indices such as TN90p, TX90p, SU25, and TR20 significantly increase from 1961 to 2016 at 3.0, 2.6, 2.1, and 2.2 d/10a, respectively, while the WSDI nonsignificantly increases at 0.9 d/10a. The GSL in the basin significantly increases from 1961 to 2016 at 1.4 d/10a, while the DTR shows a nonsignificant upward trend at 0.03°C/10a. The change rates of warm and cold indices before 1990 are mainly decreased, while after 1990, the change rates of warm indices are mainly increased and cold indices are mainly decreased and the change rate of warm index is higher than that of cold index.

5. Discussion

Surface warming due to global warming has changed the thermal difference between land and sea and large-scale circulation, intensified the regional and global water cycle, and further affected the spatial distribution characteristics of precipitation and heavy rainfall. Surface warming has also increased the frequency of floods, droughts, and other disasters, resulting in serious adverse effects on agricultural production and food security. Although the Minjiang River Basin has also shown a warming trend during the past 50 years, the increasing trend of temperature is 0.15°C/10a, but significantly lower than the average level of 0.22°C/10a seen in China. Under different ranges of mean temperature, the characteristics of extreme temperature will be different. In addition, the Minjiang River Basin is mainly on the eastern side of the Qinghai-Tibet Plateau, which is in a transitional area between plateau terrain and the eastern plain of China. The Minjiang River Basin gradually lowers in elevation from the western mountain areas to the eastern plain areas. The altitude difference is large, and it is among the most complex topographic areas in China. Complex topographic conditions lead to temporal and spatial distribution characteristics of extreme temperature in the Minjiang River Basin that are not exactly the same as the overall trend in China.

(1) The extreme high temperature days (TX90 and TN90) in the Minjiang River Basin show an increasing trend, while the extreme low temperature days (TX10 and TN10) show a decreasing trend, which is consistent with the trend in most other parts of China owing to global warming [12]. However, at the same time, the intensity of short-term extreme precipitation is decreasing, resulting in a downward trend in the total precipitation [30] which is different from the runoff in the Yangtze River Basin [31]. The warming and drying of the climate in the Minjiang River Basin has led to a significant reduction in runoff, providing conditions for the occurrence of regional extreme climate.

(2) TR20 in the Minjiang River Basin shows a consistent upward trend. TR20 in China has a strong interdecadal variation, but the long-term linear trend is not obvious [17]. This is related to the fact that the Minjiang River Basin is on the western periphery of the subtropical high during summer. The westward advance of the subtropical high is stronger. The Minjiang River Basin is subject to hot weather, the eastward recession of the subtropical high is weakened, and the Minjiang River Basin is on the edge of the subtropical high. Previous studies also show that [32, 33] since the 1980s, the subtropical high intensity has gradually increased and the western boundary has moved west. The northern boundary is in the south, which results in the Minjiang River Basin being affected by the lower airflow of a subtropical high for a long period creating conditions for a heat wave. As a result, heat wave events in the Minjiang River Basin have significantly increased. The frequency and intensity of cold wave events in the Minjiang River Basin have obviously decreased, which is the same as the overall trend of cold wave weather in the Yangtze River Basin [17]. This may lead to faster warming during winter at midhigh latitudes under global warming, leading to a decrease in the north-south temperature gradient and atmospheric baroclinicity at midlatitudes of the Northern Hemisphere. Disturbances in the midlatitude atmosphere are also reduced. The decrease in weather disturbance also leads to a decrease in cold waves during winter (October to April).

(3) The variation in minimum temperature (TNx and TXx) and maximum temperature (TNn and TXn) in the Minjiang River Basin is not significant. Studies show that the average minimum temperature in most other regions of China has increased significantly more than the average maximum temperature; this can be related to urbanization [12, 34]. This asymmetric variation in minimum and maximum

temperatures results in a significant decrease in the diurnal temperature range [35, 36].

(4) FD0 in the Minjiang River Basin is significantly decreasing, with a change rate of −1.3 d/10a. Correspondingly, the GSL is ahead of schedule, showing a significant growth trend. The change trend of the Minjiang River Basin is 1.4 d/10a. These changes lead to an increased instability in agricultural production, increased local drought and high temperature, and earlier crop development; they can be attributed to climate warming [37].

The Minjiang River Basin, as an important tributary of the Yangtze River, is also an important food-producing area in China. Changes in climate and runoff in the region play a significant role in the sustainable development of regional resources, the environment, and society. In this case, understanding the characteristics of regional climate change and the response of runoff is of great importance for promoting agricultural development, economic growth, and harmonious coexistence between people and society in the region. The factors affecting extreme temperature change and the mechanism their effects bring about are worth studying and will be further explored in future research.

Data Availability

The data used in this paper are provided by the State Meteorological Administration of China. Relevant station data are available at https://data.cma.cn/ through registered scientific research users.

Conflicts of Interest

There are no conflicts of interest regarding the publication of this paper.

Acknowledgments

This research was financially supported by the National Natural Science Foundation of China (no. 50979062); Sichuan Key Laboratory of Rainstorm, Drought and Flood Disasters in Plateau and Basin (no. Provincial Heavy Laboratory 2018-Youth-09); Sichuan Science and Technology Department's Key Research and Development Project (no. 2018SZ0343); and Sichuan Meteorological Service Center Project (no. SCQF2019007).

References

[1] P. Y. Groisman, T. R. Karl, D. R. Easterling et al., "Changes in the probability of heavy precipitation: important indicators of climatic change," *Weather and Climate Extremes*, vol. 42, no. 6, pp. 243–283, 1999.

[2] T. J. Osborn, M. Hnhne, P. D. Jones, and T. A. Basnett, "Observed trends in the daily intensity of United Kingdom precipitation," *International Journal of Climatology*, vol. 20, no. 5, pp. 247–364, 2000.

[3] D. R. Easterling, J. L. Evans, P. Y. Groisman, T. R. Karl, K. E. Kunkel, and P. Ambenje, "Observed variability and trends in extreme climate event: a brief review," *Bulletin of the American Meteorological Society*, vol. 81, no. 3, pp. 417–425, 2000.

[4] A. M. G. Klein Tank, T. C. Peterson, D. A. Quadir et al., "Changes in daily temperature and precipitation extremes in central and south Asia," *Journal of Geophysical Research*, vol. 111, no. 16, article D16105, 2006.

[5] E. Aguilar, A. Aziz Barry, M. Brunet et al., "Changes in temperature and precipitation extremes in western central Africa, Guinea Conakry, and Zimbabwe, 1955–2006," *Journal of Geophysical Research*, vol. 114, no. 2, article D02115, 2009.

[6] D. H. Burn, "Climatic influences on streamflow timing in the headwaters of the Mackenzie River Basin," *Journal of Hydrology*, vol. 352, no. 1-2, pp. 225–238, 2008.

[7] G. Choi, D. Collins, G. Ren et al., "Changes in means and extreme events of temperature and precipitation in the Asia-Pacific network region, 1955–2007," *International Journal of Climatology*, vol. 29, no. 13, pp. 1906–1925, 2009.

[8] G. Gruza, E. Rankova, V. Razuvaev, and O. Bulygina, "Indicators of climate change for the Russian Federation," *Climatic Change*, vol. 42, no. 1, pp. 219–242, 1999.

[9] L. V. Alexander, X. Zhang, T. C. Peterson et al., "Global observed changes in daily climate extremes of temperature and precipitation," *Journal of Geophysical Research*, vol. 111, no. 5, 2006.

[10] M. J. Manton, P. M. Della-Marta, M. R. Haylock et al., "Trends in extreme daily rainfall and temperature in Southeast Asia and the south pacific: 1961–1998," *International Journal of Climatology*, vol. 21, no. 3, pp. 269–284, 2001.

[11] Y. Ding, G. Ren, G. Shi et al., "National assessment report of climate change (I): climate change in China and its future trend," *Advances in Climate Change Research*, vol. 2, no. 1, pp. 3–8, 2006.

[12] G. Y. Ren, G. L. Feng, Z. W Yan et al., "Progresses in observation studies of climate extremes and changes in mainland China," *Climatic and Environmental Research*, vol. 4, pp. 337–353, 2010.

[13] N. Zhang, Z. B. Sun, and G. Zeng, "Change of extreme temperatures in China during 1955–2005," *Journal of Nanjing Institute of Meteorology*, vol. 31, no. 1, pp. 123–128, 2008.

[14] Q. Wang, M. Zhang, S. Wang, S. Luo, B. Wang, and X. Zhu, "Extreme temperature events in Yangtze River Basin during 1962–2011," *Acta Geographica Sinica*, vol. 68, no. 5, pp. 611–625, 2013.

[15] X. Wu, Z. Wang, X. Zhou, C. Lai, W. Lin, and X. Chen, "Observed changes in precipitation extremes across 11 basins in China during 1961–2013," *International Journal of Climatology*, vol. 36, no. 8, pp. 2866–2885, 2016.

[16] Y. Zhou and G. Ren, "Variation characters of extreme temperature indices in main land China during 1956–2008," *Climatic and Environmental Research(in Chinese)*, vol. 15, no. 4, pp. 405–417, 2010.

[17] Y. Ding, X. Li, Y. Tian et al., "Climatic characteristics and variability of summer thunderstorms at Capital Airport," *Meteorological Science and Technology*, vol. 37, no. 4, pp. 420–424, 2009, in Chinese.

[18] D. Zhou, R. Huang, and G. Huang, "Variations of climate and vegetation cover over the upper reaches of Yangtze River in the past decades," *Transactions of Atmospheric Sciences*, vol. 32, no. 3, pp. 377–385, 2009.

[19] B. Zhou, H. Xue, G. O. U. Shang et al., "Characteristics of extreme climate in downstream catchment of Yangtze River during 1960–2012," *Water Power*, vol. 43, no. 9, pp. 26–30, 2017.

[20] C. Zhong, N. Cui, C. Tan et al., "Spatiotemporal of Yangtze River in 53 years," *Journal of Irrigation and Drainage*, vol. 35, no. 12, pp. 88–96, 2016.
[21] Y. Wang, T. Jiang, and Y. Shi, "Changing trends of climate and runoff over the upper Reaches of the Yangtze River in 1961-2000," *Journal of Glaciology and Geocryology*, vol. 27, no. 5, pp. 709–714, 2005.
[22] H. B. Mann, "Nonparametric tests against trend," *Econometrica*, vol. 13, no. 3, pp. 245–259, 1945.
[23] M. G. Kendall, *Rank Correlation Methods*, Griffin, Spokane Valley, WA, USA, 1970.
[24] A. M. G. Klein and G. P. Konnen, "Trends in indices of daily temperature and precipitation extremes in Europe, 1946–99," *Journal of Climate*, vol. 16, no. 22, pp. 3665–3680, 2003.
[25] K. Vijay and K. J. Sharad, "Trends in seasonal and annual-rainfall and rainy days in Kashmir Valley in the last century," *Quaternary International*, vol. 212, pp. 64–69, 2010.
[26] Z. X. Xu, J. Y. Li, and C. M. Liu, "Long-term trend analysis for major climate variables in the Yellow River basin," *Hydrological Processes*, vol. 21, no. 14, pp. 1935–1948, 2007.
[27] H. Wu, L.-K. Soh, A. Samal, and X.-H. Chen, "Trend analysis of streamflow drought events in Nebraska," *Water Resources Management*, vol. 22, no. 2, pp. 145–164, 2008.
[28] J. Zhang, J. Wang, L. Yan, and S. Zhang, "Study on runoff trends of the main rivers in China in the recent 50 years," *China Water Resources*, vol. 2, pp. 31–34, 2008.
[29] S. J. Wang, "Changing pattern of the temperature, precipitation and runoff in Chuanjiang section of the Yangtze River," *Resource Science*, vol. 31, pp. 1142–1149, 2009.
[30] H. Du and S. He, "The analysis on characteristics of precipitation and trends in drought and flood disasters in Minjiang River Basin," *Research of Soil and Water Conservation*, vol. 22, no. 1, pp. 153–157, 2015.
[31] W. Zhang and S. Wan, "Detection and attribution of abrupt climate changes in the last one hundred years," *Chinese Physics B*, vol. 17, no. 6, pp. 2311–2316, 2008.
[32] Q. Mu, S. Wang, J. Zhu et al., "Variations of the wetern pacific subtropical high in summer during the last hundred years," *Chinese Journal of Atmospheric Sciences*, vol. 25, no. 6, pp. 787–797, 2001.
[33] Y. Chen, H. Zhang, R. Zhou et al., "Relationship between the ground surface temperature in Asia and the intensity and location of subtropical high in the western pacific," *Chinese Journal of Atmospheric Sciences*, vol. 25, no. 4, pp. 515–522, 2001.
[34] Y. Zhou and G. Ren, "Urbanization effect on trends of mean maximum, minimum temperature and daily temperature range in North China," *Plateau Metrology*, vol. 28, no. 5, pp. 1158–1166, 2009, in Chinese.
[35] H. Lijuan, Z. Ma, D. Luo et al., "Analysis of temperature range from 1961 through 2000 across China," *Acta Geographica Sinica*, vol. 59, no. 5, pp. 680–688, 2004, in Chinese.
[36] H. Tang, P. Zhai, and Z. Wang, "On change in mean maximum temperature , minimum temperature and diurnal range in China during 1951–2002," *Climatic and Environmental Research*, vol. 10, no. 4, pp. 728–735, 2005, in Chinese.
[37] E. Lin, X. U. Yin-long, J. Jiang et al., "National assessment report of climate change (II): climate change impacts and adaptation," *Advances in Climate Change Research*, vol. 2, no. 2, pp. 51–56, 2006.

Hindawi
Advances in Meteorology
Volume 2019, Article ID 1587034, 16 pages
https://doi.org/10.1155/2019/1587034

Research Article

Effects of Climate Finance on Risk Appraisal: A Study in the Southwestern Coast of Bangladesh

Firdaus Ara Hussain and Mokbul Morshed Ahmad

Regional and Rural Development Planning (RRDP), School of Environment, Resources and Development (SERD), Asian Institute of Technology, Klong Luang, Pathum Thani 12120, Thailand

Correspondence should be addressed to Firdaus Ara Hussain; st116549@ait.asia

Received 1 March 2019; Accepted 3 June 2019; Published 1 July 2019

Guest Editor: Bimal K. Paul

Utilising climate funds properly to reduce the impact of potential risks of climate change at the local level is essential for successful adaptation to climate change. Climate change has been disrupting the lives of millions of households along the coastal region of Bangladesh. The country has allocated support from its national funds and accessed international funds for the implementation of adaptation interventions. With the focus of the scientific community on climate finance mechanisms and governance at the global and the national level, there is a lacuna in empirical evidence of how climate finance affects risk appraisal and engagement in adaptation measures at the local level. This paper aims to examine how the support from climate finance affects risk appraisal in terms of the perceived probability and severity and the factors which influence risk appraisal. A field survey was conducted on 240 climate finance recipient households (CF HHs) and 120 nonclimate finance recipient households (non-CF HHs) in Galachipa Upazila of Patuakhali District in coastal Bangladesh. The results indicate that both CF and non-CF HHs experience a high probability of facing climatic events in the future; however, CF HHs anticipated a higher severity of impacts of climatic events on different dimensions of their households. With higher income and social capital, the overall risk appraisal decreases for CF HHs. CF HHs have higher engagement in adaptation measures and social groups and maintain alternative sources of income. Climate finance played a critical role in supporting households in understanding the risks that they were facing, assisting them in exploring as well as enhancing their engagement in adaptation options.

1. Introduction

Risk appraisal at the household level plays a crucial role in the adaptation pathway and towards exploring available adaptation measures. Reasons for this are manifold, recognising the centrality of the household unit in governing responses to external stimuli as cited by Jones and Tanner [1]. Risk appraisal comprises of perceived probability, which is the person's expectancy of being exposed to the threat, while perceived severity is the person's appraisal of how harmful the consequences of the threat would be to things he or she values if the threat were actually to occur [2]. Households are concerned about how climatic events may affect their livelihoods and assets based on past experiences. However, project planning and budgetary allocation for the local level are considerably done at the national level in Bangladesh, mainly by the ministries and their subordinated departments and agencies, and do not consider the household needs. The implementation is left to the local level. Hence, the approach is rather top-down. This limits consideration of local needs and participation within the process. This is also similar for adaptation projects, although climate change is localised and needs to consider localised adaptation responses. Local governments are less involved in the planning process of the adaptation measures, which results in the local needs being insufficiently considered [3]. Furthermore, localised encounters contrast significantly with the techno-scientific accounts through which scientists, policymakers, and practitioners often conceptualise climate change risks and operationalise responses [4]. Customised adaptation interventions at the household level are also limited. In fact, households contribute from their

own resources to participate in the planned adaptation measures, increasing the overall adaptation cost for the affected households. Indeed, many of the assets, capacities, and functions required to respond to climate risk are dictated by household-level dynamics [1]. Adaptation funding is scarce and has to be used effectively [5]. External assistance facilitates, secures, and improves the process of climate risk reduction [6].

Some authors argue that the bottom-up approach prevalent in development assistance brings flexibility and innovation and that such an approach fits well with the many motivations for providing aid, with the diverse willingness and capabilities to contribute to development finance efforts [7]. Local governments are the authorities who need to react at the earliest in case of any calamities or disasters. The local governments in Bangladesh have the mandate of developing and maintaining infrastructure and basic public services such as water, sanitation, health, and educational facilities, which can be adapted to make the localities resilient. In addition, although local governments are often better informed on how to go about making development activities climate-adapted in a participatory manner with the involvement of local political leaders, communities, practitioners, and authorities, they are often unable to respond as they are provided limited funding from the central level as they have little involvement in the budgetary decisions. The insufficient funding can be followed back to the planning and budgeting done at the national level, which often does not take account of the local dimensions and cost estimates of climate change into the development planning. A more participatory bottom-up approach with the engagement of local governments and local people in the adaptation project planning, budgeting, and implementation process is needed. The challenge, however, is to channel climate finance towards adaptation measures, which fit the local context and support the most vulnerable and marginalised population.

During the Conference of Parties (COP) 15 in 2011, the Green Climate Fund was agreed upon which offers an equal funding window for adaptation and mitigation. However, almost a quarter of a century into climate change negotiations, an adequate system for defining, categorising, tracking, and evaluating climate change finance, is still absent [7]. Despite the "polluter-pays-principle" at the climate negotiations, the gap in the availability of climate finance is prevalent. The inadequacy of climate finance to meet the adaptation needs will be analysed further through this study.

At the national level, Bangladesh has taken initiatives to finance climate change interventions from national and international financial sources. By 2050, total investments of $5,516 million and $112 million in annual recurrent costs will be needed to protect Bangladesh against climate change [8]. The country is not helpless, therefore, against coping with sea-level rise, but it might need financial and technical assistance with providing practical mitigation measures [9]. Climate finance comes from different sources such as from the national budget, Bangladesh Climate Change Trust Fund (BCCTF), Bangladesh Climate Change Resilience Fund (BCCRF), and bilateral donors through Fast Start Finance, among others [10].

To analyse the perception of risk, a field survey was conducted in Patuakhali, on the southwestern coast of Bangladesh, on the beneficiaries of a climate finance project (referred to as CF Project) run by an international NGO. The aim of the CF Project was to support the vulnerable communities against a changing and uncertain climate. This study limits itself to the adaptation interventions at the household level due to the focus of the research on the effect of climate finance on the risk appraisal at the household level.

The paper sets out to analyse how climate financial makes a difference in the risk appraisal of households in comparison with households which do not receive support. One of the objectives of the study is to examine the influencing factors of risk appraisal, which were identified through multiple regression analysis. This research contributes to the existing literature through a comparative analysis of risk appraisal and adaptation measures of CF and non-CF households. To date, much of the adaptation literature has been theoretical, reflecting the absence of empirical data from activities on the ground [11]. Effective utilisation of climate funding requires a critical analysis of where climate finance should be focused and which factors influence the household in engaging in adaptation. Risk appraisals of climate change and influencing factors are critical to understanding adaptation behaviour [12, 13]. It has become important to adaptation strategies because the way individuals interpret their risks affects what adaptation behaviour they are likely to take [13].

2. Literature Review

Climate change is disrupting the socioeconomic conditions of people, which are difficult to overcome especially by the poor households. Natural calamities will reinforce preexisting socioeconomic divide by damaging natural resources that support the poor's long-term livelihood prospects and destroying their current produce, and by repeatedly rendering the poor homeless and destroying whatever little material possessions they might have [14]. Risk appraisal is derived from the premise that people comprehend their abilities and limitations. A large number of definitions, frameworks, and approaches have been proposed for explaining and quantifying risk [3, 13]. Nearly all studies on the effects of personal experience on self-protective behaviour regarding natural hazards show preparedness increasing with the severity of past damage [2].

The discourse around the provision of climate finance has been focused at the international level. Without efforts to marry adaptation theory with real-world adaptation practices, the adaptation field will continue to be siloed between theory and practice [11]. In the last 20 years, there has been an increase in bilateral and multilateral funds providing climate finance such as Global Environmental Facility (GEF), Climate Investment Fund (CIF), Fast Start Finance, Adaptation Fund, and most recently, the Green Climate Fund (GCF); each responds to needs that emerged at different times. However, the proliferation of funds has led policymakers to question whether such a diverse landscape

of funds can effectively channel climate finance to support the necessary transformation to low-emission, climate-resilient societies [15]. The IPCC special report in 2018 argued that the world only had until 2030 to keep the global temperature increase at a maximum of 1.5°C if immediate action is not taken [16]. This collates with the Paris Agreement in 2015 with the goal of keeping the temperature between 1.5°C and 2°C.

Adaptation finance is primarily allocated to multilateral entities and national governments, rather than local organisations [17]. BCCTF has allocated almost USD 400 million as of date for climate change. BCCRF, a multidonor trust fund, had committed USD188 million in grant funds to build resilience but was discontinued after 2016. The Pilot Program for Climate Resilience (PPCR) has allocated USD 110 million in grants (45%) and interest credits (55%). Until 2019, Bangladesh has received commitments of USD 88.13 million from the GCF through three approved adaptation projects. The funds are mostly in the form of loans or grants when the funding is from international sources.

The climate-relevant budget data of five key ministries for climate change from FY 2014-15 to FY 2017-18 were analysed [18]. An increase is evident for the period 2014 to 2017, with a slight decrease in the FY 2017-18, as illustrated in Table 1. One of the barriers for shifting investments' allocation to green sectors and assets is the poor understanding of the relation between climate risks, the economy, and finance [16].

An analysis of the budget allocation according to Bangladesh Climate Change Strategy and Action Plan (BCCSAP) thematic areas for the four fiscal years 2014–2018 is presented in Table 2, which indicates that the majority of the budget allocation went towards adaptation. On the contrary, the budget allocation for mitigation and low carbon development decreases from 1.74% in FY 2014-15 to 1.16% in FY 2017-18 of the total climate-relevant budget [18].

3. Theoretical and Empirical Basis of Research

For measuring risk appraisal to climate change, this paper follows the Model of Private Proactive Adaptation to Climate Change (MPPACC) to examine why some people exhibited adaptation behaviour while other people did not [2]. The MPPACC was based on the Protection Motivation Theory, which was recognised as one of the four major theories in psychological research conducted on health behaviour.

(i) First, the perceived probability is the person's expectancy of being exposed to the threat (to use a natural-hazard example that a flood reaches the house in which a person lives).

(ii) Second, perceived severity is the person's appraisal of how harmful the consequences of the threat would be to things he or she values if the threat were actually to occur.

Grothmann and Patt's framework was expanded further by Frank et al.'s study which identified social identity as an important additional component of an individual's perceived risk and adaptation capacity [1]. For risk appraisal, the framework was operationalised further through quantitative analysis. The formula utilised was followed by this study as well, with some modifications explained in the succeeding section, and is as follows:

$$\text{risk appraisal} = \text{perceived probability} \times \text{perceived severity}. \tag{1}$$

The concept of threat appraisal formulated by [13] in their conceptual framework is as follows:

$$\text{risk appraisal} = \text{uncertainty} \times \text{adverse consequences}, \tag{2}$$

where uncertainty = perceived probability and adverse consequences = perceived severity.

$$\text{Overall risk appraisal} = \sum_{i=1}^{n} \text{uncertainty}_i \times \text{adverse consequences}_i. \tag{3}$$

4. Materials and Methods

4.1. Study Area. In South Asia, Bangladesh is the most densely populated delta of the Ganges-Brahmaputra-Meghna (GBM) Basin [19]. The country drains out approximately 92.5% of the water that is generated in the GBM Basins (an area of 175,106 ha) [20] to the Bay of Bengal. Bangladesh has 19 coastal districts and with a coastal population of 50 million people, nearly about one-third of its total population. The coastal area represents an area of 47,211 km^2 equalling 32% of the country's total geographical area [21]. The coastal zone has been affected by 174 natural disasters during the period 1974–2007 [22]. Current predictions claim that this coastal area will be increasingly submerged up to 3 per cent by the 2030s, 6 per cent in the 2050s, and 13 per cent by 2080s as a result of the sea-level rise [21].

Galachipa Upazila (a subdistrict/administrative region in Bangladesh) is one of the thirteen subdistricts under the Patuakhali district in the southwestern coast of Bangladesh. Galachipa, as shown in Figure 1, has been selected as the study area as it had interventions under the CF Project concluded in 2016. Galachipa is around 925 km^2 large and is around 35–50 feet above the mean sea level. It has been affected by cyclones, tidal surges, coastal flooding, thunderstorms, nor'westers, heavy/irregular rainfall, and salinity. Besides these, river erosion is a severe problem in this area as the two large rivers, Agunmukha and Tetulia, flow on both sides of Galachipa and several smaller rivers flow cross-terrain through Galachipa. It has around 109 km of the embankment at different points, with around 12 door sluice gates.

4.2. Sampling. The field survey was conducted as a comparative study of the risk assessment of households who received support from the climate finance interventions (CF HHs hereafter) in relation to households who did not receive support from climate finance interventions (referred to as

Table 1: Climate-relevant budget allocation in selected ministries from 2014 to 2018 [18].

Budget description	Annual budget (amount in thousand taka)			
	2014-15	2015-16	2016-17	2017-18
Nondevelopment budget	270,827,806	300,456,768	309,209,969	358,797,697
Climate-relevant allocation	65,982,855	77,193,807	84,036,986	85,334,676
% of nondevelopment budget	24.36	25.69	27.18	23.78
Development budget	253,047,122	297,119,124	350,529,332	403,219,100
Climate-relevant allocation	28,066,412	46,513,505	53,701,881	61,001,430
% of development budget	11.09	15.65	15.32	15.13
Total budget	523,874,928	597,575,892	659,739,301	762,016,797
Climate-relevant allocation	94,049,267	123,707,312	137,738,867	146,336,106
% of total budget	17.95	20.70	20.88	19.20
% of GDP	0.62	0.71	0.70	0.66

Source: Climate Protection and Development: Budget Report, 2017-18.

Table 2: Allocation in BCCSAP thematic areas in the selected ministry budget [18].

BCCSAP themes	CC-relevant allocation (amount in thousand taka)			
	2014-15	2015-16	2016-17	2017-18
Food security social protection and health	13,304,421	16,146,944	16,678,265	17,353,924
% of total CC-relevant allocation	14.15	13.04	12.11	11.86
% of ministry budget	1.75	2.12	2.19	2.28
Comprehensive disaster management	20,687,257	30,318,387	29,434,227	34,671,966
% of total CC-relevant allocation	22.00	24.49	21.37	23.69
% of ministry budget	2.71	3.98	3.86	4.55
Climate resilient infrastructure	6,559,625	13,248,641	23,947,171	24,743,940
% of total CC-relevant allocation	6.97	10.70	17.39	16.91
% of ministry budget	0.86	1.74	3.14	3.25
Research and knowledge management	2,631,410	4,165,926	2,804,454	3,658,676
% of total CC-relevant allocation	2.80	3.37	2.04	2.50
% of ministry budget	0.35	0.55	0.37	0.48
Mitigation and low carbon development	1,639,602	1,653,730	1,613,205	1,699,220
% of total CC-relevant allocation	1.74	1.34	1.17	1.16
% of ministry budget	0.22	0.22	0.21	0.22
Capacity building and institutional strengthening	49,226,953	58,246,322	63,261,544	64,208,380
% of total CC-relevant allocation	52.34	47.06	45.93	43.88
% of ministry budget	6.46	7.64	8.30	8.43
Total CC relevance (Tk)	94,049,267	123,779,950	137,738,867	146,336,106
% of total budget for 6 ministries	17.95	20.71	20.88	19.20

Source: Climate Protection and Development, Budget Report, 2017-18.

non-CF HHs). The unit of analysis was at the household level. Crucially, household-level assessments also offer value in capturing the interactions of individual-level decisions and traits with broader social norms, behaviour, and institutions that collectively affect responses to climate hazards [1]. The CF HHs functioned as the experimental group while the non-CF HHs were the control group. Other risk assessment studies opted for an experimental and control group, allowing for comparison and reliability of results [23]. Also, both CF and non-CF HHs were of similar criteria and lived within similar geographical conditions and allowed comparison. The study employed mixed sampling methods to select households. From the 19 districts in the coast of Bangladesh, Patuakhali was chosen through purposive sampling. From within the seven subdistricts of Patuakhali, Galachipa was chosen through purposive sampling as a CF Project was implementing adaptation activities at the household level. The beneficiaries of the CF Project had been selected by the NGO based on the criteria that the household did not have more than 10 decimal or 0.004 hectares of productive lands and had less than USD 62.5 in productive assets. Some other criteria included the nonengagement of households in microcredit programmes or projects similar to the CF Project. The last criteria were that each household had a monthly income of less than USD 62.5.

A list of 489 CF HHs supported in the Galachipa Upazila was provided by the project managers of the CF Project to the researcher. Based on the formula of Yamane (1967) for computing the size of the sample under equation (1), the sample size of 220 CF HHs was estimated. Finally, a sample of 240 CF HHs was collected through random sampling. The list of sample beneficiary households then underwent random sampling in MS Excel to determine which households should be surveyed:

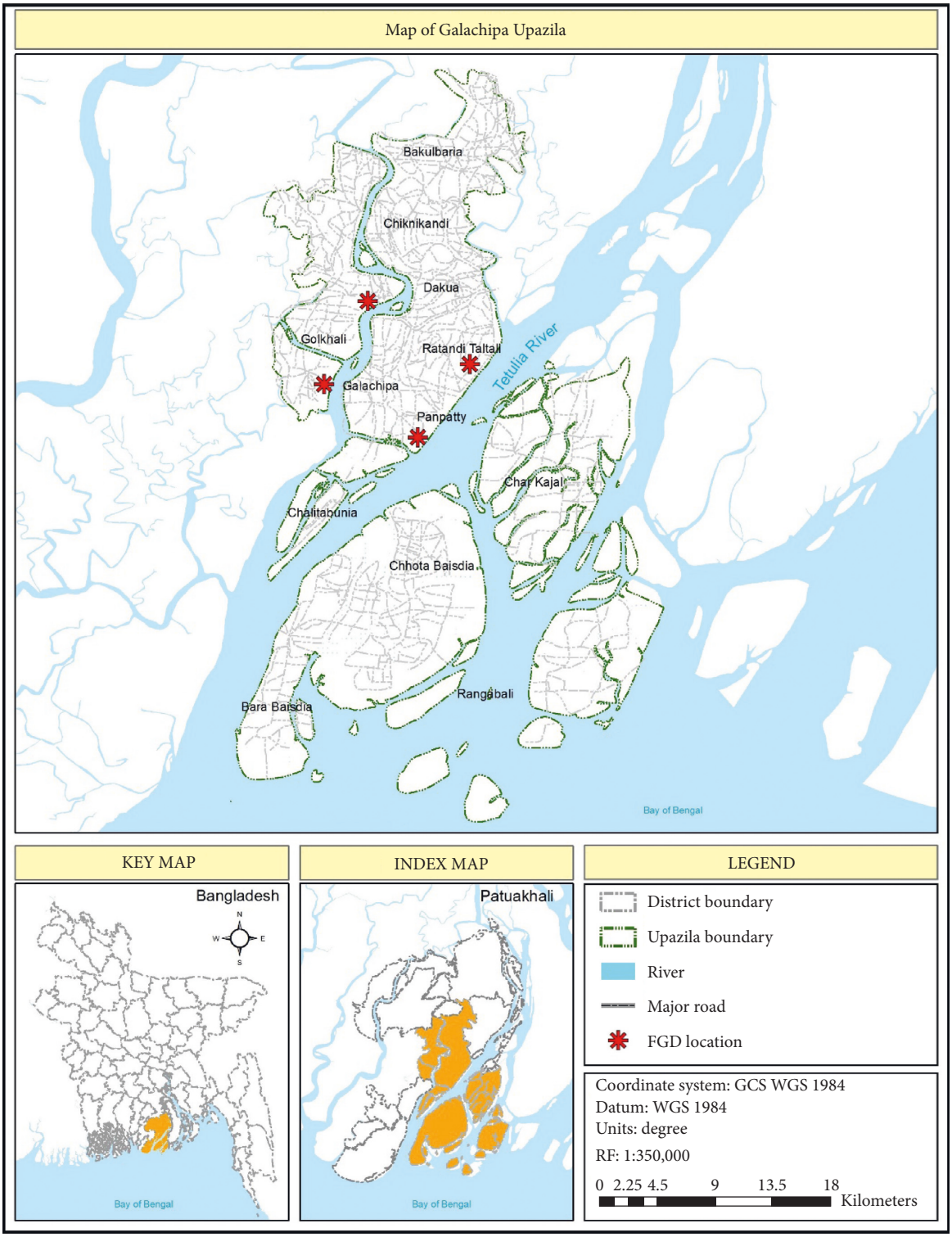

Figure 1: Galachipa Upazila.

$$n = \frac{N}{1 + Ne^2}, \tag{4}$$

where n is the sample size in each area, N is total numbers of households in an area, and e is the precision value, set as 10% (0.10).

The CF HHs received support for adaptation measures such as plinth raising, construction of new housing, homestead gardening, agricultural support, and income diversification activities such as livestock, small businesses, small solar home systems, among others. A control group from the same study area (indicated as non-CF HHs)

which did not receive support from climate finance was also surveyed to allow the comparison and reliability of results. Unlike the CF households, there was no existing name list for the non-CF HHs. Therefore, four focus group discussions (FGDs) were conducted in the study area to identify those households, which met the same criteria for choosing CF households of the households, those who had less than 10 decimal or 0.004 hectares land, had less than USD 62.5 in productive assets, were not engaged in microcredit or similar projects, and had a monthly income below USD 62.5. Participants of the FGDs included Upazila members, members of the local disaster management committee, and local leaders who were able to identify around 240 households in the study area, which met the selection criteria. The names of the households obtained from the FGDs were then entered into an Excel sheet. However, budget constraints in conducting the survey were considered while maintaining a comparable sample size. Therefore, the number of non-CF HHs was limited to 120 households. The percentage of simulated studies with an elevated effect increases as control group size increases (30 participants: 85%; 60 participants: 92%; 100 participants: 96%; and 200 participants: 99%) [24]. Through random sampling in MS Excel, a list of non-CF households of 120 HHs was shortlisted and surveyed. In case any of the households were unwilling to be surveyed or were unavailable, the next household was chosen from the randomized list.

The field survey was conducted in April and May 2016 using a structured questionnaire. Eight interviewers were chosen based on the experience of data collection and previous knowledge of the area, and they were provided with a three-day training. Before the actual survey, the questionnaire was pretested on 15 households by the interviewers. The interviewees were read out a uniform introduction on the purpose of the survey. The interviews were conducted between one and a half hours to two hours.

4.3. Variable Measurement. The questionnaire included two main aspects of risk appraisal, namely, perceived probability and perceived severity. The variables were chosen based on previous studies on risk appraisal [13, 25] and cross-checked during pretesting. For perceived probability, the households were asked about how likely they were to experience the seven main climatic events in the future, as identified in the Patuakhali Disaster Management Plan 2014. The scale ranged from 1 to 5 (1 = not likely; 2 = less likely; 3 = likely; 4 = more likely; and 5 = very likely). For perceived severity, the households were asked about how each of the climatic events could affect different features of their lives. Perceived severity had the scales of 1 to 5 (1 = not affected; 2 = less affected; 3 = affected; 4 = more affected; and 5 = highly affected).

A number of methods, frameworks, and approaches were applied for risk assessment [13, 26–29]. For this study, it utilised the method by Le Dang et al., in which the risk appraisal was computed by multiplying perceived probability with perceived severity as given in equation (1). The probability was based on the likelihood of the household facing these natural calamities in the future. A summation was drawn from all the perceived severity corresponding to a particular climatic event to obtain a single perceived severity. The perceived probability was then multiplied by the corresponding severity for the event to obtain the risk appraisal for that climatic event. Then, a summation was drawn to estimate an overall risk appraisal. This overall risk appraisal was used as the dependent variable for the multiple linear regression model. Le Dang followed the multiple regression model risk appraisal = f (risk experience, information, belief in climate change, trust in public adaptation, farm household characteristics, farm characteristics, and income).

Drawing on dimensions developed by Le Dang et al., the model was executed under the following function for this research and with independent variables identified for adaptation efficacy under the bivariate analysis such as x_1 = HH size, x_2 = income, and x_3 = immobile assets:

$$Y_{\text{opr}} = b_0 + b_1 x_1 + \ldots + b_p x_p + \ldots + \varepsilon, \tag{5}$$

where b_0 is the intercept, b_1 to b_p are the regression coefficients corresponding to the covariates $x_1, \ldots, x_p$, ε is the error term of the model, x_1 = HH size, x_2 = income, x_3 = immobile assets, x_4 = productive assets (livestock, etc.), x_5 = mobile assets (rickshaw), x_6 = participation in social circle, x_7 = information on climate change from NGO, x_8 = support from social safety net, x_9 = monetary/in-kind support from social circle (relatives, friends, neighbours, and self-help groups) for adaptation measures, x_{10} = financial support from loans (microcredit, bank, cooperative, and mohajan) for adaptation responses, x_{11} = financial support from govt. for adaptation responses, x_{12} = financial support from NGOs (cash, materials, labour costs, and advisory services) for adaptation responses, x_{13} = self-financed adaptation responses through selling assets, and x_{14} = self-financed adaptation measures through income/savings/reducing expenditure on food, health, and education.

4.4. Data Analysis Techniques. Statistical Analysis Software (SAS) was used to analyse the household data including descriptive statistics—chi-square, Pearson's correlation coefficient, factor analysis, R^2 and adjusted R^2, variance inflation factor, Durbin–Watson statistic, normality, and homoscedasticity were used.

To identify significant variables, bivariate analysis was conducted on all relevant independent variables which were important to the dependent variable, overall perceived risk. Those variables which had an association in the bivariate analysis were included under the independent variables for the multiple linear regression analysis in the model for this study. One regression model under equation (5) was fitted, with CF and non-CF as the independent variables. By including CF and non-CF as independent variables, we can assess the impact that CF and non-CF have on the dependent variable for the overall perceived risk.

5. Results and Discussion

Both the climate and nonclimate finance households were from Galachipa subdistrict and lived under similar conditions. This study examined the differences in the socioeconomic profile of the CF HHs and the non-CF HHs through chi-square test and corresponding P values, as shown in Table 3. The adaptation measures engaged in by CF and non-CF HHs are given under Table 4. As shown in Table 3, more CF HHs lived outside or on the embankment, which may have been related to the loss of land due to river erosion. Those without land inside the embankment remained outside of the embankment mainly on government land or the embankments.

Moreover, the housing structure of CF HHs was made of less durable materials. There were also a higher number of wage labourers, traders, and fishers in the CF HHs. About 18% of CF HHs pursued a secondary source of income. The average monthly income of CF households was higher at USD 59.9 in comparison with USD 54.9 for non-CF HHs. About 96.2% of the CF HHs participated in a social group such as self-help groups, producer groups, or cooperatives while only 16.7% of the non-CF HHs participated in some form of social groups. More non-CF households received support from the social safety net at 78.3% compared with 63.8% of CF HHs receiving support.

Data showed that non-CF HHs participated in most of the 26 adaptation measures on self-initiatives while the CF HHs received support in 14 adaptation measures, partially supported by the climate finance interventions. At an aggregated level, the main categories of adaptation measures all saw a higher engagement of CF HHs than non-CF HHs as shown in Table 4. Higher income levels were likely to significantly increase the likelihood of planting trees and using supplementary irrigation as adaptation choices [29]. The two highest engagements for both groups were in housing and livestock. The socioeconomic profile of the CF HHs showed that a significant number lived outside or on the embankment and needed support for housing. Livestock was perceived as an instant cash source and was the preferred option for receiving external support as they could quickly reproduce.

Furthermore, households did not need a new skill set to maintain their livestock. Both groups participated least in agriculture and fisheries. From the aggregated level, a significant difference based on the chi-square and P value between CF and non-CF HHs was seen for gardening, agricultural land and crops, livestock, fisheries, safe water, and access to power and fuel resources. From the socioeconomic profile and focus group discussions, support was least given to agriculture and crops as the CF HHs had lost their arable and homestead land due to river erosion. Most of the households who had lost land and could no longer do farming worked as day-labourers. About 55.4% of the CF HHs had the main source of income as day-labourers. The occupation of a day-labour is also critical as they are out of work 6 to 8 months in the whole year. This analysis is indicative of the selection bias of the climate finance project towards selecting households who had lost their land to river erosion and who now work as day-labourers, i.e., without a stable or regular income. This bias might have caused barriers to climate finance reaching other households, who were also in dire conditions.

Engaging in adaptation measures was made possible through some households' own financial resources or external sources. Poor households, however, had fewer income sources, often had to sell assets to sustain their family's expenditure, and had limited access to financial services. There exists growing evidence of the beneficial impact of access to financial services on all aspects of social and economic outcomes at the household and firm level [30]. The absence of financial services makes diversification of income sources a livelihood strategy, as well as an adaptation response for climate-affected households. The first step is to stabilising their socioeconomic conditions. For this, it is essential to understand how the poor farmers manage their cash flows, their preferences, attitudes, and behaviours to determine the scope of diversifying income sources as an effective path out of poverty [30].

Once climate funds reach the national level, a further breakdown of the allocated amounts for hard and soft measures ensues. Studies have shown that 65% of climate funding was allocated to infrastructure investments, including coastal protection measures for flooding and erosion [11], that caused a significant portion of climate finance to be preplanned for infrastructures such as embankments. At the local level, the projects with "soft" measures, such as those related to capacity building, policy reform, and planning and management, are traditionally low cost [11] and inadequately meet the adaptation needs of the households. Data generated from this study showed that the households engaged in 24 adaptation measures whereas climate finance had 14 adaptation measures available (Table 4). Thus, it can be argued that climate finance was inadequate and the support received was beneficial to a limited extent.

The perceived probability in this study is defined as how likely households expect to face a climatic event in the future on the basis that it will affect a household's ability to rebound, i.e., overcome the effects of the climatic events. Risk experiences tend to induce people to think of the risks more often, thereby increasing their risk appraisals [13].

5.1. Perceived Probability. The perceived probability, as shown in Table 5, had the highest mean of 3.6667 and 3.9750, which ranged between likely and quite likely for both CF and non-CF HHs. The P value for cyclone and river erosion showed a significant correlation, however, with river erosion indicating a negative association. T-tests indicated that there is indeed a significant difference between the perceived probability of climate finance and nonclimate finance households. Significant differences between CF and non-CF HHs have also been observed based on the means of the CF and non-CF HHs for all climatic events as indicated by the P value.

5.2. Perceived Severity. The perceived severity was measured by multiple aspects of households that are affected by

Table 3: Summary of differences in socioeconomic profiles of climate finance (CF HHs) and nonclimate finance households (non-CF HHs).

	Findings (P value)	CF households	Non-CF households
Household size	No significant difference	4.07	4.27
Educational attainment	Significant difference at 10% confidence interval P value (0.062)	(i) The lower level of illiteracy with 69.6% (ii) Higher completion of the primary level with 26.3% (iii) Higher completion of the secondary level with 4.2%	(i) A higher level of illiteracy with 75.8% (ii) Lower completion of primary level with 25.6% (iii) No completion of secondary level
Land-holding size	No significant difference	However, more men have land than women; both CF men and CF women have more land than non-CF women	
Housing conditions	Significant difference at 0.01% and 0.05% confidence interval		
	Tenancy P value (0.049)	(i) 4.2% CF live free (ii) Only 1 CF rents (iii) 85% own housing (iv) More (10%) inherited from parents	(i) More non-CF (11.7%) live free (ii) 0 non-CF rents (iii) More non-CF (80%) own housing (iv) Less (8.3%) inherited from parents
	Location now $P < 0.001$	(i) More CF (10.4%) live outside embankment (ii) 7 CF live on embankment (iii) Less CF (74.6%) live inside embankment (iv) More CF (12.1%) live upland	(i) Less non-CF (2.5%) live outside embankment (ii) 0 non-CF live on embankment (iii) More non-CF (94.2%) live inside embankment (iv) Less non-CF (3.3%) live upland
	Household construction material P value (0.016)	(i) More CF (3.8%) houses made of mud (ii) More CF (22.9%) houses made of leaves (iii) Less CF (66.7%) houses made of corrugated tin (iv) More CF (2.9%) houses made of brick and cement (v) More CF (3.8%) houses made of others (wicker)	(i) Fewer non-CF (0.8%) houses made of mud (ii) More non-CF (13.3%) houses made of leaves (iii) More non-CF (83.3%) houses made of corrugated tin (iv) Fewer non-CF (1.7%) houses made of brick and cement (v) Fewer non-CF (0.8%) houses made of others (wicker)
	Water purification methods $P < 0.001$	(i) Less CF (1.3%) use water purification tablets (ii) More CF (2.5%) use filtering systems (iii) Less CF (21.7%) use boiling (iv) More CF (62.1%) use fitkari (aluminium sulfate, also known as alum) as others (v) Less CF do not use any purification method (12.5%)	(i) More non-CF (2.5%) use water purification tablets (ii) 0 non-CF use filtering systems (iii) More non-CF (23.3%) use boiling (iv) Fewer non-CF (45%) use fitkari (aluminium sulfate, also known as alum) as others (v) More non-CF do not use any purification method (29.2%)
Primary source of income	Significant difference at 0.05% confidence interval	(i) More CF wage labourer (55.4%) (ii) Less CF in service (6.3%) (iii) More CF in trade (8.8%) (iv) More CF fishermen (7.5%)	(i) Less non-CF wage labourer (40.8%) (ii) More non-CF in service (25.5%) (iii) Fewer non-CF in trade (7.5%) (iv) Less non-CF fishermen (5.8%)
Secondary source of income	Significant difference at 0.01% confidence interval	(i) More CF as pastoralist (12.5%) and wage labourer (5.4) (ii) 71.7% CF does not have any secondary source	(i) Only 1 farmer, 1 domestic worker, 1 begging non-CF (ii) 96.7% non-CF do not have any secondary source
Average monthly income	Difference	USD 59.9	USD 54.9

Table 3: Continued.

	Findings (P value)	CF households	Non-CF households
Membership in social groups	Significant difference at 0.01% confidence interval		
	Self-help groups $P < 0.001$	More CF (64.6%) participation in self-help group	Less non-CF (1.7%) participation in self-help group
	Producer group $P < 0.001$	More CF (48.8%) participation in producer group	Less non-CF (0.8%) participation in producer group
	DMC $P < 0.001$	More CF (10.5%) participation in disaster management committee (DMC)	Less non-CF (0.8%) participation in disaster management committee (DMC)
	Cooperatives $P < 0.001$	More CF (76.3%) participating in cooperatives	Less non-CF (16.7%) participating in cooperatives
	No membership in any social group $P < 0.001$	Less CF (3.8%) not participating in any social group	More non-CF (83.3%) not participating in any social group

Table 4: Percentage of climate finance (CF) and nonclimate finance (non-CF) households who engaged in the adaptation measures.

Group	Adaptation measures	Groups		Chi^2 (P value)
		CF (%)	Non-CF (%)	
Housing	Plinth raising and reinforcement of housing**	78.8	64.2	8.82 (0.003)
	Construction of new housing*	70.8	51.7	13.76 (<0.001)
	Repair of damaged housing**	28.8	31.7	0.33 (0.568)
Garden	Homestead gardening**	55.0	42.5	5.00 (0.025)
	Community nursery*	11.3	0.83	12.10 (<0.001)
	Social forestry*	19.2	12.5	2.53 (0.112)
Agricultural land and crops	Changed crop varieties**	7.5	1.7	5.19 (0.023)
	Changed crop patterns*	7.1	1.7	4.70 (0.030)
	Changed irrigation management	3.8	0	6.57 (0.037)
Livestock	Poultry farming**	85.4	72.5	8.71 (0.003)
	Duck farming**	70.8	58.3	5.63 (0.018)
	Raised poultry housing**	53.8	38.3	7.61 (0.006)
	Goat rearing**	35.8	19.2	10.53 (<0.001)
	Cow rearing**	75.8	45.8	32.01 (<0.001)
	Raised barn**	42.9	12.5	33.59 (<0.001)
	Cow fattening**	30.4	2.5	37.43 (<0.001)
Fisheries	Change in fish culture**	7.9	2.5	4.09 (0.043)
Safe water	Installation of deep tube wells*	54.6	40.8	6.05 (0.014)
	Elevated tube wells**	32.5	30	0.23 (0.631)
	Water storage tanks	4.6	0	5.67 (0.017)
Access to power and fuel sources	Solar systems*	60.8	50	3.84 (0.050)
IGA	Rickshaw/Thela**	5.8	9.2	1.38 (0.241)
	Three-wheeler*	5	3.3	0.52 (0.469)
	Trading/small business**	17.9	16.7	0.09 (0.769)

Source: Survey conducted under this study. **Adaptation measures fully supported by climate finance; *partial support from climate finance.

climatic events. To obtain a single perceived severity, all the perceived severities were aggregated corresponding to a particular climatic event such as cyclone, storm surge, and river erosion, among others. As shown in Table 6, the perceived severity to cyclones had the highest effect on the different dimensions of households such as housing, gardening, crops, and livestock and with a mean of 1.93 for the CF HHs and 1.66 for the non-CF HHs. The P value for all values shows a significant correlation, however, in a negative direction, derived from the t-test. The t-tests also indicated that there is indeed a significant difference between the perceived severity of climate finance and nonclimate finance households. CF HHs have a higher severity on the different dimensions of the households compared to non-CF HHs. Significant differences between CF and non-CF HHs have also been observed for the means of the CF and non-CF HHs for all climatic events as indicated by the P value.

5.3. Risk Appraisal and Overall Risk Appraisal. All the perceived severity for each of the climatic event was added to reach a single perceived severity, as presented in Table 7. The perceived probability was multiplied by the corresponding severity for the event to obtain the risk appraisal for that climatic event. After which, all the risk appraisals were added to estimate an overall risk appraisal which indicated a significant difference between the

Table 5: Mean, standard deviation, and standard error of the perceived probability, i.e., likelihood of facing the climatic events in the future.

	CF/non-CF	Mean	Std. deviation	*T*-test	*P* value
Cyclone	CF	3.667	1.541	1.963	0.051
	Non-CF	3.975	1.331		
Storm surge	CF	2.988	1.451	1.798	0.073
	Non-CF	3.242	1.160		
Flooding	CF	3.346	1.281	−0.551	0.583
	Non-CF	3.258	1.487		
River erosion	CF	2.829	1.818	−7.110	<0.001
	Non-CF	1.558	1.477		
Irregular rains	CF	2.992	1.284	0.795	0.428
	Non-CF	3.108	1.327		
Nor'wester (Kalboishakhi)	CF	4.158	1.094	0.502	0.616
	Non-CF	4.225	1.233		
Salinity	CF	1.471	1.420	−3.271	<0.001
	Non-CF	1.000	1.216		

Table 6: Mean, standard deviation, and standard error of the perceived severity, i.e., the effect of climatic events on different dimensions of the households.

	CF/non-CF	*N*	Mean	Std. deviation	Std. error	*T*-test	*P* value
Cyclone	CF	240	1.937	0.560	0.036	−4.575	<0.001
	Non-CF	120	1.663	0.522	0.048		
Storm surge	CF	240	1.692	0.630	0.041	−5.516	<0.001
	Non-CF	120	1.373	0.447	0.041		
Flooding	CF	240	1.723	0.675	0.044	−4.380	<0.001
	Non-CF	120	1.442	0.510	0.047		
River erosion	CF	240	0.892	0.697	0.045	−7.009	<0.001
	Non-CF	120	0.418	0.553	0.051		
Irregular rains	CF	240	1.021	0.458	0.030	−3.056	0.002
	Non-CF	120	0.883	0.371	0.034		
Nor'wester (Kalboishakhi)	CF	240	1.710	0.533	0.034	−4.384	<0.001
	Non-CF	120	1.466	0.465	0.043		
Salinity	CF	240	0.540	0.471	0.030	−5.011	<0.001
	Non-CF	120	0.315	0.362	0.033		

Table 7: Mean, standard deviation, and standard error of the risk appraisal of the households.

	CF/non-CF	*N*	Mean	Std. deviation	Std. error	*T*-test	*P* value
Risk appraisal_Cyclone	CF	240	7.332	3.805	0.246	−1.448	0.149
	Non-CF	120	6.773	3.259	0.296		
Risk appraisal_Storm surge	CF	240	5.340	3.539	0.229	−2.821	0.005
	Non-CF	120	4.466	2.284	0.209		
Risk appraisal_Flood	CF	240	6.114	3.408	0.220	−2.909	0.004
	Non-CF	120	5.057	3.151	0.289		
Risk appraisal_River erosion	CF	240	3.256	3.091	0.199	−8.207	<0.001
	Non-CF	120	1.142	1.784	0.163		
Risk appraisal_Irregular rains	CF	240	3.250	2.127	0.137	−2.247	0.025
	Non-CF	120	2.794	1.633	0.149		
Risk appraisal_Nor'wester	CF	240	7.165	3.097	0.200	−2.596	0.010
	Non-CF	120	6.306	2.881	0.264		
Risk appraisal_Salinity	CF	240	1.092	1.399	0.090	−5.118	<0.001
	Non-CF	120	0.501	0.791	0.072		

overall risk appraisal of CF and non-CF HHs, where the CF HHs have a higher overall risk assessment than non-CF HHs. This overall risk appraisal was used as the dependent variable for the multiple linear regression model to assess the impact of selected independent variables on it (Table 8).

Table 8: Independent variables with details for the dependent variable (overall risk appraisal).

Categories	Independent variables	Measurement/ explanation	Scale	Recoded for regression analysis	Types of data
Socioeconomic factors	HH size	Numbers of household members			Continuous
	Income	Total annual income in number			Continuous
Assets	Immobile Assets (land)	Agricultural land in acre in number			Continuous
	Productive Assets (livestock, etc.)	In number			Continuous
	Mobile Assets	In number			Continuous
Involvement in social groups	Participation in self-help groups, producer group, DMC, cooperatives	Participation	1 = yes; 0 = no	1 = yes; 0 = no	Binary
Information on climate change	SISCH: information on climate change from social circle, i.e., relatives/ neighbours/friends/ community	Information received	1 = yes; 0 = no	1 = yes; 0 = no	Binary
External sources of finance	Support from social safety net	Support received from	1 = vulnerable group development (VGD) 2 = vulnerable group feeding (VGF) 3 = food for work (KABIKA) 4 = cash for work (KABITA) 5 = old age allowance 6 = allowance for the widowed, deserted, and destitute 7 = housing support 8 = test relief (TR) programme 9 = zakat in cash 10 = zakat in kindness 11 = scholarship 12 = others	1 = yes; 0 = no	Binary
	Monetary/in-kind support from Social Circle (relatives, friends, neighbours, self-help groups) for adaptation responses	Support received from	1 = relatives 2 = friends 3 = neighbours 4 = self-help groups	1 = yes for all options; 0 = no for all options	Binary
	Financial support from loans (microcredit, bank, cooperative, mohajan) for adaptation responses	Support received from	1 = microcredit 2 = bank 3 = cooperatives 4 = mohajan	1 = yes for all options; 0 = no for all options	Binary
	Financial support from govt. for adaptation responses	Support received from	1 = yes; 0 = no	1 = yes; 0 = no	Binary
	Financial support from NGOs (cash, materials, labour costs, advisory services) for adaptation responses	Support received from	1 = cash 2 = materials 3 = labour costs 4 = advisory services 5 = training	1 = yes for all options; 0 = no for all options	Binary
	Self-financed adaptation responses through selling		1 = land or building 2 = durable HH assets 3 = livestock 4 = mobile assets 5 = agricultural/fisheries equipment	1 = yes for all options; 0 = no for all options	Binary
	Self-financed adaptation responses through reduced household expenditure		1 = reduced expenditure on food, health, and education 2 = relied on savings 3 = paid from income 4 = HH members took other employment	1 = yes for all options; 0 = no for all options	Binary

6. Multiple Linear Regression Model for Overall Risk Appraisal

6.1. Regression Model for Overall Risk Appraisal for CF and Non-CF HHs. From the model for overall risk appraisal for CF HHs and non-CF HHs with 240 and 120 observations, respectively, the summary of statistical tests and the regression analysis results are given in Tables 9 and 10. The models were statistically significant at $F = 15.16$, $P < 0.01$ for CF HHs and $F = 6.30$, $P < 0.01$ for non-CF HHs, respectively. Positive auto-collinearity was observed. As shown in Table 10, a highly significant ($P < 0.01$) and negative relationship between overall risk appraisal and the independent variables was observed for income and participation in a social circle for CF HHs, while a significant and negative relationship was observed for non-CF HHs for income and information on climate change from the social circle. For CC HHs, positive and highly significant association ($P < 0.01$) between overall risk appraisal and the independent variables was seen for household size, immobile assets, and support from the social safety net. Significant relationship for CF HHs was observed between overall risk appraisal productive assets and financial support from government. On the contrary, for non-CF HHs, highly significant and positive relationship can be observed between overall risk assessment and immobile and productive assets and financial support from NGOs, while the significant and positive relationship is observed for social safety net.

Table 9: Summary of results from statistical tests for CF and non-CF models for overall risk appraisal.

	CF HHs	Non-CF HHs
Number of observations	240	120
Model	10	8
Error	229	111
Corrected total	239	119
F value	15.16	6.30
P value	<.001	<.001
Root MSE	52.470	41.537
Dependent mean	142.163	112.350
Coefficient of variance	36.908	36.971
R-square	0.398	0.312
Adj R-square	0.372	0.263
Durbin–Watson D	1.420	1.375

7. Discussion

7.1. Climate Hazards, Risk Appraisal, and Role of the Climate Finance Project. Galachipa is vulnerable to natural hazards such as cyclones, storm surges, and river erosion, among others. It was one of the hardest hit upazilas by the 2007 super cyclone SIDR [31]. For the CF HHs, the analysis from Table 5 indicated a significant correlation between cyclone with perceived probability based on previous exposure of the households to cyclones and their perception that they will be affected by cyclones in the future. Table 5 also shows that there is a significant difference between climate finance recipient households and nonrecipients in their correlation between river erosion and perceived probability, indicating that CF HHs were severely affected by river erosion, given that the CF HHs and non-CF HHs were taken from the same study area. A possible reason is the staff of the CF Project may have had a selection bias towards selecting those households who have lost land to river erosion as beneficiaries. Loss of places is a significant risk from climate change for physical loss of land and resources [4]. Furthermore, Table 6 shows that CF HHs had a higher perceived severity than non-CF HHs, which indicates that the CF HHs were sensitised by the climate finance project towards the exposure to climatic events on their lives and livelihoods. Climate change and its risks can be understood through memories of past weather, current experience, and future imaginaries, which are attached to particular places and practices [4].

The CF HHs were trained through a household adaptation plan to interpret the exposure they were facing and identify adaptation measures. The climate finance project organised exchanges between the households on the effects on climate change on their households and the precautionary measures they take, thus building awareness within the wider social circle of the households. As argued by Granderson, discourses play a significant role in how climate change and its risks are interpreted and made meaningful for communities [4]. Furthermore, climate finance supported the development of consensus and of a common understanding within the households on how to adapt. According to Granderson, responses required the adoption of a particular vision of the future, the course of action rather than another [4], and an understanding of sharing common resources and labour between the households to adapt.

7.2. Household Size. The estimated coefficient for overall risk appraisal was statistically positive and highly significant for household size, indicating that overall risk perception increases with more household members. From the household profile in Table 3, it can be seen that the average household size of the surveyed household is 4.07 and 4.27 for CF and non-CF HHs, respectively, while the Upazila average is 4.5 people per household. The possible reasons of higher risk perception may be due to the awareness that evacuated household members during climatic events leads to higher consumption costs borne by members during and after climatic effects when resources and commodities are scarce as well as adaptation costs in the future.

7.3. Income. Table 10 shows that as income increased, the overall risk perception of both the CF and non-CF households decreased. Results from this research are consistent with the findings of Alauddin and Sarker that higher-income households engaged in adaptive measures and undertook more associated risks [32]. The study also showed that risk appraisals to production, physical health, and income dimensions received greater priority while farmers paid less attention to risks to happiness and social relationships [13]. Sociodemographic characteristics like farm experience,

Table 10: Multiple linear regression results for CF and non-CF models for overall risk appraisal.

Independent variables	CF			Non-CF		
	Parameter estimate	Standard error	*P* value	Parameter estimate	Standard error	*P* value
HH size	6.251	2.387	0.009	—	—	—
Income	−0.003	<0.001	0.002	−0.004	0.002	0.023
Immobile assets	8.169	1.438	<0.001	8.649	2.165	<0.001
Productive assets (livestock, etc.)	1.882	0.921	0.042	3.310	1.210	0.007
Participation in self-help groups, producer group, DMC, cooperatives	−14.806	4.029	<0.001	—	—	—
SISCH: information on climate change from social circle, i.e., relatives/neighbours/friends/community	—	—	—	−7.285	2.815	0.011
Support from social safety net	23.182	7.411	0.002	21.881	8.385	0.010
Monetary/in-kind support from social circle (relatives, friends, neighbours, self-help groups) for adaptation responses	−15.206	7.325	0.039	—	—	—
Financial support from govt. for adaptation responses	18.830	7.547	0.016	—	—	—
Financial support from NGOs (cash, materials, labour costs, advisory services) for adaptation responses	—	—	—	39.503	13.963	0.006

education, and income level are the most significant factors in increasing the likelihood of farmers' adaptation practices [33]. The inverse association between income and overall risk appraisal may be due to higher income; the households perceive less risk as they engage more in adaptation measures and ascertain that they are in a better position to deal with the impacts of climate change.

Findings from the study, as seen in Table 3, also revealed that the CF HHs had a higher average income than the non-CF HHs and had an increase in assets and livestock received from the CF interventions. However, more assets expanded the risk of losing the assets they have gained through the CF intervention. Perceived probability, production, physical health, and income are the essential dimensions farmers perceive to be threatened by climate change [13]. A negative and significant association was observed between overall risk and income and involvement in social circles for overall risk appraisal. This may indicate that social circles affect the spending behaviour of households towards engaging in adaptation measures, resulting in a decrease in income and a simultaneous decrease in overall risk appraisal.

7.4. Immobile and Productive Assets. Table 10 shows that an increase in immobile assets, in terms of land, increases overall risk perception of CF and non-CF households alike. Furthermore, Table 10 also indicates a positive and highly significant association is observed between risk appraisal and productive assets in terms of livestock, poultry, agricultural equipment, and fisheries equipment for CF HHs, while for non-CF the association is highly significant. A considerable proportion of the households have been affected by river erosion and are landless; therefore, this explains the high-risk perception between overall risk perception and immobile assets. Furthermore, Vatsa argues that assets play a critical role in risk situations, and households try to resist and cope with adverse consequences of disasters and other risks through the assets that they can mobilise in the face of shocks [34]. However, if immobile assets are affected, then the households lose their ability to cope with the effects of climatic events.

However, Islam et al. argue that a household's involvement in a diverse set of income-generating livelihood activities or strategies reduces the vulnerability of the household [25]. Income-generating activities provide households with additional income in addition to their main source of income and support in having savings and investing in building assets. Assets help in engaging in activities to address the household vulnerability. While people from different occupations are affected differently, farmers, pastoralists, and fishers are especially affected by climate change as they rely on natural resources and are, at the same time, exposed to meteorological events as well. Most decisions by farmers to adapt to climate change vary directly with livestock ownership since it serves as a store of value and encourages adaptation to climate change [32].

7.5. Participation in Social Circles. As shown in Table 10, results demonstrate increased participation in social circles causes a highly significant decrease in the overall risk appraisal of household, especially for the non-CF HHs. As hypothesised by Le Dang et al., social discourse is hypothesised to affect risk perception and adaptation assessment [13]. In fact, social capital facilitates access to a broader source of information [35]. The involvement in the social circle gives the households a better support system to gain information and even jointly face the different climatic events as social circles can act as sources of financial support and even interpersonal relationships, such as kinship networks, social obligations, trust, and reciprocity, mobilise capacity directly by enabling material responses to climate hazards or indirectly via institutional modifications [4]. Islam et al. have derived similar findings [25]. The non-CF

households' ability to cope and adapt was constrained because of their lack of participation in community organisations or the absence of community organisations as a whole, indicating that social relationships received less attention [36] from non-CF HHs.

7.6. Information on Climate Change from the Social Circle. Access to information from the social circle has a significant impact on the overall risk appraisal of non-CF HHs, as shown in Table 10. From Table 3, it is seen that around 83.3% of the non-CF HHs do not engage in any social groups. Therefore, information received from the social circle on climate change informed the households on the exposure of climate change and could have prepared accordingly, thus decreasing their risk appraisal. Information and discussion, therefore, can influence perception [13]. Information from the social circle could also have given the non-CF households a better understanding of how to interpret the information and also explore new ways of adapting from their social circle, also contributing to a decrease in the overall risk appraisal. However, other scholars have found that farmers who believe that climate change is happening and influencing their family's lives perceive higher risks in most dimensions [13].

7.7. Support from Social Safety Nets and Financial Support from Government and NGOs. The regression analysis of social safety net programmes under Table 10 illustrated a positive and highly significant relationship with overall risk appraisal for CF HHs and a positive and significant relationship for non-CF HHs. Social protection or safety net programs assist individuals, households, and communities in managing better a wide range of risks that leaves people vulnerable [34]. One of the reasons for this could be that these programs deal with both the deprivation and vulnerability of the poorest people; thus, when these programmes supported the households, they perceived themselves being at risk. Similarly, the CF HHs perceive significant and positive risk, when they received support from the government, as the assistance is aimed towards people who are at risk and need support. Furthermore, as seen in Table 10, a relationship between financial support from NGOs for adaptation measures and overall risk appraisal for non-CF HHs is evident. Possible reasons could be that when they receive the support for adaptation measures from government or NGOs, they believe that they are at risk.

7.8. Monetary/In-Kind Support from Social Circle (Relatives, Friends, Neighbours, and Self-Help Groups) for Adaptation Measures. As seen in Table 10, a negative and highly significant relationship is evident between monetary support and in-Kind support from social circle for the CF HHs and overall risk appraisal. Instead of being at risk of facing the effects of climate change alone, the CF HHs could rely on getting support from their social circle. While risk appraisal played a crucial role in motivating the household to explore adaptation options which are crucial and which they can afford, households also could share common resources within their social circle to adapt, which did not cause them to incur additional costs and yet benefit from them. Correspondingly, support from the social circle increases the effectiveness of climate finance through enhancing the utilisation of the household's own resources towards contributing towards adaptation needs of the social circle.

8. Conclusions

This study conducted a comparative analysis between CF and non-CF HHs regarding the anticipated climatic events and the severity of the events on their lives as well as factors which influenced their risk appraisal. Both CF and non-CF HHs resided in the same geographical and meteorological conditions and dealt with the same climatic events. Both groups anticipated climatic events such as river erosion and cyclones, among others, occurring in the future. However, the findings of the study indicated that CF HHs expected higher severity of climatic events on the various dimensions of their households such as housing, income, crops, equipment, among others. This result suggests that the CF HHs are more aware of the consequences of climate change and therefore engaged in more adaptation measures than non-CF HHs. Barrett had similar findings in a study in Malawi of adaptation finance-assisted villages [6]. Programs that provide technical assistance or compensation to change practices may be a positive opportunity for agricultural communities to address climate change and help offset the transaction costs associated with changing practices [25]. This analysis implies that climate finance support informed the households about the risks that they were facing, assisted them in exploring adaptation options and engaging in them. Awareness and training sessions, climate information, increased accessibility to public extensions services, and exchange within the social groups about the effects of climate change affect the potential severity or effect of climate change on the households.

Furthermore, several factors influenced the risk appraisal of the CF and non-CF HHs, respectively. The socioeconomic conditions of the households played a key role in the risk appraisal. Particularly, household size increased the risk assessment for CF HHs. While the increase in income caused a decrease in the risk assessment, increase in assets caused an increase in the risk perception of the households. These results could indicate that households do not have stable socioeconomic conditions yet.

The benefits by strengthening the social circle of the CF HHs under the climate finance project became evident as participation in the different groups and the monetary/in-Kind support from the social circle resulted in a decrease in overall risk appraisal. On the contrary, Le Dang et al. argue that social circles play a significant role in facilitating decisions on using adaptation measures based on information obtained from friends, relatives, and neighbours, which increases the overall perceived risk [13].

Furthermore, awareness is not sufficient for households to engage in adaptation measures as the households were extremely poor and lacked adequate resources to adapt. In

fact, households, which intend to reduce the risks associated with climate change and have the resources or access to resources needed to make the appropriate changes, are generally more resilient and have a greater capacity to adapt [37]. Information variables can increase or decrease risk appraisals. Therefore, information from social circles is significant for non-CF HHs as they are less engaged in social circles and value the information on climate change received.

Different sources of external finance such as from the government, social safety net programmes, or financial support from NGOs, all increased the risk appraisal of the households. One of the reasons could be that finance is mainly provided to the households if they are at risk. Secondly, since the financial support is limited, the households have to examine the dimensions that are at risk from climatic events, hence making them more aware of the risks, which increases their risk appraisal correspondingly. Furthermore, this causes the households to explore adaptation options which are crucial and which they can afford to address those dimensions of the households that are at risk. Thus, risk appraisal may increase the effective utilisation of external climate finance, and the households own resources for adaptation measures.

This study tried to address the knowledge gap on the effect of climate finance on risk appraisal at the local level. The findings of this research reinforce the pattern of the inadequacy of climate finance to meet the local needs of the most vulnerable communities. At the global level, adequate funding is not provided to the developing countries by the Annex 1 countries, which include the industrialized countries and members of the OECD (Organisation for Economic Co-operation and Development) in 1992, plus countries with economies in transition (the EIT Parties), including the Russian Federation, the Baltic States, and several Central and Eastern European States. When climate finance reaches the national level, a significant proportion was allocated on hard components of adaptation such as infrastructure and recurring costs such as staff salaries. At the local level, limited climate finance remains actually to meet the adaptation needs of the households.

A dilemma remains in the pursuit of channelling climate finance support to the households. This study possibly identified a selection bias by the project team towards including people affected by river erosion as beneficiary. This could have caused other households, who were similarly vulnerable, to be not chosen as a beneficiary of the CF project as they were not affected by river erosion. In addition, some households could try to obtain more support from different projects if they have a better relationship with the project teams. Moreover, inequality could increase for the poorest and marginalised groups if climate finance does not reach them but is channelled towards the influential people who can exert more pressure to access the funding.

This research provides insights for policymakers, development partners, researchers, and practitioners that climate financing needs to be available for the exposed and marginalised households and that localised adaptation measures need to be initiated to support the affected households. Mechanisms to locally generate and integrate customised and contextualised adaptation measures into planning processes should be studied further. How to channel the climate finance into reaching the vulnerable population in the coastal region of Bangladesh so that inequality is not increased and marginalisation is avoided was not covered under this research and may be explored further. Finally, future research may be conducted on the costs of various adaptation actions together with a cost-benefit analysis which may contribute towards the future adaptation implementation at the local level.

Data Availability

The data used to support the findings of this study are available from the corresponding author upon request.

Disclosure

This article is an outcome of the research study of Ms Firdaus Ara Hussain for her PhD at the Asian Institute of Technology.

Conflicts of Interest

The authors declare that there are no potential conflicts of interest concerning the research, authorship, and publication of this paper.

References

[1] L. Jones and T. Tanner, "'Subjective resilience': using perceptions to quantify household resilience to climate extremes and disasters," *Regional Environmental Change*, vol. 17, no. 1, pp. 229–243, 2017.

[2] T. Grothmann and A. Patt, "Adaptive capacity and human cognition: the process of individual adaptation to climate change," *Global Environmental Change*, vol. 15, no. 3, pp. 199–213, 2005.

[3] I. A. Rana and J. K. Routray, "Actual vis-à-vis perceived risk of flood prone urban communities in Pakistan," *International Journal of Disaster Risk Reduction*, vol. 19, pp. 366–378, 2016.

[4] A. A. Granderson, "Making sense of climate change risks and responses at the community level: a cultural-political lens," *Climate Risk Management*, vol. 3, pp. 55–64, 2014.

[5] R. Barr, S. Fankhauser, and K. Hamilton, "Adaptation investments: a resource allocation framework," *Mitigation and Adaptation Strategies for Global Change*, vol. 15, no. 8, pp. 843–858, 2010.

[6] S. Barrett, "Local level climate justice? Adaptation finance and vulnerability reduction," *Global Environmental Change*, vol. 23, no. 6, pp. 1819–1829, 2013.

[7] J. T. Roberts and R. Weikmans, "Postface: fragmentation, failing trust and enduring tensions over what counts as climate finance," *International Environmental Agreements: Politics, Law and Economics*, vol. 17, no. 1, pp. 129–137, 2017.

[8] M. Sarraf, S. Dasgupta, and N. Adams, *Bangladesh Development Series: The Cost of Adapting to Extreme Weather Events in a Changing Climate*, World Bank, Washington, DC, USA, 2011.

[9] H. Brammer, "Bangladesh's dynamic coastal regions and sea-level rise," *Climate Risk Management*, vol. 1, pp. 51–62, 2014.

[10] S. Huq, S. M. M. H. Khan, and M. Shamsuddoha, *The Bangladesh National Climate Funds—A Brief History and Description of the Bangladesh Climate Change Trust Fund and the Bangladesh Climate Change Resilience Fund*, LDC Paper Series, Bangladesh, 2012.

[11] B. Biagini, R. Bierbaum, M. Stults, S. Dobardzic, and S. M. McNeeley, "A typology of adaptation actions: a global look at climate adaptation actions financed through the global environment facility," *Global Environmental Change*, vol. 25, no. 1, pp. 97–108, 2014.

[12] E.-L. Sundblad, A. Biel, and T. Gärling, "Cognitive and affective risk judgements related to climate change," *Journal of Environmental Psychology*, vol. 27, no. 2, pp. 97–106, 2007.

[13] H. Le Dang, E. Li, I. Nuberg, and J. Bruwer, "Farmers' perceived risks of climate change and influencing factors: a study in the Mekong Delta, Vietnam," *Environmental Management*, vol. 54, no. 2, pp. 331–345, 2014.

[14] Butardo-Toribio, M. Zita, and E. R. Tenefrancia, "Land, livelihood, Poverty: assessment of selected socio-economic factors influencing community adaptive capacity to climate change," *COMCAD Arbeitspapiere Working Paper*, vol. 94, 2011.

[15] N. Amerasinghe, J. Thwaites, G. Larsen, and A. Ballesteros, *The Future of the Funds: Exploring the Architecture of Multilateral Climate Finance*, World Resources Institute, Washington, DC, USA, 2017.

[16] F. Lamperti, A. Mandel, M. Napoletano et al., "Towards agent-based integrated assessment models: examples, challenges, and future developments," *Regional Environmental Change*, vol. 19, no. 3, pp. 747–762, 2019.

[17] S. Colenbrander, D. Dodman, and D. Mitlin, "Using climate finance to advance climate justice: the politics and practice of channelling resources to the local level," *Climate Policy*, vol. 18, no. 7, pp. 902–915, 2018.

[18] Government of Bangladesh, *Climate protection and development finance division ministry of finance government of the people's republic of Bangladesh*, Government of Bangladesh, Dhaka, Bangladesh, 2017.

[19] M. Ataur Rahman and S. Rahman, "Natural and traditional defense mechanisms to reduce climate risks in coastal zones of Bangladesh," *Weather and Climate Extremes*, vol. 7, pp. 84–95, 2015.

[20] M. M. Q. Mirza, "Climate change, flooding in South Asia and implications," *Regional Environmental Change*, vol. 11, no. S1, pp. 95–107, 2011.

[21] B. Mallick and J. Vogt, "Population displacement after cyclone and its consequences: empirical evidence from coastal Bangladesh," *Natural Hazards*, vol. 73, no. 2, pp. 191–212, 2014.

[22] M. S. Hossain, J. A. Dearing, M. M. Rahman, and M. Salehin, "Recent changes in ecosystem services and human well-being in the Bangladesh coastal zone," *Regional Environmental Change*, vol. 16, no. 2, pp. 429–443, 2016.

[23] M. R. Karim and A. Thiel, "Role of community based local institution for climate change adaptation in the Teesta riverine area of Bangladesh," *Climate Risk Management*, vol. 17, pp. 92–103, 2017.

[24] S. S. Hutchins, C. Brown, R. Mayberry, and W. Sollecito, "Value of a small control group for estimating intervention effectiveness: results from simulations of immunization effectiveness studies," *Journal of Comparative Effectiveness Research*, vol. 4, no. 3, pp. 227–238, 2015.

[25] M. M. Islam, S. Sallu, K. Hubacek, and J. Paavola, "Vulnerability of fishery-based livelihoods to the impacts of climate variability and change: insights from coastal Bangladesh," *Regional Environmental Change*, vol. 14, no. 1, pp. 281–294, 2014.

[26] M. T. Niles, M. Lubell, and V. R. Haden, "Perceptions and responses to climate policy risks among California farmers," *Global Environmental Change*, vol. 23, no. 6, pp. 1752–1760, 2013.

[27] H. B. Truelove, A. R. Carrico, and L. Thabrew, "A socio-psychological model for analyzing climate change adaptation: a case study of Sri Lankan paddy farmers," *Global Environmental Change*, vol. 31, pp. 85–97, 2015.

[28] S. van der Linden, "The social-psychological determinants of climate change risk perceptions: towards a comprehensive model," *Journal of Environmental Psychology*, vol. 41, pp. 112–124, 2015.

[29] J. J. Hyland, D. L. Jones, K. A. Parkhill, A. P. Barnes, and A. P. Williams, "Farmers' perceptions of climate change: identifying types," *Agriculture and Human Values*, vol. 33, no. 2, pp. 323–339, 2016.

[30] United Nations, "Financing development gaps in the countries with special needs in the asia-pacific region," in *Proceedings of the Third International Conference on Financing for Development*, Addis Ababa, Ethiopia, July 2015.

[31] U. Kulatunga, G. Wedawatta, D. Amaratunga, and R. Haigh, "Evaluation of vulnerability factors for cyclones: the case of Patuakhali, Bangladesh," *International Journal of Disaster Risk Reduction*, vol. 9, pp. 204–211, 2014.

[32] M. Alauddin and M. A. R. Sarker, "Climate change and farm-level adaptation decisions and strategies in drought-prone and groundwater-depleted areas of Bangladesh: an empirical investigation," *Ecological Economics*, vol. 106, pp. 204–213, 2014.

[33] M. N. Uddin, B. Lei, M. A. Sarker, M. Z. Rahman, and M. M. Hasan, "Role of a coastal NGO in attaining climate resilience in Bangladesh," *American Journal of Climate Change*, vol. 7, no. 2, pp. 187–203, 2018.

[34] K. S. Vatsa, "Risk, vulnerability, and asset-based approach to disaster risk management," *International Journal of Sociology and Social Policy*, vol. 24, no. 10-11, pp. 1–48, 2004.

[35] G. M. M. Alam, K. Alam, and S. Mushtaq, "Climate change perceptions and local adaptation strategies of hazard-prone rural households in Bangladesh," *Climate Risk Management*, vol. 17, pp. 52–63, 2017.

[36] H. Le Dang, E. Li, I. Nuberg, and J. Bruwer, "Farmers' assessments of private adaptive measures to climate change and influential factors: a study in the Mekong Delta, Vietnam," *Natural Hazards*, vol. 71, no. 1, pp. 385–401, 2014.

[37] W. Ullah, T. Nihei, M. Nafees, R. Zaman, and M. Ali, "Understanding climate change vulnerability, adaptation and risk perceptions at household level in Khyber Pakhtunkhwa, Pakistan," *International Journal of Climate Change Strategies and Management*, vol. 10, no. 3, pp. 359–378, 2017.

Hindawi
Advances in Meteorology
Volume 2019, Article ID 2767018, 12 pages
https://doi.org/10.1155/2019/2767018

Research Article

Climate Change Impacts on Winter Wheat Yield in Northern China

Xiu Geng,[1,2] Fang Wang,[1,2] Wei Ren,[3] and Zhixin Hao[1,2]

[1]*Key Laboratory of Land Surface Pattern and Simulation, Institute of Geographic Sciences and Natural Resources Research, Chinese Academy of Sciences, Beijing 100101, China*
[2]*College of Resources and Environment, University of Chinese Academy of Sciences, Beijing 101408, China*
[3]*College of Agriculture, Food and Environment, University of Kentucky, Lexington 40506, USA*

Correspondence should be addressed to Zhixin Hao; haozx@igsnrr.ac.cn

Received 22 February 2019; Revised 6 May 2019; Accepted 19 May 2019; Published 19 June 2019

Guest Editor: Sushil K. Dash

Exploring the impacts of climate change on agriculture is one of important topics with respect to climate change. We quantitatively examined the impacts of climate change on winter wheat yield in Northern China using the Cobb–Douglas production function. Utilizing time-series data of agricultural production and meteorological observations from 1981 to 2016, the impacts of climatic factors on wheat production were assessed. It was found that the contribution of climatic factors to winter wheat yield per unit area (WYPA) was 0.762–1.921% in absolute terms. Growing season average temperature (GSAT) had a negative impact on WYPA for the period of 1981–2016. A 1% increase in GSAT could lead to a loss of 0.109% of WYPA when the other factors were constant. While growing season precipitation (GSP) had a positive impact on WYPA, as a 1% increase in GSP could result in 0.186% increase in WYPA, other factors kept constant. Then, the impacts on WYPA for the period 2021–2050 under two different emissions scenarios RCP4.5 and RCP8.5 were forecasted. For the whole study area, GSAT is projected to increase 1.37°C under RCP4.5 and 1.54°C under RCP8.5 for the period 2021–2050, which will lower the average WYPA by 1.75% and 1.97%, respectively. GSP is tended to increase by 17.31% under RCP4.5 and 22.22% under RCP8.5 and will give a rise of 3.22% and 4.13% in WYPA. The comprehensive effect of GSAT and GSP will increase WYPA by 1.47% under RCP4.5 and 2.16% under RCP8.5.

1. Introduction

In recent years, the frequency of various meteorological disasters such as drought, flood, and frost has increased due to climate change, which seriously impaired many climate-sensitive sectors [1]. It is understood that agriculture is likely to be affected most by climate change and variability because of its high dependence and sensitivity to climatic conditions [2–5]. Nevertheless, the impacts of climate change on crops in different regions are not the same [6]. Previous studies have shown that the warming caused by greenhouse gases is more pronounced at higher latitudes [7], which could lengthen growing seasons and reduce the risk of freezing injury due to low temperature and have positive effects on crops here [8, 9]. In contrast, higher temperature will adversely affect growing conditions in lower latitudes, especially in areas where temperatures are close to or at the optimal level for crop growth to begin with [10, 11]. Impacts on agriculture are likely to be especially severe in developing countries because of their low agricultural investment, technological levels, and capability to cope with climate change [12, 13]. China is the most populous developing country as well as one of the largest agricultural production countries. Agriculture in China feeds 22% of the global population with only 7% of the world's arable lands [14]. However, some studies have shown that China's agriculture might suffer from climate change. The loss in yield for each degree Celsius increase in global mean temperature is about 8.0% for maize and 2.6% for wheat [15]. It is urgent for us to understand the possible impacts of climate change on China's agriculture production, so that the planting strategies can be provided timely to avoid or mitigate the negative impacts from climate change.

There is now a substantial number of assessment studies demonstrating the link between climate change and agriculture, with the study methods ranging from simple equations to complex models, the study scope ranging from single sector to multiple sectors, and the study core ranging from intuitive phenomenon to mechanism analysis [16]. Crop models and statistical models are two main tools for quantitatively assessing the effects of climate change on crop yields [17]. Crop models such as DSSAT (America), APSIM (Australia), and CCSODS (China) can integrate knowledge on physiology, agronomy, soil science, and agrometeorology to the models using mathematical equations to quantitatively and dynamically describe the process of crop growth, development, and yield formation. Crop models are dominant tools for the Third and Fourth Assessment Reports of the IPCC to assess the impacts of climate change on agricultural sector because of their relatively clear ecological mechanism [18]. However, the results of crop models are highly sensitive to soil, meteorology, and field management and require extensive input data. These models also can be very difficult to calibrate because of complex model structures and a large number of uncertain parameters [19–22]. Statistical models such as time-series models, panel data models, and cross section models can predict crop indicators by using historical data on crop indicators and weather data to develop a regression equation [23]. However, the statistical data of Food and Agriculture Organization of the United Nation (FAO) showed that global wheat yield did not reduce with climate warming in the premise of stable planting areas (http://www.fao.org/faostat/zh/#data/QC/visualize), which indicated that with the development of agricultural technology, agricultural production is not only related to meteorological factors such as temperature and precipitation but also to economic factors such as labor and fertilizer. Therefore, researchers combined meteorological factors and economic factors as independent variables to establish regression models so as to explore the impacts of climate change on agricultural production [24–27]. Chou et al. [28, 29] developed a new model (C-D-C) for assessing and predicting the effect of climate change on grain yield by introducing climatic factors into the C-D (Cobb–Dauglas) production function, and the preliminary simulation and verification of the model were performed.

In terms of planting area and yield, wheat is the third most important crop in China, only behind rice and maize, and winter wheat accounts for approximately 95% of the total (winter and spring) wheat yields. The northern winter wheat production areas (NWPA) are the main areas that produce winter wheat and make up approximately 80.1% of the wheat production (National Bureau of Statistics of China, http://data.stats.gov.cn/easyquery.htm?cn=E0103). Winter wheat is mainly used for food in this region because of its high quality and flour yield. The goal of this paper was to quantitatively study the impacts of climate change on the winter wheat yield per unit area (WYPA) in NWPA by introducing growing season average temperature (GSAT) and precipitation (GSP) for winter wheat into the C-D production function, so as to provide reference for planting strategies and wheat import and export trade strategies in the future.

2. Materials and Methods

2.1. Study Area and Data. Our study area covers Jing-Jin-Ji region (including Beijing, Tianjin, and Hebei provinces), Shanxi, Shaanxi, Shandong, and Henan provinces (Figure 1), located in the midlatitude temperate zones of northern hemisphere (32–42°N) and influenced by East Asian monsoon climate. Crops are harvested twice a year or three times every two years. The climatic conditions in the region are suitable for planting winterness or strong-winterness wheat varieties with an annual precipitation of 440–980 mm, annual average temperature of 9–15°C, and active accumulated temperature ranges from 2750 to 4900°C. The growing season of winter wheat in this area is from this September to next June [30, 31].

The data used in this study included meteorological data and agricultural data. The meteorological data consisted of observations data for estimating the parameters of models and scenario data for forecasting future climate change. Observations data were available from China Meteorological Administration (CMA), which provided time series on the daily temperature and precipitation of meteorological stations (black dots in Figure 1) across the study area from 1981 to 2016, so as to calculate the GSAT and GSP for winter wheat. Greenhouse gas emission scenarios are the basis for future climate change projections, and one of the most important scenarios is RCPs (representative concentration pathways). RCPs include four greenhouse gases concentration trajectories adopted by the IPCC AR5, which represent integrated socioeconomic standards, emissions, and climate scenarios to construct the definite mitigation scenario. The four RCPs including RCP2.6, RCP4.5, RCP6.0, and RCP8.0 stabilized the radiative forcing at approximately 490, 650, 850, and 1370 ppm CO_2-equivalent in 2100, respectively [32]. RCP4.5, a medium emissions scenario, is possibly consistent with the future economic development of China and meets the mitigation plan for responding to climate change [33]. RCP8.5 corresponds to a high greenhouse gas emissions pathway and also to the upper bound of the four RCPs. The greenhouse gases emissions and concentrations in this scenario increase considerably over time, and there is not any specific climate mitigation target [34]. Therefore, the RCP4.5 and RCP8.5 were used in this study. Climate scenario data from the RCP4.5 and RCP8.5 for 2021–2050 were downloaded from the Inter-Sectoral Impact Model Intercomparison Project (ISI-MIP). The data include 5 climate models simulation outputs: HadGEM2-ES (MOHC, England), IPSL-CM5A-LR (IPSL, France), MIROC-ESM-CHEM (MIROC, Japan), GFDL-ESM2M (GFDL, America), and NorESM1-M (NCC, Norway), which have been bias-corrected based on the raw data from the 5 CMIP5 models listed above. The variability of the simulated data about their monthly means is modified to match the observed data to preserve the long-term absolute or relative trend of the simulated data. Then, these data are bilinearly interpolated in space to $0.5^\circ \times 0.5^\circ$ grid [35]. The

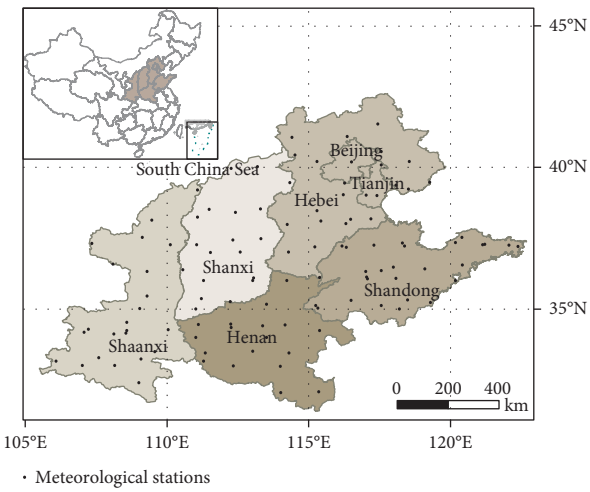

Figure 1: Location of study area and the distribution of meteorological stations.

multimodel ensemble (MME) of the climate variables was used in this paper, including daily mean temperature and precipitation.

Agricultural data were available from the National Bureau of Statistics of the People's Republic of China and an agricultural statistical datasets [36], which included provincial WYPA and related inputs from 1981 to 2016, that is, fertilizer use, machinery, labor, and irrigated area for winter wheat.

2.2. Model Specification and Evaluation. Cobb–Douglas production function is a multifactor analysis model, which can effectively describe the relationship between production factors and output. The production factors used in this study included both agricultural inputs and climatic factors, and we introduced climatic factors GSAT and GSP into the Cobb–Douglas production function to quantitatively investigate the impacts of climate change on wheat yield for the five provinces (region) in Northern China. We specified the empirical production function where the WYPA was a function of the meteorological variables and agricultural inputs for any province (region) i at year t:

$$Y_{\mathrm{it}} = \alpha_0 \times F_{\mathrm{it}}^{\alpha_1} \times M_{\mathrm{it}}^{\alpha_2} \times L_{\mathrm{it}}^{\alpha_3} \times I_{\mathrm{it}}^{\alpha_4} \times T_{\mathrm{it}}^{\beta_1} \times P_{\mathrm{it}}^{\beta_2} \times e^{\gamma \mathrm{Te}_{\mathrm{it}}} \times e^{\varepsilon_{\mathrm{it}}}. \tag{1}$$

We linearized the equation by taking the logarithm of both sides:

$$\begin{aligned} \ln(Y_{\mathrm{it}}) = {} & \alpha_0 + \alpha_1 \ln(F_{\mathrm{it}}) + \alpha_2 \ln(M_{\mathrm{it}}) + \alpha_3 \ln(L_{\mathrm{it}}) \\ & + \alpha_4 \ln(I_{\mathrm{it}}) + \beta_1 \ln(T_{\mathrm{it}}) + \beta_2 \ln(P_{\mathrm{it}}) + \gamma \mathrm{Te}_{\mathrm{it}} + \varepsilon_{\mathrm{it}}, \end{aligned} \tag{2}$$

where Y was the WYPA (kg/ha) and the agricultural inputs F, M, L, and I were fertilizers used (10,000 tons), machinery (10,000 kw), labor (10,000 persons), and irrigated area (1000 ha) for winter wheat, respectively. More importantly, we introduced average temperature (T, °C) and precipitation (P, 100 mm) during winter wheat growing season (from this September to next June) as climatic factors to the model. Additionally, we allowed for time varying effects on winter wheat production, represented by a time series, Te, and intended to capture the factor of technological progress influence. ε was white noise. The α, β, and γ were the coefficients to be estimated.

One should note that the agricultural inputs for winter wheat were included in the total agricultural inputs and needed to be calculated by some formulas. They can take the following form:

$$\begin{aligned} F_{\mathrm{it}} &= \mathrm{TF}_{\mathrm{it}} \times \mathrm{RA}_{\mathrm{it}}, \\ M_{\mathrm{it}} &= \mathrm{TM}_{\mathrm{it}} \times \mathrm{RA}_{\mathrm{it}}, \\ L_{\mathrm{it}} &= \mathrm{TL}_{\mathrm{it}} \times \mathrm{RG}_{\mathrm{it}} \times \mathrm{RA}_{\mathrm{it}}, \\ I_{\mathrm{it}} &= \mathrm{TI}_{\mathrm{it}} \times \mathrm{RA}_{\mathrm{it}}, \end{aligned} \tag{3}$$

where TF was total fertilizer use of farm crops; TM was total power of agricultural machinery; TL was total labor of agriculture, forestry, animal husbandry, and fishery; TI was total agricultural irrigated area; RA was sown area of winter wheat/total sown area of farm crops; RG was gross output of agriculture/gross output of agriculture, forestry, animal husbandry, and fishery.

Panel data involved two dimensions: a cross-sectional dimension and a time-series dimension [37], which required testing the temporal stability of variables before establishing a regression model to avoid spurious regressions. The approaches of LLC that assumes common unit root process [38] and ADF-Fisher that assumes individual unit root process [39] were used in this study to test for a unit root. The regression analysis can be carried out when all of the variables are stationary time series. However, as analyzed by Zhao [40], we can also establish a regression model if the variables pass the cointegration criterion in the premise that the integrated order of dependent variable is not more than that of independent variables and there are at least two independent variables having the integrated orders more than that of dependent variable, although some of the variables are nonstationary time series.

We adopted "leave-one-out cross validation" [41], the measures of "normalized root mean square error" (NRMSE), and "index of agreement" (IA) [42] to evaluate model performance. The two measures, NRMES and IA, summarize the average difference and agreement between observed and model-predicted values, respectively. They can take the following form:

$$\begin{aligned} \mathrm{NRMSE} &= \sqrt{\frac{\sum_1^n (P_i - O_i)^2}{n}} \times \frac{100}{\overline{O}}, \\ \mathrm{IA} &= 1 - \left[\frac{\sum_1^n (P_i - O_i)^2}{\sum_1^n \left(\left| P_i - \overline{O} \right| + \left| O_i - \overline{O} \right| \right)^2} \right], \end{aligned} \tag{4}$$

where P_i is the model-predicted value, O_i is observed value, n is the number of cases, and $\overline{O}$ is the average of observed values. Following Yang et al. [43], we considered NRMSE ≤ 15% as "good" agreement; 15–30% as "moderate"

agreement; and ≥30% as "poor" agreement. IA is intended to be a descriptive measurement, and it is both a relative and bounded measure [42], with IA = 0 indicating no agreement and IA = 1 indicating perfect agreement or zero error. Also as recommended by Yang et al. [43], when IA ≥ 0.9, it is considered as "excellent" agreement; 0.8 ≤ IA < 0.9 as "good" agreement; 0.7 ≤ IA < 0.8 as "moderate" agreement; and IA < 0.7 as "poor" agreement.

The impacts of climate trends and agricultural inputs changes on the WYPA were calculated in the following processes. First, we set three scenarios: (i) actual climatic factors and actual agricultural inputs for each province (region) for the period 1981–2016; (ii) detrended climatic factors and actual agricultural inputs; (iii) actual climatic factors and fixed agricultural inputs. We obtained the detrended datasets of GSAT and GSP for winter wheat in the five provinces (region) by the method of "linear detrending" [44]. For the agricultural inputs, we fixed them at the values in 1980. They can take the following form:

$$\begin{aligned} \mathrm{Cd}_{i,t} &= \text{detrended climatic variable} = C_{i,t} - s_i * t, \\ \mathrm{AF}_{i,t} &= \text{fixed agricultural input} = A_{i,1980}, \end{aligned} \tag{5}$$

where $C_{i,t}$ is the climatic variable for province (region) i at year t, including GSAT and GSP; s_i is the slope of one climatic variable for province (region) i, based on linear fit for 1981–2016; and $A_{i,1980}$ is the agricultural inputs for province (region) i in 1980, including fertilizer use, machinery, labor, irrigated area, and technological progress. We then used the "Climate-Economy" model $F(C, A)$ to compute the following:

(i) $F(C, A)$ = predicted WYPA with observed climatic data and agricultural inputs

(ii) $F(\mathrm{Cd}, A)$ = predicted WYPA with detrended climatic data and observed agricultural inputs

(iii) $F(C, \mathrm{AF})$ = predicted WYPA with observed climatic data and fixed agricultural inputs

We computed the trends of (i)-(ii) and (i)–(iii) to quantify the yield effects of climate trends and agricultural inputs changes, respectively.

3. Results

3.1. Panel Regression and Model Evaluation. The results of unit root test suggested that a cointegration test should be carried out, and the variables passed the cointegration criterion (Table 1), which indicated that we can establish a regression model and the model will not be spurious. F test suggested us to choose a fixed-effects model, and the estimation results are presented in Table 2. We also reported the adjusted R^2, F statistic, NRMSE, and IA used to evaluate the model performance in Table 2. The value of adjusted R^2 was 0.91, and F statistic was significant at the 1% level, which indicated that the model had the feature of high fitting precision. NRMSE and IA were 8.14% and 0.98, respectively, showing a high extrapolating performance of the model. The coefficients on all of the agricultural inputs were positive and significant as expected for WYPA, except the labor with a negative coefficient. This indicated that WYPA increased with more fertilizer use, machinery, and irrigation but decreased with more labor. The reason why labor had a negative impact on YWPA was explicable that, since 1980, the agricultural mechanization improved rapidly, which resulted in a large surplus of agricultural labor. For climatic factors, the sign was negative for GSAT and was positive for GSP. This suggested that WYPA increased with more precipitation and decreased with higher temperature during the growing season.

3.2. Impacts of Climate Change on the Fluctuation of Winter Wheat Yield. From Table 2, the elastic coefficient of temperature was −0.109, which indicated that the WYPA will decrease 0.109% for each 1% increase in GSAT. Higher temperature negatively affect winter wheat yield, both directly and indirectly. With the increase of temperature, wheat tends to overgrow due to excessive accumulated temperatures before the winter, which makes wheat seedlings weak and lack resistance to the cold [45]. Higher temperature will also shorten winter wheat growing season, leading to the decrease of 1000-grain weight and damaging the quality of grain [46]. In addition, the occurrence probability of extreme high temperature events in the later stage of winter wheat growing season will increase, which is not conducive to the formation of wheat yield. However, due to the large demand of winter wheat for water and the low precipitation in study area, GSP had a positive and significant impact on WYPA, with the elastic coefficient of 0.186, that is, each 1% increase in GSP will increase WYPA by 0.186%. However, in the terms of the whole study area, GSAT for winter wheat experienced a significant increase by 0.49°C per decade since 1980; yet, the GSP had a slight but inconspicuous increasing trend with the slope of 1.138 (Figure 2).

Figure 3 showed the model-simulated results of $F(C, A)$, $F(\mathrm{Cd}, A)$, and $F(C, \mathrm{AF})$ for each province (region), so as to measure the impacts of climatic factors and agricultural inputs on WYPA. From Figure 3, agricultural inputs and technological progress played an important role in the formation of wheat yield. If these variables have remained at the values of the 1980s, the WYPA would be stagnant (green arrows). We computed the differences of $F(C, A)$ and $F(C, \mathrm{AF})$ for each province (region) to quantify the impacts of agricultural inputs on wheat yield variability and found that Shandong province was most influenced by agricultural inputs, followed by Jing-Jin-Ji region and Henan province, with the WYPA increase rate of 60.438%, 59.279%, and 56.369%, respectively. The effects of agricultural inputs on WYPA for Shanxi and Shaanxi provinces were less, and the WYPA only increased by 28.448% for Shanxi province and by 27.193% for Shaanxi province. However, the effects of climate trend on wheat yield were relatively low, and the degree of the effects was different within the five provinces (region). The actual climate change in Jing-Jin-Ji region and Shandong province, that is relatively weak rise in temperature ($\text{Jing-Jin-Ji}_{\text{slope}} = 0.032$; $\text{Shandong}_{\text{slope}} = 0.034$) and large increase in precipitation ($\text{Jing-Jin-Ji}_{\text{slope}} = 1.775$;

Table 1: Unit root test and cointegration test.

	ln$Y$	ln$F$	ln$M$	ln$L$	ln$I$	ln$T$	ln$P$
LLC	−5.73***	−8.08***	−4.21***	−1.63* −11.28***	−0.30 −10.33***	−6.48***	−7.28***
ADF	48.25***	47.05***	18.24**	12.22 94.82***	7.23 86.39***	77.30***	79.58***
Cointegration Test							
ADF	−6.78[a]						

*, **, and *** represent that the null hypothesis of nonstationary is rejected at 10%, 5%, and 1% level, respectively. When there are two statistics in a cell, the top number is for the test on the original variable, and the bottom number is for the test on the variable after it has been differenced once. [a] represents that the null hypothesis of no cointegration is rejected at 1% level.

Table 2: Estimated parameters for fixed-effects model.

Variables	Coefficient	Prob.
C	6.192***	<0.001
ln$F$	0.094**	0.026
ln$M$	0.157***	0.004
ln$L$	−0.223**	0.016
ln$G$	0.265***	0.008
ln$T$	−0.109	0.327
ln$P$	0.186***	<0.001
Te	0.003	0.361
Fixed Effects (corss)		
Jing-jin-ji_C	−0.088	
Shanxi_C	0.110	
Shaanxi_C	0.048	
Shandong_C	−0.042	
Henan_C	−0.028	
Model Performance Evaluation		
Adj R^2	0.91	
F-statistic	167.70***	<0.001
NRMSE	8.14%	
IA	0.98	

** and *** represent the parameters are significant at the 5% and 1% levels, respectively.

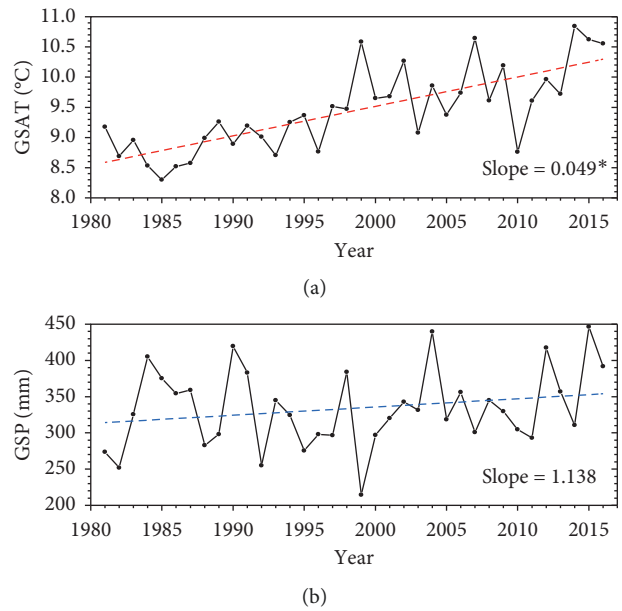

Figure 2: GSAT and GSP for winter wheat in 1981–2016. The red and blue dashed lines represent linear fitting of GSAT and GSP. *indicates that the slope is significant at the 1% level.

Shandong$_{slope}$ = 1.116), positively affected the wheat yield in the two regions during 1981–2016. The WYPA increased by 1.884% for Jing-Jin-Ji region and by 0.762% for Shandong province, relative to those without the climate trend. On the contrary, due to relatively rapid temperature rise and insignificant or negative precipitation change trend, wheat yield exhibited negative impacts for Shaanxi (GSAT$_{slope}$ = 0.04; GSP$_{slope}$ = −0.013), Shanxi (GSAT$_{slope}$ = 0.063; GSP$_{slope}$ = 0.92), and Henan (GSAT$_{slope}$ = 0.039; GSP$_{slope}$ = 0.071), with the loss of 0.917%, 1.316%, and 1.921%, respectively. If just from the aspect of quantitative values above, agricultural inputs were likely to be more important factors contributing to the formation of wheat yield. Nevertheless, one should note that agricultural inputs changes are mainly controlled by technological development level, and the impacts of agricultural inputs on crops can be stable in the premise that social and technological development are stable and the government pays more attention to the agricultural harvests, whereas climate change itself and its impacts on crops are both more complicated. Short-term extreme weather events such as flood, drought, and frost will directly exert deadly effects on crops and sharply decrease their yield, while the effects of long-term trend of climate change is gradual and potential. Long-term climate changes can greatly influence the cropping system, planting boundary, and planting structure and further influence the allocation and trade of national agricultural products. Therefore, the impacts of climatic factors on crops cannot be ignored, although apart from extreme climate events, it may be small in the short term.

3.3. Scenario Simulation Analysis of Climate Change. Figure 4 and Table 3 show the differences of GSAT and GSP projected for 2021–2050 relative to the baseline period of 1981–2005 for the medium emission scenario (RCP4.5) and high emission scenario (RCP8.5). The GSAT will increase by 1.33–1.44°C under RCP4.5 and by 1.43–1.68°C under RCP8.5 for the five provinces (region), relative to the baseline period. Shanxi province will experience the most warming. In terms of the whole study area, GSAT is projected to experience a rise of about 1.37°C for RCP4.5°C and 1.54°C for RCP8.5. The results also suggested that there will be an increasing trend in GSP for the majority of the regions under the two RCP scenarios, except for a slight decrease in western Shaanxi province. Shandong province will experience the most precipitation increasing. The precipitation increment

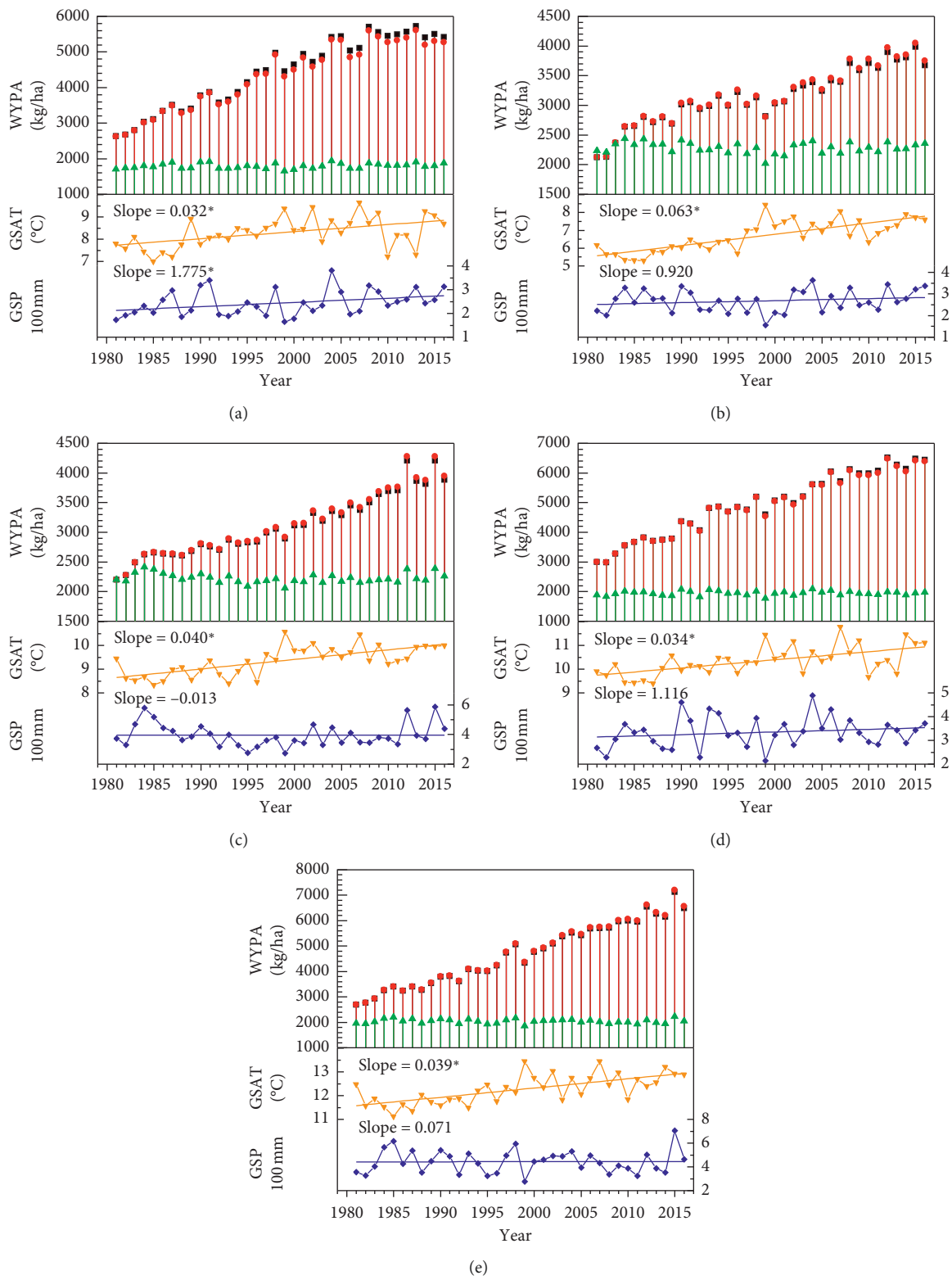

Figure 3: Model-predicted WYPA with observed climatic data and agricultural inputs (black squares) detrended climatic data and observed agricultural inputs (red dots) and observed climatic data and fixed agricultural inputs (green triangles). Yellow triangles (lines) and blue diamonds (lines) represent the (trends of) GSAT and GSP for winter wheat. * represents the trends are significant at 5% level. (a) Jing-jin-ji. (b) Shanxi. (c) Shaanxi. (d) Shandong. (e) Henan.

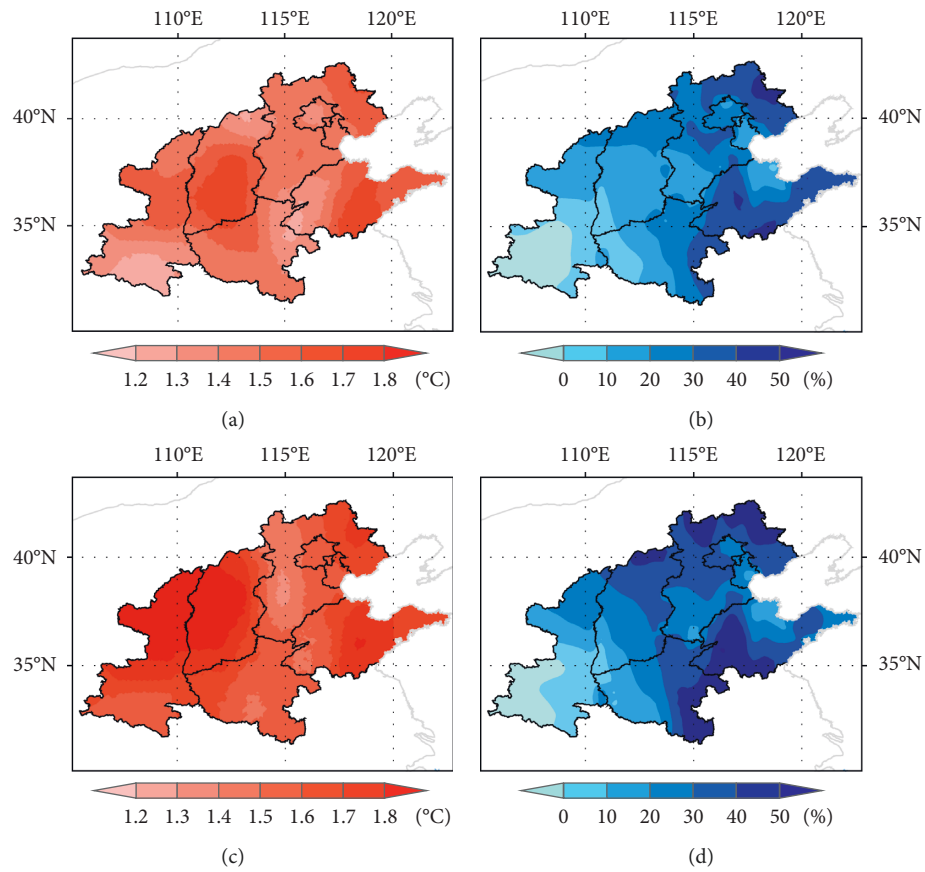

Figure 4: The differences of GSAT and GSP projected for 2021–2050 relative to 1981–2005 under RCP4.5 and RCP8.5. (a) GSAT under RCP 4.5. (b) GSP under RCP 4.5. (c) GSAT under RCP 8.5. (d) GSP under RCP 8.5.

Table 3: The differences of GSAT and GSP for each province (region) in 2021–2050 relative to that in 1981–2005 under RCP4.5 and RCP8.5.

	GSAT (°C)		GSP (%)	
	RCP4.5	RCP8.5	RCP4.5	RCP8.5
Jing-jin-ji	1.38	1.43	25.13	30.38
Shanxi	1.44	1.68	17.12	19.33
Shaanxi	1.33	1.63	2.72	4.53
Shandong	1.40	1.55	31.82	33.00
Henan	1.34	1.47	17.14	25.30
All	1.37	1.54	17.31	22.22

Table 4: Effects of climate change on WYPA for each province (region) in 2021–2050 under RCP4.5 and RCP8.5.

	Effects of GSAT (%)		Effects of GSP (%)		Comprehensive effect (%)	
	RCP4.5	RCP8.5	RCP4.5	RCP8.5	RCP4.5	RCP8.5
Jing-jin-ji	−1.46	−1.51	4.67	5.65	3.22	4.14
Shanxi	−2.71	−3.16	3.18	3.60	0.47	0.43
Shaanxi	−1.80	−2.21	0.51	0.84	−1.30	−1.37
Shandong	−1.79	−1.98	5.92	6.14	4.13	4.16
Henan	−1.56	−1.72	3.19	4.71	1.62	2.99
All	−1.75	−1.97	3.22	4.13	1.47	2.16

under high emissions scenario is much more than that under medium emissions scenario. The GSP increment for the five provinces (region) under RCP4.5 and RCP8.5 are 2.72–31.82% and 4.53–33.0%, respectively. In terms of the whole study area, precipitation is projected to increase by 17.31% for RCP4.5 and by 22.22% for RCP8.5.

Finally and for perspective, we used the estimates of climate change under RCP4.5 and RCP8.5 (Table 3) to obtain estimates of the effects of projected GSAT and GSP changes on WYPA variance in the five provinces (region) (Table 4). The change tendency of WYPA is opposite to GSAT but is consistent with GSP. For RCP4.5, temperature rising gives a decrease of 1.75% in average WYPA for the whole study area and a decrease of 1.46% (Jing-Jin-Ji region) to 2.71% (Shanxi province) for the selected five provinces (region). However, precipitation increasing is beneficial to the improvement of WYPA, with the increase of 3.22% for the whole study area and 0.51% (Shaanxi province) to 5.92% (Shandong province) for the five provinces (region). For RCP8.5, WYPA decreases by 1.97% for the whole study area and by 1.51% (Jing-jin-ji region) to 3.16% (Shanxi province) for the selected five provinces (region). Precipitation increasing gives a rise of 4.13% in WYPA for the whole study area, and 0.84% (Shaanxi province) to 6.14% (Shandong province) for the five provinces (region). In terms of the comprehensive effect of GSAT and GSP, the majority of study area experiences a WYPA increase, due to the substantial increase of GSP counteracting the negative effect of GSAT rising. However, the small increase in Shaanxi's GSP is not enough to offset

the negative effects driven by the large increase in GSAT, which causes Shaanxi to be the only province whose WYPA suffering from the projected changes of GSAT and GSP. For RCP4.5, WYPA increases by 1.47% for the whole study area and by 0.47–4.13% for Shanxi, Henan, Jing-Jin-Ji, and Shandong provinces, but decreases by 1.3% for Shaanxi province. For RCP8.5, WYPA increases by 2.16% for the whole region and by 0.43–4.16% for Shanxi, Henan, Jing-Jin-Ji, and Shandong provinces, while Shaanxi province experiences a wheat yield decrease of 1.37%.

4. Discussion

4.1. Climate Model Uncertainty. Climate models are one of the most important tools to simulate and forecast future climate change, but there exists uncertainty about the results simulated by different climate models, which represents a key challenge for adaptation planning. For example, Ding et al. [47] simulated the climate change of China by the 40 models and suggested that there is a potential significant warming in China in the twenty-first century under different emission scenarios. However, large uncertainty exists in the projection of precipitation, and further studies are needed. Xu and Xu [48] assessed the performance in simulating the climate over China based on the CMIP3 and CMIP5 experiments and found that models appeared to have a good performance on reproducing the warming tendency but showing limited skills for precipitation, and most models overestimate precipitation. Uncertainty in future climate change derives from various sources such as emission scenarios, model structure, downscaling/bias-correction methods, and impact models [49].

In this study, we dealt with the uncertainty of the model from the following three aspects. Firstly, in emissions scenarios, we selected RCP4.5 as the lower one because it is possibly most consistent with the future economic development of China and meets the mitigation plan for responding to climate change [33]. The upper bound of four RCPs, RCP8.5, was used as the contrast scenario. Secondly, the climate simulation datasets used in this study were obtained from the ISI-MIP, which have been bias-corrected in the fast-track of ISI-MIP using the trend-preserving method and can reproduce the observed climate very well [35]. Several studies have demonstrated the value of using the same projections by the 5 GCMs in climate change impact assessments for different sectors at the global and regional scales [50–54]. Thirdly, we used the MME to reduce the uncertainty because combining models can generally increase the skill, reliability, and consistency of model forecasts [55]. The combined information of an equally weighted average of several models (the method used in this study) is usually found to agree better with observations than any single model [56]. These solutions can effectively reduce the uncertainty of the models and improve the accuracy of our analysis.

4.2. Food Security and Adaptation Strategies. China is a large producer and consumer of food. China's domestic demand for food maintained a self-sufficiency rate of 95%, while the other 5% depended on the international market for balance, since joining the WTO in 1980 [57]. However, with the growing population and rising consumption levels, China needs more food to feed itself. According to the forecast of the DRC (Development Research Center of the State Council), total domestic grain demand will reach 584.87–592.02 million tons, and the gap between food supply and demand will be up to 40–50 million tons [58]. The problem of food shortage has become more and more serious in recent years, and the reasons for food shortage are various factors, among which included are the increase of population, the decrease of cultivated land area, and the degradation of cultivated land quality. In addition, climate change has altered the agro-meteorological conditions and posed a certain impact on crops growth. As shown in the results of this paper, the contribution of temperature rising to winter wheat yield in Northern China was negative since 1981, and the degree of influence will increase with the temperature rising further, while precipitation had a positive impact.

It is suggested that China could take the following two aspects to ensure the supply of domestic wheat, i.e., domestic wheat production and international wheat trade. From the aspect of domestic wheat production, climate change has been a concern of policy-makers, scientists, and farmers due to its far-reaching impacts on agriculture, and appropriate adaptation strategies should be taken immediately. Because Northern China is the principal wheat production base, the climate adaptation measures proposed in the following are based on the climate change of this region. Firstly, one of the most realistic and convenient measures for the local farmers is adjusting the sowing dates of winter wheat. Studies found that the suitable sowing dates of winter wheat in the region have been delayed in the last few decades and are projected to be further delayed in the future due to the temperature rising [59, 60]. The properly delayed sowing dates could result in significant differences in environmental conditions during crop grain filling and usually help the grains grow with increasing temperatures, which will minimize the decreasing rate of wheat yield under global warming [61, 62]. It is noticeable, however, that the freeze injury before winter wheat overwintering must be considered in this region, so the sowing dates cannot be delayed too late. Secondly, the strategy that copes with the challenges of climate change is to plant new grains which have higher heat requirement and longer duration of reproductive growth period. Better adaption to warmer climatic conditions makes these new grains more favorable than old ones under climate change and significantly increases wheat yield [63, 64]. Thirdly, converting the tillage system from conventional plow tillage to rotary tillage is beneficial to improve the efficiency of local agriculture production and enhance crop yield. The conventional plow tillage is time-consuming and energy-intensive, and farmers prefer to burn crop residues in order to save time for seeding the next crop, which has some adverse impacts on soil and hinders crops growth. However, rotary tillage can chop crop residue and mix it into the soil, which will increase retention of rainfall in the soil and enhance SOC sequestration. This can enhance the ability of wheat to cope with climate change during its growing period

[65]. Fourthly, it is necessary to expand irrigation infrastructure for Northern China. Although this study found that the precipitation likely increases during wheat growing season over the region, winter wheat is generally cultivated under irrigation conditions due to the small amount and large fluctuation of precipitation [66]. Optimizing irrigation facilities can ensure the water supply for wheat during the critical growth period, which is beneficial to improve its ability to cope with adverse climatic conditions and reduce the losses of wheat yield. In addition, there are many other options of agricultural adaptation to climate change for the region, such as developing crop diversity, improving fertilization, and natural resource management. Finally, we should be aware that the negative impacts of climate change could be moderated by implementing these adaptations duly and steadily rather than missing the appropriate timing to implement adaptations.

In terms of international wheat trade, China should make full use of the grain production resources in other countries and regions and expand the sources of domestic food supply through food trade and cooperation, so as to keep the balance between food supply and demand and guarantee the quantity of the grain stored. However, China's import market of wheat in international trade mainly focuses in the United States, Canada, and Australia. For instance, China imported 99% of its wheat from the three countries in 2011, which will raise the potential risk for China's wheat import market in the future. China should try to reduce the risk of wheat imports by analyzing the potential of wheat yield increase and export in various countries and seeking more stable sources for wheat importing. For example, from climate perspective, the United States, the largest wheat exporter to China, is projected to experience a wheat yield decrease in the future while Canada is inversed [15, 67–70]. This indicates that China's wheat import market center in North America may slowly shift from the United States to Canada. Moreover, as emerging export countries in the international wheat trade market, Russia, Ukraine, and Kazakhstan have witnessed a rapid increasing in the proportion of wheat export and a growing market influence [71]. Climate change has effectively increased their grain production potential because of the location in mid- and high-latitudes [72, 73]. The food self-sufficiency rate of the three countries has been stable at more than 100%, and the export potential is also increasing (FAOSTAT food balance sheet). Therefore, China can increase its wheat import from these countries to ensure the domestic food security in the future.

5. Conclusion

The relative contribution of climatic factors to wheat yield was about 0.762–1.921% in absolute terms for the period 1981–2016, which was smaller than the contribution of agricultural inputs and technological progress that ranged from 27.193 to 60.438%. Warming trends during winter wheat growing season had a negative effect on WYPA, whereas the increasing trend of precipitation had a positive effect in 1981–2016, and the elastic coefficients were −0.109 and 0.186, respectively. This indicated that a 1% rise in GSAT tends to lower yield of 0.109%, and a 1% increase in GSP increases yield of 0.186%, up to a point at which further rainfall becomes harmful. The GSAT and GSP are both projected to increase in the study area for the period of 2021–2050, the increment of which for high emission scenario (RCP8.5) is more than that for medium emission scenario (RCP4.5). GSAT is projected to rise 1.37°C under RCP4.5 scenario and 1.54°C under RCP8.5 scenario for the whole study area, which will lower the average WYPA by 1.75% and 1.97%, respectively. GSP is tended to increase by 17.31% under RCP4.5 scenario and 22.22% under RCP8.5 scenario for the whole region, which will give a rise of 3.22% and 4.13% in WYPA, respectively. In terms of the comprehensive effect of GSAT and GSP, average WYPA will increase by 1.47% under RCP4.5 scenario and 2.16% under RCP8.5 scenario for the whole study area. At provincial scale, the changes of climatic factors will have a positive effect on WYPA for Jing-Jin-Ji region, Shanxi, Shandong, and Henan provinces, while they will have a negative effect for Shaanxi province.

Data Availability

The meteorological observation data were taken from http://data.cma.cn/data/cdcindex/cid/6d1b5efbdcbf9a58.html. The climate scenario data were downloaded from https://esg.pik-potsdam.de/search/isimip-ft/. The agricultural data were provided by http://data.stats.gov.cn/. The other data used to support the findings of this study are available from the corresponding author upon request.

Conflicts of Interest

The authors declare that there are no conflicts of interest regarding the publication of this paper.

Acknowledgments

This research was supported by the grants (to IGSNRR) from the Ministry of Science and Technology of the People's Republic of China (2016YFA0602704) and the National Natural Science Foundation of China (41831174 and 41671201).

References

[1] IPCC, *Climate Change 2013: the Physical Scientific Basis. Contribution of Working Group* I *to the Fifth Assessment Report of the Intergovernmental Panel on Climate Change*, Cambridge University Press, Cambridge, UK, 2013.

[2] R. P. Motha and W. Baier, "Impacts of present and future climate change and climate variability on agriculture in the temperate regions: North America," *Climatic Change*, vol. 70, no. 1-2, pp. 137–164, 2005.

[3] M. J. Salinger, "Climate variability and change: past, present and future: an overview," *Climatic Change*, vol. 70, no. 1-2, pp. 9–29, 2005.

[4] K. Boomiraj, S. P. Wani, K. K. Garg, P. K. Aggarwal, and K. Palanisamp, "Climate change adaptation strategies for agro-ecosystem—a review," *Journal of Agrometeorology*, vol. 12, no. 2, pp. 145–160, 2010.

[5] C. Rosenzweig, J. Elliott, D. Deryng et al., "Assessing agricultural risks of climate change in the 21st century in a global gridded crop model intercomparison," *Proceedings of the National Academy of Sciences*, vol. 111, no. 9, pp. 3268–3273, 2014.

[6] R. Mendelsohn, W. Morrison, M. E. Schlesinger, and N. G. Andronova, "Country-specific market impacts of climate change," *Climatic Change*, vol. 45, no. 3-4, pp. 553–569, 2000.

[7] C. Baker-Austin, J. A. Trinanes, N. G. H. Taylor, R. Hartnell, A. Siitonen, and J. Martinez-Urtaza, "Emerging vibrio risk at high latitudes in response to ocean warming," *Nature Climate Change*, vol. 3, no. 1, pp. 73–77, 2013.

[8] C. Rosenzweig and D. Hillel, *Climate Change and the Global Harvest: Potential Impacts on the Greenhouse Effect on Agriculture*, Oxford University Press, New York, NY, USA, 1998.

[9] J. Wilcox and D. Makowski, "A meta-analysis of the predicted effects of climate change on wheat yields using simulation studies," *Field Crops Research*, vol. 156, no. 2, pp. 180–190, 2014.

[10] P. Kurukulasuriya and S. Rosenthal, *Climate Change and Agriculture: A Review of Impacts and Adaptations*, World Bank, Washington, DC, USA, 2003.

[11] G. Fischer, M. Shah, F. N. Tubiello, and H. van Velhuizen, "Socio-economic and climate change impacts on agriculture: an integrated assessment, 1990–2080," *Philosophical Transactions of the Royal Society B: Biological Sciences*, vol. 360, no. 1463, pp. 2067–2083, 2005.

[12] B. Smit and O. Pilifosova, "Adaptation to climate change in the context of sustainable development and equity," in *Climate Change 2001: Impacts, Adaptations and Vulnerability. The Third Assessment Report of the Intergovernmental Panel on Climate Change*, J. McCarthy, O. Canziana, N. Leary, D. Dokken, and K. White, Eds., pp. 879–967, Cambridge University Press, Cambridge, UK, 2001.

[13] D. S. G. Thomas and C. Twyman, "Equity and justice in climate change adaptation amongst natural-resource-dependent societies," *Global Environmental Change*, vol. 15, no. 2, pp. 115–124, 2005.

[14] National Bureau of Statistics of China, *China Statistical Year Book 2009*, China Statistics Press, Beijing, China, 2009, in Chinese.

[15] C. Zhao, B. Liu, S. Piao et al., "Temperature increase reduces global yields of major crops in four independent estimates," *Proceedings of the National Academy of Sciences*, vol. 114, no. 35, pp. 9326–9331, 2017.

[16] J. X. Song, "A review of research methods of the effect of climate change on agriculture," *Science and Technology for Development*, vol. 12, no. 6, pp. 765–776, 2016.

[17] W. Shi, F. Tao, and Z. Zhang, "A review on statistical models for identifying climate contributions to crop yields," *Journal of Geographical Sciences*, vol. 23, no. 3, pp. 567–576, 2013.

[18] H. Gitay, W. Easterling, and B. Jallow, "Ecosystems and their goods and services," in *Climate Change 2001: Impacts, Adaptation, and Vulnerability. The Third Assessment Report of the Intergovernmental Panel on Climate Change*, J. McCarthy, O. Canziana, N. Leary, D. Dokken, and K. White, Eds., pp. 235–342, Cambridge University Press, Cambridge, UK, 2001.

[19] D. B. Lobell and C. B. Field, "Global scale climate–crop yield relationships and the impacts of recent warming," *Environmental Research Letters*, vol. 2, no. 1, article 014002, 2007.

[20] W. Schlenker and D. B. Lobell, "Robust negative impacts of climate change on African agriculture," *Environmental Research Letters*, vol. 5, no. 1, article 014010, 2010.

[21] F. Tao and Z. Zhang, "Adaptation of maize production to climate change in North China Plain: quantify the relative contributions of adaptation options," *European Journal of Agronomy*, vol. 33, no. 2, pp. 103–116, 2010.

[22] S. Asseng, F. Ewert, P. Martre et al., "Rising temperatures reduce global wheat production," *Nature Climate Change*, vol. 5, no. 2, pp. 37–64, 2014.

[23] D. B. Lobell and M. B. Burke, "On the use of statistical models to predict crop yield responses to climate change," *Agricultural and Forest Meteorology*, vol. 150, no. 11, pp. 1443–1452, 2010.

[24] C.-C. Chen, B. A. McCarl, and D. E. Schimmelpfennig, "Yield variability as influenced by climate: a statistical investigation," *Climatic Change*, vol. 66, no. 1-2, pp. 239–261, 2004.

[25] S. Barrios, B. Ouattara, and E. Strobl, "The impact of climatic change on agricultural production: is it different for Africa?," *Food Policy*, vol. 33, no. 4, pp. 287–298, 2008.

[26] M. Dell, B. F. Jones, and B. A. Olken, "What do we learn from the weather? The new climate-economy literature," *Journal of Economic Literature*, vol. 52, no. 3, pp. 740–798, 2014.

[27] E. Blanc and W. Schlenker, "The use of panel models in assessments of climate impacts on agriculture," *Review of Environmental Economics and Policy*, vol. 11, no. 2, pp. 258–279, 2017.

[28] J. Chou, W. Dong, and D. Ye, "Construction of a novel economy-climate model," *Chinese Science Bulletin*, vol. 51, no. 14, pp. 1735-1736, 2006.

[29] J. Chou, W. Dong, and G. Feng, "The methodology of quantitative assess economic output of climate change," *Chinese Science Bulletin*, vol. 56, no. 13, pp. 1333–1335, 2011.

[30] G. C. Zhao, "Study on Chinese wheat planting regionalization," *Journal of Triticeae Crops*, vol. 30, no. 5, pp. 886–895, 2010.

[31] S. B. Jin, *Wheat Science in China*, China Agriculture Press, Beijing, China, 1996, in Chinese.

[32] D. P. van Vuuren, J. Edmonds, M. Kainuma et al., "The representative concentration pathways: an overview," *Climatic Change*, vol. 109, no. 1-2, pp. 5–31, 2011.

[33] C. Gao, Z. T. Zhang, S. Chen, and Q. Liu, "The high-resolution simulation of climate change model under RCP4.5 scenarios in the Huaihe River Basin," *Geographical Research*, vol. 33, no. 3, pp. 467–477, 2014.

[34] K. Riahi, S. Rao, V. Krey et al., "RCP 8.5—a scenario of comparatively high greenhouse gas emissions," *Climatic Change*, vol. 109, no. 1-2, pp. 33–57, 2011.

[35] S. Hempel, K. Frieler, L. Warszawski, J. Schewe, and F. Piontek, "A trend-preserving bias correction – the ISI-MIP approach," *Earth System Dynamics*, vol. 4, no. 2, pp. 219–236, 2013.

[36] National Bureau of Statistics of China, *China Compendium of Statistics 1949–2008*, China Statistical Press, Beijing, China, 2010, in Chinese.

[37] C. Hsiao, *The Analysis of Panel Data*, Cambridge University Press, Cambridge, UK, 2003.

[38] A. Levin, C.-F. Lin, and C.-S. J. Chu, "Unit root tests in panel data: asymptotic and finite-sample properties," *Journal of Econometrics*, vol. 108, no. 1, pp. 1–24, 2002.

[39] G. S. Maddala and S. Wu, "A comparative study of unit root tests with panel data and a new simple test," *Oxford Bulletin of Economics and Statistics*, vol. 61, no. s1, pp. 631–652, 1999.

[40] G. Q. Zhao, *Econometrics*, China Renmin University Press, Beijing, China, 2012, in Chinese.

[41] K.-C. Li, "Asymptotic optimality for C_p, C_L, cross-validation and generalized cross-validation: discrete index set," *The Annals of Statistics*, vol. 15, no. 3, pp. 958–975, 1987.

[42] C. J. Willmott, "Some comments on the evaluation of model performance," *Bulletin of the American Meteorological Society*, vol. 63, no. 11, pp. 1309–1313, 1982.

[43] J. M. Yang, J. Y. Yang, S. Dou, X. M. Yang, and G. Hoogenboom, "Simulating the effect of long-term fertilization on maize yield and soil C/N dynamics in Northeastern China using DSSAT and CENTURY-based soil model," *Nutrient Cycling in Agroecosystems*, vol. 95, no. 3, pp. 287–303, 2013.

[44] J. Moncrieff, R. Clement, J. Finnigan, and T. Meyers, "Averaging, detrending, and filtering of eddy covariance time series," in *Handbook of Micrometeorology*, X. Lee, W. Massman, and B. Law, Eds., vol. 29, pp. 7–31, Atmospheric and Oceanographic Sciences Library, Springer, Dordrecht, Netherlands, 2004.

[45] Z. Sun, S. F. Jia, A. F. Lv, K. J. Yang, J. Svensson, and Y. C. Gao, "Impacts of climate change on growth period and planting boundaries of winter wheat in China under RCP4.5 scenario," *Earth System Dynamics Discussions*, vol. 6, no. 2, pp. 2181–2210, 2015.

[46] S. Thaler, J. Eitzinger, M. Trnka, and M. Dubrovsky, "Impacts of climate change and alternative adaptation options on winter wheat yield and water productivity in a dry climate in Central Europe," *Journal of Agricultural Science*, vol. 150, no. 5, pp. 537–555, 2012.

[47] Y. Ding, G. Ren, Z. Zhao et al., "Detection, causes and projection of climate change over China: an overview of recent progress," *Advances in Atmospheric Sciences*, vol. 24, no. 6, pp. 954–971, 2007.

[48] Y. Xu and C. H. Xu, "Preliminary assessment of simulations of climate changes over China by CMIP5 multi-models," *Atmospheric and Oceanic Science Letters*, vol. 5, no. 6, pp. 489–494, 2012.

[49] G. Leng, Q. Tang, and S. Rayburg, "Climate change impacts on meteorological, agricultural and hydrological droughts in China," *Global and Planetary Change*, vol. 126, pp. 23–34, 2015.

[50] F. Piontek, C. Müller, T. A. M. Pugh et al., "Multisectoral climate impact hotspots in a warming world," *Proceedings of the National Academy of Sciences*, vol. 111, no. 9, pp. 3233–3238, 2014.

[51] J. Elliott, D. Deryng, C. Müller et al., "Constraints and potentials of future irrigation water availability on agricultural production under climate change," *Proceedings of the National Academy of Sciences*, vol. 111, no. 9, pp. 3239–3244, 2014.

[52] Y. Yin, D. Ma, S. Wu, and T. Pan, "Projections of aridity and its regional variability over China in the mid-21st century," *International Journal of Climatology*, vol. 35, no. 14, pp. 4387–4398, 2015.

[53] K. Frieler, S. Lange, F. Piontek et al., "Assessing the impacts of 1.5°C global warming—simulation protocol of the inter-sectoral impact model intercomparison project (ISI-MIP2b)," *Geoscientific Model Development*, vol. 10, no. 12, pp. 4321–4345, 2017.

[54] X. Ma, C. Zhao, H. Tao, J. Zhu, and Z. W. Kundzewicz, "Projections of actual evapotranspiration under the 1.5°C and 2.0°C global warming scenarios in sandy areas in Northern China," *Science of the Total Environment*, vol. 645, no. 15, pp. 1496–1508, 2018.

[55] C. Tebaldi and R. Knutti, "The use of the multi-model ensemble in probabilistic climate projections," *Philosophical Transactions of the Royal Society A: Mathematical, Physical and Engineering Sciences*, vol. 365, no. 1857, pp. 2053–2075, 2007.

[56] S. J. Lambert and G. J. Boer, "CMIP1 evaluation and intercomparison of coupled climate models," *Climate Dynamics*, vol. 17, no. 2-3, pp. 83–106, 2001.

[57] X. N. Ren, *The Impacts of Climate Change on China's Grain Production and Trade*, Chinese Academy of Agricultural Sciences, Beijing, China, 2012, in Chinese.

[58] Development Research Center of the State Council, *Research on Modernization of Agriculture with Chinese Characteristics*, China Development Press, Beijing, China, 2012, in Chinese.

[59] D. Xiao, F. Tao, Y. Liu et al., "Observed changes in winter wheat phenology in the North China Plain for 1981–2009," *International Journal of Biometeorology*, vol. 57, no. 2, pp. 275–285, 2013.

[60] Z. Hao, X. Geng, F. Wang, and J. Zheng, "Impacts of climate change on agrometeorological indices at winter wheat overwintering stage in Northern China during 2021–2050," *International Journal of Climatology*, vol. 38, no. 15, pp. 5576–5588, 2018.

[61] K. D. Subedi, B. L. Ma, and A. G. Xue, "Planting date and nitrogen effects on grain yield and protein content of spring wheat," *Crop Science*, vol. 47, no. 1, pp. 36–44, 2007.

[62] D. Y. Ding, H. Feng, Y. Zhao, J. Q. He, Y. F. Zou, and J. M. Jin, "Modifying winter wheat sowing date as an adaptation to climate change on the loess plateau," *Agronomy Journal*, vol. 108, no. 1, pp. 53–63, 2016.

[63] F. Tao, S. Zhang, and Z. Zhang, "Spatiotemporal changes of wheat phenology in China under the effects of temperature, day length and cultivar thermal characteristics," *European Journal of Agronomy*, vol. 43, pp. 201–212, 2012.

[64] X. Zhang, S. Wang, H. Sun, S. Chen, L. Shao, and X. Liu, "Contribution of cultivar, fertilizer and weather to yield variation of winter wheat over three decades: a case study in the North China Plain," *European Journal of Agronomy*, vol. 50, pp. 52–59, 2013.

[65] H.-L. Zhang, X. Zhao, X.-G. Yin et al., "Challenges and adaptations of farming to climate change in the North China Plain," *Climatic Change*, vol. 129, no. 1-2, pp. 213–224, 2015.

[66] J. Li, S. Inanaga, Z. Li, and A. E. Eneji, "Optimizing irrigation scheduling for winter wheat in the North China Plain," *Agricultural Water Management*, vol. 76, no. 1, pp. 8–23, 2005.

[67] J. Tack, A. Barkley, and L. L. Nalley, "Effect of warming temperatures on US wheat yields," *Proceedings of the National Academy of Sciences*, vol. 112, no. 22, pp. 6931–6936, 2015.

[68] B. Liu, S. Asseng, C. Müller et al., "Similar estimates of temperature impacts on global wheat yield by three independent methods," *Nature Climate Change*, vol. 6, no. 12, pp. 1130–1136, 2016.

[69] B. Qian, H. Wang, Y. He, J. Liu, and R. De Jong, "Projecting spring wheat yield changes on the Canadian Prairies: effects of resolutions of a regional climate model and statistical processing," *International Journal of Climatology*, vol. 36, no. 10, pp. 3492–3506, 2016.

[70] B. D. Qian, R. D. Jong, T. Huffman, H. Wang, and J. Y. Yang, "Projecting yield changes of spring wheat under future climate scenarios on the Canadian Prairies," *Theoretical and Applied Climatology*, vol. 123, no. 3-4, pp. 651–669, 2016.

[71] I. Fehér and A. F. Fieldsend, *The Potential for Expanding Wheat Production in Kazakhstan. Analysis from a Food*

Security Perspective, Publications Office of the European Union, Luxembourg, Europe, 2019.

[72] P. Mitra, M. Selowsky, and J. Zalduendo, *Turmoil at Twenty: Recession, Recovery, and Reform in Central and Eastern Europe and the Former Soviet Union*, World Bank, Washington, DC, USA, 2009.

[73] W. Liefert, O. Liefert, G. Vocke, and E. Allen, "Former Soviet Union region to play larger role in meeting world wheat needs," *Amber Waves*, vol. 8, no. 2, pp. 12–19, 2010.

Hindawi
Advances in Meteorology
Volume 2019, Article ID 7341465, 19 pages
https://doi.org/10.1155/2019/7341465

Research Article

Climate Variability and Farmers' Perception in Southern Ethiopia

Befikadu Esayas,[1] **Belay Simane**,[1] **Ermias Teferi**,[1] **Victor Ongoma**,[2] **and Nigussie Tefera**[3]

[1]*Center for Environment and Development Studies, Addis Ababa University, P.O. Box 1176, Addis Ababa, Ethiopia*
[2]*School of Geography, Earth Science and Environment, The University of the South Pacific, Laucala Campus, Private Bag, Suva, Fiji*
[3]*The United Nations, World Food Programme (WFP), Addis Ababa, Ethiopia*

Correspondence should be addressed to Befikadu Esayas; befikadu.esayas@aau.edu.et

Received 1 February 2019; Accepted 11 April 2019; Published 2 June 2019

Academic Editor: Gabriele Buttafuoco

The study aims to analyze climate variability and farmers' perception in Southern Ethiopia. Gridded annual temperature and precipitation data were obtained from the National Meteorological Agency (NMA) of Ethiopia for the period between 1983 and 2014. Using a multistage sampling technique, 403 farm households were surveyed to substantiate farmers' perceptions about climate variability and change. The study applied a nonparametric Sen's slope estimator and Mann–Kendall's trend tests to detect the magnitude and statistical significance of climate variability and binary logit regression model to find factors influencing farm households' perceptions about climate variability over three agroecological zones (AEZs). The trend analysis reveals that positive trends were observed in the annual maximum temperature, 0.02°C/year ($p < 0.01$) in the lowland and 0.04°C/year ($p < 0.01$) in the highland AEZs. The positive trend in annual minimum temperature was consistent in all AEZs and significant ($p < 0.01$). An upward trend in the annual total rainfall (10 mm/year) ($p < 0.05$) was recorded in the midland AEZ. Over 60% of farmers have perceived increasing temperature and decreasing rainfall in all AEZs. However, farmers' perception about rainfall in the midland AEZ contradicts with meteorological analysis. Results from the binary logit model inform that farmers' climate change perceptions are significantly influenced by their access to climate and market information, agroecology, education, agricultural input, and village market distance. Based on these results, it is recommended to enhance farm households' capacity by providing timely weather and climate information along with institutional actions such as agricultural extension services.

1. Introduction

The global average temperature has increased by 0.78°C between 1850 and 2012. Intergovernmental Panel on Climate Change (IPCC) [1] noted the projected increase will range from 1.5°C to 2°C towards the end of the 21st century. Many scholars have produced evidence of global climate change and their projections show that the rate of change will likely increase [2–4]. The case in Africa will be more pronounced than the global average, suggesting warming in all seasons [1]. Most regional studies use long-term changes in rainfall and temperature patterns as a proxy indicator of climate change.

East Africa region is not an exception. Studies have reported high variability in rainfall and the associated adverse effects of rainfall changes in East Africa [5–7]. The impact is primarily associated with higher instability in the interannual rainfall primarily affecting rainfall fed livelihood groups [8].

Various studies have investigated historical trends of climate change and variability in Ethiopia. For instance, a 0.2°C to 0.28°C rise per decade in the average annual maximum temperature between 1960 and 2006 was reported in recent studies [4, 9], whereas, 0.37°C/decade increase was observed in the minimum temperature between 1951 and 2006 [10]. A projection suggests that

Ethiopia will experience a 1.7°C–2.1°C increase in the mean temperature by 2050 [11].

As [12] pointed out, special attention should be paid to assessing farmers' climate change perception as it requires continued data collection from different contexts and dissemination of new knowledge due to the complex and dynamic nature of climate change [13]. Moreover, Broomer et al. [14] noted that perceived personal experiences can affect climate change belief and the corresponding adaptation and mitigation measures to be taken.

Some attempts have been made on the climate trend analysis in Ethiopia, reporting mixed findings. For example, an insignificant trend was reported on the annual rainfall amount in the Nile basin [15–21]. Similarly, a nonsignificant trend in annual and seasonal rainfall was reported in Southwestern Ethiopia [22] and North Ethiopia [23]. Other studies show positive trends in air temperature and negative trends in rainfall [24–27]. Other studies [28–30] observed both increasing and decreasing trends in the climate parameters, including extreme climate in the study area. However, none of the previous studies have linked their climate trend analysis with farmers' perceptions and its influencing factors.

The existing evidence for farmers' perception of climate change suggests that studies are of three types. The first group includes [31–34] that used Heckman probit selection model to study factors affecting farmers' perception of climate change and their adaptation strategies. The second group comprises of [35–37], which applied binary logit/probit and multinomial logit models focusing on factors influencing only adaptation strategies. Finally, [38, 39] used binary logit/probit/recursive bivariate probit model to examine factors impeding households' perception of climate change and their link with meteorological data.

The mentioned studies tried to document the trends in rainfall and temperature data at national, regional, and local levels. They reported complex patterns in the climate parameters. However, most of the studies emphasized on mean climate trend analysis using either station-based or downscaled data. Accessing the latter is difficult in the situation like the study Agroecological Zones (AEZs). Other studies focused on climate change perception with an emphasis on either factors affecting climate change perception and adaptation or both based on household surveys, mainly geographically confined to the Nile basin and Northern Ethiopia, with few others conducted in other parts of Ethiopia.

Even recent studies in Wolaita and its surroundings by other researchers [28, 29, 40] assessed only trends in extreme and mean climate and adaptation strategies to climate change, respectively. Others have examined the link between farmers' perception of climate change and trends of change in the meteorological data using station-based data and household surveys at national and subnational levels, which may not fully explain the situation at the local level. Cross-sectional data from farm households located at different AEZs have also been used for exploring factors affecting farmers' perception of climate change and linking recently promoted gridded time series data for analyzing trends in the climate parameters. There is a paucity of studies that use gridded data set *s* to analyze climate trends relating to the household perception of climate change in Ethiopia.

This study puts emphasis on disaggregation by AEZs because of the increasing role of agroecology. This explains why agroecological-based approach is rapidly advancing as a sustainable farming approach, social movement, and scientific discipline [41]. Understanding the relation between national and Local level climate parameters as and farmers' views is crucial for drafting development plans and programs, early warning systems, and integrated adaptation strategies that fit the local reality. This study contributes to the rapidly advancing climate change and farmers' perception literature by providing empirical evidence of the climate trend analysis and factors affecting perceptions and their correlation with the trend results over AEZs in Southern Ethiopia.

In summary, the purpose of this study is to give a better understanding of recent changes and variability in the rainfall and temperature data and factors affecting farm households' perception of climate variability and change over three AEZs in Wolaita Zone, Southern Ethiopia. This paper is organized into four sections. Section 2 gives a brief account of the data and methodology. Section 3 presents and discusses the study results. Conclusions and recommendations are provided in Section 4.

2. Study Area, Sample Size, and Procedure and Methodology

2.1. Study Area. Wolaita Zone is located in Southern Nations and Nationalities People (SNNP) region. It lies between 6.4°–7.1°N and 37.4°–38.2°E (Figure 1). It is subdivided into three traditional AEZs: 56% of the area is a Midland (*Woyna-Dega*); 35% of the area is Lowland (*Kola*); and the rest 9% of the area is covered by Highland (*Dega*) [42]. The area generally has a highland relief that covers most parts of the midland while the peripheries are lowland areas (Figure 1). The altitude ranges from 501 meters in the lowlands at Bilate Tena to 3000 meters above sea level in the highlands of Damota mountain. The lowest average annual rainfall was recorded as 800 mm in Bilate Tena and the highest was 1200 mm in Wolaita Sodo. Rainfall is unpredictable by nature and variable, occurring in two different seasons. The pattern of rainfall distribution is bimodal. The main rainy season (*Kirmet*) begins in mid-June and extends to the end of September, whereas the *Belg* season/short rains extents from end of February to early April [42]. The average annual minimum temperature was observed to range between 15.1°C and 25.1°C in 2015/2016. However, temperature is usually high with minimal seasonal variability. The average maximum temperature was between 17.1°C and 29.7°C. In terms of livelihood activities, the area is characterized by a mixed farming involving the production of cereals, root crops, *Enset*, and coffee. Crop production is the main means of livelihood while livestock serves as a source of food, cash income, and insurance against uncertainty [42]. After [43], this study adopted the traditional AEZ grouping approach to

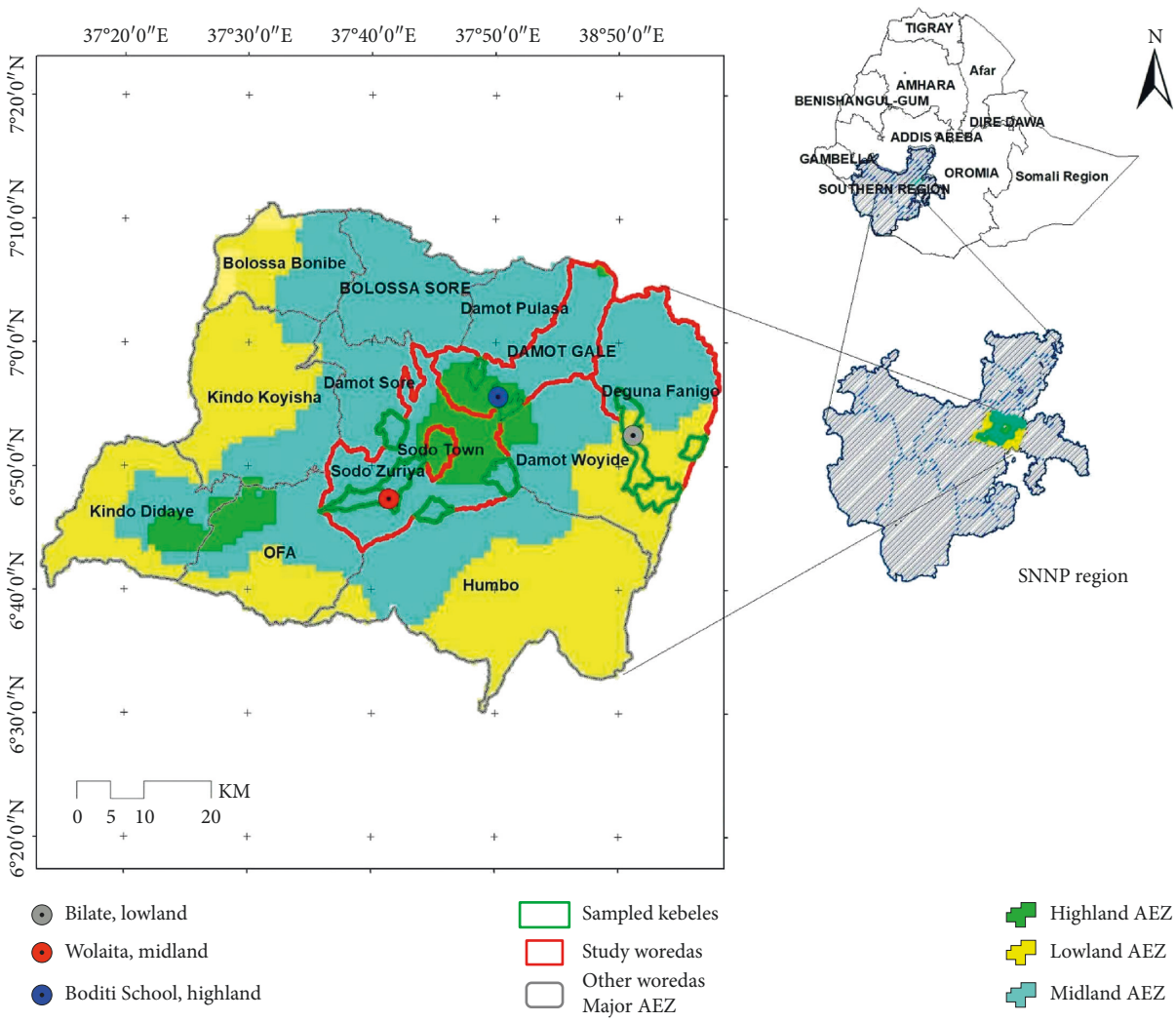

Figure 1: Location of the study agroecological zones.

compare and represent highland, midland, and lowland AEZ, respectively (Figure 1).

2.2. Sample Size and Procedure. Following Esayas et al. [30], this study is based on a gridded daily (4 km by 4 km spatial resolution) temperature and rainfall data running from 1983 to 2014. The data are a combination of two data sets. First, station data were used sourced from the National Meteorological Agency (NMA) of Ethiopia. Second, the satellite rainfall and temperature approximations obtained from the European Organization for the Exploitation of Meteorological Satellites (EUMETSAT) and the US National Aeronautics and Space Administration (NASA) were used. Data reconstruction was conducted by NMA in corporation with the International Research Institute for Climate and Society at Columbia University, USA. In other words, the gridded data set integrated quality-controlled station data from the national observation network with locally calibrated satellite-derived data that were used to fill spatial and temporal gaps in the Ethiopian national observations. Data reconstruction was undertaken by the NMA in partnership with International Research Institute for Climate and Society at Columbia University, USA, whereas data calibration and validation were carried out by Reading University, UK.

Due to high missing values, poor data quality, and measurement errors on the station based data, the aforementioned gridded data set were used to address the data quality problems. On this account, this study considered three existing stations, which are located over the AEZs using the gridded data set for the purpose of comparison by AEZ, which in turn is assumed to represent each AEZ with the available climate data over the study period (1983–2014). The stations include Bilate (Lowland), Wolaita (Midland), and Boditi School (Highland) (Figure 1). The stations were selected purposively as they have long years (over 30 years) of observed temperature and rainfall data. The analysis period, 1983–2014, was chosen due to available data and to explore recent changes in temperature and rainfall, which help to recognize trends and data coverage across the AEZs. The gridded data can be accessed at NMA (http://www.ethiomet.gov.et/) for the climatic stations located in the AEZs.

In terms of survey design, the study employed a quantitative-dominant, qualitative mixed research design to select farmers for analyzing factors affecting perception of climate variability [44]. In selecting representative sample households, this research followed a three-stage sampling procedure. The approach allows taking small sample units from larger ones that offers an equal chance for all the elements chosen [45]. In the first stage, three districts, including Damote Gale (highland AEZ), Sodo Zuria (midland AEZ), and Duguna Fango (lowland AEZ), were selected purposively (Figure 1). The criteria include a district with dominant AEZ, long years of climate data availability (i.e., above 30 years), existence of meteorological stations, and demographic and livelihood conditions. In the second stage, following the characterization of the AEZs by Gecho et al. [42], list of all villages in the selected AEZs were used to further cluster them into the respective AEZs. Hence, a proportional three highland, five midland, and three lowland villages were selected randomly (Figure 1). Lastly, a probability proportional to size sampling technique [44] was applied to select 403 farm household heads in the area of study. The total sample size was calculated using a sample size computation technique that was proposed by Kothari [46]. We also used a purposive sampling technique to identify and undertake 11 focus group discussions (one per village) and 15 key informant interviews (five per district) to gather qualitative information to corporate climate change perceptions, both on temperature and rainfall indicators, and demographic, socioeconomic, and contextual factors affecting climate change perception. Instrument validation and piloting was conducted in a nearby nonsurvey district aimed to check the appropriateness, completeness, and validity of the data collection tools through a household survey for the quantitative data and expert judgment and elders' feedback for the qualitative tools. Scientific jargons, inappropriate variables, and indicators were dropped and corrected accordingly.

2.3. Data Analysis. ClimPACT2 Software in *R* was used for meteorological data quality control [47]. It was tested to label potentially wrong values and to remove them from the analysis. Outliers were detected and rejected for daily maximum and minimum temperatures exceeding ±3 standard deviation. After quality control, the trend was computed for daily maximum, daily minimum, and daily rainfall amount on annual time scale. The parameters for annual time scale include annual maximum temperature (ATmax), annual minimum temperature (ATmin), and annual total rainfall (ATR) using XLSTAT® 16. The households survey data management and analysis was carried out in Cspro® 6.3 and Stata® 14. To statistically compare variables between perceived and not perceived households, a *t*-test was employed for interval variables. A thematic analysis including description and classification of data and seeing how concepts interconnect was employed for qualitative information [48] to explain and triangulate the survey results. To see the presence of trends in both annual temperature and rainfall data, we used the nonparametric Mann–Kendall (MK) test statistic [49, 50] and Sen's estimator test [51].

2.3.1. Mann–Kendall Test. The MK uses the relationship between the ranks of a time series and their sequence. A hypothesis test is formulated as a null hypothesis (H_o) when there is no trend and the alternate hypothesis (H_1), as a trend in mean climate, where there is an increasing or decreasing monotonic trend. The Z score is computed and the confidence limits of the standard normal Z are equally determined. For a ranked set of observations n, $X = x_1, x_3, \ldots, x_n$, the MK trend statistic S is computed using

$$S = \sum_{i=1}^{n-1} \sum_{j=i+1}^{n} \operatorname{sgn}\left(x_j - x_i\right), \tag{1}$$

where x_j are the sequential data values, n is the data length of the time series, and

$$\operatorname{sgn}\left(x_j - x_i\right) = \begin{cases} 1, & x_j > x_i, \\ 0, & x_j = x_i, \\ -1, & x_j < x_i. \end{cases} \tag{2}$$

The variance of S is calculated using

$$\operatorname{Var}(S) = \frac{n(n-1)(2n+5) - \sum_{i=1}^{p} t_i\left(t_i - 1\right)\left(2t_i + 5\right)}{18}, \tag{3}$$

where n is the number of data points, ρ is the number of tied groups, and t_i is the number of data values in the ρth group. A tied group is sample data with the same value, where there is zero variance between the compared values. The summary of Equation (3) can be ignored if there are no tied groups. The significance of a trend is calculated by the Z-score using

$$\left.\begin{aligned} Z &= \frac{S-1}{\sqrt{\operatorname{Var}(S)}}, && \text{if } S > 0, \\ &= 0, && \text{if } S = 0, \\ &= \frac{S+1}{\sqrt{\operatorname{Var}(S)}}, && \text{if } S < 0. \end{aligned}\right\} \tag{4}$$

When Z value exceeds either of the confidence limit lines, it shows a significant trend at a given significance level. Hence, H_o is rejected and in place H_1 is accepted.

2.3.2. Sen's Slope Estimator Test. The Sen's slope estimator (SSE) [51] is employed to estimate the magnitude of the trends in the time series data. Thus, if a linear trend exists in a time series, then the true slope of the trend is estimated using a Sen-Theil trend line [51, 52], an alternative to linear regression, in combination with the MK test. The slope (T_i) of all data sets is calculated as

$$T_i = \frac{X_j - X_k}{j - k}, \quad \text{for } i = 1, 2, \ldots, N, \tag{5}$$

where X_j and X_k are taken as data values at time j and k ($j > k$), respectively. The median of these N values of T_i is denoted as Sen's estimator of slope, which is expressed as

$$Q_i = \begin{cases} T_{(N+1)/2}, & N \text{ is odd}, \\ \frac{1}{2}\left(T_{N/2} + T_{(N+2)/2}\right), & N \text{ is even}. \end{cases} \quad (6)$$

Sen's estimator is calculated as $Q_{\text{med}} = T_{(N+1)/2}$ if N appears odd, and it is used as $Q_{\text{med}} = T_{N/2} + T_{(N+2)/2}$ if N appears even. Lastly, Q_{med} is computed by a two-sided test at $100(1-\alpha)\%$ confidence interval, which is then used to obtain the true slope through the nonparametric test. A positive value of Q_i suggests an increasing trend and a negative value of Q_i offers a decreasing trend in the time series. Both the MK and SSE tests were performed using R software.

Rainfall variability was examined using standardized rainfall anomaly (SRA), precipitation concentration index (PCI), and coefficient of variation (CV). The descriptors were computed using equations (7) and (8). SRA was obtained using equation (7) [53]. The SRA features have contributed to its acceptance for drought monitoring while enabling to identify the dry and wet years in the record [54]. Therefore, the drought severity is categorized as, extreme drought (SRA < −1.65), severe drought (1.28 > SRA > −1.65), moderate drought (−0.84 > SRA > −1.28), and no drought (SRA > −0.84).

$$\text{SRA} = \frac{\text{P}_t - \text{P}_m}{\sigma}, \quad (7)$$

where SRA is Standardized Rainfall Anomaly, P_t is annual rainfall in year t, P_m is long-term mean annual rainfall for the period 1983–2014, and σ is the standard deviation of annual rainfall for the period 1983–2014.

Oliver [55] recommends the use of PCI to get information about any possible variations in the rainfall distribution over the year. Hence, PCI values are interpreted as typical of a uniform monthly rainfall distribution (PCI below 10), seasonality in rainfall distribution (PCI between 11 and 20), and a high variability in monthly rainfall amounts (PCI above 20). Using the PCI, data related to the long-term variability in rainfall amount were obtained and computed using equation (8) on annual scale, which was applied to examine heterogeneity of annual rainfall:

$$\text{PCI}_{\text{annual}} = \frac{\sum_{i=1}^{12} \rho_i^2}{\left(\sum_{i=1}^{12} \rho_i\right)^2} * 100. \quad (8)$$

Moreover, interannual variability of rainfall and temperature for the selected AEZs was determined by CV (i.e., standard deviation divided by the mean of ATmax, ATmin, and ATR), respectively. Z-score was adapted to compute the temperature anomalies, which is commonly used for rainfall anomalies.

2.3.3. Binary Logit Model Estimation. Methodologically, so far farmers' perception of climate change has been studied in three different ways as discussed under the introduction section. Nevertheless, following the assumption of standard logistic probability distribution like the previous studies, including [39, 56–58] and the suggestions made by Gujarati [59], we applied binary logit model, mainly to identify factors affecting farmers' perception of climate variability and change over AEZs.

The logit model considers that the outcome variable is dichotomous in nature, which assumes a value of 1 or 0. It also adopts a discrete vector of repressors X, which are assumed to influence the outcome Y. In line with Abid et al. [60], our dependent variable (*i.e., perceive climate change, $Y = 1$ or not perceive climate change, $Y = 0$*) was taken as a combination of an increase in temperature being accompanied by a decrease in rainfall, which results in accurate perception coded as 1 "*perceive climate change*" and coded as 0 "*not perceive climate change*". Gujarati [59] stated the functional form of logistic model (the log-odds ratio) as

$$P_i = \text{E}\frac{Y_i}{X_i} = \frac{1}{1 + e^{-(\beta_o + \beta_1 \text{X}_i)}}, \qquad P_i = \text{E}\frac{Y_i}{X_i} = \frac{1}{1 + e^{-\text{Z}_i}}, \quad (9)$$

where P_i is the probability of ith household to be in the first category-perceive climate change, which ranges from 0 to 1 and Z_i is a functional form of m explanatory variables (X), which is

$$\text{Z}_i = \beta_o + \sum_{i=1}^{m} \beta_i \text{X}_i, 1, 2, 3, \ldots, m, \quad (10)$$

where β_o is an intercept and β_i are slope parameters of the model or slopes of the equation. It indicates that how the log-odds are in favor of a given household which perceives climate change as an independent variable change. If P_i shows the probability of a given household which perceives climate change, then $1 - \text{P}_i$ shows the probability of a given household is not perceiving climate change, which is expressed as

$$1 - \text{P}_i = \frac{1}{1 + e^{\text{Z}_i}}. \quad (11)$$

When equation (9) is divided by equation (10), the simplified form is stated as

$$e^{\text{Z}_i} = \frac{\text{P}_i}{1 - \text{P}_i} = \frac{1 + e^{\text{Z}_i}}{1 + e^{-\text{Z}_i}}. \quad (12)$$

It explains a ratio of the probability that a household perceives climate change to the probability a household does not perceive climate change. Finally, the logit model is obtained by taking the natural log of

$$\text{Z}_i = \ln\left(\frac{\text{P}_i}{1 - \text{P}_i}\right) = \beta_o + \beta_i \text{X}_i. \quad (13)$$

Including an error term ε_i into the model is expressed as

$$\text{Z}_i = \beta_o + \beta_i \text{X}_i + \varepsilon_i. \quad (14)$$

In order to interpret and compute the results, it is relevant to compute the marginal effects using equation (15). It describes the effect of a unit change in the explanatory variable on the probability of a dependent variable, i.e., $\Pr(Y = 1)$. Marginal effects can be computed using

$$\frac{\partial P_\kappa}{\partial X_\kappa} = \frac{\beta_\kappa e^{-Z_\kappa}}{(1 + e^{-Z_\kappa})^z}. \quad (15)$$

The logit model was regressed on a set of relevant explanatory variables hypothesized based on literature and data availability that are assumed to affect farmers' perception of climate variability and change (Table 1). Factors included are of two types. The internal factors include farm-specific, socioeconomic, and demographic variables such as gender, age, education, landholding, age dependency ratio, nonfarm participation, food secured months, and household productive assets [26, 32–35, 38, 39].

External factors that affect farmers' perception to climate variability and change comprise access to the village market, climate information, market information, credit services, trainings, agroecology, access to irrigation, and agricultural input use [33, 34, 38, 39, 57, 60]. Variables such as total farm size (ha), household productive assets (local currency-*birr*), age dependency ratio (number), distance to the village market (km), age of the farmer (years), and food secured months (number) are continuous variables and measured in the respective unit, while all other variables are dummies and take the value of one and zero (Table 1). Using these variables, the empirical specification of the logit model was described as

$$\begin{aligned} Z_i = {} & \beta_o + \beta_1 \text{age} + \beta_2 \text{land} + \beta_3 \text{mard} + \beta_4 \text{adr} + \beta_5 f\,\text{sec} \\ & + \beta_6 \text{asset} + \beta_7 \text{sex} + \beta_8 \text{edu} + \beta_9 cli\text{inf} + \beta_{10} mar\text{inf} \\ & + \beta_{11} \text{nonfarm} + \beta_{12} \text{credit} + \beta_{13} \text{aez} + \beta_{14} \text{input} \\ & + \beta_{15} \text{train} + \beta_{16} \text{irruse} + \varepsilon_i. \end{aligned} \quad (16)$$

3. Results and Discussion

3.1. Variability and Trends in Temperature

3.1.1. Variability and Trends in Annual Maximum Temperature. The CV of the highland AEZ is nearly double that of the midland and lowland AEZs, suggesting a high variability in the ATmax over the 32 years under study. The year 2012 was observed as the hottest year in AEZs while 1989 was the lowest ATmax year for the midland and lowland AEZs (Table 2 and Figure 2). The hottest and coldest years are consistent with a study by Mengistu et al. [17], which reported that AEZs in the Upper Nile basin experienced relatively cold years in the 1980s and warm years from the early 1990s to the 2000s.

Table 3 and Figure 2 show the temporal and spatial variability and trend of ATmax in the AEZs. It exhibited an upward trend of 0.02°C/year ($p < 0.01$), signifying 0.64°C increase between 1983 and 2014 in the lowland AEZ. The highland AEZ experienced significantly increased temperature in the ATmax. The rate of change in the ATmax was 0.04°C/year ($p < 0.001$). However, the result for midland AEZ reveals a nonsignificant downward trend in the ATmax (0.01°C/year) (Table 3). In terms of AEZs, the highland AEZ experienced 1.28°C change ($p < 0.001$) compared to the lowland AEZ that exhibited 0.64°C increase ($p < 0.01$), notifying highly rapid rate of change in the ATmax over three decades. The warming trend observed in the study area is relatively higher than the historical trend reported at national and subnational levels. For instance, a warming trend of 0.1°C/decade was observed in Ethiopia between 1953 and 1999 [61] while it was 0.2°C/decade for Addis Ababa from 1951 to 2002 [62].

The interannual variability of the ATmax presented in (Figure 2) indicates that the AEZs have experienced both warm and cool years during the 32 years. Therefore, the anomaly detected was complex for midland AEZ. A warming trend in lowland and highland AEZs was reported, informing the recent years are warmer than the earlier years. Even though the magnitude in the ATmax differs, the general warming trend matches with studies reported both at national level [61] and local level [17, 32].

Several other studies at various spatial and temporal scales have recognized warming trends in maximum temperature [4, 20, 21, 28, 63]. On the rate of increase, without adaptation, more than 1°C warming has adverse impacts [3]. In this case, the trend analysis over three decades suggests that the highland AEZ has exhibited warming of 1.28°C while the lowland experienced 0.64°C increase, implying some possible negative impacts on the lives and livelihoods of smallholder farmers mainly in the highland AEZ. Relating rapid change in the climate, the shifting nature of the AEZ and its contributing factors, farmers in the highland AEZ stated:

> "Previously, there were big trees that used to pull down rain and cold air. Today, these trees are not there due to high deforestation and expansion of farmland. These trees have been cleared and the land is open for wind. Rather, the lands are covered by eucalyptus, which does not maintain soil fertility. Because of the change in climate, we are not sowing crops during the same time as we used to do before. The farm calendar of both cultivation and harvesting has changed over time. This was a highland before as cold as Damota-highest point. It is like a lowland now. We have thus suffered from high temperatures day in and day out." [Discussions in Highland AEZ, March 2017].

Supporting this idea, one of the key informants from the same AEZ shared his experiences:

> "Malaria was one of the major shocks that claimed the lives of many people before the recent expansion of health services in the lowland areas. Currently, with the change of temperature from lowland to highland areas, malaria occurred in areas where there were no incidences before, indicating that the highland AEZ is no longer highland in its main characteristics." [Discussions in Highland AEZ, March 2017].

Table 1: Results of the binary logit model for aggregate sample and agroecological zones.

Explanatory variables	Mean	SD	Aggregate (1)		Highland AEZ (2)		Midland AEZ (3)		Lowland AEZ (4)	
			Regression	Marginal effect	Regression	Marginal effect	Regression	Marginal effect	Regression	Marginal effect
Age (years)	44.62	14.06	−0.014	−0.003	−0.019	−0.004	−0.013	−0.003		
Total land size (ha)	0.78	0.79	−0.200	−0.046			−0.041	−0.010	−0.338	−0.081
Distance to village market (km)	2.87	4.98*	−0.082**	−0.019**	−0.161*	−0.030	−0.047	−0.011		
Dependency ratio (number)	0.87	0.73	−0.231	−0.053	−0.563	−0.107				
Food secured months (number)	7.29	2.85	−0.148***	−0.034***	−0.063	−0.012	−0.141**	−0.033**	−0.249***	−0.060***
ln (household productive assets)	6.21	1.10			−0.243	−0.046				
Gender (1 = male)	264	65.51%	−0.666***	−0.148***	−0.894	−0.157	−0.489	−0.111	−1.253***	−0.276***
Education (1 = primary)	154	38.21%	0.654***	0.147***	0.855	0.149			0.103*	0.025*
Climate information (1 = yes)	280	69.48%	1.113***	0.264***			1.650***	0.387***	0.030	0.007
Market information (1 = yes)	234	58.06%	0.590**	0.137**	1.193*	0.229*			0.960**	0.228**
Participation in nonfarm (1 = yes)	109	27.05%	−0.585**	−0.139**	−1.621**	−0.341**	−0.408	−0.096		
Access to credit (1 = yes)	120	29.78%	−0.177	−0.041			−0.250	−0.059		
Agroecology (1 = lowland)	115	28.54%	−0.774***	−0.184***						
Improved seed (1 = yes)	154	38.21%	0.851***	0.189***	2.418***	0.388***			0.868*	0.208*
Received training (1 = yes)	80	19.85%	1.078***	0.220***	0.340	0.062	1.305***	0.257***		
Irrigation use (1 = yes)	19	4.71%							−0.786	−0.194
Constant			1.808***		3.945*		1.528**		1.671*	
N			403		90		198		115	
LR chi^2			85.95		34.16		47.14		28.73	
Prob > chi^2			0.001		0.001		0.001		0.001	
Pseudo R^2			0.160		0.302		0.178		0.183	

*** Significant at $p < 0.01$; ** significant at $p < 0.05$; * significant at $p < 0.1$.

Table 2: Annual maximum temperature variability by agroecological zones.

Station	AEZ	Mean (°C)	Std. deviation	Max (°C)	Year	Min (°C)	Year	CV (%)
Bilate	Lowland	27.87	0.45	28.65	2012	26.75	1989	1.62
Wolaita	Midland	26.59	0.36	27.59	2012	26.01	1989	1.35
Boditi school	Highland	25.50	0.66	26.76	2012	23.33	2006	2.59

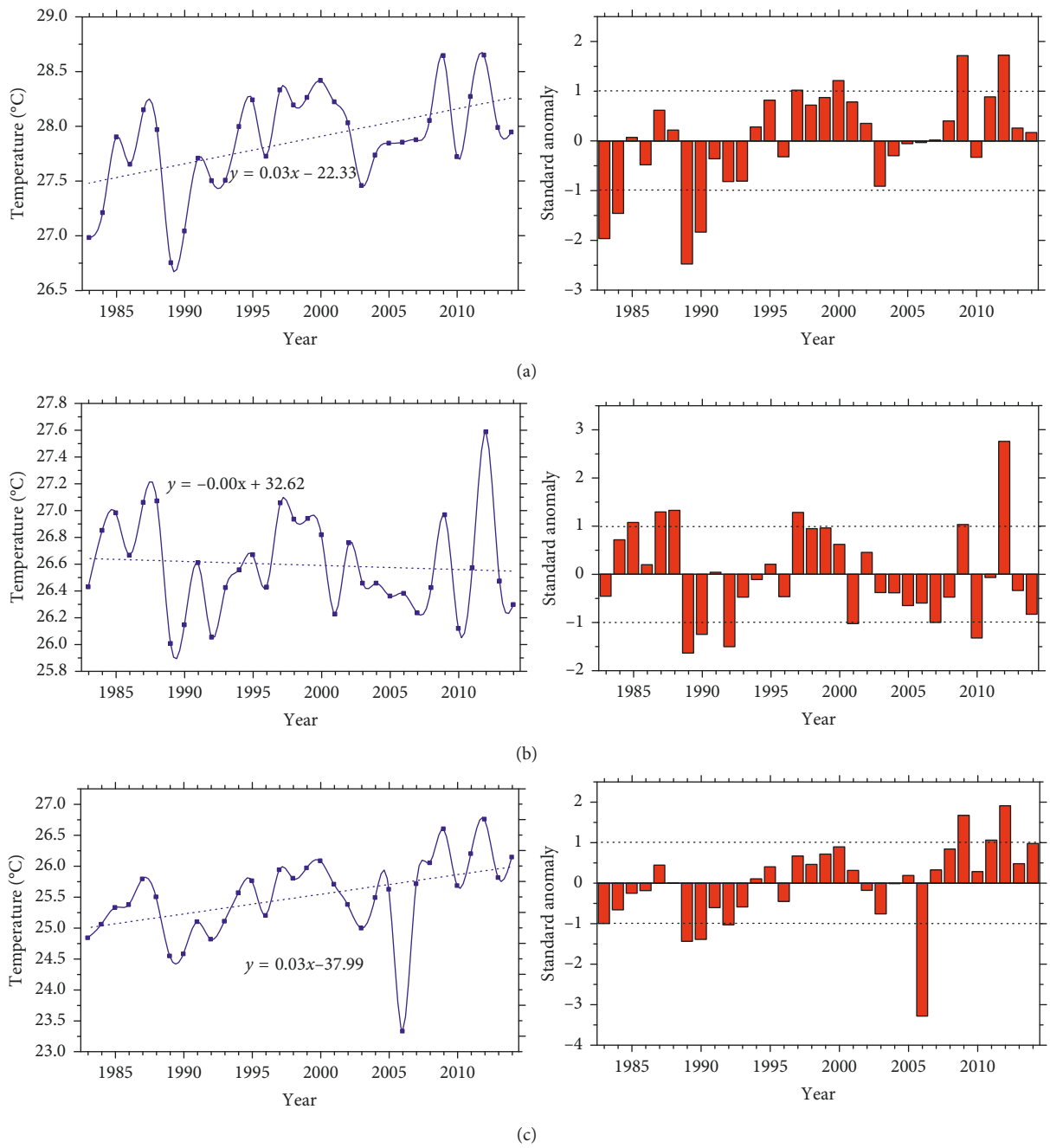

Figure 2: Spatial and temporal variations in the annual mean maximum temperature over the three agroecological zones, (a) lowland, (b) midland, and (c) highland, for the period 1983–2014: trends (left) and anomalies (right).

The rapid change in the ATmax reveals the shift in the AEZ where the highland AEZ is changing in its main features and showing somewhat different patterns in the climate components, specifying changes in the climate in the past years in Wolaita.

3.1.2. Variability and Trends in Annual Minimum Temperature. The ATmin is 14.80°C (CV = 6.49%), 14.86°C (CV = 5.10%), and 13.64°C (CV = 7.26%) for lowland, midland, and highland AEZ, respectively (Table 4). It shows relatively high variability in the highland AEZ than the other

Table 3: Trend statistics of annual maximum temperature by AEZs (1983–2014).

Station	AEZ	MKZ	S	Sen's slope (°C/year)
Bilate	Lowland	0.35	172	0.02***
Wolaita	Midland	−0.11	−56	−0.01
Boditi school	Highland	0.46	226	0.04***

***Significant at $p < 0.01$; **significant at $p < 0.05$; *significant at $p < 0.1$.

Table 4: Annual minimum temperature variability by agroecological zones.

Station	AEZ	Mean (°C)	Std. deviation	Max (°C)	Year	Min (°C)	Year	CV (%)
Bilate	Lowland	14.80	0.96	15.97	2010	12.74	1986	6.49
Wolaita	Midland	14.86	0.76	15.97	2012	12.96	1986	5.10
Boditi school	Highland	13.64	0.99	15.04	2014	11.11	1986	7.26

AEZs. The year 1986 was the coldest year in all AEZs. The finding agrees with the cold and warm years reported among AEZs of the Upper Nile basin [17].

It is clear that the change in the ATmin both for lowland and midland AEZs was the same (Table 4). It accounts for 0.05°C/year, signifying 1.6°C increase in the ATmin in lowland and midland AEZs $p < 0.001$ and $p < 0.01$, respectively. The result for highland AEZ was 0.07°C/year ($p < 0.001$), suggesting a highly warming trend observed in highland AEZ compared to other AEZs (Table 5). For example, Conway et al. [62] observed an increasing trend in ATmin from 1951 to 2002 (0.4°C/decade) for Addis Ababa; Mengistu et al. [17] found 0.15°C/decade in the Upper Nile basin while Tekleab et al. [15] reported significant increases in ATmin at the annual times cale for many stations studied in the Abay basin. Moreover, ATmin increased by about 0.37°C/decade between 1951 and 2006 [10]. Earlier studies have also shown [64, 65] that most parts of the Greater Horn of Africa (GHA) show warming trends for both ATmax and ATmin. On a global scale, studies [66, 67] reported an increase in the annual maximum temperature by 0.15°C/decade. However, in this study, findings show relatively higher rate of changes in the ATmax and ATmin than was reported by Camberlin [65] for GHA and other studies at national level [4, 9].

ATmin shows a significantly increasing trend across all AEZs, but ATmax has revealed both increasing and decreasing trends. The rate of change for ATmin is faster than the ATmax both in time and space. The faster rate of change in the ATmin than the ATmax is in line with trends found by NMA [61]. As suggested by Peterson et al. [68], the changes are attributed to the decreasing night-time cooling. McSweeney et al. [10] thus indicated that at national level, the average number of hot nights has increased by 137 whereas the hot days by 73 days per year from 1960 to 2003.

The results in Figure 3 affirm that all AEZs have experienced both warm and cool years during three decades. Starting from 1998, a warming trend was observed in all AEZs except in 2006 which was the coldest year both in the midland and highland AEZs. In contrast, the 1980s were the coldest years with the ATmin below the mean across all AEZs, which concur with the observation made by Mengistu et al. [17]. Hence, the rapid rate of changes both in the ATmax and ATmin signifies the change in temperature is one of the climate elements in the studied AEZs.

3.2. Variability and Trends in Annual Rainfall. On annual scale, rainfall is variable in the AEZs (Table 6). The ATR in the study AEZs varies from 697 mm in the lowland AEZ to 1,181 mm in the midland AEZ. The CV ranges from 18.57% in the highland AEZ to 25% in the lowland AEZ, suggesting a high rainfall variability in the lowland AEZ while similar patterns being observed in the midland and highland AEZs.

The CV of rainfall exhibits nearly similar patterns, both in the midland and highland AEZs (above 18%) on an annual scale, whereas the highest CV(25%) was reported in the lowland AEZ, signifying moderate rainfall variability (Table 6). From Table 7, similar PCI values were detected in the midland and highland AEZs while lower PCI value was sensed in lowland AEZ, showing irregularity in the rainfall distributions between and among AEZs. On the variability of PCI values, empirical studies reported differently in different contexts. For example, a moderate-to-high interannual rainfall concentration was observed in Amhara region [69] while the same pattern was reported by Kassie [8] in the Central Rift. In contrast, Gebre et al. [70] found that high and very high concentrations were observed in the Northern Ethiopia, suggesting poor monthly rainfall distribution.

Table 7 and Figure 4 show the trend test results of rainfall on the annual time scale. Though not statistically significant, a decreasing trend was observed (1.80 mm/year and 0.11 mm/year) in the lowland and highland AEZ, respectively, while an increasing trend (10 mm/year) ($p < 0.05$) was exhibited in the midland AEZ. The increasing trend in the ATR in the midland AEZ was in line with findings of other researchers [28, 30], in which the midland AEZ experienced an increasing trend in the ATR. Likewise, Weldegerima et al. [21] reported an increase in ATR in three stations in Northern Ethiopia. To this end, the figures suggest that the ATR trend was neither decreasing nor increasing between 1983 and 2014 in all except the midland AEZ. The findings are consistent with a study in three meteorological stations, including Bilate, which did not show a significant trend in ATR [29]. Similarly, the total rainfall trend in the selected AEZs is in agreement with most

Table 5: Trend statistics of annual minimum temperature by AEZs (1983–2014).

Station	AEZ	MKZ	S	Sen's slope (°C/year)
Bilate	Lowland	0.64	318	0.05*
Wolaita	Midland	0.44	220	0.05*
Boditi school	Highland	0.57	284	0.07*

*Significant at $p < 0.01$.

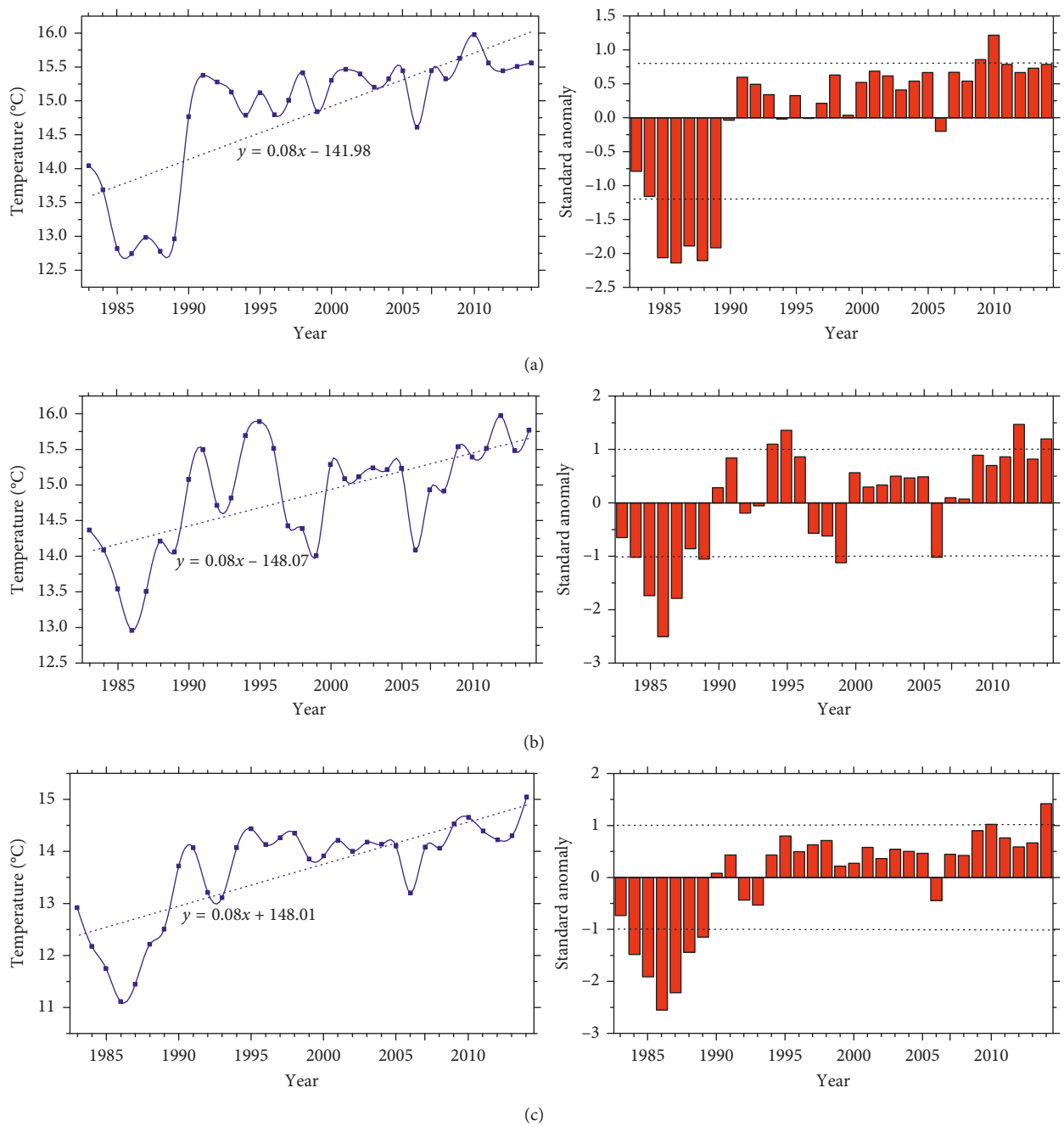

Figure 3: Spatial and temporal variations in the annual mean minimum temperature over the three agroecological zones, (a) lowland, (b) midland, and (c) highland, for the period 1983–2014: trends (left) and anomalies (right).

Table 6: Annual rainfall variability by agroecological zones.

Station	AEZ	Mean (mm)	Std. deviation	Max (mm)	Year	Min (mm)	Year	CV (%)	PCI
Bilate	Lowland	696.66	173.47	1064	1987	435	1999	24.90	10.88
Wolaita	Midland	1180.91	223.89	1474	2006	605	1984	18.96	11.38
Boditi school	Highland	881.13	163.64	1252	2007	555	2009	18.57	11.13

Table 7: Trends statistics of total rainfall by AEZs (1983–2014).

Station	AEZ	MKZ	S	Sen's slope (mm/year)
Bilate	Lowland	−0.075	−37.00	−1.80
Wolaita	Midland	0.274	136	10*
Boditi school	Highland	−0.01	−5	−0.11

*Significant at $p < 0.05$.

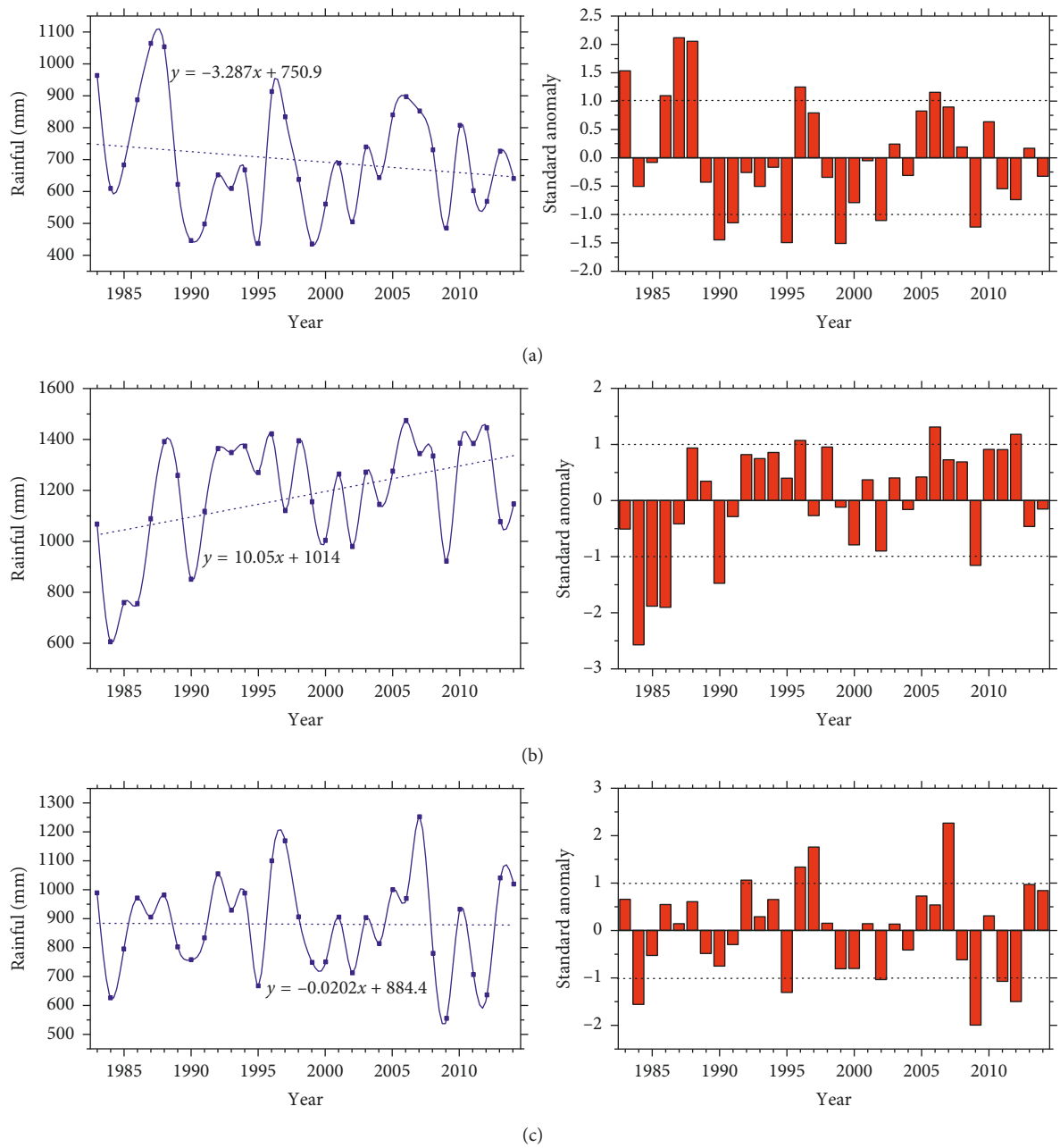

Figure 4: Annual total rainfall trends over the three agroecological zones, (a) lowland, (b) midland, and (c) highland, for the period 1983–2014.

of the empirical studies in Ethiopia that reported neither decreasing nor increasing patterns of rainfall amounts over time [15–17].

The interannual rainfall variability informs that AEZs have experienced negative and positive anomalies in the ATR (Figure 4). Hence, 1999, 1984, and 2009 were the driest and 1987, 2006, and 2007 were the wettest years in the lowland, midland, and highland AEZ, respectively. Drought categories are summarized in Table 8 based on McKee et al.'s [71] drought classification. As a result, 13 (40.63%), 10 (31.25%), 4 (12.50%), and 2 (6.25%) were observed as mild drought, normal, moderate drought, and severe drought years in the lowland AEZ, respectively. Only, 2 (6.25%) was reported as extreme wet years in the lowland AEZ, signifying nearly 60% of observed drought conditions. Likewise, the 1980s were detected as a wet decade in the lowland AEZ (Figure 4(a)). In midland, 17 (53.13%) were normal years while extreme wet conditions have not been observed at all. In highland, 16 (50%) was a normal year, whereas 2 (6.26%) were reported as severe wet and extreme wet years. 14 (44%) were drought years with varying levels of severity (Table 8 and Figure 4(c)). One key informant vividly noted the frequent occurrence of drought in the area as follows:

> "Hitherto, drought occurred at least on a decadal basis, which was the case for the introduction of the bigger nongovernmental organizations like World Vision in Wolaita. Its occurrence continuously increased from time to time and begun to happen on a yearly basis. For example, due to El Niño, we faced a drought last year (2016), which affected animals and caused even complete crop failure. There was also the outbreak of pest (virus) that damaged maize. This was a strange phenomenon." [Key informant Interview in Lowland AEZ, March 2017].

In general, 44% were observed as normal years across AEZs while 50% were drought years (Figure 5). The study result partly agrees with the national level anomaly trend reported by McSweeney et al. [10]. The national worst drought years also fits with realities in the study area. However, the anomaly trend in the study area partly differs with the national level figures when seen from the AEZs perspectives. In the lowland, 1980s was the wettest decade, while it was the 1990s in the midland and partly wettest in the highland in the 2000s (Figures 4 and 5), respectively. The differences in the anomaly years suggest the high annual rainfall variability among the AEZs.

3.3. Spotting Farmers' Perception of Local Climate Variability and Change. Depending of the research contexts, different studies have been carried out to examine how farmers perceive changes in the climate system. Understanding farmers' perception levels and the various adaptation strategies individual households employ would benefit to gather supplementary information relevant to policy and intervention to tackle the challenges of climate change.

The descriptive analysis show that about 248 (61.54%) of the farmers perceived changes in the climate parameters (i.e., increased temperature and decreased rainfall) in the aggregate sample. As for AEZ, 61 (67.78%), 121 (61.11%), and 66 (57.39%) farmers perceived the changes in highland, midland, and lowland AEZs, respectively (Figure 6). This is in agreement with the household perception regarding increased temperature and decreased rainfall reported in Ethiopia and other countries [25, 26, 31, 32, 38, 39, 58, 72–74]. In our case, the proportion of farmers who perceived increasing temperature and decreasing rainfall is slightly different compared to studies in Ethiopia and other countries, being influenced by factors affecting their level of perception in general and the type of meteorological data (station vs. gridded data) and climate data availability (longer vs. shorter time period) in particular. Moreover, Schwartz [75] pointed that people believe climate may change owing to fresh climate experiences, such as the recent 2015/2016 El Niño events prior to the data collection period may contribute to their perception in the study area context.

The data on the temperature indicators also revealed that farmers perceived an increase in dry season temperature and hot days' temperature, which are consistently increasing over the AEZs. In addition, over 60% of farmers in the highland AEZ perceived an increase in rainy season temperature while a comparable proportion of farm households perceived increased temperature in the rainy season both in the midland and lowland AEZs (Figure 7). The farmers' perception results are in line with a recent study in the same AEZs [30]. Others studies observed similar patterns in different parts of Ethiopia [25, 26, 32, 38, 39, 76].

Farmers in all AEZs perceived that rainfall comes late. Farmers in the highland AEZ perceived that the rainfall goes early and observed decreasing trend in the short rains. In the same AEZ, farmers have better perceived for all rainfall indicators compared to those in the lowland AEZ. In general, farmers in all AEZs perceived declining trends both for the *belg*/short-rains and *meher*/long-rains over the last two decades, which makes rainfall erratic (Figure 8). The result agrees with empirical studies [25, 26, 32, 38, 39], which reported that farmers perceived declining trend in the rainfall amount over years in Ethiopia. Similarly, a study by Mkonda et al. [74] reported that a significant increasing temperature was observed locally in all the AEZs in Tanzania.

Regarding the perceived impacts of climate change, farm households witnessed impacts, including, crop productivity decline (98.26%), food price inflation (98.01%), increased frequency of drought (94.79%), increased crop pest (70.72%), increased frequency of floods (68.73%), shortage of water for human use (63.03%), emergence of new pests (61.79%), shortage of water for irrigation (61.04%), increased livestock disease (58.81%), and conflict over diminishing resources (55.83%) in order of severity across AEZs (Figure 9). Similarly, Tesso et al. [32] documented perceived impacts of climate change among AEZs in North Shewa, Ethiopia. Hence, farmers' perception of the climate-induced impacts over years is indicative of Ethiopia's vulnerability to climate change and variability. Thus, studies recognized that Ethiopia suffers from problems associated with high rainfall

Table 8: Standardized rainfall indices over the three agroecological zones, (a) lowland, (b) midland, and (c) highland, for the period 1983–2014.

Drought category	SRA ranges	Percentage and frequency of occurrence (Years)							
		Lowland (a)		Midland (b)		Highland (c)		Total (d)	
		N	%	*N*	%	*N*	%	*N*	%
Extreme drought	−2.0 or less	—	—	1	3.13	—	—	1	1.04
Severe drought	−1.5 to −1.99	2	6.25	2	6.25	3	9.38	7	7.29
Moderate drought	−1.0 to −1.49	4	12.50	2	6.25	3	9.38	9	9.38
Mild drought	−0.99 to 0	13	40.63	10	31.25	8	25	31	32.29
Normal	+0.01 to +1.49	10	31.25	17	53.13	16	50	43	44.79
Severe wet	+1.5 to +1.99	1	3.13	—	—	1	3.13	2	2.08
Extreme wet	+2.0 or more	2	6.25	—	—	1	3.13	3	3.13

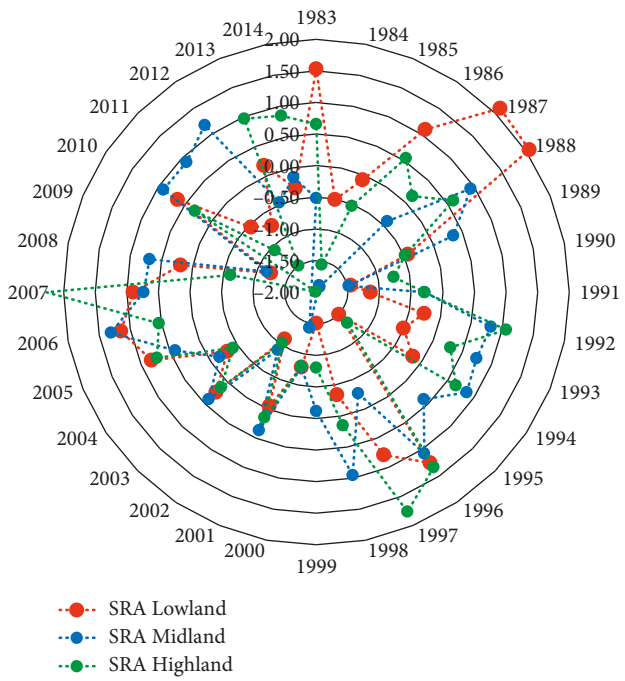

Figure 5: Drought occurrence years over the period of 1983 to 2014 in the three agroecological zones.

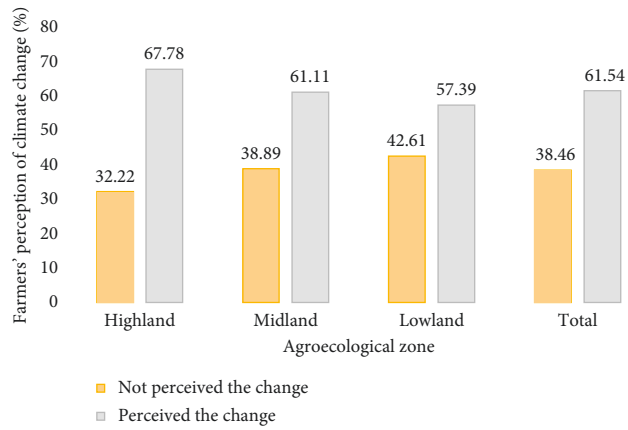

Figure 6: Farmers' perception of climate change.

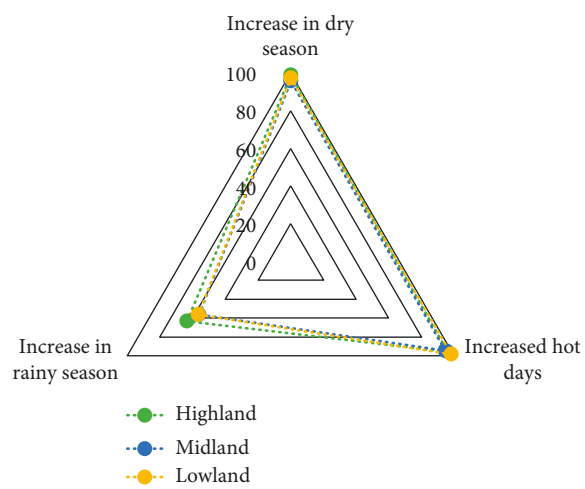

Figure 7: Farmers' perception of temperature indicators.

variability [77]. Specifically, Amsalu and Adem [78] show that climate change has both direct and indirect impacts on the occurrence and spread of pests and diseases. Moreover, extracts from qualitative information supports the changes in the climate parameters and the corresponding impacts over the last two decades as follows:

> "Before 1999, the area was very green and we had adequate pasture for the cattle. Now, there is no grass for grazing, and there is a movement in search of grass. Since 1999, we have witnessed a decrease in rainfall and an increase in temperature warming. The springs have dried, and the vegetation cover has been declining. Where there is irrigation, production of crops is good." [Discussions in Lowland AEZ, March 2017].

Ethiopia has faced many droughts and floods since 1980 [79]. Since 1990, Ethiopia has confronted 47 major floods that killed nearly 2000 people and affected a population of about 2.2 million [80]. It also experienced 12 major droughts between 1900 and 2010 that claimed the lives of over 400,000 people and affected more than 54 million [80]. Very recently, the 2015/2016 El Niño-induced drought caused food security affecting an estimated 10.2 million people; one of the most severe on record [81]. Therefore, although the farmers' perception of climate change differs in the study AEZs and parts of Ethiopia, farmers' perceptions and the trends in climate change complement each other, showing a warming trend.

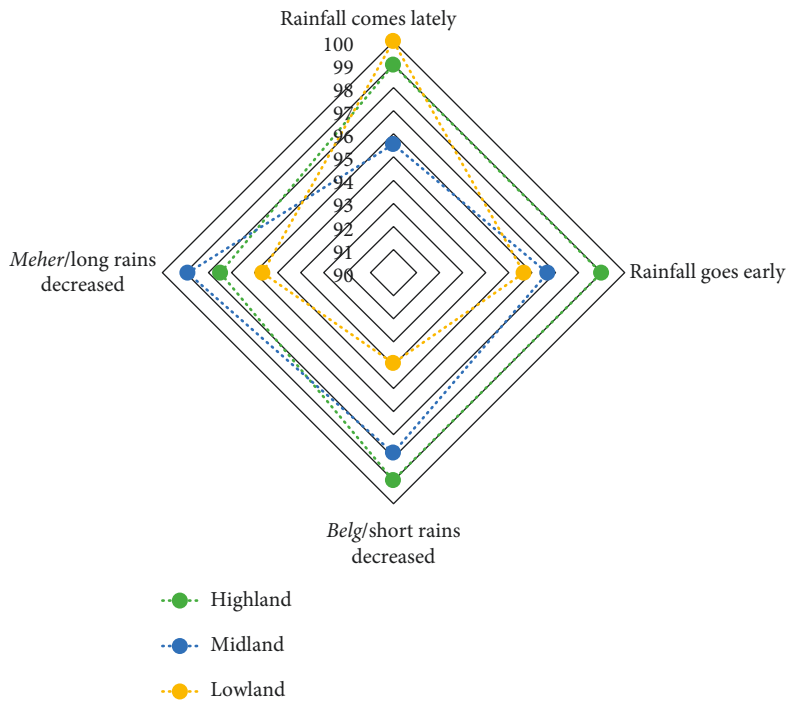

Figure 8: Farmers' perception of precipitation indicators.

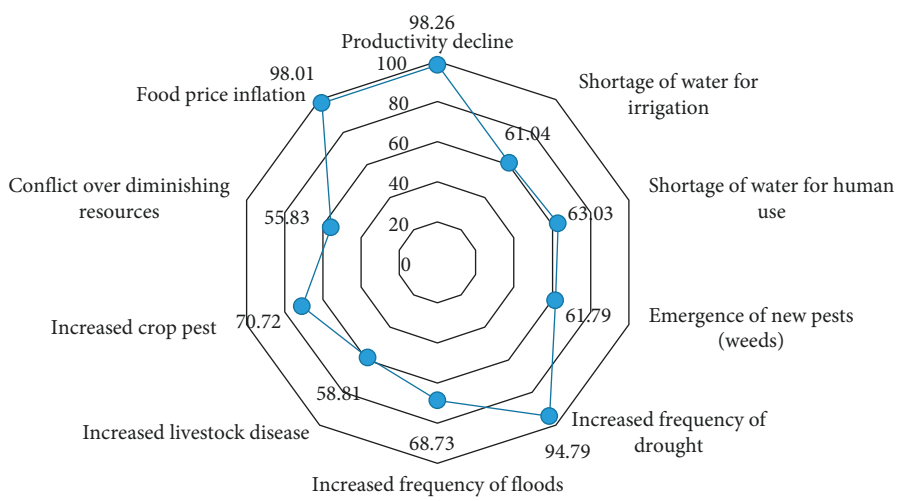

Figure 9: Perceived impacts of climate change and variability.

3.4. Econometric Model Results. A descriptive statistic of the explanatory variables used is summarized in Table 1. The average age was 44.62 years, suggesting that farmers are in the productive age category (16–64 years) [82]. The land-holding accounts for 0.78 hectare in all AEZs. A statistically significant difference was observed between farmers who perceived climate change (0.71 ha) and not perceived climate change (0.88 ha) ($t = 1.96$, $p < 0.1$). The average distance farmers travel to reach to the village market was 2.87 km. This was statistically significant between the perceived and not perceived farmers, 2.30 km and 3.79 km, respectively ($t = 2.43$, $p < 0.05$). Regarding food secured months, farmers in all AEZs were able to feed their families for 7.29 months. A statistically significant difference was exhibited between farmers who perceived climate change (6.89 months) and not perceived climate change (7.92 months) ($t = 3.65$, $p < 0.01$), suggesting food-secured households are less likely to perceive climate change compared to their counterparts.

Most of the famers' households were male-headed (65.51%), with 38.21% having completed primary school (grade 1 to 8). In terms of access to information, it was evident that 69.48% had access to climate information and 58.06% to market information in all AEZs, supporting the positive role of information to farmers' livelihood improvement and preparedness to climate change impacts. Of the sample, 27.05% of farmers were involved in the nonfarm

income activities as a way to diversify livelihoods in the face of climate change and enable them to address food and income gaps. The result agrees with Gecho et al. [42], where they reported 37% of farmers derive income from farm and nonfarm activities in Wolaita. Only 29.78% had access to credit, indicating that farm household had limited access to credit services in AEZs. 38.21% farm households used improved seed in the production seasons, and a negligible percent of farmers had access to irrigation use. Likewise, only 19.85% of the sampled farmers received trainings important for their livelihood activities across AEZs. The binary logit model was first tested for its suitability and explanatory power for the variables used. In addition, the likelihood function of the binary logit model was significant (Likelihood-ratio (LR) $chi^2 = 85.95$ with $p < 0.01$), signifying its strong explanatory power. The estimated coefficients of the parameters and the marginal effects in the binary logit model ($p < 0.1$) for aggregate sample, highland AEZ, midland AEZ, and lowland AEZ are presented in Table 1.

Factors such as agroecological zone, head gender, nonfarm participation, food secured months, and distance to village market are significantly negatively correlated with climate change perception while access to climate and market information, attended training, use of improved seed, and completed primary school are significantly positively associated with climate change perception. Unlike our expectations, farmers who live in the lowland AEZ are less likely to perceive change than farmers who reside both in the midland and highland AEZ. Thus, the probability of perceiving climate change declines by 18.4% if a farmer resides in the lowland AEZ ($p < 0.01$). This could be due to their inherent vulnerability to impacts of climate change while a small change in the climate parameters in other AEZs more likely affects the farmers to perceive climate change. In support of this, Ethiopian Panel on Climate Change (EPCC) [83] has recognized highland areas among the most vulnerable agroecology in Ethiopia. Esayas et al. [30] also reported that the highland AEZ in Wolaita experienced a rapid rate of change in the extreme climate events compared to the lowland AEZ over three decades. Deressa et al. [31] further noted that farmers from the highland AEZ in the Nile basin perceived climate change more than those in the lowland AEZ.

In this study, the gender of household head is inversely correlated with climate change perception. The probability of male-headed farmers' perception of climate change declines by 14.8% compared to female headed households ($p < 0.01$). In terms of AEZ, the probability of perceiving the climate change for male headed households in the lowland AEZ decreases by 27.6% whereas it is nonsignificant both in the highland and midland AEZs. This might be because female headed households are more confined to home the most part of the day and, hence, are more concerned about environmental problems that impede their families and local people [84]. Nevertheless, previous studies [31, 38, 58] testified that there was no significant variation between male- and female-headed households on the perception of climate change. Hence, gender is not always positively associated with the perception of climate change; rather, it is a mixed factor depending on the environmental issues studied.

Similarly, participation in nonfarm income, food-secured months, and distance to village market have negatively influenced farmers' perception of climate change. The probability of perceiving climate change, thus, decreases by 13.9% when a farm household is involved in nonfarm income across AEZs. This could be because nonfarm activities are less susceptible to climate change impacts. Ndambiri et al. [56] similarly reported an inverse relationship between participation in off-farm income and perceiving climate change.

The estimated marginal effect for one additional food-secured month of the household head decreases the probability of perceiving climate change by 3.4% ($p < 0.01$) for the aggregate sample. The same pattern was observed both in the midland and lowland AEZs, where the probability of perceiving climate change decreases by 3.3% ($p < 0.05$) for midland AEZ and by 6% for lowland AEZ ($p < 0.01$), respectively. This signifies that food-secure farm households are less likely to perceive the climate change compared to the food insecure households, since the latter may attribute the food shortage to environmental challenges such as climate change.

The study revealed that there is an inverse relationship between distance to the village market and farmers' perception of climate change. Therefore, one extra km traveled to the village market by the household head decreases the probability of perceiving climate change by 1.9% ($p < 0.05$) for all samples. Farmers residing farther away from the nearest input/output market are less likely to perceive climate change than farmers residing closer to the market. Market outlets offer a crucial linkage for farmers to collect and disseminate information between and among fellow farmers, and the further the farmer's distance from such a market linkage, the less likely the farmer would be to perceive climate change. Similarly, a negative influence of distance to village market on the perception of climate change was reported in other studies [32, 34, 39].

As expected, the logit model shows that there is a positive association between farmers' access to climate information and perception of climate change. Farmers' access to climate information increases the probability of perceiving climate change by 26.4% in an aggregate sample ($p < 0.01$) while it enhances the probability of farmers' perception of climate change by 38.7% ($p < 0.01$) in the midland AEZ. Studies also reported that farmers who have better access to climate information are more likely to perceive climate change [34, 38, 39]. Though farmers recognized these sources of information as vital, they still had their own ways of perceiving climate change [85].

Likewise, the availability of market information has significant positive correlation with farmers' perception of climate change. Hence, farmers who have access to market information are 13.7% more likely to perceive the climate change in the aggregate sample ($p < 0.05$). In terms of AEZ, the probability of farmers who have access to market information increases the perception to climate change by 22.9% in the highland AEZ and 22.8% in the lowland AEZ.

This can be attributed to better access to input and output market information. The study shows that farmers using improved seeds are 18.9% more likely to perceive climate change in the aggregate sample ($p < 0.01$), 38.8% in the highland AEZ ($p < 0.01$) and 20.8% in the lowland AEZ ($p < 0.10$).

The other variable of interest that influences the probability of farmers' perception of climate change is farmers' education level and received capacity building trainings (proxy variables for level of awareness). The marginal effect revealed that farmers who have completed primary school are 14.7% more likely to perceive climate change ($p < 0.01$) in all samples while the increases was by 2.5% in the lowland AEZ ($p < 0.10$). In this regard, the more educated the household head, the higher the probability of perceiving the climate change and vice versa. The result agrees with previous studies which reported the positive influence of household education on climate change perception in different contexts [32, 34, 38, 39]. Although a small number of farmers have attended capacity building trainings, the results imply that training has a positive influence on farmers' perception of climate change. The computed marginal effect indicates that receiving training increases the probability of perceiving climate change by 22% for an aggregate sample ($p < 0.01$), whereas the increase was by 25.7% in the midland AEZ ($p < 0.01$).

3.5. Climate Trend Analysis Nexus with Farmers' Perceptions. It is evident that farmers' perceptions of climate change in the last two decades correlates with the meteorological data in the study area. Over 60% of farmers have perceived increasing temperature and decreasing rainfall in all AEZs. Likewise, the trend analysis reveals that positive trends were observed in the ATmax, 0.02°C/year ($p < 0.01$) in the lowland AEZ and 0.04°C/year ($p < 0.01$) in the highland AEZ, respectively. The trend for ATmin was consistent in all AEZs and significant ($p < 0.01$). Regarding rainfall trend, a nonsignificant decreasing trend was observed (1.80 mm/year) and (0.11 mm/year) in the lowland and highland AEZs, respectively. However, an increasing trend in the ATR (10 mm/year) ($p < 0.05$) was experienced in the midland AEZ between 1983 and 2014. There are increasing temperature and decreasing rainfall trends both in the lowland and midland AEZs. Similarly, many studies in Ethiopia reported positive trends in the average ATmax [4, 20, 28, 38, 63] and increasing trend in the average ATmin [4, 9, 10, 17]. The total rainfall trend in two of the AEZs agrees with most of the empirical studies in Ethiopia [10, 15, 16, 61] that found neither decreasing nor increasing patterns in the total rainfall amounts. Nevertheless, the positive trend on the average total rainfall in the midland AEZ contradicts with household perceptions in the same AEZ over the study periods. The increasing trend in the ATR in the midland AEZ corroborates the earlier findings [28, 30] that reported that the midland AEZ experienced an increasing trend in the average ATR.

Nonetheless, the discrepancy between farmers' perception of rainfall amount in the midland AEZ and the climate trend could be attributed to farmers' level of perception which are influenced by a number of factors including, agroecology, education, farm experience, resource endowments, access to climate information, and early warning systems [32, 34, 38, 39] while the trend is a cumulative result over three decades. Tadesse et al. [26] observed similar discrepancies between the climate trend analysis and farmers' perception in the adjacent area of the study AEZs. Therefore, farmers' perception cannot merely depend on the actual climate conditions and a change in the climate parameters. Instead, it can be affected by a number of social, economic, demographic, and institutional factors [32, 34, 38].

4. Conclusion and Recommendations

This study has analyzed trends of climate variability and farmers' perception in Southern Ethiopia using meteorological time series data from 1983 to 2014. Understanding the temperature and rainfall variability trends and farmers' perception of changes in the climate among agroecological settings would offer valuable information for the planning and implementing local level adaptations. The livelihood activities of most rain-fed farmers of the study area depend on the numerous climatic variables, mainly rainfall. The annual trend analysis of temperature and rainfall was carried out at agroecological zone level, while the survey was conducted at households' level representing three different (highland, midland, and lowland) AEZs. The Mann–Kendall trend analysis confirms that there was a significant upward trend in the annual minimum temperature across AEZs while the annual maximum temperature has exhibited both upward and downward trends.

Sen's slope confirms that the magnitude of change for the minimum temperature is faster than the maximum temperature both in time and space. The interannual variability of the annual maximum temperature suggests that AEZs have unveiled both warm and cool years during the 32 years, informing the recent years are warmer compared to the earlier years. The general warming trend observed in the study area agrees with empirical studies reported both at the national and local levels. The Mann–Kendall trend analysis reveals that there was an insignificant downward trend observed in the annual total rainfall both in the highland and lowland AEZs, whereas a significant upward trend was detected in the midland AEZ, indicating mixed results. Standardized rainfall anomaly confirms that the study AEZs have experienced many drought years between 1983 and 2014 that also fits to the nation's worst drought years.

The study established that farm households are becoming aware of local climate change more. Hence, farmers of Wolaita Zone have been facing the adverse impacts of climate variability and change as it impacted their lives and livelihoods over the last three decades. Results from the binary logit model inform that farmers' climate change perceptions are significantly influenced by their access to climate and market information, agroecology, education, agricultural input, and village market distance. The study concluded that farmers' perception of climate change reflects

the meteorological analysis, although their perceptions were grounded on local climate factors. Based on these results, it is recommended to enhance farm households' capacity by providing timely weather and climate information along with institutional actions, including agricultural extension services, farm input supplies, and viable livelihood diversification options. However, this study was limited in scope and sample size; it is suggested to undertake further studies at a larger scale to figure out the links between farmers' perceptions of climate change with meteorological data, in general, and explore socioeconomic and contextual factors affecting climate change perceptions, in particular.

Data Availability

The climate data used to support the findings of this study are available from the corresponding author upon request.

Conflicts of Interest

The authors declare that there are no conflicts of interest regarding the publication of this article.

Acknowledgments

The study was carried out with the financial support from both Wolaita Sodo University and Addis Ababa University as part of the first author's PhD program. The authors appreciate the National Meteorological Agency for providing the gridded daily temperature and precipitation data. The authors are thankful to local-level government offices, farmers, and enumerators for their time and cooperation during field data collection.

References

[1] Intergovernmental Panel on Climate Change (IPCC), "Climate Change 2013: The Physical Science Basis," in *Contribution of Working Group I to the Fifth Assessment Report of the Intergovernmental Panel on Climate Change*, T. F. Stocker, D. Qin, G.-K. Plattner et al., Eds., Cambridge University Press, Cambridge, UK, 2013.

[2] Intergovernmental Panel on Climate Change (IPCC), "Climate Change 2007: Impacts, Adaptation and Vulnerability," in *Contribution of Working Group II to the Fourth Assessment Report of the Intergovernmental Panel on Climate Change*, M. L. Parry, O. F. Canziani, J. P. Palutikof, P. J. van der Linden, and C. E. Hanson, Eds., Cambridge University Press, Cambridge, UK, 2007.

[3] Intergovernmental Panel on Climate Change (IPCC), "Climate change 2014: synthesis report," in *Contribution of Working Groups I, II and III to the Fifth Assessment Report of the Intergovernmental Panel on Climate Change Core Writing Team*, R. K. Pachauri and L. A. Meyer, Eds., IPCC, Geneva, Switzerland, 2014.

[4] A. Amsalu, W. Negatu, N. Canales Trujillo et al., *Climate Finance in Ethiopia,* 2014, https://www.odi.org/sites/odi.org.uk/files/odi-assets/publications-opinion-files/8995.pdf.

[5] E. Viste, D. Korecha, and A. Sorteberg, "Recent drought and precipitation tendencies in Ethiopia," *Theoretical and Applied Climatology*, vol. 112, no. 3-4, pp. 535–551, 2013.

[6] V. Ongoma and H. Chen, "Temporal and spatial variability of temperature and precipitation over East Africa from 1951 to 2010," *Meteorology and Atmospheric Physics*, vol. 129, no. 2, pp. 131–144, 2017.

[7] V. Ongoma, H. Chen, and G. W. Omony, "Variability of extreme weather events over the equatorial East Africa, a case study of rainfall in Kenya and Uganda," *Theoretical and Applied Climatology*, vol. 131, no. 1-2, pp. 295–308, 2018.

[8] B. T. Kassie, *Climate Variability and Change in Ethiopia: Exploring Impacts and Adaptation Options for Cereal Production*, Wageningen University, Wageningen, Netherlands, 2014.

[9] M. Keller, *Climate Risks and Development Projects, Assessment Report for a Community-Level Project in Guduru, Oromiya, Ethiopia. Bread for All,* 2009, https://www.iisd.org/cristaltool/documents/BFA-Ethiopia-Assessment-Report-Eng.pdf.

[10] C. McSweeney, M. New, and G. Lizcano, "UNDP climate change Country profiles Ethiopia," 2008, http://country-profiles.geog.ox.ac.uk.

[11] Ethiopian Environmental Protection Agency (EPA), "National report of Ethiopia," in *The United Nations Conference on Sustainable Development (Rio 20+)*, Ethiopian Environmental Protection Agency, Addis Ababa, Ethiopia, 2012.

[12] M. T. Niles, M. Lubell, and M. Brown, "How limiting factors drive agricultural adaptation to climate change," *Agriculture, Ecosystems & Environment*, vol. 200, pp. 178–185, 2015.

[13] S. J. Vermeulen, E. Grainger-Jones, and X. Yao, "Climate change, food security and small-scale producers. CCAFS info brief, CGIAR research program on climate change," *Agriculture and Food Security*, 2014, https://cgspace.cgiar.org/handle/10568/35215.

[14] S. B. Broomell, D. V. Budescu, and H.-H. Por, "Personal experience with climate change predicts intentions to act," *Global Environmental Change*, vol. 32, pp. 67–73, 2015.

[15] S. Tekleab, Y. Mohamed, and S. Uhlenbrook, "Hydro-climatic trends in the abay/upper blue Nile Basin, Ethiopia," *Physics and Chemistry of the Earth, Parts A/B/C*, vol. 61-62, pp. 32–42, 2013.

[16] T. G. Gebremicael, Y. A. Mohamed, G. D. Betrie, P. van der Zaag, and E. Teferi, "Trend analysis of runoff and sediment fluxes in the Upper Blue Nile basin: a combined analysis of statistical tests, physically-based models and landuse maps," *Journal of Hydrology*, vol. 482, pp. 57–68, 2013.

[17] D. Mengistu, W. Bewket, and R. Lal, "Recent spatiotemporal temperature and rainfall variability and trends over the upper blue nile river basin, Ethiopia," *International Journal of Climatology*, vol. 34, no. 7, pp. 2278–2292, 2014.

[18] C. Onyutha and P. Willems, "Spatial and temporal variability of rainfall in the Nile Basin," *Hydrology and Earth System Sciences*, vol. 19, no. 5, pp. 2227–2246, 2015.

[19] E. Teferi, S. Uhlenbrook, and W. Bewket, "Inter-annual and seasonal trends of vegetation condition in the Upper Blue Nile (Abay) Basin: dual-scale time series analysis," *Earth System Dynamics*, vol. 6, no. 2, pp. 617–636, 2015.

[20] M. Gedefaw, D. Yan, H. Wang et al., "Innovative trend analysis of annual and seasonal rainfall variability in Amhara regional state, Ethiopia," *Atmosphere*, vol. 9, no. 9, p. 326, 2018.

[21] T. M. Weldegerima, T. T. Zeleke, B. S. Birhanu, B. F. Zaitchik, and Z. A. Fetene, "Analysis of rainfall trends and its relationship with SST signals in the lake tana basin, Ethiopia," *Advances in Meteorology*, vol. 2018, Article ID 5869010, 10 pages, 2018.

[22] G. Eshetu, T. Johansson, and W. Garedew, "Rainfall trend and variability analysis in Setema-Gatira area of Jimma, South-western Ethiopia," *African Journal of Agricultural Research*, vol. 11, no. 32, pp. 3037–3045, 2016.

[23] T. G. Gebremicael, Y. A. Mohamed, P. v. Zaag, and E. Y. Hagos, "Temporal and spatial changes of rainfall and streamflow in the Upper Tekezē–Atbara river basin, Ethiopia," *Hydrology and Earth System Sciences*, vol. 21, no. 4, pp. 2127–2142, 2017.

[24] A. Hagos, K. Tesfaye, and A. J. Duncan, "Trends in daily observed temperature and precipitation extremes over three Ethiopian eco-environments," *International Journal of Climatology*, vol. 34, no. 6, pp. 1990–1999, 2014.

[25] Z. B. Weldegebriel and M. Prowse, "Climate variability and livelihood diversification in northern Ethiopia: a case study of Lasta and Beyeda districts," *Geographical Journal*, vol. 183, no. 1, pp. 84–96, 2017.

[26] G. Tadesse, M. Bekele, and B. Tesfaye, "Farmers' perceptions and adaptation strategies to climate change and variability the case of Kacha bira Woreda, Kembata tembaro zone, southern nations, Nationalities and peoples Ethiopia," *Journal of Environmental and Earth Science*, vol. 7, no. 3, pp. 52–61, 2017.

[27] A. Asfaw, B. Simane, A. Hassen, and A. Bantider, "Variability and time series trend analysis of rainfall and temperature in northcentral Ethiopia: a case study in Woleka sub-basin," *Weather and Climate Extremes*, vol. 19, pp. 29–41, 2018.

[28] M. A. Degefu and W. Bewket, "Variability and trends in rainfall amount and extreme event indices in the Omo-Ghibe River Basin, Ethiopia," *Regional Environmental Change*, vol. 14, no. 2, pp. 799–810, 2014.

[29] G. G. Wodaje, Z. Eshetu, and M. Argaw, "Temporal and spatial variability of rainfall distribution and evapotranspiration across altitudinal gradient in the Bilate River Watershed, Southern Ethiopia," *African Journal of Environmental Science and Technology*, vol. 10, no. 6, pp. 167–180, 2016.

[30] B. Esayas, B. Simane, E. Teferi, V. Ongoma, and N. Tefera, "Trends in extreme climate events over three agroecological zones of southern Ethiopia," *Advances in Meteorology*, vol. 2018, Article ID 7354157, 17 pages, 2018.

[31] T. T. Deressa, R. M. Hassan, and C. Ringler, "Perception of and adaptation to climate change by farmers in the Nile basin of Ethiopia," *Journal of Agricultural Science*, vol. 149, no. 1, pp. 23–31, 2011.

[32] G. Tesso, B. Emana, and M. Ketema, "A time series analysis of climate variability and its impacts on food production in North Shewa zone in Ethiopia," *African Crop Science Journal*, vol. 20, no. 2, pp. 261–274, 2012.

[33] S. Addisu, G. Fissha, B. Gediff, and Y. Asmelash, "Perception and adaptation models of climate change by the rural people of lake Tana Sub-Basin, Ethiopia," *Environmental Systems Research*, vol. 5, no. 1, pp. 1–10, 2016.

[34] P. Asrat and B. Simane, "Farmers' perception of climate change and adaptation strategies in the Dabus watershed, North-West Ethiopia," *Ecological Processes*, vol. 7, no. 1, pp. 7–13, 2018.

[35] B. Legesse, Y. Ayele, and W. Bewket, "Smallholder farmers' perceptions and adaptation to climate variability and climate change in Doba district, west Hararghe, Ethiopia," *Asian Journal of Empirical Research*, vol. 3, no. 3, pp. 251–265, 2013.

[36] N. Debela, C. Mohammed, K. Bridle, R. Corkrey, and D. McNeil, "Perception of climate change and its impact by smallholders in pastoral/agropastoral systems of Borana, South Ethiopia," *SpringerPlus*, vol. 4, no. 1, p. 236, 2015.

[37] G. Hadgu, K. Tesfaye, G. Mamo, and B. Kassa, "Farmers climate change adaptation options and their determinants in Tigray Region, Northern Ethiopia," *African Journal of Agricultural Research*, vol. 10, no. 9, pp. 956–964, 2015.

[38] L. T. Habtemariam, M. Gandorfer, G. A. Kassa, and A. Heissenhuber, "Factors influencing smallholder farmers' climate change perceptions: a study from farmers in Ethiopia," *Environmental Management*, vol. 58, no. 2, pp. 343–358, 2016.

[39] M. G. Abrha and S. Simhadri, "Local climate trends and farmers' perceptions in Southern Tigray, Northern Ethiopia," *American Journal of Environmental Sciences*, vol. 11, no. 4, pp. 262–277, 2017.

[40] S. Bedeke, W. Vanhove, M. Gezahegn, K. Natarajan, and P. Van Damme, "Adoption of climate change adaptation strategies by maize-dependent smallholders in Ethiopia," *NJAS-Wageningen Journal of Life Sciences*, vol. 88, pp. 96–104, 2019.

[41] L. Silici, *Agroecology-What it is and What it has to Offer*, Issue Paper 14629IIED, International Institute for Environment and Development, London, UK, 2014.

[42] Y. Gecho, G. Ayele, T. Lemma, and D. Alemu, "Rural household livelihood strategies: options and determinants in the case of Wolaita Zone, Southern Ethiopia," *Social Sciences*, vol. 3, no. 3, pp. 92–104, 2014.

[43] H. Hurni, "Agroecological belts of Ethiopia: explanatory notes on three maps at a scale of 1: 1,000,000," in *Soil Conservation Research Program of Ethiopia, Addis Ababa, Ethiopia*, Wittwer Druck AG, Bern, Switzerland, 1998.

[44] Central Statistical Agency (CSA), *Report on Area and Production of Major Crops 584, The Federal Democratic Republic of Ethiopia*, Statistical Bulletin, Addis Ababa, Ethiopia, 2016.

[45] D. Boansi, J. A. Tambo, and M. Müller, "Analysis of farmers' adaptation to weather extremes in West African Sudan Savanna," *Weather and Climate Extremes*, vol. 16, pp. 1–13, 2017.

[46] C. R. Kothari, *Research Methodology: Methods and Techniques*, New Age International, New Delhi, India, 2004.

[47] L. Alexander, H. Yang, and S. Perkins, "ClimPACT—indices and software," in *User Manual*, 2018, http://www.wmo.int/pages/prog/wcp/ccl/opace/opace4/meetings/documents/ETCRSCI_software_documentation_v2a.doc.

[48] P. Bazeley, "Analysing qualitative data: more than 'identifying themes'," *Malaysian Journal of Qualitative Research*, vol. 2, no. 2, pp. 6–22, 2009.

[49] H. B. Mann, "Nonparametric tests against trend," *Econometrica*, vol. 13, no. 3, pp. 245–259, 1945.

[50] M. G. Kendall, "A new measure of rank correlation," *Biometrika*, vol. 30, no. 1-2, pp. 81–93, 1938.

[51] P. K. Sen, "Estimates of the regression coefficient based on Kendall's tau," *Journal of the American Statistical Association*, vol. 63, no. 324, pp. 1379–1389, 1968.

[52] H. Theil, "A rank-invariant method of linear and polynominal regression analysis (Parts 1-3)," *Proceedings of the Koninklijke Nederlandse Akademie van Wetenschappen Series A*, vol. 53, pp. 1397–1412, 1950.

[53] W. Bewket and D. Conway, "A note on the temporal and spatial variability of rainfall in the drought-prone Amhara region of Ethiopia," *International Journal of Climatology*, vol. 27, no. 11, pp. 1467–1477, 2007.

[54] M. Svoboda, M. Hayes, and D. Wood, *Standardized Precipitation Index User Guide*, World Meteorological Organization, Geneva, Switzerland, 2012.

[55] J. E. Oliver, "Monthly precipitation distribution: a comparative index," *Professional Geographer*, vol. 32, no. 3, pp. 300–309, 1980.

[56] H. K. Ndambiri, C. Ritho, S. G. Mbogoh et al., "Analysis of farmers' perceptions of the effects of climate change in Kenya: the case of Kyuso district," *Analysis*, vol. 2, no. 10, pp. 74–83, 2012.

[57] E. Bryan, C. Ringler, B. Okoba, C. Roncoli, S. Silvestri, and M. Herrero, "Adapting agriculture to climate change in Kenya: household strategies and determinants," *Journal of environmental management*, vol. 114, pp. 26–35, 2013.

[58] M. L. Amadou, G. B. Villamor, E. M. Attua, and S. B. Traoré, "Comparing farmers' perception of climate change and variability with historical climate data in the Upper East Region of Ghana," *Ghana Journal of Geography*, vol. 7, no. 1, pp. 47–74, 2015.

[59] D. N. Gujarati, *Basic Econometrics*, Tata McGraw-Hill Education, New York, NY, USA, 2009.

[60] M. Abid, J. Scheffran, U. A. Schneider, and E. Elahi, "Farmer perceptions of climate change, observed trends and adaptation of agriculture in Pakistan," *Environmental Management*, vol. 63, no. 1, pp. 110–123, 2019.

[61] National Meteorological Agency of Ethiopia (NMA), *Climate Change National Adaptation Programme of Action (NAPA) of Ethiopia*, National Meteorological Services Agency, Ministry of Water Resources, Federal Democratic Republic of Ethiopia, Addis Ababa, Ethiopia, 2007.

[62] D. Conway, C. Mould, and W. Bewket, "Over one century of rainfall and temperature observations in Addis Ababa, Ethiopia," *International Journal of Climatology*, vol. 24, no. 1, pp. 77–91, 2004.

[63] G. Worku, E. Teferi, A. Bantider, and Y. T. Dile, "Observed changes in extremes of daily rainfall and temperature in Jemma sub-basin, upper blue Nile basin, Ethiopia," *Theoretical and Applied Climatology*, vol. 135, no. 3–4, pp. 839–854, 2019.

[64] P. A. O. Omondi, J. L. Awange, E. Forootan et al., "Changes in temperature and precipitation extremes over the Greater Horn of Africa region from 1961 to 2010," *International Journal of Climatology*, vol. 34, no. 4, pp. 1262–1277, 2014.

[65] P. Camberlin, "Temperature trends and variability in the Greater Horn of Africa: interactions with precipitation," *Climate Dynamics*, vol. 48, no. 1-2, pp. 477–498, 2017.

[66] R. S. Vose, D. R. Easterling, and B. Gleason, "Maximum and minimum temperature trends for the globe: an update through 2004," *Geophysical Research Letters*, vol. 32, no. 23, 2005.

[67] D. R. Easterling, G. Byron, R. S. Vose, and R. J. Stouffer, "A comparison of model produced maximum and minimum temperature trends with observed trends for the 20th and 21st centuries," in *Proceedings of the 18th Conference on Climate variability and Change*, San Antonio, TX, USA, 2006.

[68] T. C. Peterson, M. A. Taylor, R. Demeritte et al., "Recent changes in climate extremes in the Caribbean region," *Journal of Geophysical Research: Atmospheres*, vol. 107, no. D21, p. 4601, 2002.

[69] D. Ayalew, K. Tesfaye, G. Mamo, B. Yitaferu, and W. Bayu, "Variability of rainfall and its current trend in Amhara region, Ethiopia," *African Journal of Agricultural Research*, vol. 7, no. 10, pp. 1475–1486, 2012.

[70] H. Gebre, T. Kindie, M. Girma, and K. Belay, "Trend and variability of rainfall in Tigray, northern Ethiopia: analysis of meteorological data and farmers' perception," *Academia Journal of Agricultural Research*, vol. 1, no. 6, pp. 88–100, 2013.

[71] T. B. McKee, N. J. Doesken, and J. Kleist, "The relationship of drought frequency and duration to time scales," in *Proceedings of the 8th Conference on Applied Climatology*, American Meteorological Society, Boston, MA, USA, 1993.

[72] G. W. Kibue, X. Liu, J. Zheng et al., "Farmers' perceptions of climate variability and factors influencing adaptation: evidence from Anhui and Jiangsu, China," *Environmental Management*, vol. 57, no. 5, pp. 976–986, 2016.

[73] A. Han, M. Radeny, and J. F. Morton, "Comparing smallholder farmers' perception of climate change with meteorological data: a case study from Southwestern Nigeria," *Weather and Climate Extremes*, vol. 15, pp. 24–33, 2017.

[74] M. Y. Mkonda, X. He, and E. S. Festin, "Comparing smallholder farmers' perception of climate change with meteorological data: experience from seven agroecological zones of Tanzania," *Weather, Climate, and Society*, vol. 10, no. 3, pp. 435–452, 2018.

[75] M. Shwartz, *Majority of Americans Continue to Believe that Global Warming is Real*, Woods Institute for the Environment, Stanford, CA, USA, 2010, http://woods.stanford.edu/docs/surveys/Krosnick-20090312.pdf.

[76] T. S. Saguye, "Farmers' perception of climate variability and change and its implication for implementation of climate-smart agricultural practices," *American Journal of Human Ecology*, vol. 6, no. 1, pp. 27–41, 2017.

[77] M. A. Degefu, D. P. Rowell, and W. Bewket, "Teleconnections between Ethiopian rainfall variability and global SSTs: observations and methods for model evaluation," *Meteorology and Atmospheric Physics*, vol. 129, no. 2, pp. 173–186, 2017.

[78] A. Amsalu and A. Adem, *Assessment of Climate Change-Induced Hazards, Impacts and Responses in the Southern Lowlands of Ethiopia*, Forum for Social Studies (FSS), Washington, DC, USA, 2009, http://hdl.handle.net/123456789/3075.

[79] World Bank, *Ethiopia: Economics of Adaptation to Climate Change*, The World Bank Group, Washington, DC, USA, 2010.

[80] G. J. Y. You and C. Ringler, *Hydro-Economic Modeling of Climate Change Impacts in Ethiopia (No. 960)*, International Food Policy Research Institute (IFPRI), Washington, DC, USA, 2010.

[81] Food and Agricultural organization (FAO), *FAO in Ethiopia El Niño Response Plan 2016*, 2016, https://reliefweb.int/report/ethiopia/fao-ethiopia-el-ni-o-response-plan-2016.

[82] Central Statistical Agency (CSA), *Federal Democratic Republic of Ethiopia (FDRE). Population Projection of Ethiopia for all Regions: At Wereda level from 2014–2017*, CSA, Addis Ababa, Ethiopia, 2013.

[83] Ethiopian Panel of Climate Change (EPCC), "First assessment report, working group II agriculture and food security," Ethiopian Academy of Sciences, Addis Ababa, Ethiopia, 2015.

[84] Z. Liu, W. J. Smith, and A. S. Safi, "Rancher and farmer perceptions of climate change in Nevada, USA," *Climatic Change*, vol. 122, no. 1-2, pp. 313–327, 2014.

[85] J. A. Yaro, "The perception of and adaptation to climate variability/change in Ghana by small-scale and commercial farmers," *Regional Environmental Change*, vol. 13, no. 6, pp. 1259–1272, 2013.

Hindawi
Advances in Meteorology
Volume 2019, Article ID 1930453, 12 pages
https://doi.org/10.1155/2019/1930453

Research Article

Impact of Sea Surface Temperature and Surface Air Temperature on Maximizing Typhoon Rainfall: Focusing on Typhoon Maemi in Korea

Jeonghyeon Choi,[1] **Jeonghoon Lee**,[2] **and Sangdan Kim**[3]

[1]*Division of Earth Environmental System Science (Major in Environmental Engineering), Pukyong National University, Busan 48513, Republic of Korea*
[2]*Department of Civil and Environmental Engineering, Cleveland State University, Cleveland, OH 44115, USA*
[3]*Department of Environmental Engineering, Pukyong National University, Busan 48513, Republic of Korea*

Correspondence should be addressed to Sangdan Kim; skim@pknu.ac.kr

Received 28 February 2019; Revised 29 April 2019; Accepted 15 May 2019; Published 29 May 2019

Guest Editor: Sushil K. Dash

In this study, the effects of surface air temperature (SAT) and sea surface temperature (SST) changes on typhoon rainfall maximization are analysed. Based on the numerically reproduced Typhoon Maemi, this study tried to maximize the typhoon-induced rainfall by increasing the amount of saturated water vapour in the atmosphere and the amount of water vapour entering the typhoon. Using the Weather Research and Forecasting (WRF) model, which is one of the regional climate models (RCMs), the rainfall simulated by WRF while increasing the SAT and SST to various sizes at initial conditions and boundary conditions of the model was analysed. As a result of the simulated typhoon rainfall, the spatial distribution of total rainfall depth on the land due to the increase combination of SAT and SST showed a wide variety without showing a certain pattern. This is attributed to the geographical location of the Korean peninsula, which is a peninsula between the continent and the ocean. In other words, under certain conditions, typhoons may drop most of the rainfall on the southern sea of the peninsula before landing on the peninsula. For instance, the 6-hour duration maximum precipitation (MP) in Busan Metropolitan City was 472.1 mm when the SST increased by 2.0°C. However, when the SST increased by 4.0°C, the MP was found to be 395.3 mm, despite the further increase in SST. This indicates that the MP at a particular area and the increase in temperature do not have a linear relationship. Therefore, in order to maximize typhoon rainfall, it is necessary to repeat the numerical experiment on various conditions and search for the combination of SAT and SST increase which is most suitable for the target typhoon.

1. Introduction

The probable maximum precipitation (PMP) is defined as the maximum amount of precipitation that can occur physically for a specific duration in a particular area [1, 2]. The most widely applied method for estimating PMP is the hydrometeorological method, which statistically considers physical relationships with observational meteorological variables such as rainfall, dew point, and wind speed based on long-term observed weather data [3]. However, this PMP calculation method has a problem that it relies heavily on observation data [4]. It has been also reported that the physical relationship between the meteorological variables applied to the PMP estimation might not adequately reflect the processes of very complex atmosphere and precipitation [5].

In order to overcome the limitations of the PMP estimation method, researches for estimating the PMP using the regional climate model (RCM) have been conducted recently. In particular, Ohara et al. [6] and Ishida et al. [7–9] have proposed a method of maximizing rainfall occurred in the past by linking the spatial shifting of climate variables, maximizing relative humidity (RH), and increasing surface air temperature (SAT) using the fifth-generation Penn State/NCAR mesoscale model (MM5). In Korea, studies have been

carried out to estimate PMP by controlling climate variables using the Weather Research and Forecasting (WRF) model for Typhoon Rusa [10]. All of these studies commonly apply the method of maximizing the rainfall by changing the meteorological parameters of the initial and boundary conditions of the model after numerically reproducing the past rainfall events. Because RCM is used, the complex process of the atmosphere can be taken into consideration, and the dependence on observation data is relatively low compared to the existing PMP estimation method [9].

Due to global warming, SAT is increasing, and sea surface temperature (SST) is also increasing [11]. In particular, it is observed that the intensity of typhoon is getting stronger due to the rise of SST near the Western Pacific. In addition, since the warm pool around the Indian Ocean and the Pacific is expanded and the SST of the typhoon route approaching East Asia and Southeast Asia is increasing, the intensity of the typhoon is increasing, and the maximum reaching position of the typhoon is also rising [12]. It is also reported that the increase in SST around the Korean peninsula (especially during the summer season) affects the intensity of typhoons landing in China, Taiwan, Japan, Korea, and the Philippines [13]. If the increase in SAT and SST continues due to climate change, the intensity of typhoons generated in the Western Pacific will also increase gradually [14–17].

In fact, typhoons Rusa, Maemi, and Chaba, which had a great impact on the Korean peninsula in the past, suffered great damage because of the abnormally high SST, which caused the typhoon to land on the Korean peninsula while maintaining strong forces. Since the increase in the heat capacity of the surrounding ocean due to global warming and the rise of SST are likely to increase the energy supply of the typhoon, the potential risk of landing a super typhoon on the Korean peninsula is increasing gradually [18].

This study tried to maximize the rainfall by using WRF for the physical PMP estimation. The study was conducted based on the Maemi, a typhoon reproduced by Choi et al. [19] through the improvement of initial conditions and boundary conditions. Among the initial conditions and boundary conditions of WRF, this study tried to maximize typhoon rainfall by adjusting SAT, SST, and RH. The sensitivity of typhoon rainfall to SAT and SST increase by simulating typhoons in various SAT and SST conditions was also analysed.

2. Materials and Methods

2.1. Target Typhoon and Model Construction. Typhoon Maemi was a typhoon in September 2003 and landed on the Korean Peninsula, maintaining its maximum strength during the typhoon's life cycle, unlike most typhoons that affected the Korean peninsula. Recorded heavy rain and strong winds were generated because the Typhoon Maemi landed on the Korean peninsula with a steady supply of energy from the ocean due to abnormally high SST. Especially, although the Korean peninsula had been affected for a relatively short period of time, total rainfall depth of 100~450 mm was recorded in the southeastern part of the Korean peninsula. As a result, most of the Republic of Korea has been declared as a special disaster area, resulting in 131 deaths and missing persons and an enormous property damage of approximately KRW 4.2 trillion [20].

Choi et al. [19] numerically reproduced the Typhoon Maemi's rainfall by improving the initial conditions and boundary conditions through the observation data assimilation and the typhoon initialization technique using WRF. This study tried to maximize rainfall on land by typhoon based on reproduced Typhoon Maemi. WRF was composed of three domains considering the landing direction of the typhoon and the location of major rainfall. The horizontal resolution of each domain was set to 27 km, 9 km, and 3 km, respectively. In addition, a combination of physical options optimized by Choi et al. [19] was applied to this study. The details of the model are shown in Table 1. Figure 1 shows the spatial distribution of total rainfall depth reproduced by Choi et al. [19] and the spatially averaged rainfall time series in the southeastern part of the Korean peninsula.

2.2. Typhoon Rainfall Maximization. Typhoons, which generally land on the Korean peninsula, are supplied with energy sources in the Western Pacific and expand northward. At this time, the high SST plays an important role in raising the typhoon rainfall by increasing the amount of water vapour supplied to the typhoon. In addition, the high SAT affects the increase in saturated water vapour in the atmosphere. In other words, if the amount of saturated water vapour in the atmosphere is increased by the high SAT, and a large amount of water vapour is introduced into the typhoon due to the high SST, a great deal of rainfall is likely to occur.

Therefore, this study tried to maximize typhoon rainfall by increasing SAT, SST, and RH among climate variables closely related to rainfall. SAT will increase the amount of saturated water vapour in the atmosphere, SST will increase the amount of water vapour supplied to the typhoon, and additionally high RH will increase the amount of rainfall generated. Especially, considering the increase of SAT and SST due to global warming plays a major role in strengthening the typhoon's power, the increase of SAT and SST will have a great influence on the estimation of extreme rainfall in the future considering climate change.

To maximize the typhoon, the SAT and SST of the initial conditions and boundary conditions of the WRF were increased (see Figure 2(a)). However, since these two variables alone were not enough to generate the PMP, which is the physical upper limit of the rainfall, the RH of the boundary condition for entering the typhoon in Domain 3 was set to 100% (see Figure 2(b)). For reference, as a result of several numerical experiments, in the case that the RH of the boundary condition in all directions was set to 100%, the water vapour of the typhoon was saturated early and most of the rainfall occurred in the East China Sea before the typhoon landed on the peninsula. This caused very little rainfall on land. In order to prevent this simulation result, the RH of the south boundary condition of Domain 3 was changed for a specific time, as shown in Table 2, in consideration of the typhoon route and location.

Figure 3 shows the procedure performed in this study to maximize the amount of rainfall caused by Typhoon Maemi.

Table 1: Summary of the WRF model configuration [19].

Model version	WRF V3.6.1		
Domain	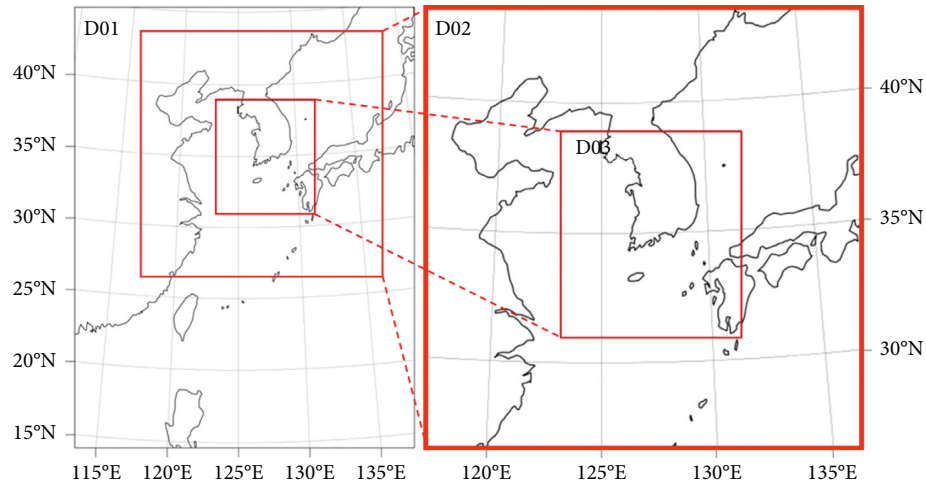		
	D01	D02	D03
Horizontal grid size	27 km × 27 km	9 km × 9 km	3 km × 3 km
Dimension	98 × 127 × 31	208 × 211 × 31	256 × 292 × 31
Microphysics	Ferrier (new Eta) microphysics, operational high-resolution window		
Cumulus parameterization	Betts–Miller–Janjic scheme		
Planetary boundary layer	Yonsei University scheme		
Land surface model	Noah land surface model		
Integration period	0000 UTC 11 to 0000 UTC 14 September 2003		

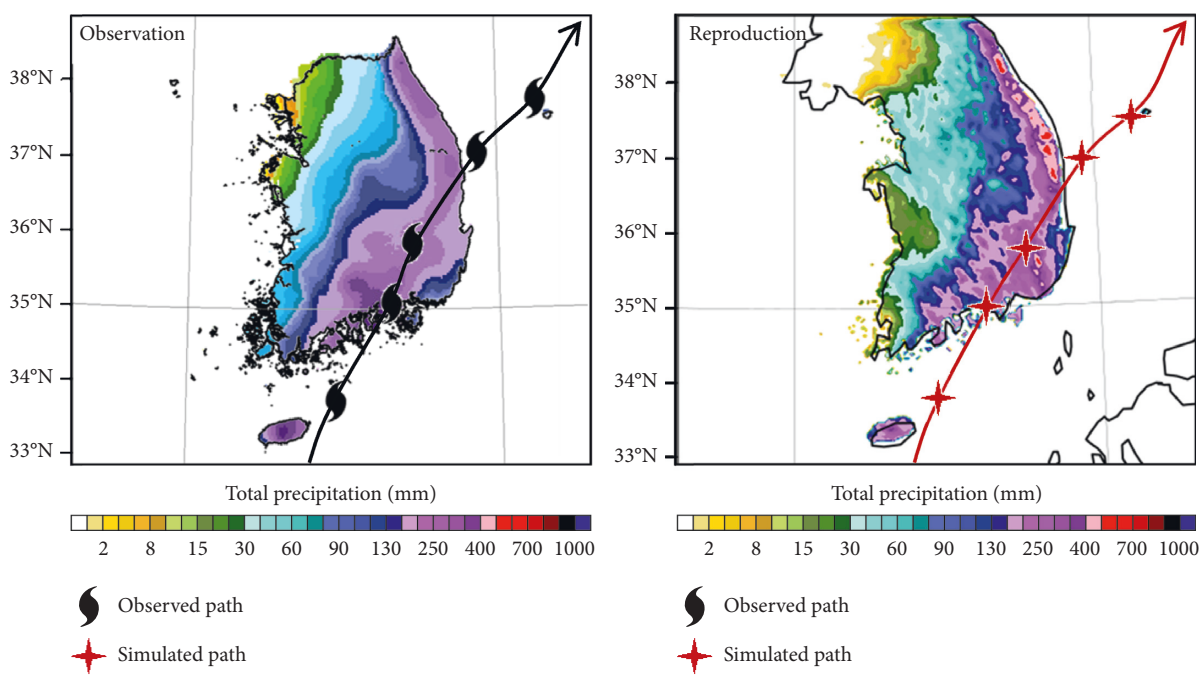

(a)

Figure 1: Continued.

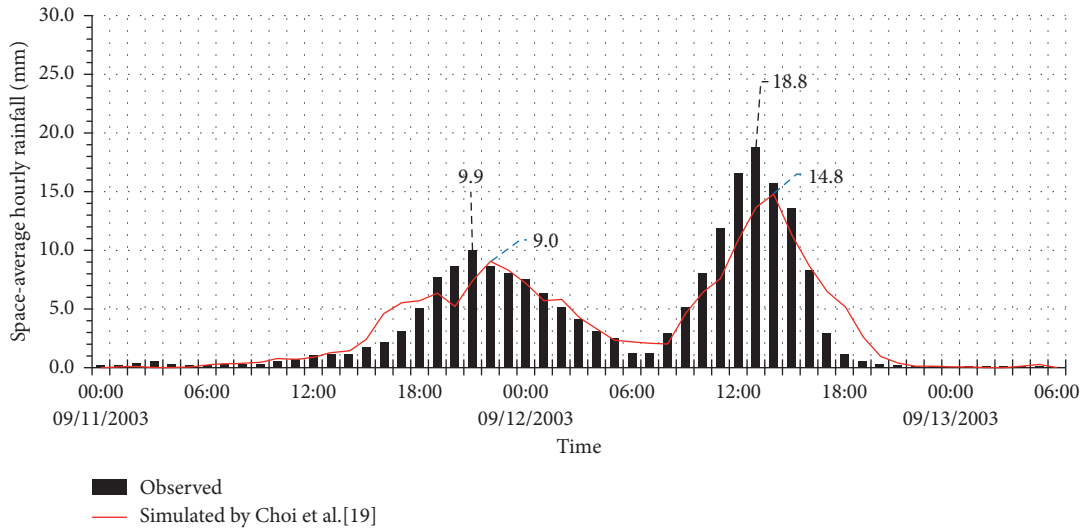

(b)

Figure 1: Comparison of observed and simulated (a) total accumulated rainfall depth and (b) hourly rainfall time series in the southeastern part of the Korean peninsula, which is the major damaged area by Typhoon Maemi [19].

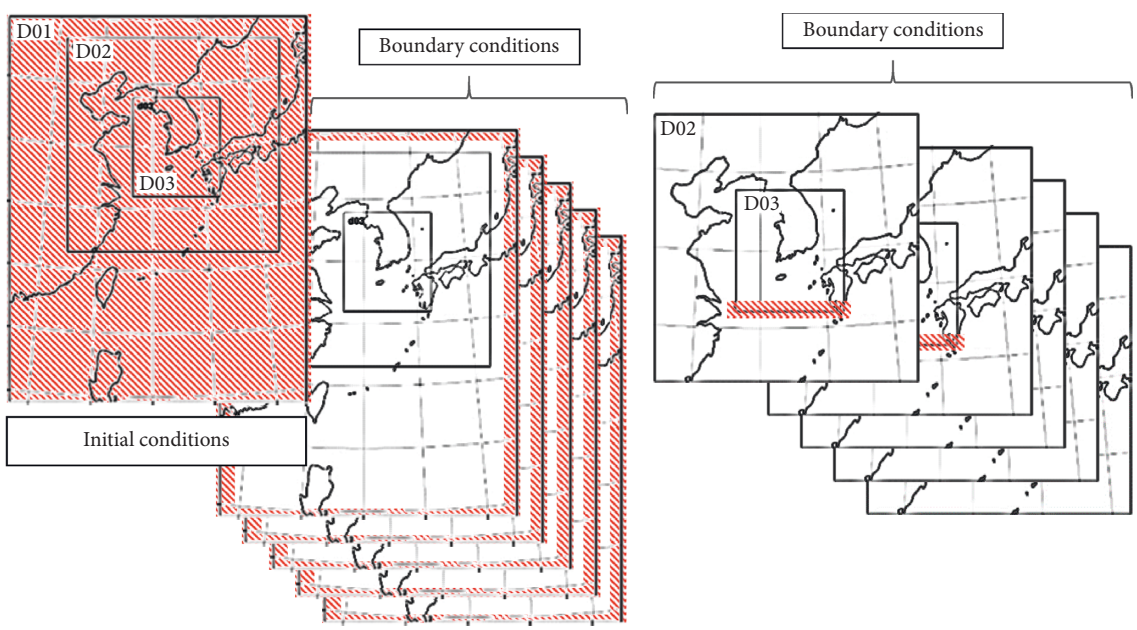

(a) (b)

Figure 2: Change in initial and boundary conditions for (a) increase of SAT and SST and (b) maximization of RH.

Table 2: Modification of RH in the south boundary condition.

Time	Before 06:00 (11-09-2003)	06:00	12:00	18:00	00:00 (12-09-2003)	06:00	After 06:00 (12-09-2003)
RH	Original condition	100%	100%	100%	100%	100%	Original condition

First, after increasing SAT and SST of the initial condition and boundary condition of each domain, Domain 1 and Domain 2 were simulated. The RHs of the grids corresponding to the south boundary condition of Domain 3 in the simulated Domain 2 were modified to 100%. The ndown method was then used to create a new boundary condition for Domain 3 from the modified Domain 2 results. The ndown method, built into the WRF model, is a function used for one-way nesting, which typically generates a lower domain boundary condition for the finer-grid resolution run using the results of the coarse-grid resolution run (upper domain). In this study, the boundary condition file of Domain 3 with RH of 100% in south

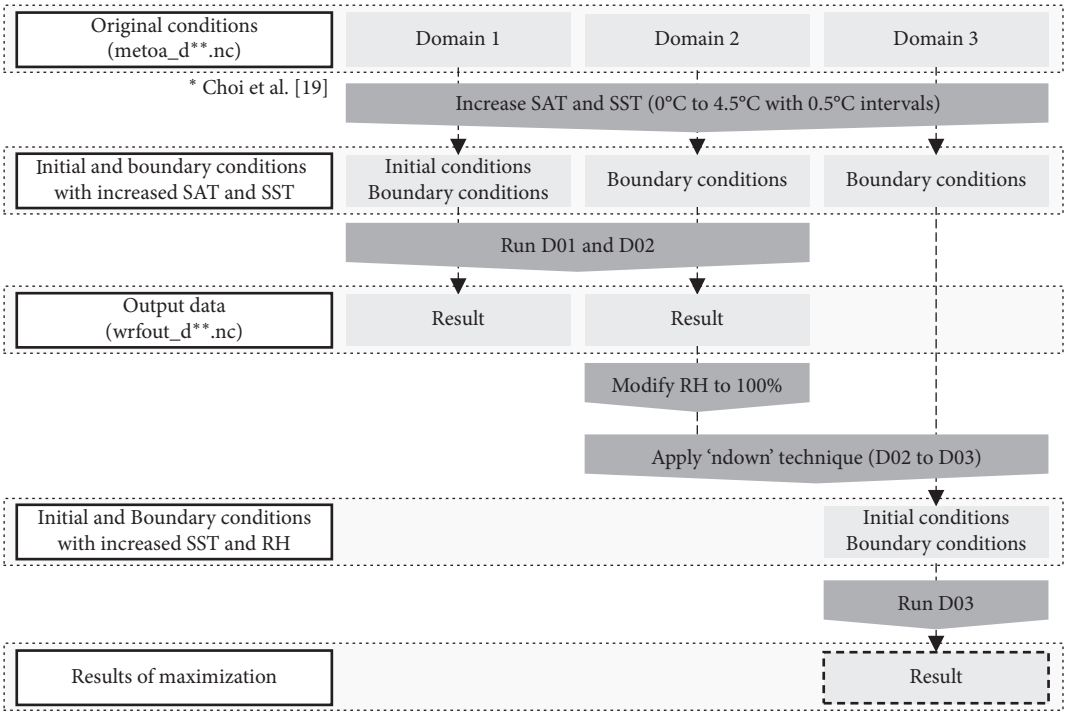

Figure 3: Procedure for maximizing Typhoon Maemi.

boundary was obtained by ndown method. For a more detailed description of the ndown method, see [21]. For reference, MATLAB was used to modify the SAT and SST of the initial and boundary conditions and the RH of the Domain 2 result.

2.3. Sensitivity Analysis and Maximum Precipitation Estimation. In order to examine the effect of increasing SAT and SST on the maximization of typhoon rainfall, numerical experiments were carried out by varying the SAT and SST increments (see Figure 4). Numerical experiments consisted of a total of 100 combinations, with SAT and SST increasing 0.5°C from 0°C to 4.5°C, respectively, with RH set at 100%, as shown in Table 2. From the results of these numerical experiments, the effect of increasing SAT and SST on the total rainfall and spatial distribution of rainfall was analysed.

In fact, Singh and Oh [22] increased the Indian Ocean's monthly mean SST by 0.6°C in their study to investigate the impact of the interannual variability of Indian Ocean SST anomaly on Indian summer monsoon precipitation. However, this study focuses on maximizing the amount of rainfall caused by a specific typhoon event, not the amount of rainfall during the entire summer season, and the target area is also a relatively small local area consisting of sea and land around the Korean peninsula. Therefore, it is necessary to reflect the extreme change range that can occur temporarily, not the average increase in the SST increase range. For reference, Ishida et al. [9] changed the SAT from 0.0°C to 8.0°C to maximize precipitation for rainfall events over the American River watershed in Northern California. The SAT range in this study was set up with reference to Ishida et al. [9]. The range of increase in SST was also set from 0.0°C to 4.5°C. In 2018, the SST on the East and the Yellow Sea of the Korean Peninsula temporarily increased by 2.0°C to 4.0°C due to extreme heat wave events [23].

Finally, the proposed typhoon rainfall maximization procedure was applied to maximize the rainfall event by Typhoon Maemi, and then, the maximized rainfall depth was calculated for each duration of the Busan Metropolitan City in the southeast of the Korean Peninsula (see Figure 5). Maximized rainfall depth estimated in this study is defined as maximum precipitation (MP) for distinction from PMP estimated by hydrologic meteorological method. MP and PMP estimated by hydrometeorological method reported by Lee et al. [3] were compared.

3. Results and Discussion

3.1. Sensitivity of Total Rainfall Depth. Before estimating MP, the effects of increased SAT, SST, and RH on typhoon rainfall were explored. As shown in Figure 6, the sensitivity of the total rainfall depth occurred in the entire Domain 3 and the sensitivity of the total rainfall depth occurred in the land area of the Domain 3 were analysed.

In Figure 6, from the comparison of the results of reproduction with the results of the increase in RH alone (SAT + 0.0°C and SST + 0.0°C), it can be found that the amount of rainfall on the entire Domain 3 or land increases with increasing RH. Therefore, it can be seen that RH plays an important role in maximizing the amount of rainfall caused by typhoons. However, the effects of SAT and SST on the maximization of rainfall caused by typhoons have been somewhat complicated.

The amount of rainfall in the entire Domain 3 shows an increasing pattern as SAT or SST increases (see Figure 6(a)). As the SAT increases for the same SST, the rainfall also

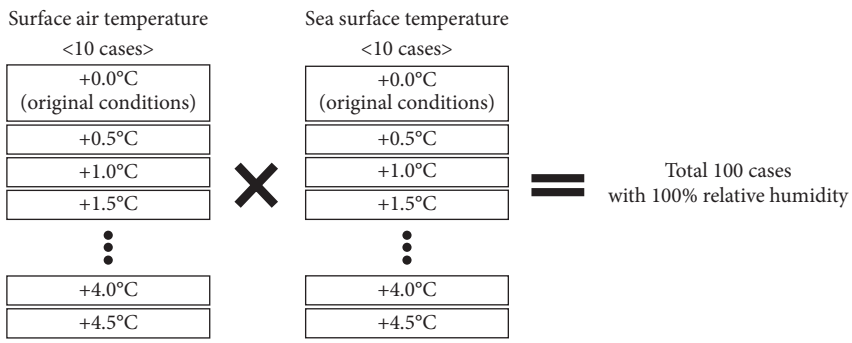

Figure 4: Composition of numerical experiments on SAT and SST incremental combinations.

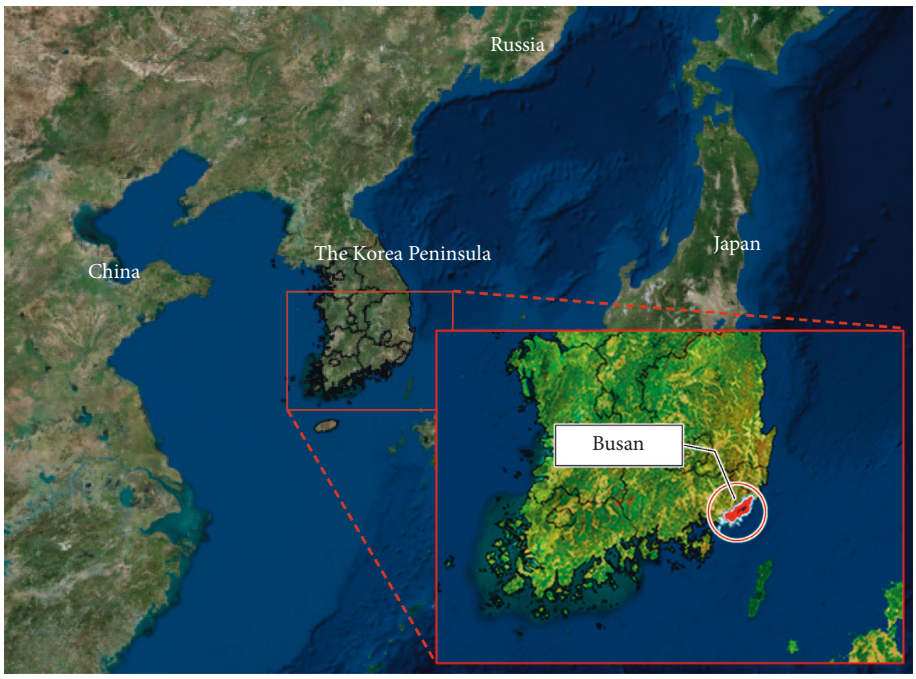

Figure 5: Location of Busan metropolitan.

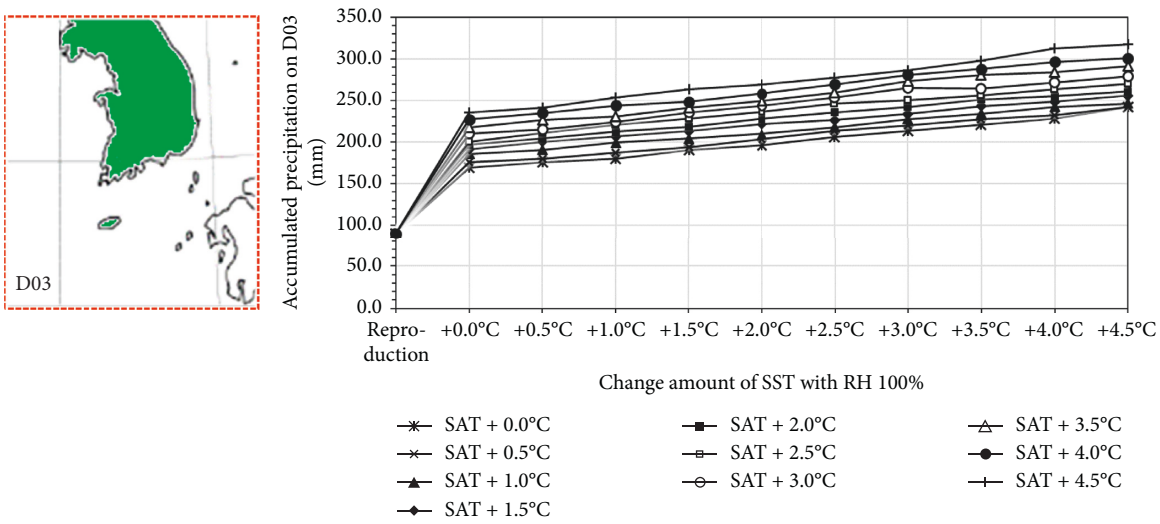

(a)

Figure 6: Continued.

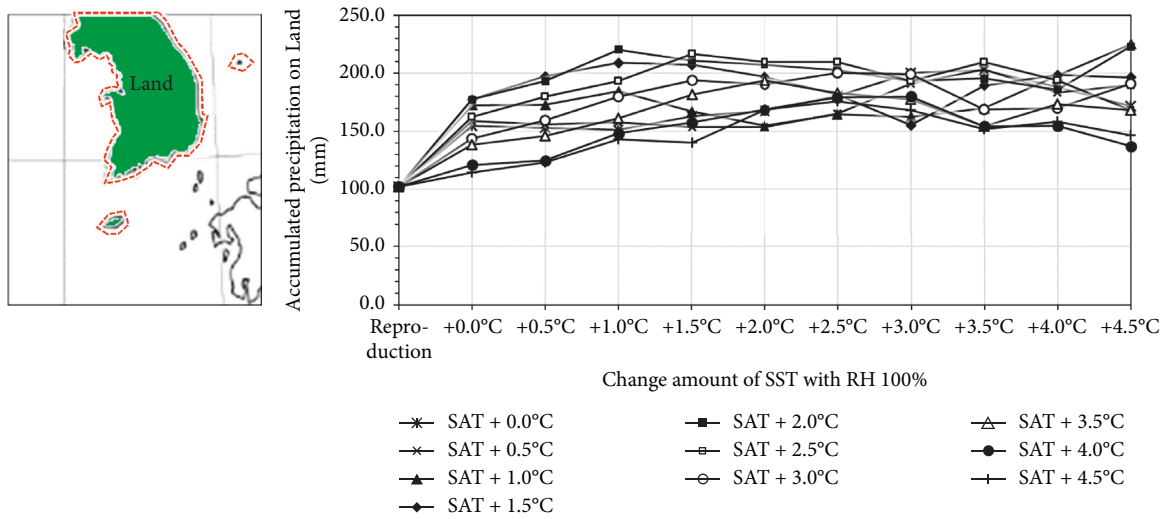

(b)

Figure 6: Comparison of accumulated rainfall depth on (a) the entire D03 and (b) the land area of D03 for SAT and SST increases.

increases. As the SST increases for the same SAT, the rainfall also increases.

On the other hand, rainfall on land did not show a consistent relationship with SAT or SST increase. As shown in Figure 6(b), although the SAT or SST increases, the amount of rainfall decreases. For instance, in the case that the SST is increased from 0°C to 2.5°C while SAT is fixed at 4.0°C increase (SAT + 4.0°C), the rainfall gradually increases. However, in the case that the SST is further increased, the rainfall decreases inversely. Also, it can be seen that the sensitivity of rainfall to the increase of SAT is very difficult to find a definite pattern.

3.2. Sensitivity of Spatial Distribution. As described in Section 3.1, the spatial distribution of total rainfall depth was examined in order to investigate the cause of the decrease in rainfall despite the increase of SAT or SST. Figure 7 shows some of the simulations of all combinations for SAT and SST increase. Similar to the observed data (see Figure 1(a)), it was observed that large rainfall occurred in the southeastern part of the Korean peninsula along the path of the typhoon.

Also, as the SAT and SST increase, the total rainfall depth increases. In the case of the same SAT increase, it was found that the total rainfall depth and range increase in the order of SST increment of 0.0°C (Figures 7(a)–7(d)), 1.5°C (Figures 7(e)–7(h)), 3.0°C (Figures 7(i)–7(l)), and 4.5°C (Figures 7(m)–7(p)) for each SAT increase. The increase in rainfall due to the increase in SST can also be found by the same method.

However, the spatial distribution of total rainfall varied somewhat by SAT/SST increase combination. In particular, it can be seen that the location of the maximum rainfall and the amount of rainfall in the ocean were greatly changed depending on which SAT/SAT increase combination was applied. Comparing the combination of 100% RH/SAT 3°C increase/SST 3°C increase (see Figure 7(k)) and the combination of 100% RH only (see Figure 7(a)), it can be seen that the amount of rainfall on the land had increased greatly in the southeast region of the peninsula as well as the increase in the amount of rainfall in the ocean. On the other hand, in the combination of RH 100%/SAT 4.5°C increase (see Figure 7(d)), a lot of rainfall occurred in the southern sea of the peninsula, and the total rainfall was large, but the amount of rainfall on land was reduced. In other words, it was found that the spatial distribution of total rainfall depth varies greatly depending on which SAT increase/SST increase combination was applied, and the amount of rainfall on the land and its spatial pattern were influenced by how much rainfall occurred on the ocean before typhoon arrived on land. This is probably because the physics-based RCM reflects the interaction of the surface with the atmosphere relatively accurately.

3.3. Effect on Point Rainfall for Busan Metropolitan. In this study, to analyse the effect of SAT and SST on the rainfall of a specific area, the analysis was performed on Busan Metropolitan City, which was the main damage area caused by Typhoon Maemi, located in the southeast of the Korean peninsula. For comparison with PMP proposed by Lee et al. [3], MP was calculated using the spatially averaged rainfall of three grids of Domain 3 (i.e., the impact area is 27 km^2). In addition, since the simulation results using the nesting grid system were generated from the input data composed of low resolution, it was not proper to calculate the MP by designating three specific grids included in Busan Metropolitan City. Therefore, in this study, maximum simulated rainfall in the range of 27 km^2 for each combination of SAT/SST in Busan metropolitan area was regarded as MP. Figure 8 shows the estimated MP corresponding to the SAT/SST increment combination for various durations (1 hour and 6, 12, and 24 hours).

As can be seen in Figure 8, the MP of Busan Metropolitan City was not consistently proportional to the increase of SAT or SST. The influence of the SAT/SST increase combination applied on the result of MP was also changed depending on the duration. For instance, in the case of a short duration, the MP of SST 2.0°C increase combination (i.e., 472.1 mm for

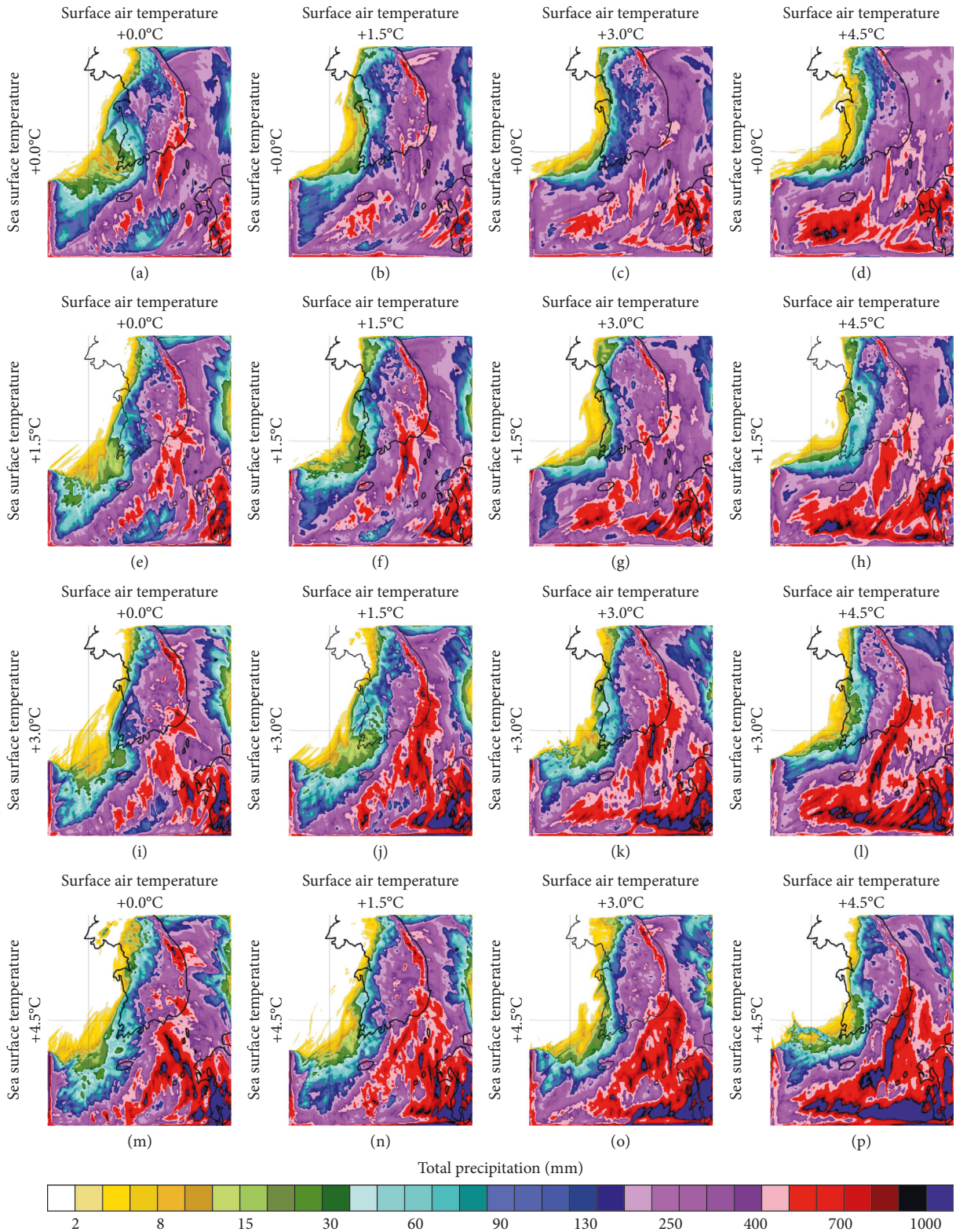

Figure 7: Total rainfall depth and its spatial distribution for various SAT/SST combinations.

6 hours in SST 2.0) was estimated to be larger than the MP of SST 4.0°C increase combination (i.e., 359.3 mm for 6 hours in SST 4.0), whereas in the case of long durations, the MP of SST 4.0°C increase combination (i.e., 698.5 mm for 12 hours in SST 4.0) is estimated to be larger than the MP of SST 2.0°C increase combination (i.e., 646.1 mm for 12 hours in SST 2.0). The same results were shown for duration 1 hour (Figure 8(a)) and 24 hours (Figure 8(d)).

As mentioned above, these causes were reflected in the complex interaction of the surface and the atmosphere.

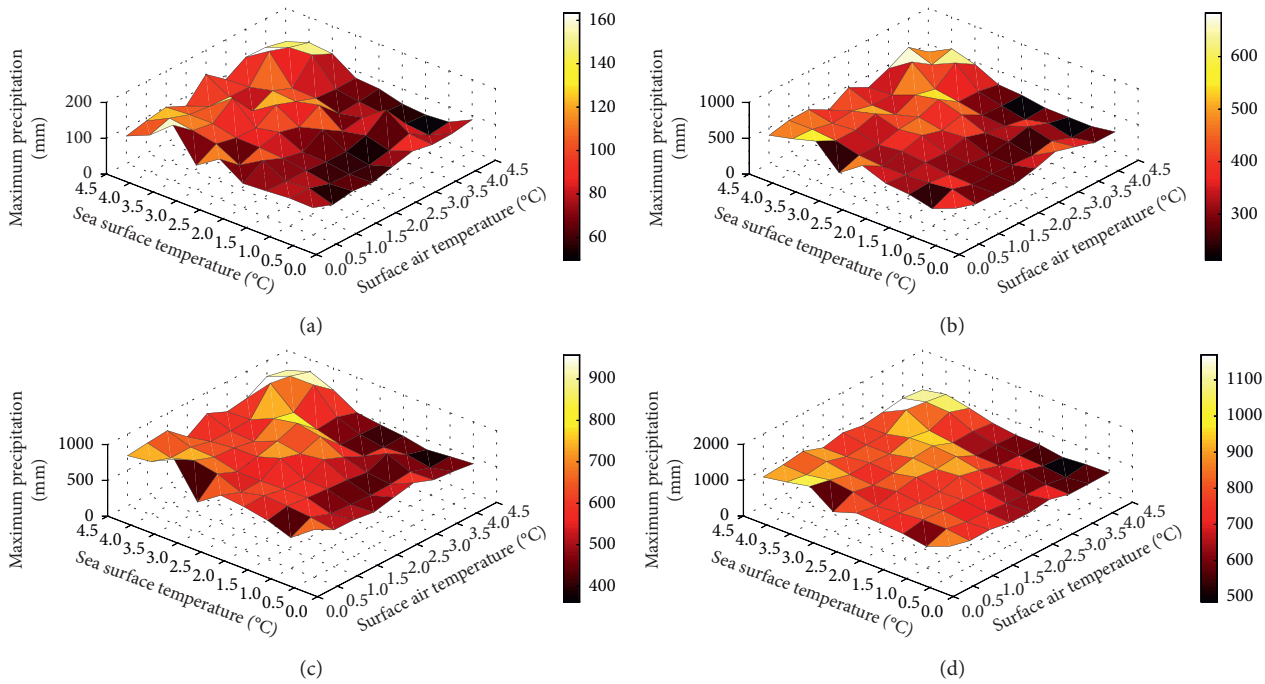

Figure 8: MP for duration (a) 1 hour, (b) 6 hours, (c) 12 hours, and (d) 24 hours at Busan.

Therefore, it is necessary to explore the optimal combination of SAT/SST by various numerical experiments in order to estimate the MP of a specific region through the increase of SAT and SST using physically based RCMs.

3.4. Estimation of Maximum Precipitation. From the results analysed so far, it has been shown that increasing the SAT or SST uniformly did not contribute to the production of MPs in a specific region using RCMs. In this study, two cases were selected among the MPs produced through numerical simulations: (1) SST/SAT increment combination in which the largest MP was simulated and (2) SAT/SST increment combination representing the MP that is closest to the previously reported hydrometeorological PMP. In addition, the selected MPs were compared with PMP calculated by hydrometeorological method of Lee et al. [3].

As shown in Figure 9, the combination of SAT 3.0°C increase/SST 3.5°C increase (MP 3.0–3.5) produced the largest MP. The MP 3.0–3.5 combination simulated 957.5 mm MP at 12 hours of duration, which is approximately 32% greater than the PMP (726.7 mm) reported by Lee et al. [3]. However, even if the MP was estimated using the physically based RCM, the result of the MP that is more than 30% above the PMP, which means the maximum amount of precipitation that can occur physically, was considered to be somewhat unreasonable.

Therefore, in this study, a combination that produces the most similar results to the previously reported PMPs was explored. As a result, it was confirmed that the combination of SAT 2.5°C increase/SST 3.0°C increase (MP 2.5–3.0) produced MPs closest to the conventional PMPs. The MP 2.5–3.0 combination simulated a rainfall depth (736.5 mm) greater than PMP (726.7 mm) for duration of 12 hours, but

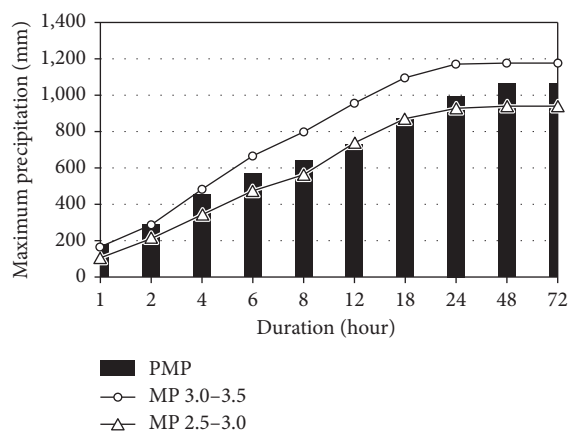

Figure 9: Comparison of PMP and selected MPs.

the difference between the two values was only about 1%, so it was judged to be acceptable. In addition, the MP 2.5–3.0 combination simulated a MP of about 6% smaller than PMP (930.9 mm) for duration of 24 hours, but this was also considered reliable enough considering the uncertainty of PMP estimation.

When MP is calculated using the physically based RCM, the rainfall is simulated at the computational time interval that drives the model. Therefore, not only the maximum rainfall depth for various durations but also the temporal distribution of total rainfall depth can be obtained. That is, there is no need to configure separately a virtual rainfall temporal distribution. This means that the results of this study can be used directly as input data to rainfall-runoff models for flood inundation maps or emergency action plans under the occurrence of mega-disaster scenarios. Figure 10 shows the rainfall hyetograph (bar graph) and

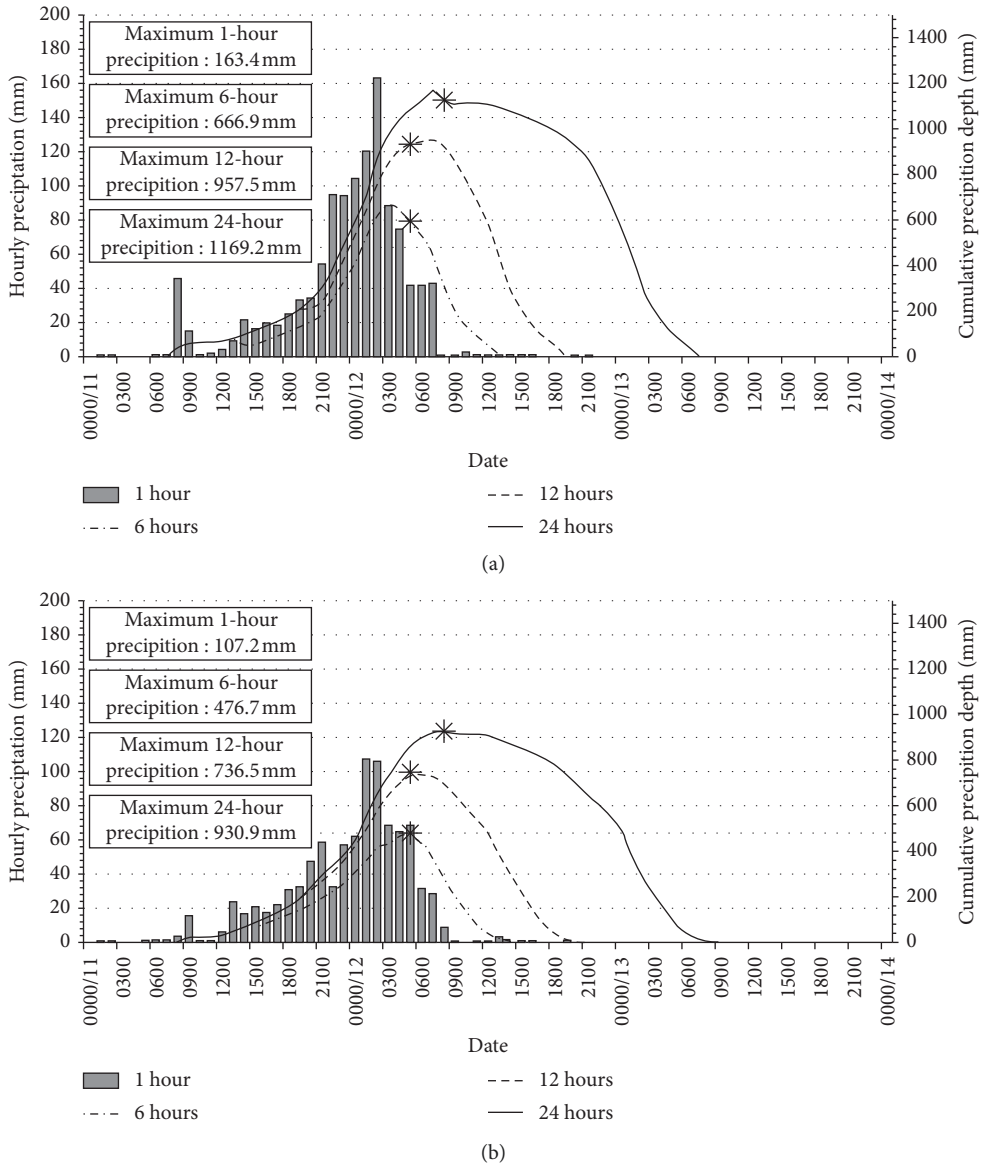

Figure 10: Rainfall hyetograph and rainfall depth for several durations produced at Busan using (a) MP 3.0–3.5 combination and (b) MP 2.5–3.0 combination.

rainfall depth for several durations (line graph) that can be obtained as a result of two selected combinations.

4. Conclusion

In this study, the influence of increasing SAT and SST on the typhoon path (see Figure 1(a)) on the total rainfall depth was analysed using WRF. In addition, the spatially averaged MP of 27 km^2 was calculated for Busan Metropolitan City and compared with PMP estimated by hydrometeorological method.

As a result of analysing the effect of increase of SAT and SST on the total rainfall depth, total rainfall amount in land area of applied domain did not show an explicit relationship with increase of SAT and SST. Since physically based RCMs reflect the complex interactions of the surface and atmosphere, the spatial distribution of rainfall produced by typhoons in peninsular terrain varies greatly in response to changes in ambient climatic conditions. Therefore, despite the increase of SAT and SST, the amount of rainfall in the land decreases. That is, even if the SAT or SST is greatly increased, the amount of rainfall occurring in a specific area does not increase as intended. The results of estimating the MP of Busan Metropolitan City showed no relation regardless of which SAT or SST increment combination was applied. For instance, the duration 6-hour MPs in the Busan area calculated through a total of 100 SAT/SST combination showed a wide range of rainfall amount results ranging from 361.7 mm (SAT + 4.0°C and SST + 1.0°C) to 957.5 mm (SAT + 3.0°C and SST + 3.5°C). However, the MP of combination of SAT + 4.0°C and SST + 4.0°C was estimated to be 720.3 mm smaller than

957.5 mm (SAT + 3.0°C and SST + 3.5°C). Therefore, it is difficult to produce extreme rainfall scenarios in a specific region simply by increasing the SAT or SST as in the method of moisture maximization for estimating PMPs, when producing MP using RCMs. This means that numerous numerical experiments on various SAT/SST increment combinations are needed.

When the rainfall of Typhoon Maemi was maximized by using WRF, the MP of Busan Metropolitan City was estimated to be the highest when SAT 3.0°C increase/SST 3.5°C increase combination was applied. Also, the SAT 2.5°C increase/SST 3.0°C increase combination produced the most similar MP as the PMP reported in the literature. The proposed method of maximizing the typhoon rainfall is expected to contribute to the improvement of the PMP estimation method. Since produced MPs provide detailed temporal distribution of the total rainfall depth as well as total rainfall depth for various durations and impact areas, they can be applied directly as input data of rainfall-runoff models for the design of massive hydraulic structures and the establishment of flood inundation maps and emergency action plans caused by mega disasters.

However, since the spatial distribution of rainfall is heavily influenced by the changes in the surrounding climatic conditions, if the meteorological variables other than SST/SAT/RH applied in this study are changed, there is a possibility that MP is also changed. Therefore, in order to produce extreme rainfall scenarios in specific regions using physically based RCMs, numerical experiments using a combination of varying climate variables rather than unconditional changes in specific climate variables will be needed. Therefore, future studies on various climate variables affecting rainfall caused by typhoons, such as air pressure, wind velocity, and SAT, SST, and RH, are required to maximize typhoon rainfall using RCMs.

Data Availability

The data used to support the findings of this study are available from the corresponding author upon request.

Conflicts of Interest

The authors declare that they have no conflicts of interest.

Acknowledgments

This work was supported by the Korea Environmental Industry and Technology Institute (KEITI) grant funded by the Ministry of Environment (RE201901073).

References

[1] E. M. Hansen, L. C. Schreiner, and J. F. Miller, *Application of Probable Maximum Precipitation Estimates—United States East of the 105th Meridian*, Hydro Meterological Report No. 52, National Weather Service, Washington, DC, USA, 1982.

[2] World Meteorological Organization (WMO), *Manual for Estimation of Probable Maximum Precipitation*, World Meteorological Organization (WMO), Geneva, Switzerland, 1986.

[3] O. Lee, Y. Park, E. S. Kim, and S. Kim, "Projection of Korean probable maximum precipitation under future climate change scenarios," *Advances in Meteorology*, vol. 2016, Article ID 3818236, 16 pages, 2016.

[4] S. M. Papalexiou and D. Koutsoyiannis, "A probabilistic approach to the concept of probable maximum precipitation," *Advances in Geosciences*, vol. 7, pp. 51–54, 2006.

[5] D. J. Abbs, "A numerical modeling study to investigate the assumptions used in the calculation of probable maximum precipitation," *Water Resources Research*, vol. 35, no. 3, pp. 785–796, 1999.

[6] N. Ohara, M. L. Kavvas, S. Kure, Z. Q. Chen, S. Jang, and E. Tan, "Physically based estimation of maximum precipitation over American River watershed, California," *Journal of Hydrologic Engineering*, vol. 16, no. 4, pp. 351–361, 2011.

[7] K. Ishida, M. L. Kavvas, S. Jang, Z. Q. Chen, N. Ohara, and M. L. Anderson, "Physically based estimation of maximum precipitation over three watersheds in northern California: atmospheric boundary condition shifting," *Journal of Hydrologic Engineering*, vol. 20, no. 4, article 04014052, 2015.

[8] K. Ishida, M. L. Kavvas, S. Jang, Z. Q. Chen, N. Ohara, and M. L. Anderson, "Physically based estimation of maximum precipitation over three watersheds in northern California: relative humidity maximization method," *Journal of Hydrologic Engineering*, vol. 20, no. 10, article 04015014, 2015.

[9] K. Ishida, N. Ohara, M. L. Kavvas, Z. Q. Chen, and M. L. Anderson, "Impact of air temperature on physically-based maximum precipitation estimation through change in moisture holding capacity of air," *Journal of Hydrology*, vol. 556, pp. 1050–1063, 2018.

[10] J. Lee, J. Choi, O. Lee, and S. Kim, "Estimation of probable maximum precipitation in Korea using a regional climate model," *Water*, vol. 9, no. 4, pp. 1–12, 2017.

[11] IPCC, "Contribution of working groups I, II and III to the fifth assessment report of the intergovernmental panel on climate change," in *Climate Change 2014: Synthesis Report*, R. K. Pachauri and L. A. Meyer, Eds., IPCC, Geneva, Switzerland, 2014.

[12] E. Weller, S. Min, W. Cai, F. W. Zwiers, Y. Kim, and D. Lee, "Human-caused indo-pacific warm pool expansion," *Science Advances*, vol. 2, no. 7, article e1501719, 2016.

[13] W. Mei and S.-P. Xie, "Intensification of landfalling typhoons over the northwest pacific since the late 1970s," *Nature Geoscience*, vol. 9, no. 10, pp. 753–757, 2016.

[14] F. Laliberte, J. Zika, L. Mudryk, P. J. Kushner, J. Kjellsson, and K. Doos, "Constrained work output of the moist atmospheric heat engine in a warming climate," *Science*, vol. 347, no. 6221, pp. 540–543, 2015.

[15] National Institute of Meteorological Research (NIMR), *Understanding Climate Change II—Climate Change on the Korean Peninsula: Present and Future*, National Institute of Meteorological Research, Seogwipo, Republic of Korea, 2009, in Korean.

[16] K. Tsuboki, M. K. Yoshioka, T. Shinoda, M. Kato, S. Kanada, and A. Kitoh, "Future increase of supertyphoon intensity associated with climate change," *Geophysical Research Letters*, vol. 42, no. 2, pp. 646–652, 2015.

[17] World Meteorological Organization (WMO), *The Second Assessment Report on the Influence of Climate Change on Tropical Cyclones in the Typhoon Committee Region*, ESCAP/WMO Typhoon Committee, Geneva, Switzerland, 2012.

[18] J. Kim, C. Son, and Y. Moon, "Super typhoon haiyan and future typhoon forecast," *Water for Future*, vol. 47, no. 2, pp. 49–54, 2014, in Korean.

[19] J. Choi, J. Lee, H.-G. Jeong, J. Jang, and S. Kim, "Effect of improvement of initial and boundary conditions in WRF model on simulating typhoon rainfall," *Journal of the Korean Society of Hazard Mitigation*, vol. 18, no. 2, pp. 445–454, 2018, in Korean.

[20] Gangwon Regional Meteorological Administration (GRMA), *Gangwon-Do Typhoon White Paper*, Gangwon Regional Meteorological Administration, Gangwon-Do, Republic of Korea, 2013, in Korean.

[21] National Center for Atmospheric Research (NCAR), *ARW Version 3 Modeling System User's Guide*, National Center for Atmospheric Research (NCAR), Boulder, CO, USA, 2015.

[22] G. P. Singh and J.-H. Oh, "Impact of Indian Ocean sea-surface temperature anomaly on Indian summer monsoon precipitation using a regional climate model," *International Journal of Climatology*, vol. 27, no. 11, pp. 1455–1465, 2007.

[23] Korean Meteorological Administration (KMA), *2018 Abnormal Climate Report*, Korea Meteorological Administration, Seoul, Republic of Korea, 2019, in Korean.

Hindawi
Advances in Meteorology
Volume 2019, Article ID 8505903, 11 pages
https://doi.org/10.1155/2019/8505903

Research Article

Understanding the Effects of Changing Weather: A Case of Flash Flood in Morogoro on January 11, 2018

Offoro Neema Kimambo,[1,2] **Hector Chikoore**,[3] **and Jabulani Ray Gumbo**[4]

[1]*Department of Geography and Environmental Studies, Solomon Mahlangu College of Science and Education, Sokoine University of Agriculture, Morogoro, Tanzania*
[2]*Department of Ecology and Resource Management, School of Environmental Sciences, University of Venda, Thohoyandou, South Africa*
[3]*Department of Geography and Geo-Information Sciences, School of Environmental Sciences, University of Venda, Thohoyandou, South Africa*
[4]*Department of Hydrology and Water Resources, School of Environmental Sciences, University of Venda, Thohoyandou, South Africa*

Correspondence should be addressed to Offoro Neema Kimambo; offoro@gmail.com

Received 8 November 2018; Revised 14 March 2019; Accepted 26 March 2019; Published 21 April 2019

Guest Editor: Sushil K. Dash

Floods are the leading cause of hydrometeorological disasters in East Africa. Regardless of where, when, and how the event has happened, floods affect social security as well as environmental damages. Understanding floods dynamics, their impacts, and management is thus critical, especially in climate risk assessment. In the present study, a flash flood (a case of an episodic hydrological event) which happened on January 11, 2018, in Morogoro, Tanzania, is examined and synthesized. Data were courtesy of the National Oceanic and Atmospheric Administration Global Forecasting System (NOAA GFS) (forecast data), Tanzania Meteorological Agency (TMA), and Sokoine University of Agriculture (for the automatic weather data). With the help of ZyGRIB-grib file visualization software (version 8.01, under General Public License (GNU GPL v3)), the forecast data and patterns of the observation from the automatic weather station (temperatures, wind speed and directions, rainfall, humidity, and pressure) and the long-term rainfall data analysis in the study area made it possible. This study contributes to the knowledge of understanding the changing weather for planning and management purposes. Both forecasts and the observations captured the flash flood event. The rain was in the category of heavy rainfall (more than 50 mm per day) as per the regional guidelines. The synergy between the forecasts and the 30-minute weather observation interval captured the fundamental weather patterns that describe the event. For studying the nature and impacts of flash floods in the region, the integration of automatic weather observation into the systems of national meteorological centers is inevitable. Additionally, as part of an integrated disaster risk reduction effort, there is a need for a review on catchment management strategies.

1. Introduction

Flash floods according to the World Meteorological Agency (WMO) are defined as floods of "*short duration with a relatively high peak discharge*" [1]. Flash floods are studied as climatological phenomena [2] or as hydrological phenomena [3]. Several factors are responsible for flash floods occurrence including meteorological (e.g., intensity, duration, amount, and time-space variation in rainfall) and watershed characteristics such as area, length, slope, type of soil, vegetation cover, and land use [4, 5]. However, there are also many other factors which are unknown [6]. Flash floods may be accompanied by other events such as mudslides, but very rare [7]. Flash floods are also ranked high among natural disasters [8]. Recent studies indicate that there is an increasing trend of floods over about half of the globe but with greater regional and local variability [9].

In East Africa, for example, flash floods are the leading hydrometeorological disaster [10]. Due to the predicted changes in climate in the region [11], for example, increased precipitation and flooding, major cities and towns are at higher risks. A recent study [12] specifically in Tanzania suggests that floods are driven by heavy rainfall patterns and are widely distributed and overtime have caused significant economic damages and causalities. On the other hand, documentation and track records of this phenomenon [13] is limited. The ability to predict flash floods is also limited and difficult due to the complex interaction between meteorological and hydrological variables. However, the prediction of flash floods has been investigated and verified using hydrological models [4]. Recent advances have demonstrated, for example, weather radar has the capability to predict these events ahead of time [5], but they can also be assisted by other means of investigations and therefore they can synergistically provide early warning to the vulnerable communities.

Recent cases (information available online at http://floodlist.com/tag/tanzania and https://reliefweb.int/country/tza) of floods in Tanzania indicate an increasing intensity, and the trend is more than ever before [14]. A recent study [15] conducted in Tanzania and Nigeria on coping strategies to climate impacts suggests differences in coping strategies across regions. Tanzania climate is very variable, and it is mostly regulated by the Intertropical Convergence Zone (ITCZ) which defines rain pattern in the country. Also, El Niño and La Niña which influence drought and floods, respectively, define rain pattern in the region as well [16]. Monsoon, thunderstorms, and local climate (e.g., orographic effects) also play an important role in the climate of Tanzania. Other causes have been studied and narrated (e.g., Kijazi and Reason [17] on the 2006 flood event in the northern part of Tanzania) strong warming over the Indian Ocean coupled with the convective zone over the western Indian Ocean, warming of the Somali Coast, and an easterly moisture flux are linked with floods in Tanzania [17].

Increase in population and urbanization as well as poor land management are among other factors that increase vulnerability to floods [16, 18]. Land use changes (e.g., pollution, erosion, and silting of the river beds) have been reported as the major contributor in reducing the Ngerengere River carrying capacity [19]. Surveys and anecdotal evidence in the Ngerengere River catchment also suggest that conversion of natural areas into agricultural field leads to increased surface runoff and the magnitude of floods specifically the upper part of the catchment [20].

According to WMO, disaster risk knowledge, forecasting, dissemination, and preparedness are key elements of early warning systems [5]. Previous studies indicate that, in Tanzania, floods are recurrent phenomena and have been ranked high on the list of hazards [16, 21]. Apart from the direct effects, indireclty heavy rainfall is also secondary key to waterborne diseases [22] and other related problems in water bodies, for example, proliferation of algal blooms [3]. It is high time now to invest in understanding the occurrence and complexities that are involved in predicting as well as setting the best resilience options (i.e., physical, ecological, and sociological).

On January 11, 2018, high rainfall event was observed in Morogoro Region in Tanzania which caused damages to properties and critical infrastructure, such as water and electricity supply lines, as well as the death of one person. Normally, the dominant weather phenomenon for the month of January is associated with the Intertropical Convergence Zone (ITCZ) as it moves south and retreats to the north from the south [17]. During the event, the tropical cyclone (TC) Berguitta was the dominant weather system in the Indian Ocean. The current study aimed to examine and synthesize the flash flood event on January 11, 2018, which occurred in Morogoro, specifically, data utilization for understanding the effects of changing weather over a catchment.

2. Materials and Methods

2.1. Study Area Description. The Ngerengere catchment is the subcatchment (Figure 1) of the main Wami Ruvu basin and located in Morogoro Region, Tanzania, within longitudes and latitudes of 37°32′E 6°51′S, 38°09′E 6°69′S, 37°38′E 7°09′S, and 38°38′E 7°05′S, respectively. It covers approximately an area of 2780 km^2 and is characterized by a tropical climate [23]. The population in the catchment is estimated to be about 1 million [24]. Climate and land use are believed to have caused significant impacts on the catchment [23]. A recent survey in Wami/Ruvu basin indicates temperatures are varying (very hot days and reducing cold days), rising evapotranspiration (normally higher than rainfall) and moisture deficits, increasing uncertainty in rainfall characteristics, increasing frequency of extreme events, floods, and a long period of no rainfall [25]. Daily temperatures range from 22 to 33°C and less agreement in rainfall [25, 26]. The uncertainities in rainfall is mainly due to the complex interaction of solar radiations, atmosphere, soil and water heat storage, topography and land cover, and vegetation type [25]. A recent study [27], for example, found significant changes (9 km^2 to 82 km^2) in impervious surfaces around Morogoro town which might be the reasons for the formation of urban heat island. This study demonstrated urban heat index which was linked to variability in climate.

The catchment is characterized by bimodal rainfall pattern, the long rains or *Masika* (March, April, and May) and the short rains or *Vuli* (September, October, and November). Most part of the catchment receives annual rainfall varying from 800 to 1500 mm, whereby the highest is received in the Uluguru Mountains [23]. In the upper Ngerengere River, there are tributaries (Mzinga, Mlali, Lukurunge, and Mgeta Rivers) which are flowing into the Mindu Dam and the discharge from the Dam is spilled into the Ngerengere River which adjoins with Morogoro, Bigwa, Mlali, and Ruvu tributaries to the main Ruvu River.

2.2. Methods. We analyzed twenty-four (24) hours of observations (at an interval of 30 minutes) for temperature (°C), dewpoint temperatures (°C), wind speed (knots) and

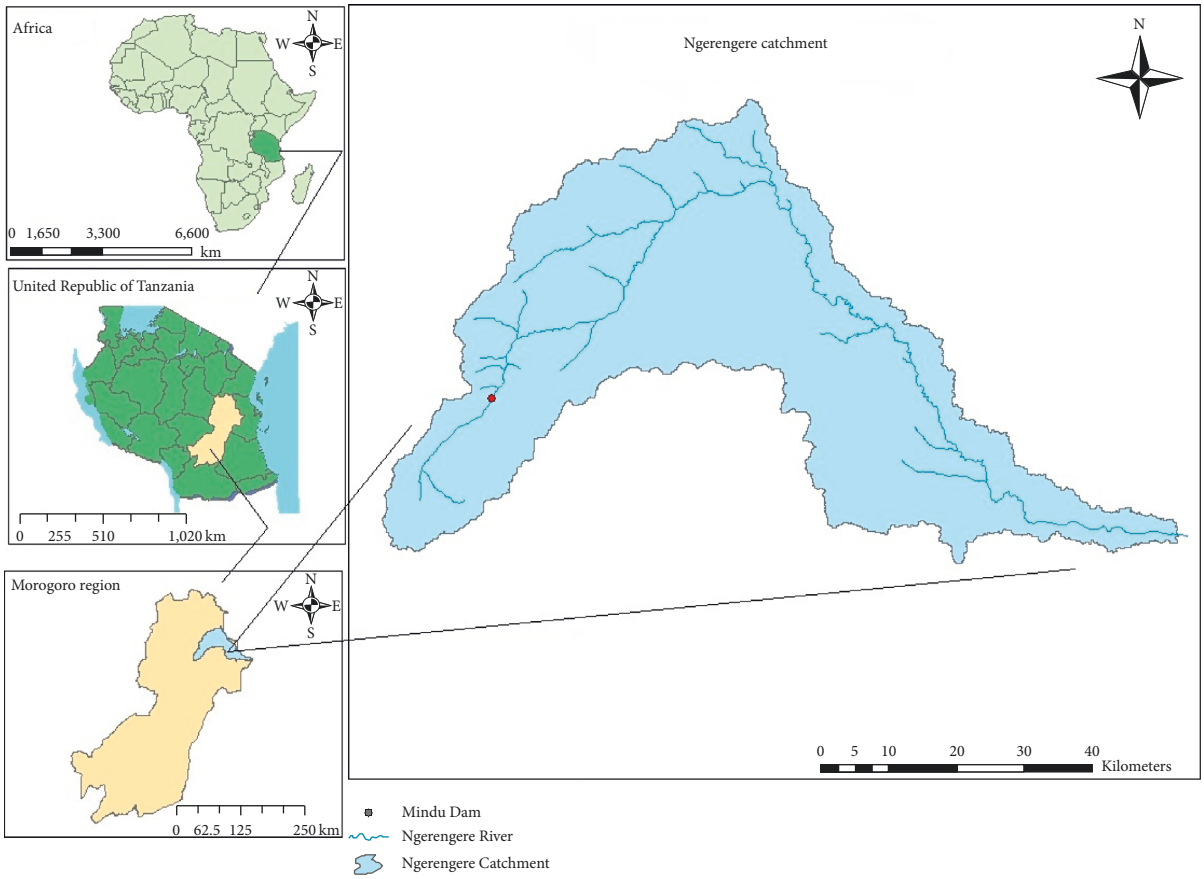

Figure 1: Map of Ngerengere catchment in Morogoro Region.

direction (degree), pressure (mmHg), rainfall (mm), and relative humidity (%) all downloaded from an automatic weather station situated at Mazimbu, Sokoine University of Agriculture, in Morogoro. We used ZyGrib (grib files visualization software, version 8.01, General Public License (GNU GPL v3 available online at http://www.zygrib.org/) to visualize a forecast of a day before (January 10, 2018) from National Oceanic and Atmospheric Administration (NOAA) Global Forecasting Services (GFS). The aim was to examine the prevailing large-scale weather pattern for January 10 and 11, 2018. ZyGrib domain settings were as follows: Weather Centre 7, Model 81, run time Wednesday 2018-01-10 06 : 00 UTC to Saturday 2018-01-20 06 : 00 UTC; area 21°S, 007°E and 007°N, 061°E; and the resolution of 0.25° ∗ 0.25°. The following parameters from the models were studied: mean sea level pressure (MSLP) (mbar), geopotential height (m) (at 850 hPa and 500 hPa), air temperature (°C) (at 2 m, 850 hPa, and 500 hPa), and dewpoint temperature (°C) (at 2 m). In addition to that, wind (at 10 m, 850 hPa, and 500 hPa), total precipitation (mm), clouds cover, surface convective inhibition (CIN) (J/kg), surface convective available potential energy (CAPE) (J/kg), and wind gust (surface) were also investigated.

2.3. Study Design and Data Analysis. This is a case study design with the intent to examine, synthesize, and describe the nature of the flash flood which happened on January 11, 2018, in Morogoro municipality and how it can be used to study catchment management. Most of the figures in the study were produced using the ZyGrib-grib file visualization software, version 8.01, under General Public License (GNU GPL v3, available at http://www.zygrib.org), and XLSTAT (Addinsoft (2019), XLSTAT statistical and data analysis solution, Boston, USA; https://www.xlstat.com) for the patterns, and statistical inferences to all the investigated parameters and cross-case synthesis were examined and used for drawing our conclusions.

3. Results and Discussion

Under this section, all the findings are presented and discussed.

3.1. Model Forecasts. Most of the flash floods result from deep convective clouds [28]. A forecast form NOAA GFS model run on Wednesday 2018-01-11 06 : 00 UTC indicated that the entire country (Tanzania) was cloudy (Figure 2(a)), and a Col (i.e., area of slack pressure between two anticyclones and two depressions) (Figure 2(b)) was situated at the central to northeastern part of the country. During the date of event (heavy rainfall), large-scale weather systems, namely, ITCZ and tropical storm (Berguitta), triggered the rainfall activity in the area of interest (Morogoro).

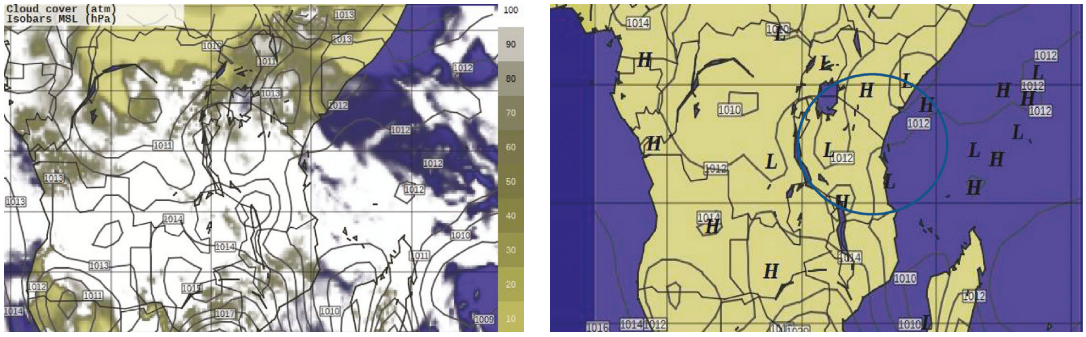

(a) (b)

Figure 2: Cloud cover overlaid with the mean sea level pressure (a) and surface high- and low-pressure centers (b) at 0900 UTC. The low-pressure centers are an indication of areas of surface convergence. All maps were from NOAA-GFS, Wednesday 2018-01-10 06 : 00 UTC, generated using zyGRID-Grib files visualization software (available at http://www.zygrib.org/).

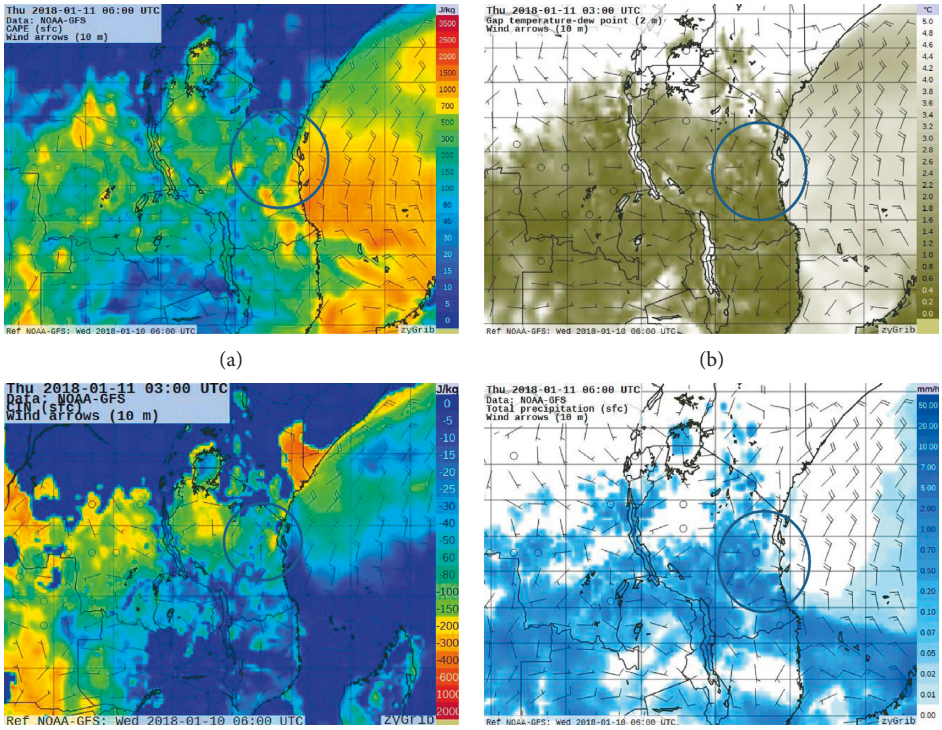

(a) (b)

(c) (d)

Figure 3: Convective available potential energy (J/kg) at 09 : 00 am (a); a gap between air temperature (°C) and dewpoint temperature (°C) (b); convective inhibition (J/kg) (c); total surface precipitation (mm) (d) all overlaid with wind at 10 m (forecast data from NOAA-GFS on Wednesday 2018-01-10 0600 UTC and generated by using zyGRID-grib files visualization software, available at http://www.zygrib.org/). The circled area is the area of interest of explicitly low pressure and converging surface wind.

For assessing the large-scale disturbances leading to severe weather, convective available potential energy (CAPE) is normally used [29, 30]. A cross-examination indicated that CAPE values increased from 450 J/Kg at around 03 : 00 UTC to 1839 J/Kg at around 15 : 00 UTC (Figure 3(a)). On the other hand, convective inhibition (CIN) (energy required to initiate convection) values were ranging from −51 to −11 J/kg (Figure 3(c)) in the specified period. Relative humidity (%) values were also high (reaching 92%) (*for the estimation of CAPE and CIN with ZyGrib, values can be extracted from the map while navigating the cursor over the area of interest*). The air and dewpoint temperature gradient (Figure 3(b)) varied from 0.2 to 0.4°C between 0300 and 0600 UTC, which is an indication of high moisture content as well. This among other factors mentioned in the previous sections were responsible for the precipitation (Figure 3(d)).

From the forecast, there was warming over the Indian Ocean and wind flows at both 850 and 500 hPa indicated a moisture flux from the western Indian Ocean (Figures 4(a) and 4(b)).

The vertical velocity (Pascal/seconds) (Figures 5(a) and 5(b)) for both 850 hPa and 500 hPa indicates a significant

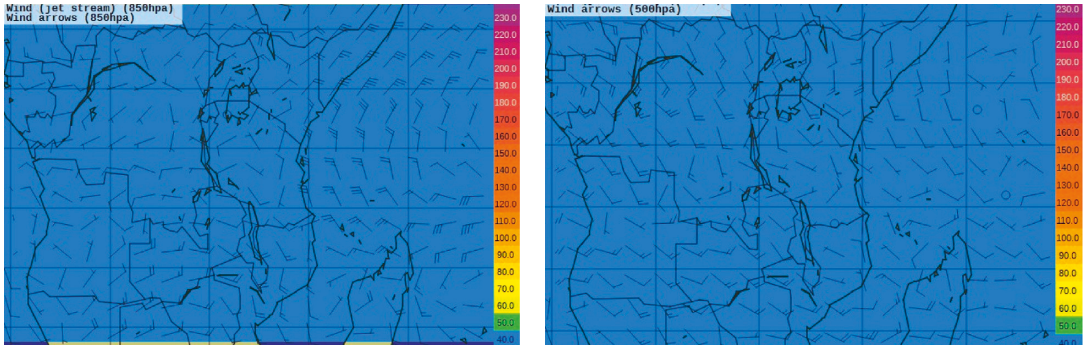

(a) (b)

Figure 4: (a) Wind at 850 hPa and (b) wind at 500 hPa all from NOAA-GFS on Wednesday 2018-01-10 06 : 00 UTC (all the graphs generated using zyGRID-grib files visualization software, available at http://www.zygrib.org/).

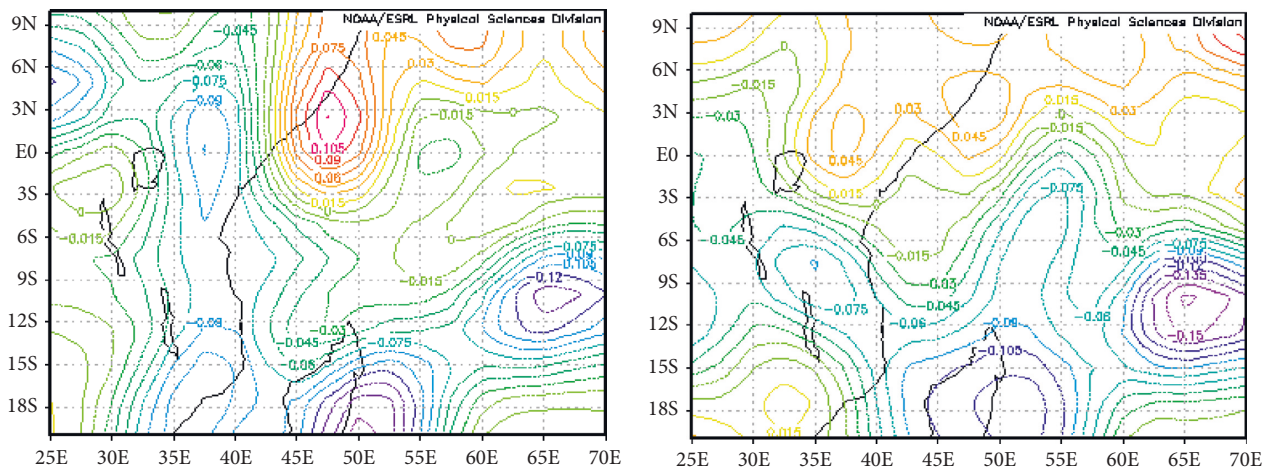

(a) (b)

Figure 5: Vertical velocity (Omega) (Pascal/second) for both 850 hPa (a) and 500 hPa (b) (images provided by the NOAA-ESRL Physical Sciences Division, Boulder Colorado from their website at https://www.esrl.noaa.gov/psd/).

area of vertical velocity which is bulging from the south-eastern tip of Tanzania connected to the one which was occurring in the Indian Ocean, East of Madagascar. The dominant weather system during the course of the event over the area was ITCZ (regions of low-pressure systems can also be depicted from Figure 2(b)) which is the normal and regular position during the month of January [17], and over the Indian Ocean, there was a tropical cyclone (TC) Berguitta (Figure 5(b), far eastern Madagascar). The two weather systems together are the ones which influenced the convergence over the area leading to the heavy weatherly activities over the area of interest (study area).

3.2. Surface Observations. As per the automatic weather station data, the event started at around 05 : 00–09 : 00 am (0300–0600 UTC) Tanzania local time. Wind speed (Figure 6(a)) was ranging from 5 to 10 knots, gusting 30 knots towards 09 : 00 am, and at the same time, wind direction registered a huge variation. On average, the whole day, more than 50% of wind direction (Figure 6(a)) distribution varied from southwesterly to northwesterly. The air temperature and dewpoint gradient were also so close during the three hours of the event (Figure 6(b)) indicating that there was moisture in the area which was one among the ingredient for the precipitation. This can be confirmed by the moisture amount in the atmosphere which was almost 92%.

At the time of the event, there was also an increase in pressure (Figure 7) which is common (follows normal diurnal variation). From the surface observation (automatic weather station data), it can be deduced that rainfall (Figure 7) intensity (92.2 mm in almost three hours) was very high. Based on this fact, one can hypothesize and test on the variation of the rainfall intensity in the region. The same can also be depicted from the analysis of water level (Figure 8) for Mindu Dam, a domestic water reservoir in the Ngerengere catchment which increased significantly. Preliminaries on the forecasts (i.e., the previous twenty-four-hour rainfall) according to the Tanzania Meteorological Agency (TMA) indicated that Morogoro synoptic station had received the highest rainfall (85.3 mm) in the country (Figure 9(a)). The satellite image as well could tell the activeness of the weather of the day (Figure 9(b)).

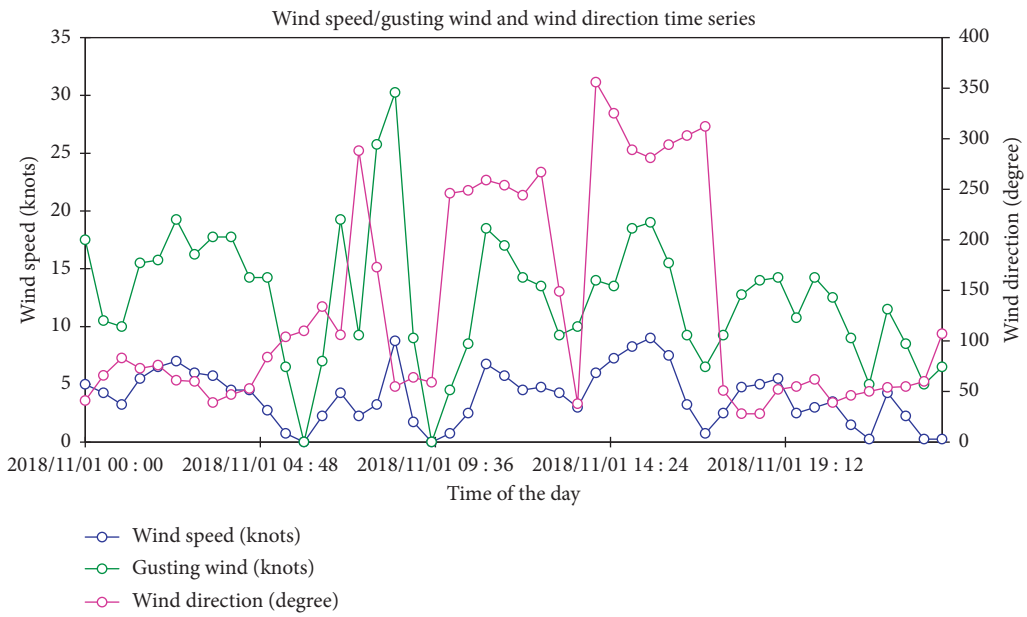

(a)

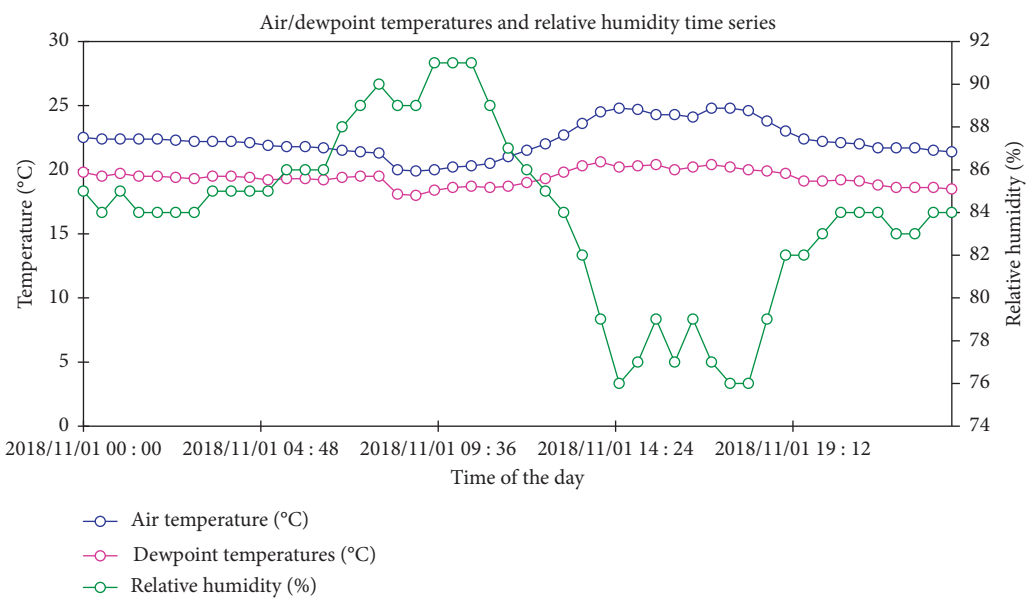

(b)

Figure 6: Twenty-four-hour wind speed, gusting wind (both in knots), and wind direction (degree) (a) and relative humidity (%), air temperature (°C), and dewpoint temperature (°C) (b) for the day of January 11, 2018.

General characteristics of the variation of weather parameters (temperature, for example) in the regions show significant variations [31]. Rainfall is more tied to sea surface temperatures (SSTs) [32]. A historical record in the study area also indicates that it is a drought-prone area [33]. To supplement that, a recent study [19] in the Ngerengere catchment which investigated the effects of climate change and land use on the discharge regime demonstrated that climate change and land use have got different effects. This study used soil and water assessment tool (SWAT) and statistical analysis to curb the problem of data. The study also pointed out that there is a huge variation in weather (sometimes, total drying out downstream the catchment and floods). According to Natkhin et al. [19] with regard to the drying out, dry periods (less than 15 mm of rainfall per week) registered an increasing trend [19]. This was also reported by Kimambo et al. [34] on the standardized precipitation and evapotranspiration index (SPEI) with alteration of positive (positive 2 for wet conditions) and negative (negative 2 for severe drought condition). A comparison for the extreme (per year and for the month of January) rainfall for the period (1971–2012) is demonstrated in Figure 10. It was found that the month of January had also contributed to the cases of extreme rainfall/year in the catchment. However,

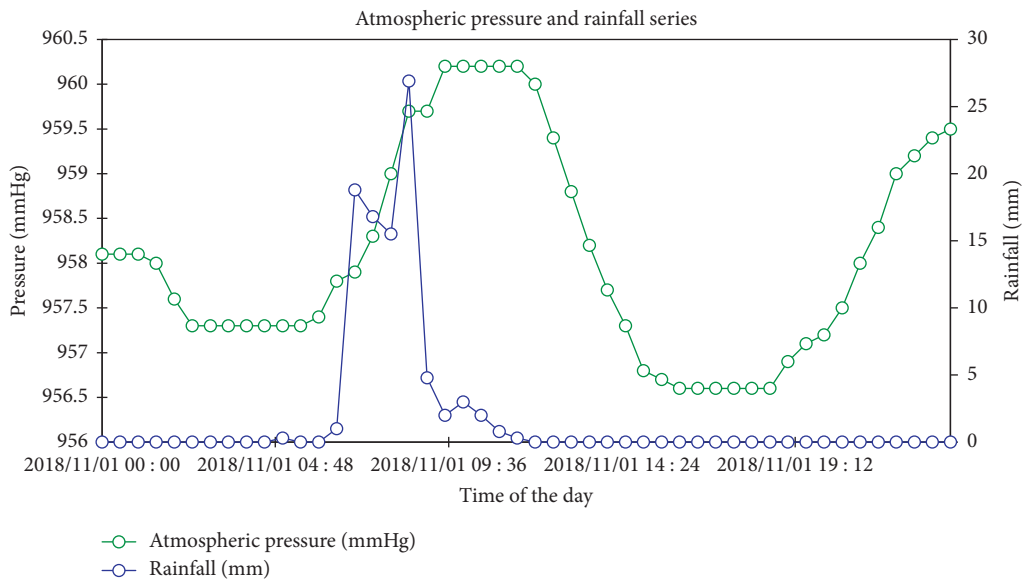

Figure 7: Atmospheric pressure (mmHg) and rainfall (mm) series on the 11th of January 2018, Morogoro.

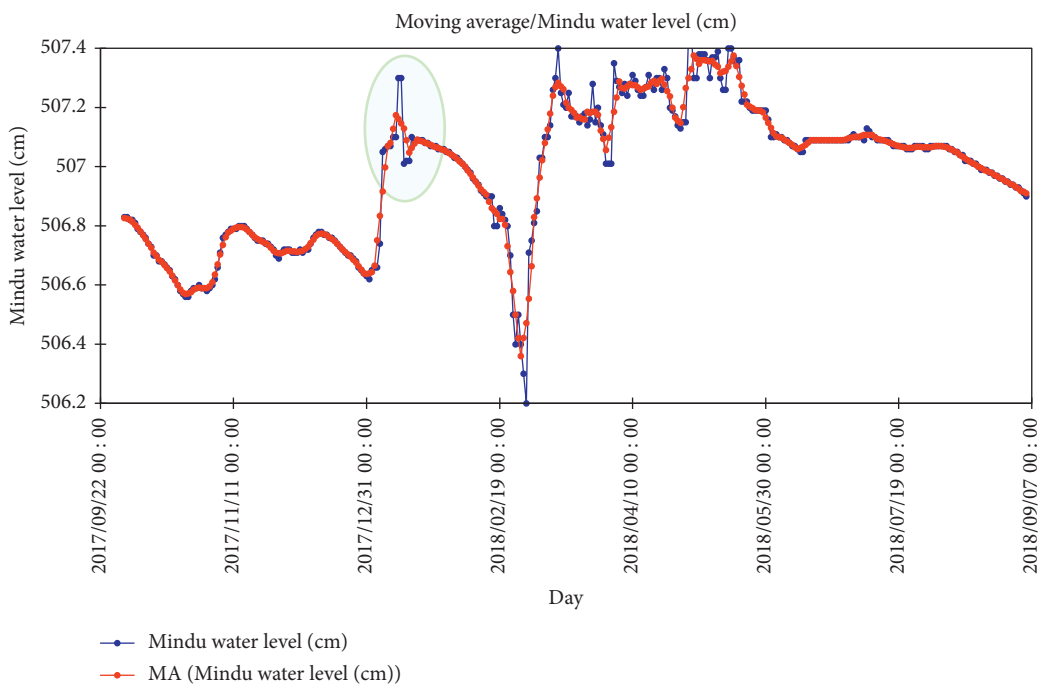

Figure 8: Moving average/water level (cm) for Mindu Dam for a period of October 2017 to August 2018 (data from Wami Ruvu basin office). A sharp increase (cycled) is attributed to the heavy rainfall (a case study being discussed) and thereafter dropping toward the end of the month of February and then an increase in the following months of March, April, and May (MAM), i.e., the rainfall seasons.

that there was a significant difference between the two data distribution meaning that most of the extreme (heavy) cases of rainfall are attributed to other months of the year. Performing Mann–Kendall trend, it was found that there is no significant trend in the two series.

3.3. Associated Impacts and Management. Weather-related extreme events such as flash floods are associated with the economic crisis, societal disturbances, and environmental impacts (e.g., nutrients transports, pollution, and species composition change in the affected area) [9, 35]. The perception prevailing is that floods are from the prolonged rainfall [14] which may not be always. Short-time rainfall like the case being studied demonstrated even a less-than-a-day rainfall event can also create havoc. The anecdotal observations (Figures 11(a) and 11(b)) showed that the event was so stressful to the locals and damaged properties and some business was inundated (https://www.youtube.com/watch?v=W1Gj-R1-mto) in the town of Morogoro. Apart from the direct impacts discussed above, the

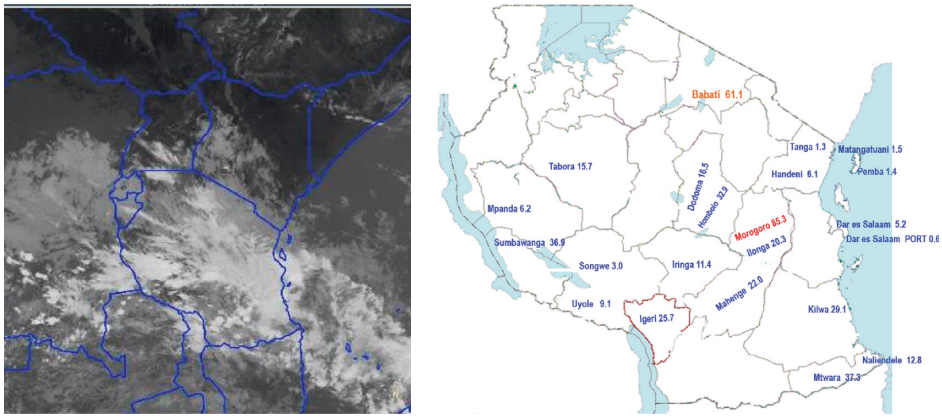

(a) (b)

Figure 9: (a) Infrared satellite (IR) image for the day (1015 UTC, 11/01/2018) (retrieved from https://en.sat24.com/en/af/infraPolair) and (b) the twenty-four-hour (January 11, 2018) rainfall (mm) distribution (preliminaries prior to the forecast of the day) in Tanzania as extracted from the official YouTube (https://www.youtube.com/watch?v=ohd4t4BMsnk) channel of the Tanzania Meteorological Agency.

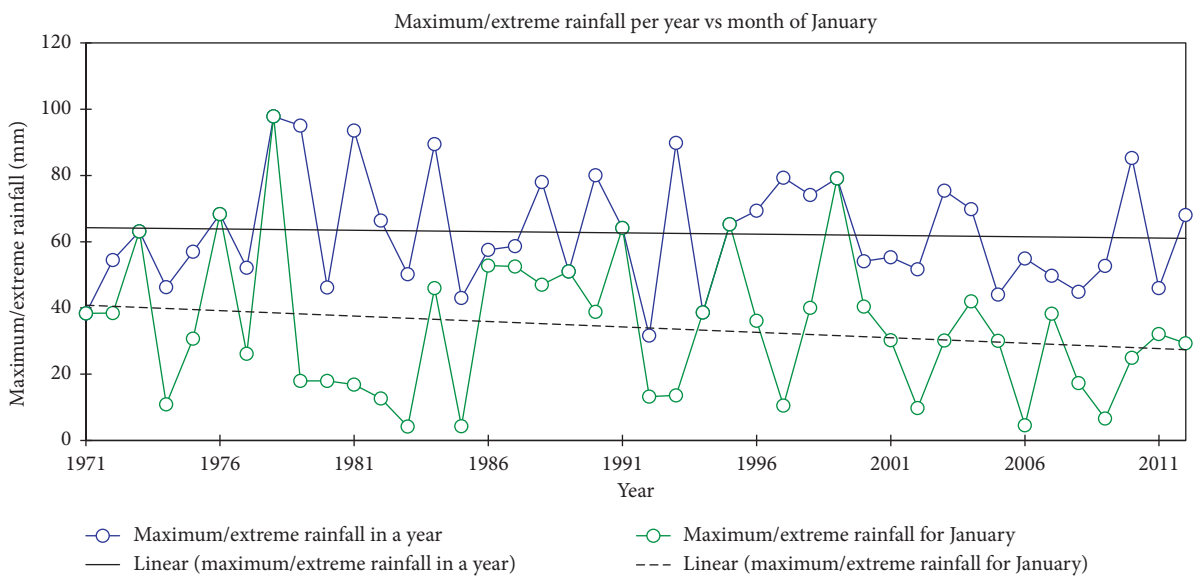

Figure 10: Trend (the Mann–Kendall trend test showed a nonsignificant trend at a 95% confidence interval, p-value > 0.05) for maximum (extreme) rainfall (per year and for the month of January) for Morogoro synoptic (daily rainfall data for the period of 1971–2012, in courtesy of the Tanzania Meteorological Agency, were extracted using an interactive Statistical Package, Instat+ for Windows, version 3.37).

effect of rainfall (for example, heavy rainfall cases) on aquatic systems has been discussed critically [3]. Anderson [36] suggests that a case study approach may be more informative to study river ecological health, for example, studying harmful algal blooms (noxious to the environment) dynamics in a catchment. Heisler et al. [37] also highlight the relationship between nutrients transfer in rivers as a result heavy rainfall (for example, an observation made by the author just a month after a rainy season in Figure 11(c)) algal blooms tend to proliferate. Algal blooms are also common in the study area and they have been associated with variations of both climate and hydrological changes [34].

Normally in risk assessment, three elements are involved, i.e., vulnerability, exposure, and threats. The national adaptation plan [14] does not address specifically what should be done on these short-term impacts. A study by Ringo [38] argues that governance and institutional structures are insufficient in providing structural measures before, during, and after flash floods. Ringo (2018) outlined core areas which can be improved such as lack of disaster experts, delays in relief, and the participatory approach in dealing with the problem. Other case studies [39] in Dar es Salaam, for example, proposed strategies that can be used for risk reduction from the same phenomenon. Wilby and Keenan [40] triangulated the best way to address the issue. This study considered information (e.g., early warning systems, education programs, and mapping the vulnerable areas), institutions (e.g., building codes, public participation, and transparencies), and preparedness (e.g., standing orders and role plays) nexus as the best approach.

(a) (b)

(c)

Figure 11: (a) Photos taken (downstream Mindu Dam) on morning hours just after the rainfall on the 11th of January 2018. No one (anecdotal observation) could have crossed the bridge (Julius Nyerere Freedom Bridge) to/from Solomon Mahlangu College of Science and Education, Mazimbu, from/to Morogoro Town; (b) for the first time (word of mouth from an aged personnel with 32 years of working experience), the security offices in the campus went flooded and (c) observation at the same point just few months after rainy season (March, April, and May).

4. Conclusion

Flash floods of any nature increase the vulnerability of humans, livestock, and aquatic resources. The paper analyzed the flash flood event which was attributed to heavy rainfall (more than 80 mm/day) on January 11, 2018, in the northern Morogoro, Tanzania. The event caused the overflow of Ngerengere River and some of its tributaries. NOAA GFS and observations (automatic weather) synergistically can be efficient in understanding (for example, local context) the nature of flash flood cases in the study area. The phenomenon was localized (enhanced by the orographic nature of the place) but also steered by the presence of the ITCZ and the tropical cyclone Berguitta (which was the dominant weather over the Indian Ocean). Anthropogenic activities (observed siltation of the Ngerengere River) could have also contributed to the magnitude/severity of the damages. For studying the nature and impacts of flash floods in the region, installation of the automatic weather stations and their integration into the systems of national meteorological centers is inevitable. Additionally, as part of an integrated disaster risk reduction and/or adoption, there is a need for reviewing catchments management policies.

Data Availability

The data used to support the findings of this study are available from the corresponding author upon request.

Conflicts of Interest

The authors declare that there are no conflicts of interest.

Acknowledgments

The authors acknowledge the support from staff at the College of Science and Education, Sokoine University of Agriculture, Morogoro, Tanzania. The authors thank Wami Ruvu Basin Authority and the Morogoro Municipal Council through Morogoro Urban Water Supply Authority (MORUWASA). This work was supported by the University of Venda, Limpopo, South Africa.

References

[1] The University Corporation for Atmospheric Research, *Flash Flood Early Warning System Reference Guide*, University Corporation for Atmospheric Research, Boulder, CO, USA, 2010, http://www.meted.ucar.edu/communities/hazwarnsys/ffewsrg/FF_EWS.pdf.

[2] E. S. Kim and H. I. Choi, "Assessment of vulnerability to extreme flash floods in design storms," *International Journal of Environmental Research and Public Health*, vol. 8, no. 7, pp. 2907–2922, 2011.

[3] E. S. Reichwaldt and A. Ghadouani, "Effects of rainfall patterns on toxic cyanobacterial blooms in a changing climate: between simplistic scenarios and complex dynamics," *Water Research*, vol. 46, no. 5, pp. 1372–1393, 2012.

[4] S. Rozalis, E. Morin, Y. Yair, and C. Price, "Flash flood prediction using an uncalibrated hydrological model and radar rainfall data in a Mediterranean watershed under changing hydrological conditions," *Journal of Hydrology*, vol. 394, no. 1-2, pp. 245–255, 2010.

[5] M. Acosta-Coll, F. Ballester-Merelo, M. Martinez-Peiró et al., "Real-time early warning system design for pluvial flash floods-A review," *Sensors*, vol. 18, no. 7, p. 2255, 2018.

[6] J. Zogg and K. Deitsch, *The Flash Flood Potential Index at WFO Des Moines, Iowa*, National Weather Service, Des Moines, LA, USA, 2013, http://www.crh.noaa.gov/Image/dmx/hydro/FFPI/FFPI_WriteUp.pdf.

[7] B. E. Montz and E. Gruntfest, "Flash flood mitigation: recommendations for research and applications," *Environmental Hazards*, vol. 4, no. 1, pp. 15–22, 2002.

[8] L. Marchi, M. Borga, E. Preciso, and E. Gaume, "Characterisation of selected extreme flash floods in Europe and implications for flood risk management," *Journal of Hydrology*, vol. 394, no. 1-2, pp. 118–133, 2010.

[9] Z. W. Kundzewicz and P. Matczak, "Extreme hydrological events and security," *Proceedings of the International Association of Hydrological Sciences*, vol. 369, pp. 181–187, 2015.

[10] J. M. Huho and R. C. Kosonei, "Understanding extreme climatic events for economic development in Kenya," *IOSR Journal Of Environmental Science Toxicology And Food Technology Ver. I*, vol. 8, no. 2, pp. 14–24, 2014, http://www.iosrjournals.org.

[11] World Wide Fund For Nature, *Climate Change Impacts on East Africa: A Review of the Scientific Literature. East Africa Climate Impacts*, World Wide Fund For Nature, Gland, Switzerland, 2006.

[12] K. B. Mafuru and T. Guirong, "Assessing prone areas to heavy rainfall and the impaction of the upper warm temperature anomaly during March–May rainfall season in Tanzania," *Advances in Meteorology*, vol. 2018, Article ID 8353296, 17 pages, 2018.

[13] T. Ja and K. M, "Review of spatial and temporal distribution of landslides in Tanzania," *Journal of Ecosystem & Ecography*, vol. 7, no. 3, 2017.

[14] The United Republic of Tanzania, *National Adaptation Programme of Action*, Global Environment Facility (GEF), Washington, DC, USA, 2007, https://unfccc.int/resource/docs/napa/tza01.pdf.

[15] S. Boamah, F. Armah, V. Kuuire, I. Ajibade, I. Luginaah, and G. McBean, "Does previous experience of floods stimulate the adoption of coping strategies? Evidence from cross sectional surveys in Nigeria and Tanzania," *Environments*, vol. 2, no. 4, pp. 565–585, 2015.

[16] M. Mollet and D. Barelli, *Rapid Agriculture Needs Assessment in Response to the El-Niño Effects in the United Republic of Tanzania*, Food and Agriculture Organization of the United Nations, Rome, Italy, 2016, http://www.fao.org/fileadmin/user_upload/emergencies/docs/TZ_final_needs_assessment_report-reformatted-new.pdf.

[17] A. L. Kijazi and C. J. C. Reason, "Analysis of the 2006 floods over Northern Tanzania," *International Journal of Climatology*, vol. 29, no. 7, pp. 955–970, 2009.

[18] S. Pavagadhi and R. Balasubramanian, "Toxicological evaluation of microcystins in aquatic fish species: current knowledge and future directions," *Aquatic Toxicology*, vol. 142-143, pp. 1–16, 2013.

[19] M. Natkhin, O. Dietrich, M. P. Schäfer, and G. Lischeid, "The effects of climate and changing land use on the discharge regime of a small catchment in Tanzania," *Regional Environmental Change*, vol. 15, no. 7, pp. 1269–1280, 2015.

[20] M. P. Schaefer and O. Dietrich, *Impact of Land Use Change and Water Abstractions on the Discharge of the Ngerengere River in Tanzania and its Implications for Agriculture and Food Security*, Institute of Landscape Hydrology, Muncheberg, Germany, 2016.

[21] The United Republic of Tanzania, *The United Republic of Tanzania. National Adaptation Programme of Action (NAPA)*, International Institute for Environment and Development, London, UK, 2007.

[22] S. L. M. Traerup, R. A. Ortiz, and A. Markandya, "The costs of climate change: a study of cholera in Tanzania," *International Journal of Environmental Research and Public Health*, vol. 8, pp. 4386–4405, 2030.

[23] M. C. Gomani, O. Dietrich, G. Lischeid et al., "Establishment of a hydrological monitoring network in a tropical African catchment: an integrated participatory approach," *Physics and Chemistry of the Earth, Parts A/B/C*, vol. 35, no. 13-14, pp. 648–656, 2010.

[24] The United Republic of Tanzania, *Population Distribution by Age and Sex*, National Bureau of Statistics, Dar Es Salaam, Tanzania, 2013, https://ihi.eprints.org/2169/1/Age_Sex_Distribution.pdf.

[25] GLOWSFIU, *Climate, Forest Cover, and Water Resources Vulnerability Wami/Ruvu Basin, Tanzania*, Florida International University, North Miami, FL, USA, 2014.

[26] M. Gomani, F. Mahay, B. Mbilinyi, O. Dietrich, and G. Lischeid, "Establishment of a hydrological monitoring system through a participatory approach in a small tropical catchment in Tanzania: learning hydrology from the local people," vol. 2069, pp. 8–11, 2009, http://www.tropentag.de/2009/abstracts/links/Dietrich_yGx508hY.pdf.

[27] S. Ernest, A. R. Nduganda, and J. J. Kashaigili, "Urban climate analysis with remote sensing and climate observations: a case of Morogoro municipality in Tanzania," *Advances in Remote Sensing*, vol. 6, no. 2, pp. 120–131, 2017.

[28] M. Borga, E. N. Anagnostou, G. Blöschl, and J.-D. Creutin, "Flash floods: observations and analysis of hydro-meteorological controls," *Journal of Hydrology*, vol. 394, no. 1-2, pp. 1–3, 2010.

[29] M. L. Apsley, K. J. Mulder, and D. M. Schultz, *Reexamining the United Kingdom's Greatest Tornado Outbreak: Forecasting the Limited Extent of Tornadoes along a Cold Front*, University of Manchester, Manchester, UK, 2016.

[30] F. Tuluri, R. S. Reddy, Y. Anjaneyulu, J. Colonias, and P. Tchounwou, "Environmental modeling, technology, and communication for land falling tropical cyclone/hurricane prediction," *International Journal of Environmental Research and Public Health*, vol. 7, no. 5, pp. 1937–1952, 2010.

[31] M. New, B. Hewitson, D. B. Stephenson et al., "Evidence of trends in daily climate extremes over Southern and West Africa," *Journal of Geophysical Research Atmospheres*, vol. 111, no. 14, 2006.

[32] W. C. Ndomeni, E. Cattani, A. Merino, and V. Levizzani, "An observational study of the variability of East African rainfall with respect to sea surface temperature and soil moisture," *Quarterly Journal of the Royal Meteorological Society*, vol. 144, pp. 384–404, 2018.

[33] J. Paavola, "Livelihoods, vulnerability and adaptation to climate change in Morogoro, Tanzania," *Environmental Science & Policy*, vol. 11, no. 7, pp. 642–654, 2008.

[34] O. N. Kimambo, J. R. Gumbo, and H. Chikoore, "The occurrence of cyanobacteria blooms in freshwater ecosystems and their link with hydro-meteorological and environmental

variations in Tanzania," *Heliyon*, vol. 5, no. 3, article e01312, 2019.

[35] T. H. Dewan, "Societal impacts and vulnerability to floods in Bangladesh and Nepal," *Weather and Climate Extremes*, vol. 7, pp. 36–42, 2015.

[36] D. Anderson, "HABs in a changing world: a perspective on harmful algal blooms, their impacts, and research and management in a dynamic era of climactic and environmental change," in *Proceedings of the 15th International Conference on Harmful Algae*, vol. 3–17, Changwon, Korea, October 2014.

[37] J. Heisler, P. M. Glibert, J. M. Burkholder et al., "Eutrophication and harmful algal blooms: A scientific consensus," *Harmful Algae*, vol. 8, no. 1, pp. 3–13.

[38] J. Ringo, "Influence of governance and institutional structures on flood management and control in Kilosa district, Tanzania," *International Journal of Scientific and Research Publications (IJSRP)*, vol. 8, no. 4, 2018.

[39] A. Gastinger, A. Neoh, A. Cardwell et al., *Building Just Responses to Flooding*, Centre for Community Initiatives (CCI), Dar es Salaam, Tanzania, 2017.

[40] R. L. Wilby and R. Keenan, "Adapting to flood risk under climate change," *Progress in Physical Geography: Earth and Environment*, vol. 36, no. 3, pp. 348–378, 2012.